Controlling the Structure of Peptide Using Ferrocene as a Molecular Scaffold

A Thesis Submitted to the College of

Graduate Studies and Research

in Partial Fulfillment of the Requirements

for the Degree of Doctorate of Philosophy

in the Department of Chemistry

University of Saskatchewan

Saskatoon

By

Somenath Chowdhury

PERMISSION TO USE

Presenting this thesis in partial fulfillment of the requirements for a degree of Doctorate of Philosophy from the University of Saskatchewan, I agree that the libraries of this university may make it available for inspection. I further agree that permission for copying of this thesis in any manner, in whole or in part, for scholarly purposes may be granted by the professor or professors who supervised my thesis work or, in their absence, by the Head of the Department of Chemistry or the Dean of the College of Graduate Studies and Research. It is understood that any copying or publication or use of this thesis or parts thereof, for financial gain shall not be allowed without my written permission. It is also understood that due recognition shall be given to me and to the University of Saskatchewan in any scholarly use which may be made of any material in this thesis.

Requests for permission to copy or to make other use of material in this thesis in whole or part should be addressed to:

Head of the Department of Chemistry

University of Saskatchewan

Saskatoon, Saskatchewan,

S7K 5C9

ABSTRACT

The *de novo* design of peptides is a central area of research in chemical biology. Although it is now possible to design helical peptide structures from first principle, designing β-sheets remains a challenge. Significant advances in this area have been made by using molecular scaffolds, which stabilize β-sheets through intramolecular H-bonding involving the scaffold or which direct supramolecular assembly of the conjugate. In my thesis, I have made use of novel strategies, using ferrocene (Fc) as a central scaffold for controlling the secondary structure of peptides. This approach has been highly successful. Four major new strategies are introduced and described in this thesis:

a) Cyclization of Fc-peptide conjugates of the type $Fc[CO\text{-}Xxx\text{-}CSA]_2$ (Xxx = Gly, Ala, Val, Leu) and $Fc[CO\text{-}Gly\text{-}Xxx\text{-}CSA]_2$ (Xxx = Val, Ile; CSA = cysteamine) leads to the clean formation of novel cyclic bioorganometallic conjugates, which exhibit strong intramolecular hydrogen bonding interactions that restrict the mobility of the podand peptide chains. In the latter system, this intermolecular hydrogen bonding interaction was exploited for the design of a novel β-barrel-like structure. For $Fc[CO\text{-}Gly\text{-}Val\text{-}CSA]_2$ and $Fc[CO\text{-}Gly\text{-}Ile\text{-}CSA]_2$ discrete cyclic supramolecular assemblies were formed in which the individual molecules assemble along the rims of the molecules, resulting in the formation of tubular peptide superstructures that possess a central cavity and are filled with water molecules.

b) Prior to my work, work by Hirao and Metzler-Nolte clearly showed that the two podand peptide chains in Fc-peptide conjugates are pointing away from each other. This would indicate that extended β-sheets cannot be formed by simply extending the podand peptide chains. In my work, I clearly demonstrate that, in contrast to earlier results, it is

possible to use the Fc scaffold to stabilize β-sheet-like interactions in longer peptide chains. Two systems are described in this thesis Fc[CO-Gly-Val-Cys(Bz)-OMe]$_2$ and Fc[CO-Gly-Ile-Cys(Bz)-OMe]$_2$. In both the cases, amino acids are employed that have a high propensity for β-sheet formation. Both Fc-peptide conjugates exhibit strong interstrand hydrogen bonding, resembling that found in β-sheets.

c) In this work, I have demonstrated the use of ferrocene amino acid (Fca) to control the structure in peptides. In contrast to previous work by Metzler-Nolte, my work is largely focusing on the design of a repetitive Fca-peptide motif. It is proposed that this repetition will enable strong interactions between the peptide portions of the conjugate, resulting in the formation of an extended structure. To this effect, a series of Fca-conjugates of the type Boc-[Fca-Ala]$_n$-OMe (n = 1-4) was synthesized and fully characterized. All systems display the expected interaction between the Ala residues having a 12-membered hydrogen bonded ring. Such a structural motif resembles that found in naturally occurring β-helical structures of the spike-region of some viral proteins.

d) I have also demonstrated the use of a novel Fc-derivative, Fc[NH-Boc]$_2$, to control the structure of podand amino acid chains. Fc-diamine was synthesized by the convenient carbazide route giving this useful scaffold in high yield. This material was converted into its peptide conjugate and the resulting conjugate displays the elusive 14-membered hydrogen bonding ring.

Thus, in my work, I have provided a new complementary tool for peptide design that will undoubtedly find applications for the design of *de novo* proteins in the near future.

ACKNOWLEDGEMENTS

I would like to acknowledge everybody who showed interest in my work and supported me during this Ph.D. work. I am especially extremely grateful and indebted to my supervisor Dr. H.-B. Kraatz, for his support and guidance throughout the course of this study. His suggestions and constructive criticisms were highly useful and necessary in the successful completion of this work. My gratitude also goes to my Advisory Committee members, Dr. Mathew Paige, Dr. Jens Müller and Dr Richard Evitts, for helping me in various ways during this project. My appreciation also goes to Dr. Gabriele Schatte, Saskatchewan Structural Science Center, for crystallographic data collections and solving the structures. The assistance given by Dr. K. Brown in performing NMR experiments and collecting mass spectral data by K. Thoms is really appreciated.

I sincerely thank the past and present members of our group for their helps and suggestions in different stages during this work.

Financial support from NSERC, Department of Chemistry and University of Saskatchewan is gratefully acknowledged.

DEDICATION

This work is dedicated to my mother Kalimati Chowdhury.

TABLE OF CONTENT Page No.

LIST OF FIGURES Page No.

LIST OF SCHEMES

Page No.

LIST OF TABLES

Page No.

LIST OF ABBREVIATIONS

A	absorption
Å	armstrong
Ala	alanine
Arg	arginine
Asn	aspartine
Asp	aspartic acid
Boc	*t*-butyloxycarbonyl
BOP	benzotriazol-1-yl-*N*-oxy-tris(dimethylamino)-phosphonium hexafluoro-phosphate
Bz	benzyl
CD	circular dichroism
COSY	correlation spectroscopy
Cp	cyclopentadiene
CSA	cystamine
CV	cyclic voltammetry
Cys	cystein
DCC	dicyclohexyl-carbodiimide
DCM	dichloromethane
DMSO	dimethylsulfoxide
DPV	differential Pulse Voltammetry
E^0	standard potential
$E_{1/2}$	half-wave potential
EDC	1-Ethyl-3-(3-dimethylaminopropyl)-carbodiimide
Et	ethyl
EtOAc	ethylacetate
FAB	fast atom bombardment
Fc	ferrocene
Fca	1-amino-1'-ferrocene carboxylic acid
FTIR	fourier transform infrared spectroscopy
Gln	glutamine
Glu	glutamic acid
Gly	glycine
HBTU	O-(benzotriazole-1-yl)-N,N,N',N'-tetramethylurionium hexafluorophosphate
His	histidine
HMBC	heteronuclear multiple bond correlation spectroscopy
HOBt	hydroxybenzotriazole
HRMS	high resolution mass spectrometry

Hz	hertz
Ile	Isoleucine
j	coupling constant
K	kelvin
Leu	leucine
LRMS	low resolution mass spectrometry
Lys	lysine
m	milli
Me	methyl
MeOH	methanol
Met	methionine
min.	minute
ml	millilitre
mM	millimolar
mmol	millimole
mol	mole
MS	mass spectrometry
MW	molecular weight
NMR	nuclear magnetic resonance
Phe	phenylalanine
ppb	parts per billion
ppm	parts per million
Pro	proline
ROESY	rotary frame overhouser and exchange spectroscopy
Ser	serin
TFA	trifluro acetic acid
Thr	threonine
TOCSY	total correlation spectroscopy
Trp	triptophan
Tyr	tyrosine
Val	valine
ε	extinction coefficient
ΔEp	potential peak separation
ΔT	change of temperature
Δδ	change of chemical shift
δ	chemical shift
λ	wavelength

Chapter 1

Introduction

1.1. General

Motivated by the important roles played by the specific secondary structural domains of proteins, enormous efforts have been devoted to the design of structurally well-defined synthetic peptides. These investigations are aimed at gaining a deeper understanding of the mechanism of protein folding and of biochemical processes,[1] generating molecules with potential biological applications,[2] and developing novel materials.[3] Various strategies have been exploited to design the controlled structures of peptides such as cyclization,[4] insertion of β-amino acids,[5] disulfide bonds,[6] D-amino acids,[7] or molecular scaffold in the peptide backbone.[8]

In this respect, ferrocene (Fc) has recently been recognized for its ability to induce secondary structures and supramolecular arrangements to its peptide conjugates.[9] Along with its ability to function as a molecular scaffold, Fc has fully reversible electrochemical behavior. The combination of these two inherent properties can enable preparation and the investigation of various electrochemical properties and molecular recognition behavior of specific structural peptides.[10,11] On the basis of these characteristics, this present work details the use of Fc as a molecular scaffold to design some structural peptides.

Before proceeding to the details of my research, I would like to briefly highlight the background and give a concise overview of this research area.

1.2. Structures of Peptides

Proteins and peptides play a crucial role in biological systems for the maintenance of biochemical and biophysical activities. They are primarily the copolymers of twenty DNA coded amino acids. The difference in structure and function of various proteins and peptides arises from the variation of their amino acid sequence.

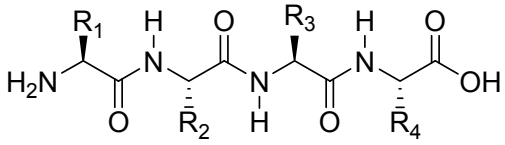

Figure 1.1. Primary structure of peptides containing four amino acids in the sequence. R_1, R_2, R_3 and R_4 represent the side groups of the amino acids.

A peptide contains two or more (generally up to fifty) amino acids linked by amide bonds, which are so called peptide bonds. Figure 1.1 illustrates the primary structure of a tetrapeptide. Peptides can adopt characteristic, well-organized three dimensional structures that are closely linked to their biological functions. A particular protein folds

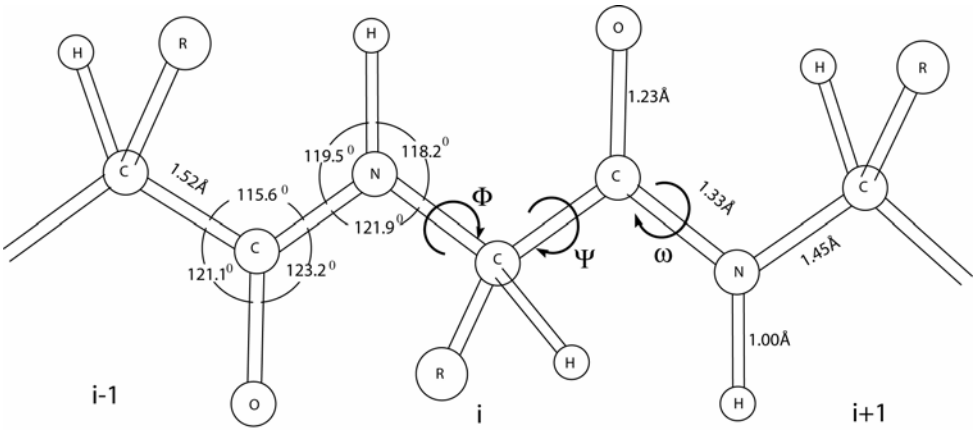

Figure 1.2. Bond angles and bond distances of a typical peptide backbone. Φ, Ψ and ω are the dihedral angels, which are the determining factors of the peptide secondary structures.[12]

in a distinct manner under physiological conditions to perform a specific function. In the folded state, various well-defined local structural domains are present in the peptide backbone. These secondary structures are helical, sheet-like and turn-like. A certain secondary structural element possesses specific torsion angles about the C^{α}, Φ (C^{α}-N) and Ψ (C^{α}-C) as shown in Figure 1.2. The torsion angles of some common peptide secondary structures are presented in Table 1.1.[12]

Table 1.1. Parameters of some regular sheet and helical peptide structures [12]

	Bond angle / º			Residues per turn	Translation per residue /Å
	Φ	Ψ	ω		
Antiparallel *β*-sheet	-139	135	-178	2.00	3.40
Parallel *β*-sheet	-119	113	180	2.00	3.20
Right-handed *α*-helix	-57	-47	180	3.60	1.50
3_{10}-helix	-49	-26	180	3.00	2.00
π-helix	-57	-70	180	4.40	1.15
Polyproline I	-83	158	0	3.33	1.90
Polyproline II	-78	149	180	3.00	3.12
Polyglycine II	-80	150	180	3.00	3.10
Left-handed *α*-helix	57	47	-180	3.60	1.50

Among the secondary structures, the helix is the most abundant. In a helix, the peptide backbone is arranged in a spiral fashion. Figure 1.3a depicts the structure of a typical α-helical peptide together with the H-bonding pattern of other helical structures. Depending upon the amino acid sequence and other external factors different helices can be formed, each with a specific set of dihedral angles (Φ , Ψ and ω) pitch length and a number of amino acid residues per turn (Table 1.1). The H-bonding pattern differs between helical types. For example, in a 3_{10}-helix, H-bonding occurs between the $C{=}O_i$

and $NH_{i=2}$, in an α-helix, it is between $C{=}O_i$ and $NH_{i=3}$ and in a π-helix between $C{=}O_i$ and $NH_{i=4}$ etc. as shown in Figure 1.3b. Both left-handed and right-handed helices can occur that are best described respectively as *M*- and *P*-helical conformations. The different helices also vary in their H-bonding pattern, where the notation n_m is used to specify the helix, with *n* being the number of amino acid residues per turn and *m* being the H-bonded ring size. The most common helical structure is the α-helix, which has a pitch length of 5.4 Å, 3.6 amino acid residues per turn and a 13-membered H-bonding ring. According to the n_m notation it can be designated as a 3.6_{13}-helix.

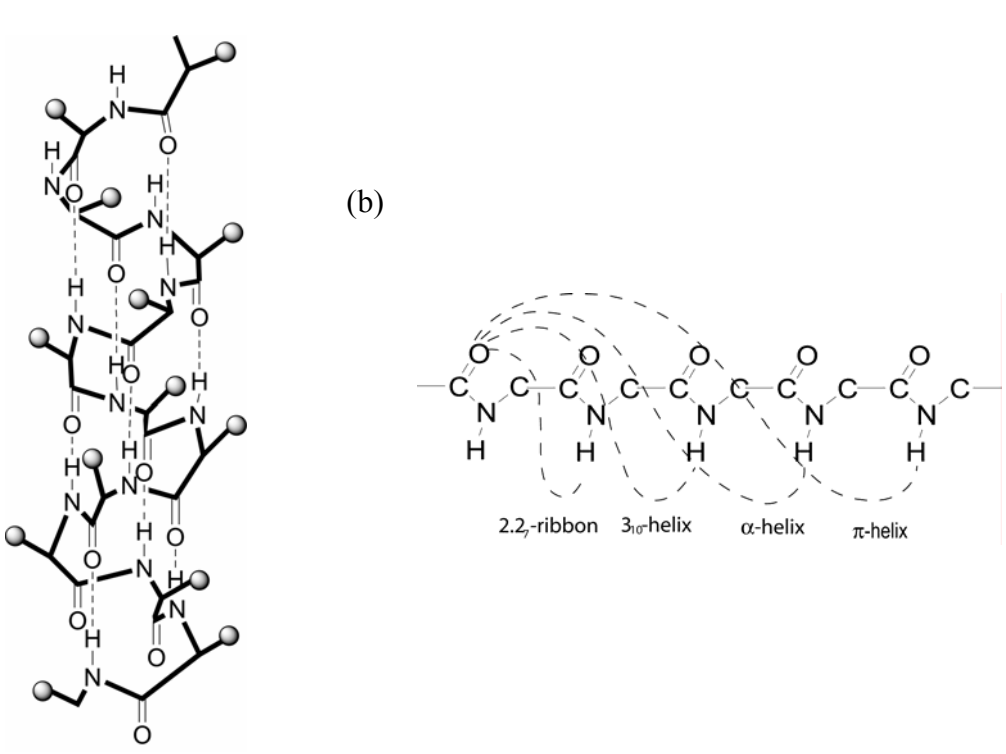

Figure 1.3. (a) Typical structure of a part of an α-helical peptide backbone, showing its spiral conformation and the hydrogen bonding. Grey spheres indicate the side groups of the amino acids. (b) Various H-bonding patterns in different helical peptides.[12]

The second most common secondary structural element is the β-sheet, in which the peptide backbone is a highly extended strand and stabilized by H-bonding with

another laterally aligned and extended peptide strand. These strands can be parallel or antiparallel to the N- and C-terminals, and correspondingly they are called parallel *β*-sheet or antiparallel *β*-sheet. Figure 1.4 illustrates the structures of typical *β*-sheet peptides and their H-bonding patterns.

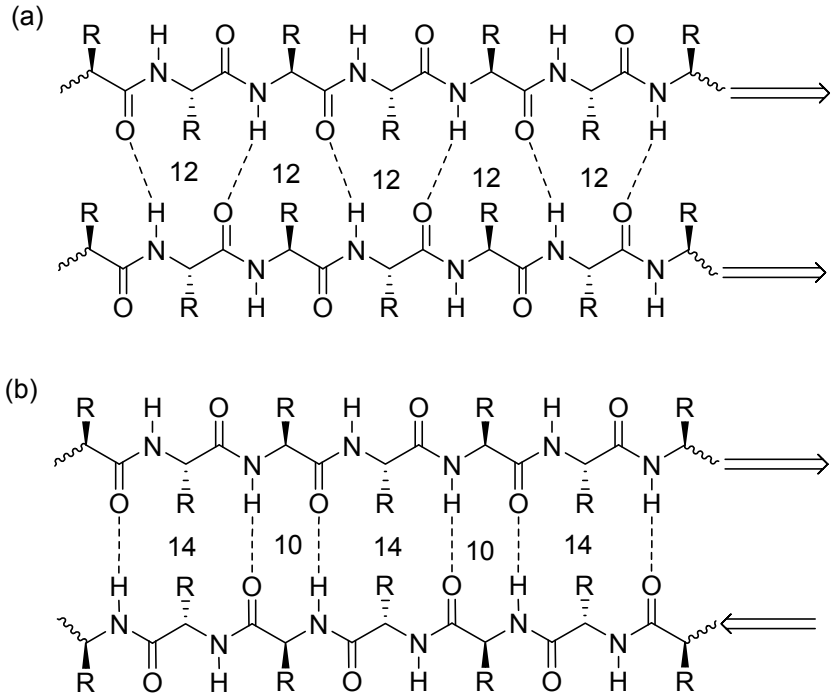

Figure 1.4. Structural drawings of *β*-sheet peptides: (a) parallel *β*-sheet peptides have 12-membered H-bonded rings; (b) Antiparallel *β*-sheet peptides have a series of alternative 10- and 14-membered H-bonded rings.[12]

To align secondary structural elements into a tertiary structure, they must be connected by some linkers, such as turns (Figure 1.5). Unlike helices and sheets, turns are aperiodic in nature and the residues in this structural element have very different torsion angles. Turn structures generally reverse the direction of the chain and they often are found on the surface of proteins. They often take part in molecular or ion recognition processes. Depending upon the radius of curvature and H-bonding pattern they are again divided into different classes as shown in Figure 1.5.

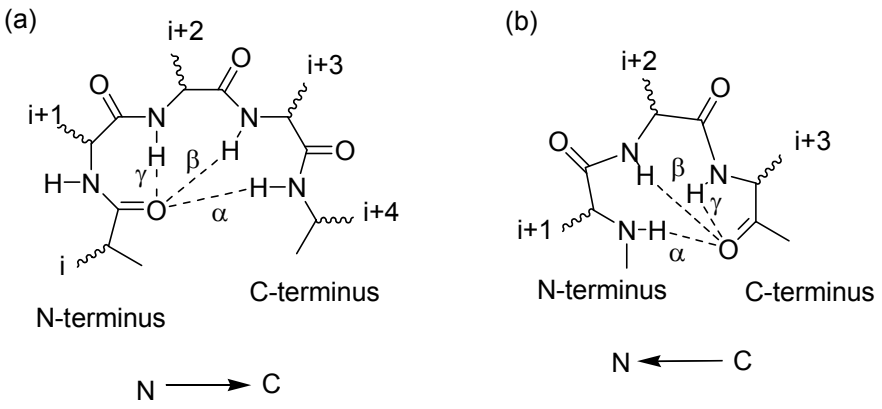

Figure 1.5. Various turn structures in peptides: (a) α, β and γ-turns and (b) reverse α, β and γ- turns.[13]

Depending upon the H-bonding ring size or directionality of the H-bonding pattern they are classified as α (13, NH_i to $CO_{-(i-4)}$), β (10, NH_i to $CO_{-(i-3)}$) and γ (7, NH_i to $CO_{-(i-2)}$) turns and reverse α (11, NH_i to $CO_{(i+3)}$), β (8, NH_i to $CO_{(i+2)}$) and γ (5, NH_i to $CO_{(i+1)}$) turns. [13]

1.3. Controlling the Secondary Structures of Peptides

The variation of secondary structures in peptides results from the differences in their sequence, indicating that it may be possible to design secondary structures by selecting appropriate amino acid sequences. From the statistical analysis of protein structures, it appears to be possible to predict the secondary structural preference of any given peptide through judicial selection of a sequence.[14] However, in many cases this approach does not provide the expected results.[15] Table 1.2 presents the propensity of certain amino acids to adopt specific secondary structure. In addition to the preference shown by amino acids for specific secondary structures, other important factors, such as

hydrophobic interactions, polar-polar interactions and van der Waals interactions need to be taken into consideration.

Table 1.2. Propensities of different amino acids for the formation of different secondary structures at different positions. [14] Preference $P_{i,j} = (n_{i,j} / n_i) / (n_j / N)$ where $n_{i,j}$ = number residue of amino acid i in the the secondary structure j, n_i = number of residue of amino acid i, n_j = number of residue in structure j and N = total number of effective residue.

	Preference			α-Helix Preference			Turn Preference		
Amino acid Residue	α-helix (P_α)	β-sheet (P_β)	Reverse turn (P_t)	N-term	Middle	C-term	Type I	Type II	Other
Glu (E)	1.59	0.52	1.01	2.12	1.18	1.21	1.12	0.84	1.06
Ala (A)	1.41	0.72	0.82	1.33	1.60	1.46	0.74	0.94	0.58
Leu (L)	1.34	1.22	0.57	1.03	1.50	1.46	0.61	0.53	0.75
Met (M)	1.30	1.14	0.52	0.75	1.44	1.92	0.66	0.73	0.96
Gln (Q)	1.27	0.98	0.84	1.39	1.22	1.24	0.79	1.45	1.02
Lys (K)	1.23	0.69	1.07	0.98	1.05	1.68	0.70	0.73	1.04
Arg (R)	1.21	0.84	0.90	1.26	1.25	1.23	0.88	1.22	0.84
His (H)	1.05	0.80	0.81	0.68	0.97	1.57	0.78	0.64	1.00
Val (V)	0.90	1.87	0.41	1.00	1.09	1.08	0.39	0.61	0.48
Ile (I)	1.09	1.67	0.47	0.96	1.31	0.99	0.39	0.43	0.93
Tyr (Y)	0.74	1.45	0.76	0.63	0.61	1.00	0.71	0.91	0.97
Cys (C)	0.66	1.40	0.54	0.78	0.66	0.56	1.38	0.99	0.78
Trp (W)	1.02	1.35	0.65	1.20	1.34	0.78	1.35	0.15	0.52
Phe (F)	1.16	1.33	0.59	0.94	1.45	1.20	0.77	0.76	0.53
Thr (T)	0.76	1.17	0.90	0.75	0.87	0.80	1.25	0.63	0.93
Gly (G)	0.34	0.58	1.77	0.60	0.47	0.31	1.14	2.61	1.38
Asn (N)	0.76	0.48	1.34	0.80	0.80	0.75	1.79	0.99	1.37
Pro (P)	0.34	0.31	1.32	0.90	0.19	0.06	0.95	1.80	1.51
Ser (S)	0.57	0.96	1.22	0.67	0.44	0.73	1.47	0.76	1.49
Asp (D)	0.99	0.39	1.24	1.35	1.03	0.67	1.98	0.71	1.28

Designing helical peptides using non-proteinogenic amino acids, especially β-amino acids, in the backbone is an excellent strategy.[16] Metal-assisted helix formation has also been explored (Figure 1.6). Sasaki and Hopkins have incorporated non-natural amino acids containing metal binding sites at different positions (i and i+3 or i and i+4

etc), which upon complexation with metal ions leads to helical structures.[17] Ghadiri and co-workers also used a similar strategy for the preparation of stable helical conformations, in which metal binding to proteinogenic amino acids was exploited.[18]

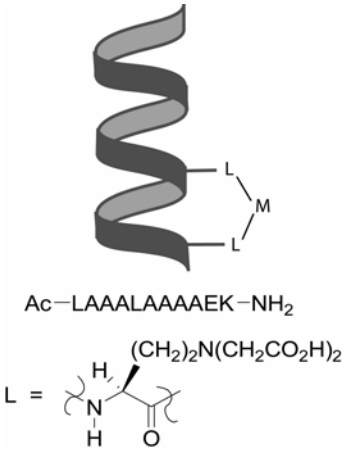

Figure 1.6. Metal-assisted stabilization of helical peptides. [17]

In addition to designing single helices, attempts have been made to design the multi-helical bundles with the ultimate goal of *de novo* protein design. Using a metal mediated strategy, the single helical backbones can be designed to contain a metal binding center in a suitable position. Ghadiri and Sasaki used bipyridine and pyridine to ensure helix-bundle formation (Figure 1.7). Additional metal binding sites enhance the stability of the helix assembly.[19] Another approach for the formation of helical bundles has been reported, where instead of conjugating the peptide with a ligand, histidine has been placed in suitable position in the peptide sequence to complex to a metal center.[20]

Whereas the design of helical peptides and their assemblies has been extensively explored, the design of β-sheets is more difficult due to their folding complexity and high tendency to self-assemble.

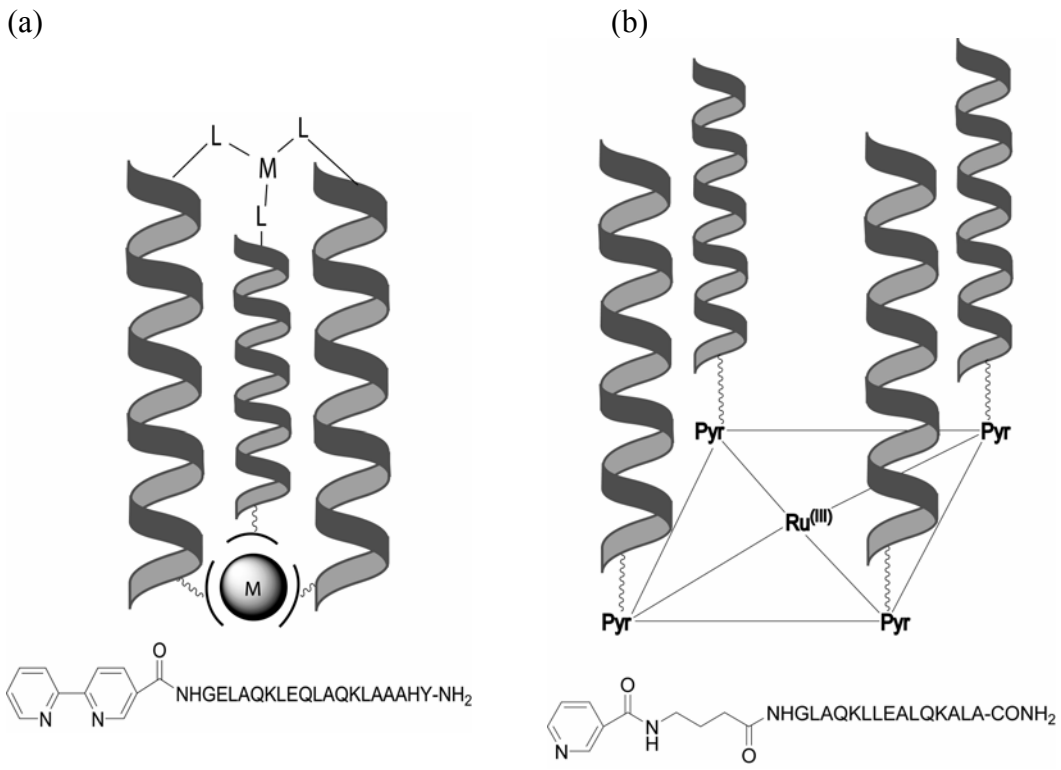

Figure 1.7. (a) Complexation of bipyridine conjugated helical peptides containing amino acids with metal binding sites at the opposite termini for the formation of very stable triple helical bundle[19] (b) Complexation of four pyridine conjugated helical peptides to form a four-helix bundle.[20]

Although several attempts were made in designing *β*-sheet peptides purely from amino acid sequences having high β-sheet propensities (Table 1.2), this strategy has only been met with limited success.[15, 21] On the other hand, the use of molecular scaffolds, ranging from simple glucose to more complex polycyclic steroids, has been successfully explored for the design and stablizing the *β*-sheet-like structures.[22] To achieve *β*-sheet conformation, Ranganathan and co-workers used norbornene as a turn inducing motif for the attached peptide strands. Using *endo*-(2*S*,3*R*)-2-amino-3-carboxynorbornene and *endo*-(2*S*,3*R*)-2,3-dicarboxynorbornene, they could obtain antiparallel (**1**) and parallel (**2**) *β*-sheet mimics respectively (Figure 1.8).[23]

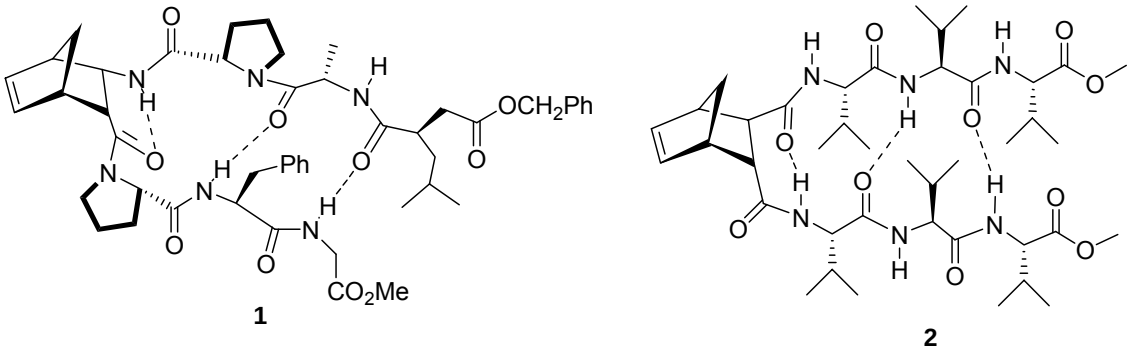

Figure 1.8. Use of norbornene as a molecular scaffold for the design of *β*-sheet-like peptides leads to the formation of offset *β*-sheet-like structure in **1** and parallel *β*-sheet-like H-bonding in **2**.[23]

Ethylenediamine derived oligourea scaffolds have been explored by Nowick and co-workers for the preparation of both parallel (**3**) and antiparallel (**4**) *β*-sheet mimics (Figure 1.9). Peptides conjugates were prepared by treating the substituted diamine with peptide isocyanate.

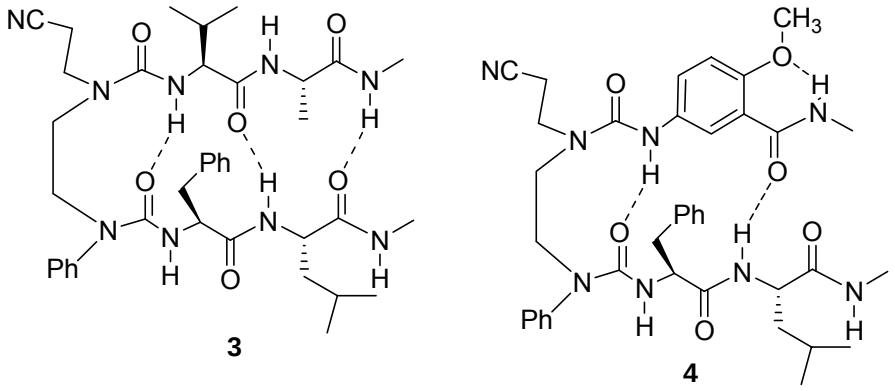

Figure 1.9. Use of ethylenediamine derivative as a scaffold for the formation of parallel *β*-sheet like H-bonds in compound **3**. Using an additional scaffold (phenyl group) in the backbone increases the stability of the *β*-sheet characteristics of compound **4**.[24]

An additional template phenyl group (see Figure 1.9) in the backbone in **4** has been found to stabilize the structure maintaining the *β*-sheet conformation. By using this

flexible ethylene-derived template, they were even able to prepare multistranded β-sheet peptides.[24] Epindolidione, a highly rigid aromatic system containing suitably positioned H-bonding donor and acceptor groups, has been explored by Bowen and co-workers.

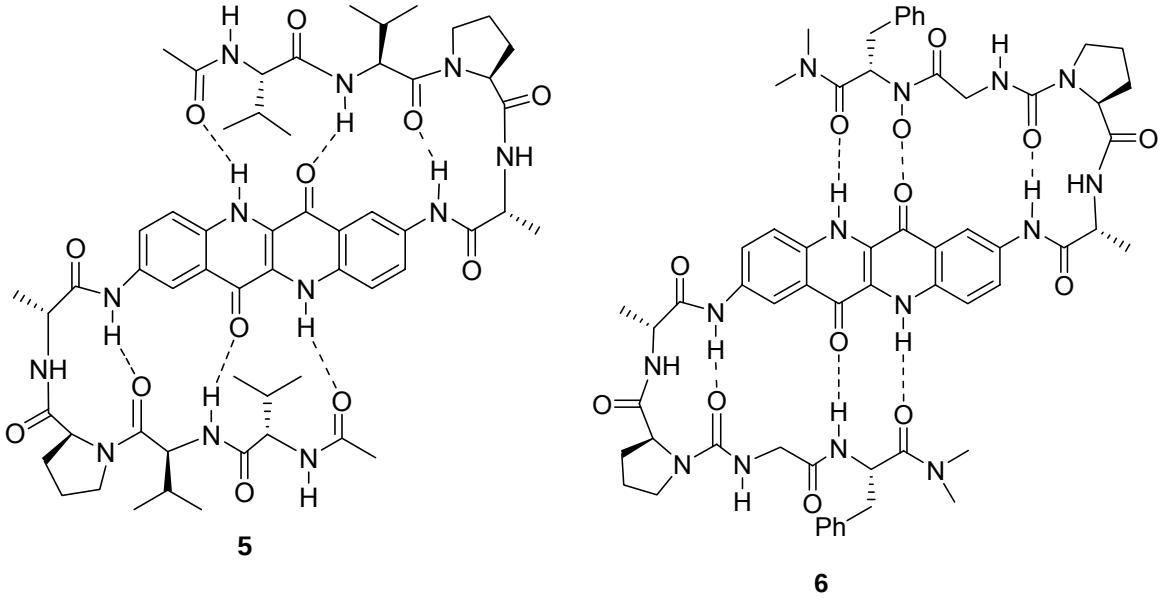

5 **6**

Figure 1.10. Upon attachment of peptide strands to the epindolidione amino groups affords a parallel β-sheet mimic **5**. Pro-D-Ala sequences are incorporated proximal to the epindolidione skeleton in order to enforce a reverse turn conformation in the attached peptide which is critical for β-sheet formation. The incorporation of two urea moieties into the peptide portion of the β-sheet mimetic affords an antiparallel β-sheet mimic **6**.[25]

To turn the peptides for the formation of H-bonds with the complementary sites on the template, a motif "L-Pro-D-Ala" was incorporated. For the formation of parallel β-sheet **5**, the peptide was conjugated to the template through amide bonds, whereas for the antiparallel β-sheet **6**, the conjugation was made through a urea linkage (Figure 1.10).[25]

Other rigid aromatic scaffolds such as 2,8-dimethyl-4-(carboxymethyl)-6-(aminomethy1)phenoxa-thiin-S-dioxide (**7**),[26] 2,8-dibenzofurandiylbis(3-propanoic

acid) (**8**)[27] and 4-(2-aminoethyl)-6-dibenzofuran propionic acid (**9**)[28] have also been utilized in the designing of *β*-sheets (Figure 1.11).

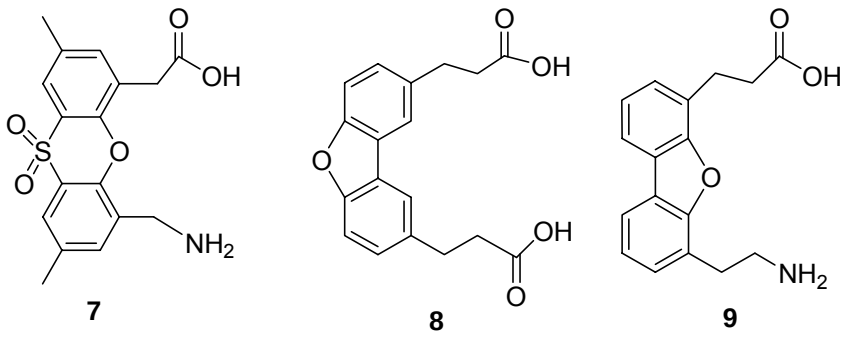

Figure 1.11. Rigid aromatic systems used to design *β*-sheet mimics; 2,8-dimethyl-4-(carboxymethyl)-6-(aminomethy1)phenoxa-thiin-S-dioxide (**7**),[26] 2,8-dibenzofuran-diylbis(3-propanoic acid) (**8**),[27] and 4-(2-aminoethyl)-6-dibenzofuran propionic acid (**9**).[28]

Metal coordination can facilitate *β*-sheet conformation, as shown by Kelly and co-workers, who have utilized disubstituted bipyridine peptide conjugates. In the absence of metal ions, the peptide strands are found to a have random coil conformation. However, upon the addition of Cu(II), the peptide conjugate adopts a *β*-sheet conformation, as shown in Figure 1.12.[29]

An alternative strategy was explored by Mutter and co-workers using a peptide template onto which other peptides were grafted, as illustrated in Figure 1.13. The peptide sequence Ac-Lys-Lys-Lys-Lys-Pro-Gly-Lys-Lys-Lys-Lys acts as a template, which contains the *β*-turning motif Pro-Gly and four Lys residues at each side of the turn. The sequence adopts a *β*-hairpin conformation, in which the side chains of Lys 1, 3, 8, and 10 are placed on the same side of the *β*-sheet.

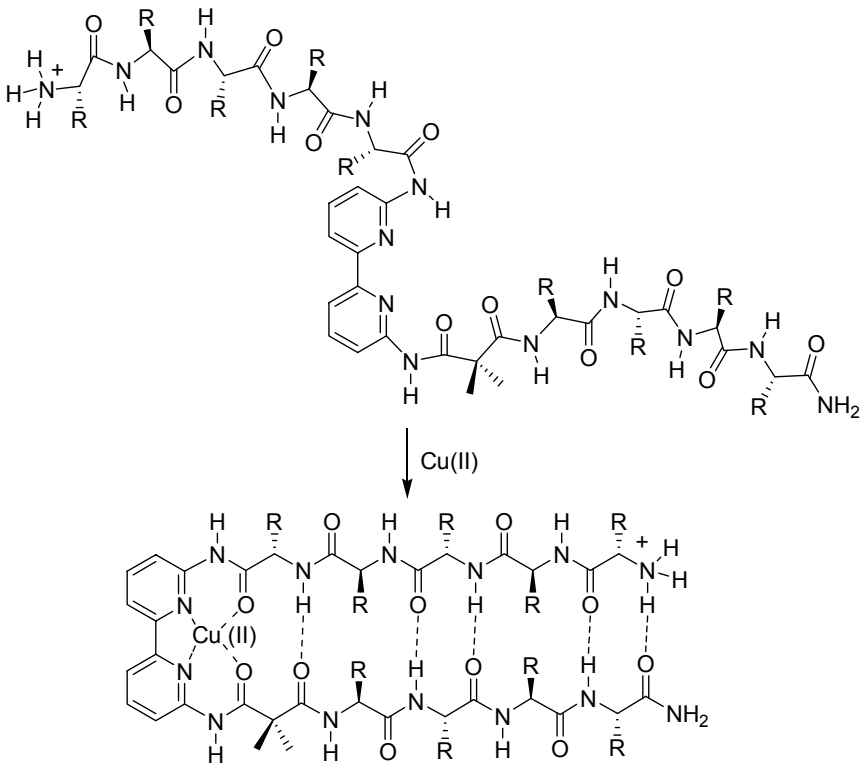

Figure 1.12. *β*-Sheet stabilization by complexation of bipyridine peptide conjugates with Cu(II).[29] R represents different side groups of the amino acids.

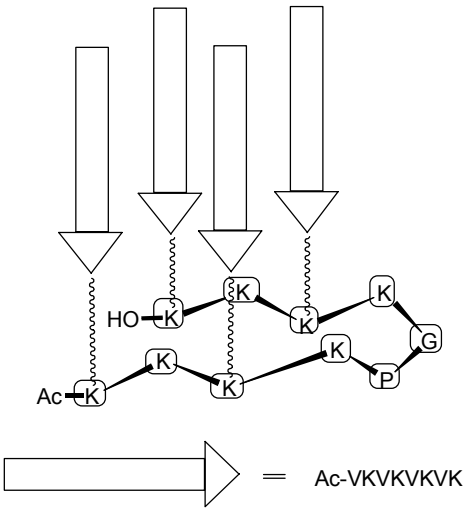

Figure 1.13. Schematic representation of a templated assembly of *β*-strands. The folding of a parallel *β*-standwich is directed via the attachment of four peptide sequences to an acyclic peptide-based template. The peptides are covalently attached at their carboxy termini, via an amide linkage to the ε-nitrogens of template lysine side chains.[30] Ac = Acetyl, V = Valine and K = Lysine.

Parallel β-strand sequences Ac-Val-Lys-Val-Lys-Val-Lys-Val-Lys were attached to the ε-amino groups of Lysine residues at 1,3,8, and 10 by solid-phase peptide synthesis for the preparation of the putative β-strand bundle. Mutter and co-workers also used an analogous template Ac-Lys-Lys-Lys-Lys-Pro-Gly-Lys-Lys-Lys-Lys-ε-6-aminohexanoic acid as a scaffold to prepare a β-barrel structure. β-strand sequences Ac-Val-Lys-Val-Lys-Val-Lys-Val-Lys were attached to the ε-amino groups of all Lys residues in the sequence, affording a putative 8-stranded β-barrel.[30]

Cyclization of peptides is another major strategy used for the formation and stabilization of β-sheet conformation. Moreover, cyclopeptides are conformationally restrained and chemically more stable, which have made them a more attractive alternative to linear peptidomimetics in designing simple β-sheet models for studying biological interactions and ion/molecular recognition.[31] Different approaches have been used for the preparation of cyclopeptides, which maintain β-sheet conformation in specific sites in the peptide backbone. Cyclization through side chains reactive sites has been widely used to obtain the desired cyclopeptide.[32] For example, formation of a disulfide bond by oxidative dimerization of two Cys thiols, as in compound **10** (Figure 1.14), is facile and has been widely used.[33] Another important approach of cyclization through side group is the formation of an ether linkage utilizing the OH groups of Tyr as shown for compound **11**.[34]

The conformational flexibility of a cyclopeptide has been further restricted by incorporating semi-rigid aromatic units into the cyclic backbone.[35] Feigel and co-workers have reported the formation of β-sheet mimics prepared from disubstituted biphenyls. The acyclic analogue is present in various stereoisomeric forms and the peptide strands do not adopt any ordered conformation.[36] However, upon cyclization,

the compounds **12** and **13** are found to form antiparallel β-sheet like structures, as depicted in Figure 1.15.

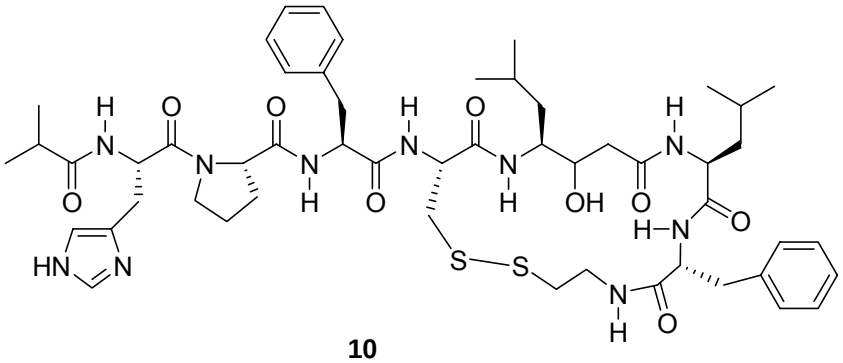

10

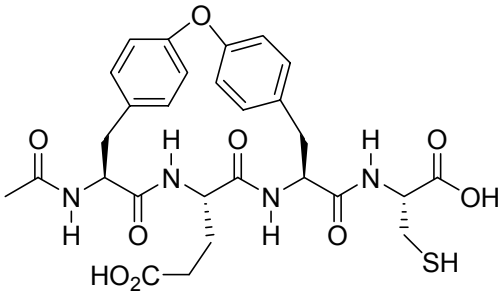

11

Figure 1.14. Cyclization, using the side groups of amino acids of peptides to achieve β-strand conformation through the formation of disulfide bond (**10**)[33] and through the formation of an ether linkage (**11**).[34]

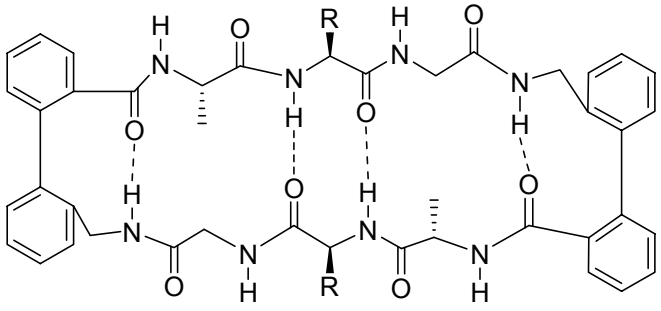

12; R = CH_2Ph
13; R = *i*-Pr

Figure 1.15. Formation of a stable antiparallel β-sheet-like conformation upon cyclization of biphenyl conjugates.[36]

A sequence of alternating D- and L-amino acids is found to adopt a *β*-strand conformation. Two such complementary strands arrange helically to form double stranded peptide helices.[37a] Ghadiri and co-workers used similar alternating sequences of D- and L-amino acids, which upon cyclization, adopt intermolecular *β*-sheet-like arrangement.

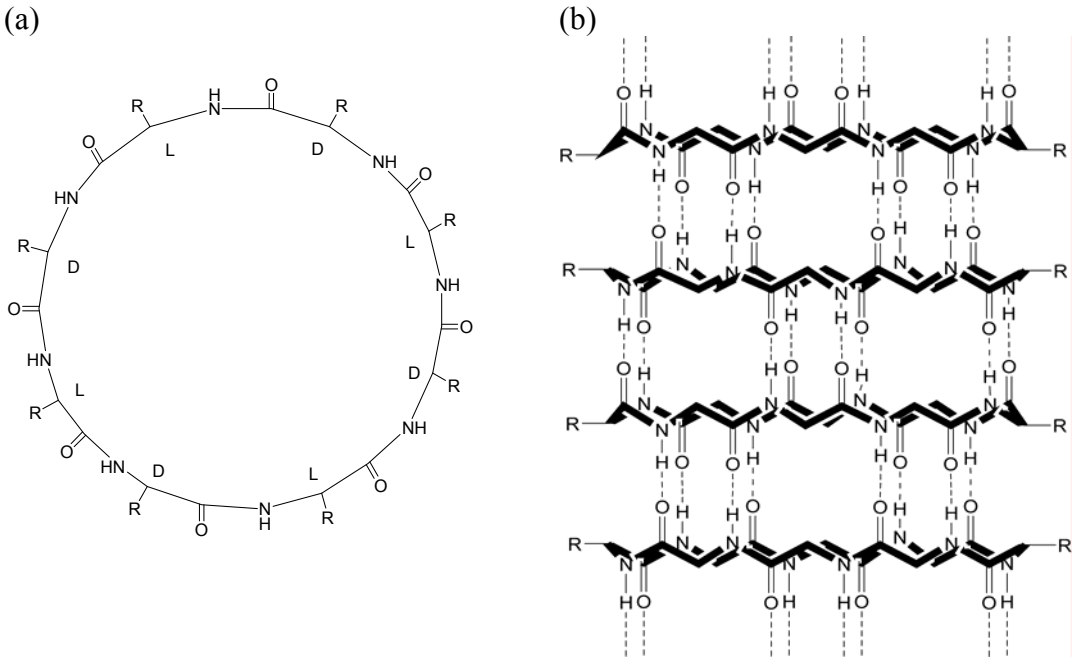

Figure 1.16. (a) Cyclopeptide from alternating D- and L-amino acids sequence, adopting circular conformation and (b) The axial stacking through H-bond to form tubular architecture.[37b]

Due to the steric interaction among the side groups of the adjacent amino acids in the backbone, the peptide strand adopts a circular geometry. The amide CO and NH groups of the molecule are projected perpendicular to the in circular plane and are able to stack over each other through *β*-sheet like H-bonding, which results in a cylindrical assembly (Figure 1.16).[37b]

1.4. Ferrocene Peptides

In the previous section, it was shown that various molecular scaffolds are able to form and stabilize specific secondary structures in peptides. Ferrocene (Fc) (**14**) has also been used for the design of well-defined peptide motifs. A brief overview of this development is described in this section.

Fc having a Fe(II) centre sandwiched between two cyclopentadienyl (Cp) rings, was first discovered by Kealy and co-workers in 1951.[38] Recently, this organometallic compound has been introduced into a peptide environment by peptide conjugation strategies.

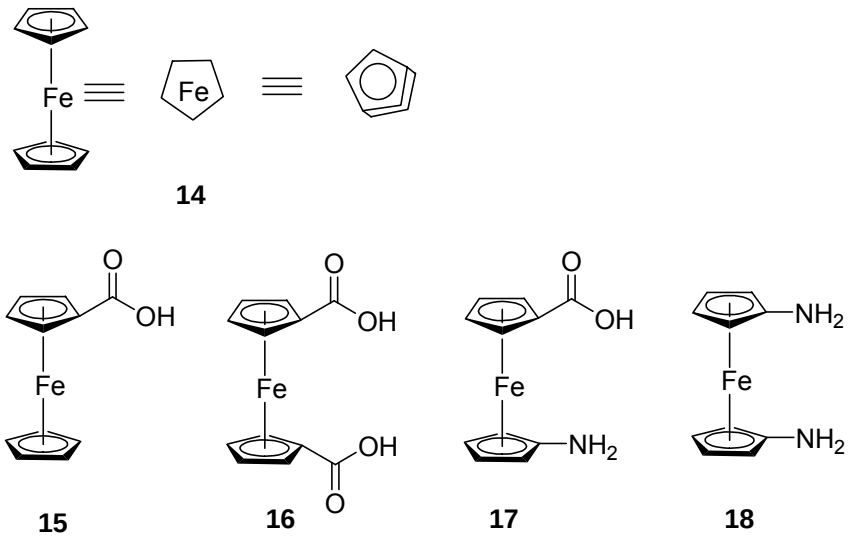

Figure 1.17. Three different sketches used to represent the ferrocene entity (**14**) and different ferrocene derivatives, **15**, **16**, **17** and **18**, used to conjugate with amino acids or peptides through amide bonds.

A series of Fc derivatives, such as ferrocene-carboxylic acid, FcCOOH (**15**), 1,1'-ferrocenedicarboxylic acid, $Fc[COOH]_2$ (**16**), 1-amino-1'-ferrocene carboxylic acid, $Fc[NH_2][COOH]$ (**17**) and 1,1'-diaminoferrocene, $Fc[NH_2]_2$ (**18**), as shown in Figure 1.17, were coupled with amino acids or peptides. It has been found that Fc is capable of

stabilizing specific intra- and intermolecular arrangements of the attached peptides through the formation of intra- and intermolecular H-bonds. This area of research has been extensively reviewed by Nolte et.al., Kraatz, and Hirao et al,[9] and only the highlights will be provided here.

When amino acids and peptides are attached to **15**, they can adopt *β*-strand conformations, which then undergo intermolecular H-bonding and as a result, assemble into *β*-sheet like architectures (Figure 1.18).[9]

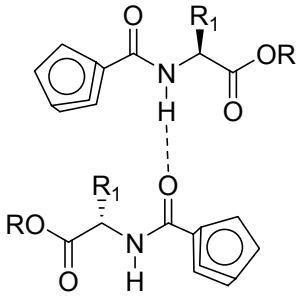

19; R = Bz, R_1 = H

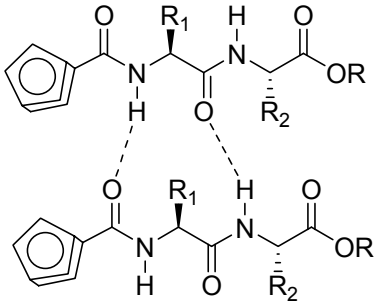

20; R = Me, R_1 = CH_3, R_2 = CH_2Ph
21; R = Et, R_1 = *i*-Bu, R_2 = CH_2Ph

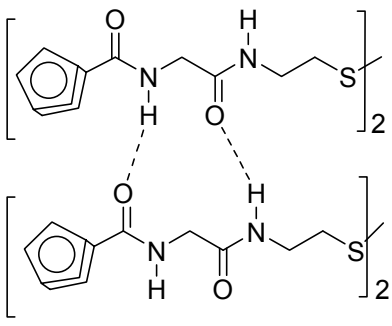

22

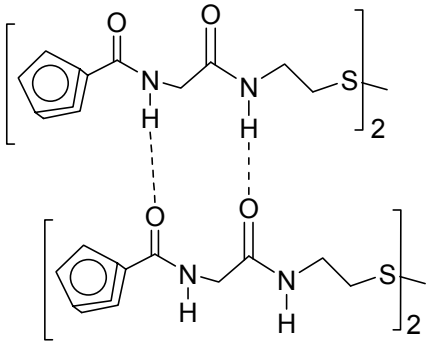

22

Figure 1.18. Intermolecular H-bond formation of various peptide conjugates of ferrocene monocarboxylic acid. Conjugate of single amino acid showing the formation of head-to-tail H-bonding in compound **19**,[39] conjugate of Fc-dipeptide showing the formation of parallel *β*-sheet like H-bonding in compounds **20** and **21**,[40] Fc-conjugate of cysteamine derived amino acid showing the parallel beta-sheet like H-bonding and Fc-conjugate of cysteamine derived amino acid showing the formation of offset H-bonding in compound **22**.[43]

Single amino acid conjugates of Fc of the general formula Fc[CO-AA-COOR] show the formation of intermolecular H-bonding between the ferrocene-carbonyl (FcC=O) and the amide NH (**19** in Figure 1.18) of adjacent molecules, resulting in the formation of one dimensional head-to-tail chain in the molecular packing.[40] In Fc-dipeptide conjugates of formula Fc[CO-AA-AA-COOR], two independent molecules are held together by H-bonding, forming a 12-membered ring similar to parallel β-sheets. Thus, they arrange themselves in a well-defined helical pattern at a supramolecular level.[40] For example, FcCO-Ala-Phe-OMe (**20**) is found to arrange in a left-handed four-fold helical supramolecular structure with the intermolecular H-bond distances of d(N-O) = 2.936 Å and 2.983 Å.[9, 41] A similar structure for FcCO-Leu-PheOEt (**21**) has been reported with a bond distances of d(N-O) = 2.977 Å and d(N-O) = 2.983 Å.[42]

Ferrocenoyl-diglycyl-cysteamine $[FcCO\text{-}Gly\text{-}CSA]_2$ (**22**), another Fc conjugate, is found to form a supramolecular helical assembly. In this case, two different H-bonding patterns are observed on different sides of the disulfide bonds (Figure 1.18). On one side, a parallel *β*-sheet like 12-membered ring is formed and on the other side, a pair of H-bond acceptors Os of C=O are arranged *syn* to each other, aligning the two Hs of NH donors in a *syn* position. This enables neighboring molecules with the same arrangement to form an asymmetric 12-membered H-bonded ring. These two different types of H-bonding lead to the formation of two different supramolecular helices.[43] Fc-carboxylic acid (**16**) has also been used to conjugate with the long peptides, both in solution and in solid phase method, mainly with the aim of studying the electrochemical properties of the conjugated peptides.[9b]

Peptide conjugates of disubstituted Fc derivatives have been most widely studied.[9] Fc containing two Cp rings parallel to each other at a distance of 3.3 Å and with a low rotational barrier of 0.8 kcal/mol, has been found suitable in imparting well-defined structure to the peptides attached to the two Cp rings (see Figure 1.19). The small rotational barrier enables Fc to function as a ball bearing that conveys flexibility to the substituent peptide strands, which can then adopt unstrained stable alignments in which the adequate inter-ring separation allows the formation of suitable inter-strand H-bonds. As a result, it has been possible to design Fc-peptide conjugates with diverse structures.

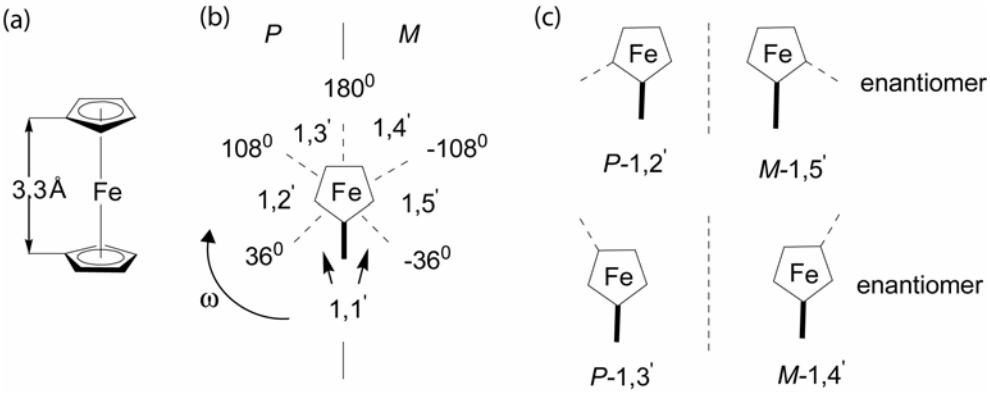

Figure 1.19. (a) Cp ring separation in Fc, (b) Possible arrangements of the two substituents at two different Cp rings and (c) Formation of optical isomers due to the variation in arrangement.[13]

For the disubstituted 1,n′-Fc systems, systematic nomenclature has been described by Kraatz and Metzler-Nolte.[13] Figure 1.19b illustrates some possible arrangements of the peptide substituents and their representation according to these rules. Depending upon the value of the rotational angle, these compounds are named as 1,n′, where n indicates the position of the substituent in the second ring with respect to the first ring in the clockwise direction. The 1,1′-isomer is defined by rotational angles

between -36^{o} and +36º , while a 1,2′-isomer would be defined as -36º < ω <108º, a 1,3′ in the range of 108º to 180º, a 1,4′ between 180 to -108º, and a 1,5′ between -108º to -36º. These different arrangements are associated with the axial chirality of the Fc unit. The clockwise alignment of the bottom ring substituent (0 < ω <180º) with respect to the top ring substituent, gives rise to a positive band in CD spectroscopy in the Fc region at 450 nm, and is termed the *P*-helical isomer. On the other hand, the alignment in the *anti*-clockwise direction (0> ω > -180) gives a negative cotton effect in the Fc region and is called the M-helical isomer (see Figure 1.20).[13] Conjugates of disubstituted Fc with chiral amino acids or peptides give rise to a series of optically isomeric compounds.

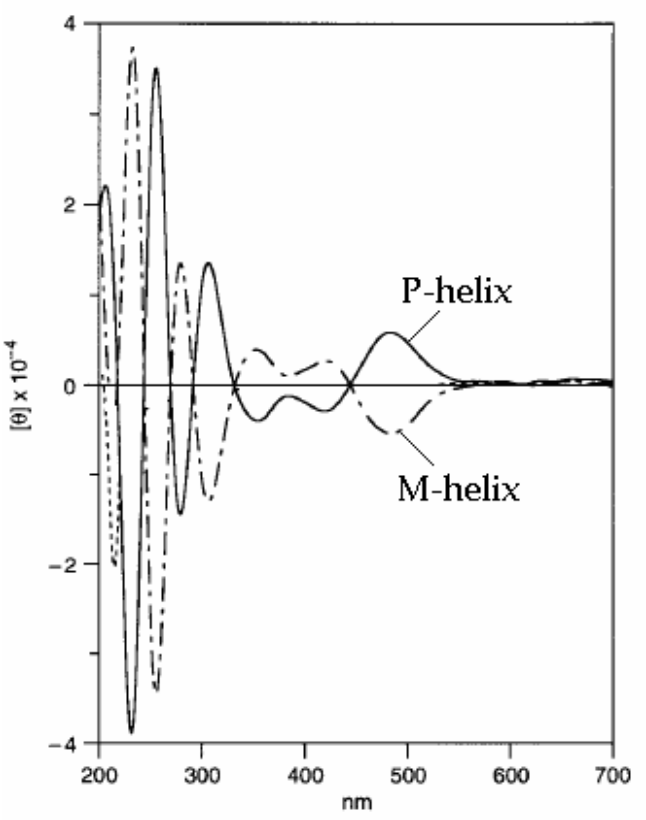

Figure 1.20. CD spectra of disubstituted Fc-peptide conjugates showing P- and M-helicity. Reprinted with permission from Ref [44]. Copyright 2001 American Chemical Society.

Generally L-amino acids are found to induce *P*-helicity while D-amino acids induce *M*-helicity.[13, 44]

The first attempt of exploiting the 1,n'-disubstituted Fc derivative for the preparation of peptide conjugates was made by Herrick and co-workers in 1996 using 1,1'-ferrocene dicarboxylic acid. The first conjugate, Fc[CO-Val-OMe]$_2$ (**23**), adopts an ordered β-sheet-like conformation in solution, as shown in Figure 1.21.[45]

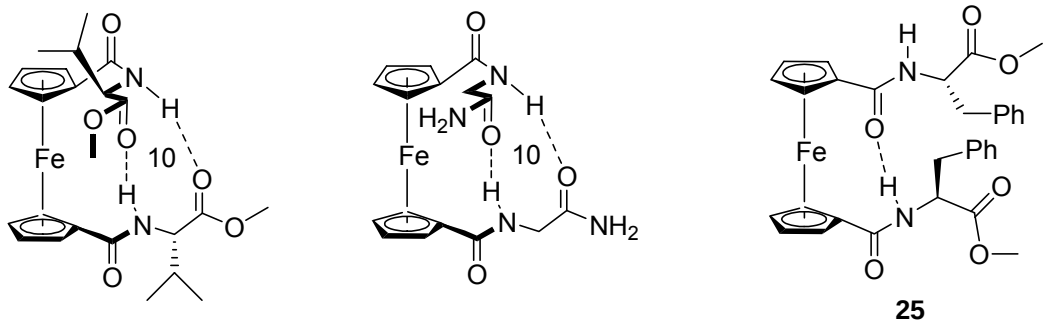

Figure 1.21. Formation of interstrand H-bonds in amino acid conjugates of 1.1'-ferrocenedicarboxylic acid.

H-Bonding, as well as the amino acid side groups, exert steric interactions and force the Fc centre into a specific helical conformation. The Gly conjugate, Fc[CO-Gly-NH$_2$]$_2$ (**24**), with the smallest side group, forms very strong H-bonds. The intramolecular H-bonding distances are d(N···O) = 2.88 Å, which has been partially attributed to the higher H-bonding ability of the carbonyl in CONH$_2$, compared to the ester carbonyl. Val having a bulkier isopropyl side group in **23**, the intramolecular H-bonding is weaker and contact distances increases to d(N···O) = 3.24 Å.[45b] For Phe, which contains a benzyl group, the structure is disrupted as observed by Metzler-Nolte and co-workers, and the

conjugate Fc[CO-Phe-OMe]$_2$ (**25**) exhibits a single cross-strand intramolecular H-bond (Figure 1.22).[41]

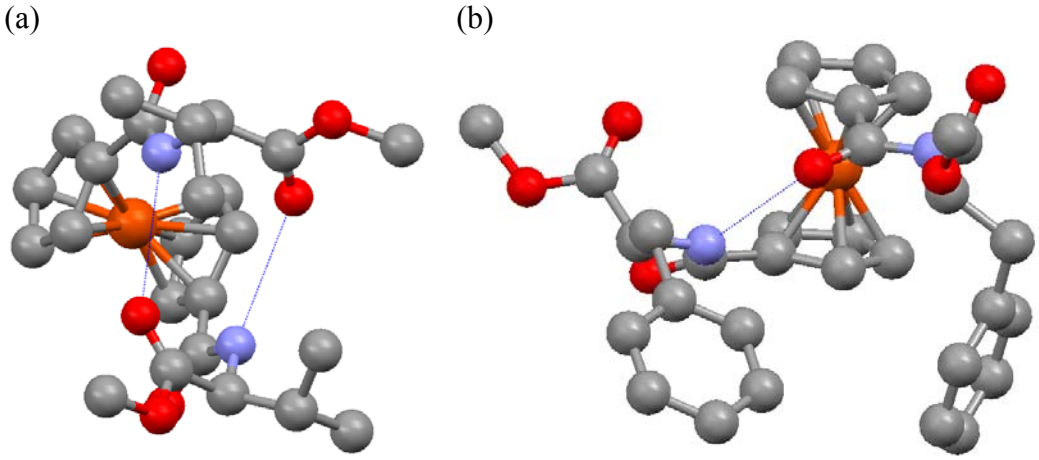

Figure 1.22. (a) Crystal structure of Fc[CO-Val-OMe]$_2$ (**23**) showing the anti-parallel *β*-sheet 10-membered H-bonded ring formation and *P*-helical arrangement, [45b] and (b) crystal structure of Fc[CO-Phe-OMe]$_2$ (**25**) showing the disruption of anti-parallel *β*-sheet-like H-bonding pattern.[41] Grey spheres represent carbon atoms, red = oxygen, blue = nitrogen, and larger red = iron atoms.

Dipeptide conjugates of 1,1'-ferrocendicarboxylic acid have been found to arrange the podand peptide strands in a helical fashion, forming similar kind intramolecular H-bonds and antiparallel β-sheet like conformation (see Figure 1.23).

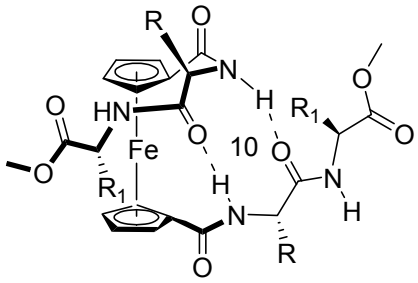

26; R = Me, R_1 = CH_2Ph

Figure 1.23. Fc-dipeptide conjugate **26**, showing the formation of an antiparallel *β*-sheet-like H-bonding pattern, indicating the formation of a 10-memered H-bonding.

In crystal structure of the conjugate Fc[CO-Ala-Phe-OMe]$_2$ (**26**), Metzler-Nolte and co-workers observed the formation of a similar 10-membered H-bonding with contact distances of 2.921 and 2.924 Å in one of the two independent molecules, and 2.901 and 2.893 Å in the second molecule.

(a)

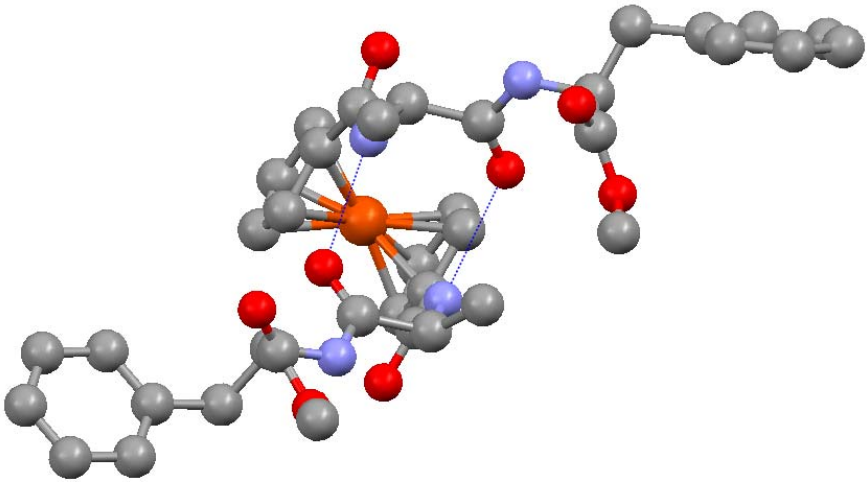

(b)

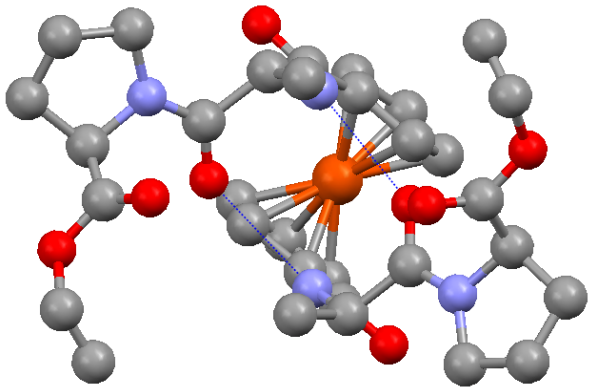

Figure 1.24. Crystal structures of (a) Fc[CO-Ala-Phe-OMe]$_2$ (**26**) showing the formation of antiparallel *β*-sheet like 10-membered hydrogen bonded ring formation aligning the peptide strand in *P*-helical conformation, [41] (b) Fc[CO-D-Ala-D-Pro-OEt]$_2$ (**28**) showing the formation of antiparallel *β*-sheet like 10-membered hydrogen bonded ring aligning the peptide strand in *M*-helical conformation.[44] Grey spheres represent carbon atoms, red = oxygen, blue = nitrogen, and larger red = iron atoms.

The torsion angles (ω) are 70º and 69º, which shows that these species are 1,2′-conformer. The crystal structure is presented in Figure 1.23a showing the intramolecular hydrogen bonding pattern and formation of a *P*-helicity.[41] With different sequences of peptides in the conjugate Fc[CO-Ala-Pro-OEt]$_2$ (**27**), Hirao and co-workers found a similar *P*-helical arrangement only with slightly different contact distances of 2.981 Å between the CO (Ala) and the NH of the other podand dipeptide chain. The conjugates of corresponding D-amino acids, Fc[CO-D-Ala-D-Pro-OEt]$_2$ (**28**) has found to arrange in a *M*-1,4'-conformtion, a mirror image of **27**.[44]

Further extention of the length of the peptide strand through heterocycles shows that the other termini of the peptide strands move farther away and form different structural motifs containing γ-turns (Figure 1.25).[46] The crystal structural study of Fc[CO-Ala-Pro-Py]$_2$ (**29**) (Figure 1.26) shows that in addition to the formation of the

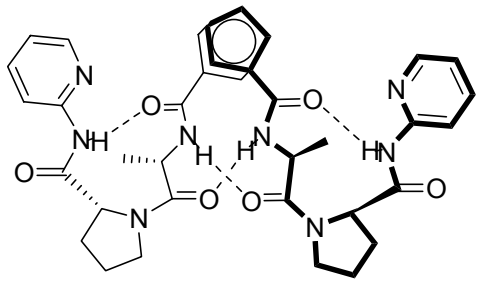

29

Figure 1.25. Extention of length provide γ-turn through the formation of intrastrand H-bond with the 1,2' arrangement in the Fc center.[46]

usual 10-membered intramolecular H-bonding with the distances of d(N···O) = 2.83 Å and 2.97 Å, it forms two extra intramolecular intrastrand H-bonds with the distances d(N···O) = 2.99 and 3.03 Å and thereby imparts a γ-turns into the podand peptide backbone. [46]

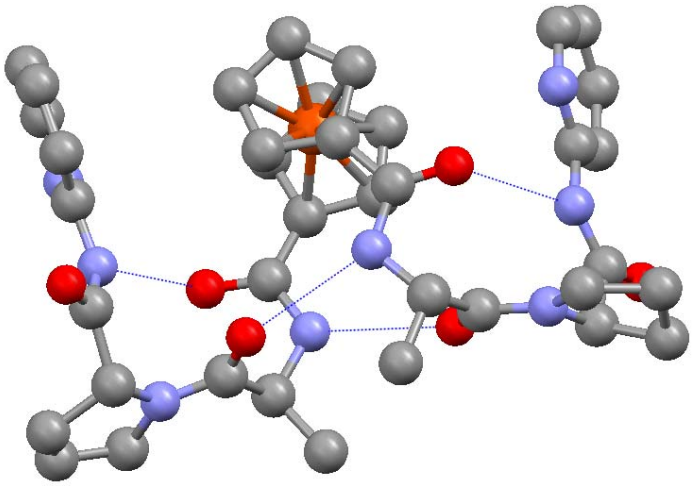

Figure 1.26. Crystal structures of Fc[CO-Ala-Pro-Py]$_2$ (**29**) showing the γ-turn through the formation of intra-strand hydrogen bonds along with keeping the antiparallel β-sheet like 10-membered H-bonded ring for the first conjugated amino acids and *P*-helical conformation intact.[46] Grey spheres represent carbon atoms, red = oxygen, blue = nitrogen, and larger red = iron atoms.

In addition to 1,1'-Fc dicarboxylic acid, other disubstituded Fc derivatives have also been used for the synthesis of peptide conjugates. In 2004, Metzler-Nolte and co-workers first reported the amino acid conjugates of 1-amino-1'-Fc carboxylic acids. [47] It was found that the conjugated amino acids are aligned in a similar helical fashion as is found for the conjugates of 1,1'-Fc dicarboxylic acid. In this case, a different H-bonding pattern, a parallel β-sheet like 12-membered H-bonded ring formation was observed. The study was extended to D-amino acids and the expected M-helical arrangement was observed.[47b] The crystal structure of Boc-Ala-Fca-Ala-Ala-OMe (**30**) shows strong intramolecular H-bonding (d(N···O) = 2.81 and 2.91 Å), displaying a 12-membered H-bonded ring and aligning the peptide strands in a *P*-helical fashion (Figure 1.27).

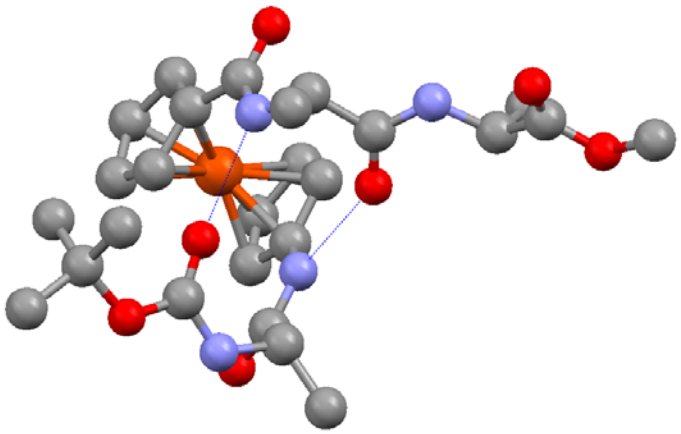

Figure 1.27. Crystal structure of Boc-Ala-Fca-Ala-Ala-OMe (**30**) showing the formation of parallel *β*-sheet like 12-membered H-bonded ring formation aligning the peptide strands in a *P*-helical conformation.[47a] Grey spheres represent carbon atoms, red = oxygen, blue = nitrogen, and larger red = iron atoms.

In the preceding sections, the characteristics of amino acids and peptides and definitions of various secondary structural elements of peptides have been described. The diverse approaches used to control the secondary structures of peptides and their assembly with the aim of achieving *de novo* protein have also been highlighted.[1a] Numerous organic and inorganic molecular templates have been used to induce specific secondary structures in the peptide conjugates.

Fc has been found to be a good template with the potential of inducing all three secondary structural motifs; a helix, a sheet (both parallel and antiparallel) and a turn, through the formation of well-defined intra- and intermolecular H-bonding. One would therefore consider this molecule as an excellent choice for the *de novo* designing of protein. In addition to controlling the secondary structure of peptides, Fc introduces redox activity to its conjugates. Presently, this characteristic is widely utilized to either investigate the electron transfer characteristics through some specific entity,[10] or study the molecular recognition property of its conjugates by electrochemical methods.[11] This

makes Fc useful also in the context of *de novo* design of redox active protein, providing the motivation to explore ferrocene peptide conjugates in detail.

1.5. Research Objectives and Approaches

The objective of my research is to explore the use of ferrocene as a molecular scaffold for controlling the β-sheet-like structure. Ferrocene has been found to be an excellent scaffold due to its multi-functional characteristics, as described in Section 1.4. When we focus our attention to the application of this multi-functional scaffold in controlling the structure of peptides, several questions arise, as illustrated in the following paragraphs. Answers to these questions provided the clue to design the above mentioned challenging and interesting peptide structural motifs.

In peptide conjugates of 1,1'-ferrocendicarboxylic acid, it was observed that when a single amino acid is linked to each of the Cp rings through an amide bond, they align themselves through the formation of antiparallel *β*-sheet-like structures, causing a large spatial separation between the carboxyl termini. This implies that the second amino acid, if linked, would not form additional interstrand H-bonding, suggesting that this approach is not useful for the formation of extended *β*-sheet. This generates my first question, "*Is it possible to bring the two termini of the amino acids together and control the conformation of the peptide so that it maintains its β-sheet characteristics*?" Macrocyclization can be an answer, which has been described in Chapter 2. There, the synthesis and structure of a series of pseudocyclopeptide of general formula Fc[CO-AA-CSA]$_2$ are described.

It was observed that upon cyclization, the amino acids retain their *β*-strand characteristics and they twist with respect to each other, aligning the H-bond donor or

acceptor sites, which do not participate in intramolecular H-bonding, to the same side. These observations raised my second question, "*Is it possible to assemble these twisted units through H-bonding*?" If so, then this approach would provide a supramolecular structure, where the *β*-sheet-like motifs will arrange in a parallel fashion providing the cylindrical hollow space inside, similar to the *β*-barrel. Through the addition of extra *β*-sheet forming amino acids, more H-bonding sites can be created in that twisted system and to achieve the desired assembly. Chapter 3 describes this strategy detailing the synthesis and structures.

In cyclic systems, it is possible to extend the *β*-sheet characteristics for the longer peptide sequences and ring strain was found negligible. This generates my third question, "*Will it be possible to achieve the similar extended β-sheet structures choosing similar amino acid sequence in acyclic conjugates*?" We have seen that the nature of the amino acids attached to Fc dictates the strength of the intramolecular H-bonds,[41,45] which are responsible for providing the 10-membered *β*-sheet-like alignment. Taking this into consideration, we were able to successfully address this question as described in Chapter 4.

Amino acid conjugates of 1,1'-diaminoferrocene are absent from the literature, largely due to a lack of convenient preparation of a suitable precursor. This poses the question as to the structural feature of amino acid conjugates of 1,1'-diaminoferrocene, "*Will they adopt a novel H-bonding motif or assemble into a certain supramolecular archetechtures*? Chapter 5 addresses this question and describing the synthesis, characterization and structures of a suitable derivative of 1,1'-diaminoferrocene and of the first amino acid conjugates of 1,1'-diaminoferrocene.

It is noted that peptide conjugates of disubstituted ferrocenes are capable of providing both the *β*-sheet characteristics and the helical alignment simultaneously, to the attached amino acids. This provides yet another question, "*Can we utilize both these characteristics of ferrocene to form larger architecture in the form of artificial β-helical peptides*?" Chapter 6 describes the utilization of 1-aminoferrocene-1'-carboxylic acid for the preparation of model parallel *β*-helical peptides. There, the synthesis and structures of a series of a series of Fca-conjugates of the type Boc-[Fca-Ala]$_n$-OMe (n = 1-4), with both L- and D-Ala, are described.

Chapter 7 provides the general discussion of my whole Ph.D. research and concludes the thesis.

1.6. References

[1] a) W. F. DeGrado, C. M. Summa, V. Pavone, F. Nastri, A. Lombardi, *Annu. Rev. Biochem.* **1999**, 68, 779-819; b) M. J. P. de Vega, M. Martin-Martinez, R. Gonzalez-Muniz, *Curr. Top. Med. Chem.* **2007**, 7, 33-62; c) D. Ghosh, V. L. Pecoraro, *Inorg. Chem.* **2004**, 43, 7902-7915.

[2] a) M. Zasloff, *Nature* **2002**, 415, 389-395; b) M. A. Shogren-Knaak, P. J. Alaimo, K. M. Shokat, *Annu. Rev. Cell Dev. Biol.* **2001**, 17, 405-433; c) S. Fernandez-Lopez, H. S. Kim, E. C. Choi, M. Delgado, J. R. Granja, A. Khasanov, K. Kraehenbuehl, G. Long, D. A. Weinberger, K. M. Wilcoxen, M. R. Ghadiri, *Nature* **2001**, 412, 452-455.

[3] a) S. G. Zhang, *Nature Biotech.* **2003**, 21, 1171-1178; b) S. Hecht, *Mater. Today* **2005**, 48-55.

[4] a) P. Li, P. P. Roller, J. C. Xu, *Current Org. Chem.* **2002**, 6, 411-440; b) U. Sprengard, M. Schudok, W. Schmidt, G. Kretzschmar, H. Kunz, *Angew. Chem. Int. Ed.* **1996**, 35, 321-324; c) T. J. Marrone, K. M. Merz, *J. Am. Chem. Soc.* **1992**, 114, 7542-7549; d) D. Ranganathan, *Acc. Chem. Res.* **2001**, 34, 919-930; e) M. R. Ghadiri, J. R. Granja, R. A. Milligan, D. E. McRee, N. Khazanovich, *Nature* **1994**, 372, 709-709; f) M. R. Ghadiri, J. R Granja, R. A. Milligan, D. E. McRee, N. Khazanovich, *Nature* **1993**, 366, 324-327.

[5] G. Lelais, D. Seebach, *Biopolymers* **2004**, 76, 206-243.

[6] a) R. Kishore, A. Kumar, P. Balaram, *J. Am. Chem. Soc.* **1985**, 107, 8019-8023; b) I. L. Karle, R. Kishore, S. Raghothama, P. Balaram, *J. Am. Chem. Soc.* **1988**, 110, 1958-1963; c) C. Garciaecheverria, F. Albericio, E. Giralt, M. Pons, *J. Am. Chem. Soc.* **1993**, 115, 11663-11670.

[7] a) J. D. Hartgerink, J. R.Granja, R. A. Milligan, M. R. Ghadiri, *J. Am. Chem. Soc.* **1996**, 118, 43-50; b) M. D. Struthers, R. P. Cheng, B. Imperiali, *Science* **1996**, 271, 342-345.

[8] a) J. S. Nowick, D. L. Holmes, G. Mackin, G. Noronha, A. J. Shaka, E. M. Smith, *J. Am. Chem. Soc.* **1996**, 118, 2764; b) T. Moriuchi, T. Hirao, *Chem. Soc. Rev.* **2004**, 33, 294-301; c) J. S. Nowick, E. M. Smith, G. Noronha, *J. Org. Chem.* **1995**, 60, 7386-7387.

[9] a) H. B. Kraatz, *J. Inorg. Organomet. Poly. Mater.* **2005**, 15, 83-106; b) D. R. van Staveren, N. Metzler-Nolte, *Chem. Rev.* **2004**, 104, 5931; c) T. Moriuchi, T. Hirao, *Top. Organomet. Chem*. **2006**, 17, 143-162.

[10] a) Y. T. Long, E. Abu-Rhayem, H. B. Kraatz, *Chem. Eur. J.* **2005**, 11, 5186-5194; b) H. B. Kraatz, I. Bediako-Amoa, S. H. Gyepi-Garbrah, T. C. Sutherland, *J. Phys. Chem. B* **2004**, 108, 20164-20172.

[11] a) F. E. Appoh, T. C. Sutherland, H. B. Kraatz, *J. Organomet. Chem.* **2005**, 690, 1209-1217; b) J. F. Gallagher, P. T. M. Kenny, M. J. Sheehy, *Inorg. Chem. Commun.* **1999**, 2, 327-330; c) A. S. Georgopoulou, D. M. P. Mingos, A. J. P. White, D. J. Williams, B. R. Horrocks, A. Houlton, *J. Chem. Soc. Dalton Trans.* **2000**, 2969-2974; d) K. Plumb, H. B. Kraatz, *Bioconjugate Chem.* **2003,** 14, 601-606.

[12] N. Sewald, H. D. Jakubke, Peptides: Chemistry and Biology, WILEY-VCH Verlag GmbH Weinheim, **2002.**

[13] S. I. Kirin, H. B. Kraatz, N. Metzler-Nolte, *Chem. Soc. Rev.* **2006**, 35, 348-354.

[14] R. W. Williams, A. Chang, D. Jureti, S. Loughran, *Biochim. Biophys. Acta*, **1987**, 916, 200-204.

[15] J. J. Osterhout, *Protein Peptide Lett.* **2005**, 12, 159-164.

[16] a) J. Venkatraman, S. C. Shankaramma, P. Balaram, *Chem. Rev.* **2001**, 101, 3131-3152; b) R. P. Cheng, S. H. Gellman, W. F. DeGrado, *Chem. Rev.* **2001**, 101, 3219-3232; c) D. J. Hill, M. J. Mio, R. B. Prince, T. S. Hughes, J. S. Moore, *Chem. Rev.* **2001**, 101, 3893-4011.

[17] a) F. Q. Ruan, Y. Q. Chen, P. B. Hopkins, *J. Am. Chem. Soc.* **1990**, 112, 9403-9404; b) F. Q. Ruan, Y. Q. Chen, K. Itoh, T. Sasaki, P. B. Hopkins, *J. Org. Chem.* **1991**, 56, 4347-4354.

[18] M. R. Ghadiri, C. Choi, *J. Am. Chem. Soc.* **1990**, 112, 1630-1632.

[19] a) M. R. Ghadiri, C. Soares, C. Choi, *J. Am. Chem. Soc*. **1992**, 114, 825-831; b) M. Lieberman, T. Sasaki, *J. Am. Chem. Soc.* **1991**, 113, 1470; c) M. R. Ghadiri, A. K. Fernholz, *J. Am. Chem. Soc.* **1990**, 112, 9633-9635.

[20] M. R. Ghadiri, C. Soares, C. Choi, *J. Am. Chem. Soc.* **1992**, 114, 4000-4002.

[21] C. K. Smith, L. Regan, *Acc. Chem. Res.* **1997**, 30, 153-161.

[22] D. S. Lawrence, T. Jiang, M. Levett, *Chem. Rev.* **1995**, 95, 2229-2260.

[23] D. Ranganathan, V. Haridas, S. Kurur, A. Thomas, K. P. Madhusudanan, R. Nagaraj, A. C. Kunwar, A. V. S. Sarma, I. L. Karle, *J. Am. Chem. Soc.* **1998**, 120, 8448-8460.

[24] *a*) J. S. Nowick, E. M. Smith and G. Noronha, *J. Org. Chem.* **1995**, 60, 7386-7387; *b*) J. S. Nowick, D. L. Holmes, G. Mackin, G. Noronha, A. J. Shaka, E. M. Smith, *J. Am. Chem. Soc.* **1996**, 118, 2764-2765; *c*) J. S. Nowick, J. H. Tsai, Q.-C. D. Bui and S. Maitra, *J. Am. Chem. Soc.* **1999**, 121, 8409-8410.

[25] a) D. S. Kemp, B. R. Bowen, *Tetrahedron Lett.*, **1988**, 29, 5077-5080; b) D. S. Kemp, B. R. Bowen, *Tetrahedron Lett.*, **1988**, 29, 5081-5082.
[26] M. Feigel, *J. Am. Chem. Soc.* **1986**, 108, 181-182.
[27] S. R. LaBrenz, J. W. Kelly, *J. Am. Chem.Soc*. **1995**,117, 1655-1656.
[28] a) H. Diaz, J. R. Espina, J. W. Kelly, *J. Am. Chem. Soc.* **1992**,114, 8316-8318; b) H. Diaz, J. W. Kelly, *Tetrahedron Lett.* **1991**, 32, 5725-5728.
[29] J. P. Schneider, J. W. Kelly, *J. Am. Chem. Soc.*, **1995**, 117, 2533-2546.
[30] a) M. Mutter, E. Altmann, K. H. Altmann, R. Hersperger, P. Koziej, K. Nebel, G. G. Tuchscherer, S. Vuilleumier, *Helv. Chim. Acta,* **1988**, 71, 835-847; b) M. Mutter, *Trends Biochem. Sci.* **1988**, 13, 260-265; c) R. Floegel, M. Mutter, *Biopolymers* **1992**, 32, 1283-1310; d) M. Mutter, S. Vuilleumier, *Angew. Chem. Int. Ed.* **1989**, 28, 535-554.
[31] a) T. J. Marrone, K. M. Merz, *J. Am. Chem. Soc.* **1992**, 114, 7542-7549; b) U. Sprengard, M. Schudok, W. Schmidt, G. Kretzschmar, H. Kunz, *Angew. Chem. Int. Ed.* **1996**, 35, 321-324; c) D. Ranganathan, *Acc. Chem. Res.* **2001**, 34, 919-930; d) M. R. Ghadiri, J. R. Granja, R. A. Milligan, D. E. McRee, N. Khazanovich, *Nature* **1994**, 372, 709-709.
[32] a) M. P. Glenn, D. P. Fairlie, *Mini. Rev. Med. Chem.* **2002,** 2, 433-445; b) J. D. A. Tyndall, D. P. Fairlie, *Current Med. Chem.* **2001**, 8, 893-907.
[33] K. Suguna, E. A. Padlan, R. Bott, J. Boger, K. D. Parris, D. R. Davies, *Proteins* **1992**, 13, 195-205.
[34] A. Marchetti, J. Ontoria, V. G. Matassa, *Synlett,* **1999**, 1000-1002.
[35] a) D. Ranganathan, V. Haridas, S. Kurur, R. Nagaraj, E. Bikshapathy, A. C. Kunwar, A. V. S. Sarma, M. Vairamani, *J. Org. Chem.* **2000**, 65, 365-374; b) R. Haubner, W. Schmitt, G. Holzemann, S. L. Goodman, A. Jonczyk, H. Kessler, *J. Am. Chem. Soc.***1996**, 118, 7881-7891.
[36] V. Brandmeier, W. H. B. Sauer, M. Feigel, *Helv. Chim. Acta* **1994**, 77, 70-85.
[37] a) G. N. Ramachandran, R. Chandrasekaran, *Ind. J. Biochem. Biophys*, **1972**, 9, 1-11; b) D. T. Bong, T. D. Clark, J. R. Granja, M. R. Ghadiri, *Angew. Chem. Int. Ed.* **2001**, 40, 988-1011.
[38] T. J. Kealy, P. L. Pauson, *Nature* **1951**, 168, 1039-1040.
[39] J. F. Gallagher, P. T. M. Kenny, M. J. Sheehy, *Inorg. Chem. Commun.* **1999**, 2, 200-202.
[40] L. Lin, A. Berces, H. B. Kraatz, *J. Organomet. Chem.* **1998**, 556, 11-20.
[41] a) D. R. van Staveren, T. Weyhermuller, N. Metzler-Nolte, *Dalton Trans.* **2003**, 210-220.
[42] P. Saweczko, G. D. Enright, H. B. Kraatz, *Inorg. Chem.* **2001**, 40, 4409-4419.
[43] I. Bediako-Amoa, R. Silerova, H. B. Kraatz, *Chem. Commun.* **2002**, 2430-2431.
[44] T. Moriuchi, A. Nomoto, K. Yoshida, A. Ogawa, T. Hirao, *J. Am. Chem. Soc.* **2001**, 123, 68-75.
[45] R. S. Herrick, R. M. Jarret, T. P. Curran, D. R. Dragoli, M. B. Flaherty, S. E. Lindyberg, R. A. Slate, L. C. Thornton, *Tetrahedron Lett.* **1996**, 37, 5289-5292; b) M. Oberhoff, L. Duda, J. Karl, R. Mohr, G. Erker, R. Fröhlich andM. Grehl, *Organometallics*, **1996**, 15, 4005-4011; c) A. S. Georgopoulou, D. M. P. Mingos, A. J. P. White, D. J. Williams, B. R. Horrocks and A. Houlton, *J. Chem. Soc. Dalton Trans.* 2000, 2969-2974.

[46] a) T. Moriuchi, T. Nagai, T. Hirao, *Org. Lett.* **2005**, 7, 5265-5268; b) T. Moriuchi, T. Nagai, T. Hirao, *Org. Lett.* **2006**, 8, 31-34.

[47] a) L. Barisic, M. Dropucic, V. Rapic, H. Pritzkow, S. I. Kirin, N. Metzler-Nolte, *Chem. Commun.* **2004**, 2004-2005.
b) L. Barisic, M. Cakic, K. A. Mahmoud, Y. N. Liu, H. B. Kraatz, H. Pritzkow, S. I. Kirin, N. Metzler-Nolte, V. Rapic, *Chem. Eur. J.* **2006**, 12, 4965-4980.

Chapter 2

Synthesis, Structure and Electrochemistry of Ferrocene Peptide Macrocycles

2.0. Connecting Text

Amino acid conjugates of 1,1'-Fc dicarboxylic acid have been found to arrange in a β-sheet like pattern, forming a10-membered intramolecular hydrogen bonded ring. The carboxyl ends of the amino acids in these conjugates are not in close proximity and consequently attaching the second amino acid does not provide access to an extended β-sheet. This Chapter discusses a methodology for controlling the structure. It describes the preparation of a series of cyclopeptide conjugates of ferrocene of general formulae $Fc[CO\text{-}AA\text{-}CSA]_2$ by macrocyclization. Structural studies show that those carboxyl termini are now in close proximity to each other making this a potential method for controlling the structure of peptides.

This paper was reproduced with the permission from *Dalton Trans* **2004**, 1726-1730. Copyright 2004, Royal Society of Chemistry. This paper was co-authored by G. Schatte and H.-B. Kraatz. All experimental works with the exception of crystallographic analysis were carried out by me. In addition I wrote the initial draft of the manuscript. The text below is a *verbatim* copy of the published paper.

2.1. Abstract

Redox active cyclopeptides $Fc[CO\text{-}CSA]_2$ (**5**), $Fc[CO\text{-}Gly\text{-}CSA]_2$ (**6**), $Fc[CO\text{-}Ala\text{-}CSA]_2$ (**7**), $Fc[CO\text{-}Val\text{-}CSA]_2$ (**8**) and $Fc[CO\text{-}Leu\text{-}CSA]_2$ (**9**) are formed by the reaction of ferrocenedicarboxylic acid with peptide cystamines at high dilutions. These systems exhibit H-bonding involving the amide NH in solution as shown by their temperature dependent NMR spectra. With exception of **5**, the ferrocene macrocycles

display intramolecular N···O cross-ring H-bonding in the solid state involving the amino acids proximal to the ferrocene.

2.2. Introduction

Peptides are ideally suited as building blocks in supramolecular synthesis based on their inherent ability to engage in inter-peptide interactions via hydrogen bonding. Novel peptidic materials were reported, such as cyclopeptide nanotubes[1] and hydrogels,[2] with potential applications in drug delivery and biomedical engineering. A number of 1,1'-disubstituted ferrocene peptide conjugates have been explored as templates in an effort to create highly ordered electroactive supramolecular systems. Structural investigations of a number of ferrocene-peptide conjugates display a rigid intramolecular cross-strand H-bonding interaction in which the amino group proximal to the Fc group on one strand engages in H-bonding with the CO group of the same amino acid on the opposite peptide strand.[3] The resulting structure resembles a β-sheet motif and was originally proposed by Herrick and coworkers based on NMR evidence of simple amino acid conjugates.[4] This structural type appears extremely robust and even withstands the presence of other strongly H-bonding compounds. In these conjugates, an interesting interplay between inter- and intermolecular H-bonding is observed. Intermolecular H-bonding is only observed if the second amino acid has available H-bonding donor sites, giving raise to H-bonded supramolecular assemblies. Connecting the two podand peptides on the two podand peptide chains on the two opposite Cp rings by a linker molecule will provide access to macrocyclic 1,1'-ferrocene cyclopeptides. While our study was underway, Cheng and coworkers reported the synthesis of a series of 1,1'-ferrocene cyclopeptides having a cystine linker and its interaction with alkali and earth alkaline ions.[5] Unfortunately, the report did not contain any structural data other than the results of the solution NMR showing strong intramolecular H-bonding. In this

regard, the structural analysis of 1,1'-ferrocene cyclopeptides is of great interest. Ferrocenophanes in general, cyclic compounds incorporating a 1,1'-disubstituted ferrocene, display a range of interesting properties, ranging from metallocryptants for the coordination of ions to starting materials for metallopolymers.[6] In this paper, we report the synthesis and spectroscopic properties of an alternative set of 1,1'-ferrocenoyl cyclopeptides possessing cystamine linkages. We provide an analysis of their solid state structures and give a full account of their electrochemical behavior in solution.

2.3. Experimental

2.3.1. General: All syntheses were carried out in air unless otherwise indicated. CH_2Cl_2 (BDH; ACS grade) used for synthesis was dried (CaH_2) and distilled prior to use. $CDCl_3$ (Aldrich) were dried by, and stored over molecular sieves (8-12 mesh; 4Å effective pore size; Fisher) before use. DCC, HOBt, CSA·2HCl (Aldrich), $MgSO_4$, $NaHCO_3$ (VWR), and 1,1'-$Fc(OH)_2$ (Strem) were used as received. Et_3N (BDH; ACS grade) used in the synthesis was used as received. For column chromatography, a column with a width of 2.7 cm (ID) and a length of 45 cm was packed 18-22 cm high with 230-400 mesh silica gel (VWR). For TLC, aluminum plates coated with silica gel 60 F_{254} (EM Science) were used. NMR spectra were recorded on a Bruker AMX-500 spectrometer operating at 500 MHz (^1H) and 125 MHz ($^{13}C\{^1H\}$). Peak positions in both ^1H and ^{13}C-NMR spectra are reported in ppm relative to TMS. The ^1H-NMR spectra are referenced to the residual $CHCl_3$ signal at δ 7.27. All $^{13}C\{^1H\}$-NMR spectra are referenced to the $CDCl_3$ signal at δ 77.23 ppm.

2.3.2. Synthesis and characterization of Cystamine-Amino acid conjugates: The procedures for the peptide conjugates syntheses are identical as described in section 2.3.2.1.

2.3.2.1. [Boc-Gly-CSA]$_2$ (1): Boc-Gly-OH (1.89 g; 10 mmol) was dissolved in 30 ml of DCM. Solid HOBt (1.68 g; 11 mmol) and of EDC•hydrochloride (2.10 g; 11 mmol) were added sequentially. After 20 minutes, the reaction mixture was cooled in an ice bath. To the reactions solution, a solution of CSA dihydrochloride (1.12 g; 5 mmol) in 50 ml of DCM and 2 ml Et_3N was added dropwise over 5 minutes. After completion, the reaction mixture was allowed to warm up and was kept at room temperature for 10 hours under constant stirring. The resulting solution was then washed successively with saturated $NaHCO_3$, 10% citric acid, saturated $NaHCO_3$ and then water. Then it was evaporated under reduced pressure in a rotorvap. The product was purified by column chromatography (silica gel 9:1 ethyl acetate : methanol, R_f = 0.33) to get the pure product in 63% yield (1.46 g). ^{1}H-NMR (δ, $CDCl_3$): 7.30 (s, 1H, amide NH), 5.78 (s, 1H, NH Boc), 3.78 (s, 2H, CH_2 of Gly), 3.53 (d, 2H, J = 6 Hz, CH_2 attached to NH), 2.77 (m, 2H, CH_2 attached to S), 1.40 (s, 9H, Boc CH_3).

2.3.2.2. [Boc-Ala-CSA]$_2$ (2): Silica gel column (EtOAc : MeOH = 93:7, R_f = 0.439 to get the pure product 3. Yield = 77). ^{1}H-NMR (δ, $CDCl_3$) 7.15 (s, 1H, amide NH), 5.56 (s, 1H, NH Boc), 4.35(s, 1H, α-CH of Ala), 3.56 (m, 2H, CH_2 attached to NH), 2.80 (m, 2H, CH_2 attached to S), 1.51 (s, 9H, Boc), 1.42 (d, 3H, J = 7 Hz Ala CH_3).

2.3.2.3. [Boc-Val-CSA]$_2$ (3): Silica gel column, (ethyl acetate : hexane = 50:50, R_f = 0.33) Yellowish powder. Yield = 79%. ^{1}H-NMR (δ, $CDCl_3$) 7.13 (s, 1H, amide NH), 5.80 (m, 1H, NH Boc), 4.26 (s, 1H, α-CH of Val), 3.60 (m, 2H, CH_2 attached to NH), 2.80 (m 2H CH_2 attached to S), 2.10 (m 1H sec. H of Val. side chain), 1.56 (s, 9H, Boc), 0.97 (d, 3H, J = 7 Hz, CH_3 of Val), 0.95 (br s, 3H, Val CH_3 of Val)

2.3.2.4. [Boc-Leu-CSA]$_2$ (4): Silica gel column, ethyl acetate : hexane 35:65.; R_f = 0.35 Yellowish powder. Yield = 80%. ^{1}H-NMR (δ, $CDCl_3$) 7.18 (s, 1H, amide NH), 5.61 (d, 1H, J = 7 Hz, NH), 4.21 (s 1H α H of Leu), 3.60 (m, 2H, CH_2 attached to NH), 2.84 (m, 2H, CH_2 attached to S), 1.75 (m, 1H, CH of Leu side chain),1.52 (m, 2H, CH_2 of Leu side chain), 1.42 (s, 9H, Boc CH_3), 0.96 (d, 3H, J = 7 Hz, CH_3 Leu), 0.95(d, 3H, J = 7 Hz, CH_3 Leu).

2.3.3. Synthesis and characterization of Ferrocene-cyclopeptides: The reactions to form the Fc-cyclopeptides follow a common procedure, which is described in detail for the formation of [FcCO-CSA]$_2$ (**5**).

2.3.3.1. Fc[CO-CSA]$_2$ (5): In an ice-bath, ferrocenedicarboxylic acid (0.055 g; 0.2 mmol) was dissolved in dichloromethane (10 mL), followed by the addition of HOBT (0.062 g; 0.4 mmol) and EDC (0.078 g; 0.4 mmol). After half an hour, the reaction mixture was diluted to 300 ml by dichloromethane. In another flask, cystamine dihydrochloride (0.045 g; 0.2 mmol) was dissolved in 10 ml of dichloromethane and 1 ml of triethylmine.The resulting solution was diluted to 100 ml. Then, the cystamine solution was added to the orange organometallic solution and allowed to warm up to room temperature. Stirring was continued for 72 hours at room temperature. Then the solution was washed consecutively with saturated $NaHCO_3$, 10% aqueous citric acid, saturated aqueous $NaHCO_3$ and water. The organic phase was then dried over anhydrous Na_2SO_4, and then evaporated at 25^0C under reduced pressure to get the crude product. It was then purified by flash chromatography on silica (EtOAc : MeOH = 95:5 v/v, R_f = 0.30) to get 26 mg (33 %) of the desired compound. (KBr, cm^{-1}): 1523 (C=O). UV-vis (λ in nm, [ε in $M^{-1}cm^{-1}$]): 440 [200]. HRMS (ES): Calc. for $C_{16}H_{19}N_2O_2FeS_2$ $[M+1]^+$ = 391.0237, observed 391.0156 $[M+1]^+$. ^{1}H-NMR (δ, $CDCl_3$): 6.75 (s, 1H, NH), 4.67 (s, 2H, 2,2'-CH Cp), 4.48 (br s, 2H, 3,3'-CH Cp), 3.89 (s, 2H, CH_2 attached to N), 3.12 (s,

2H, CH_2 attached to S). ^{13}C-NMR (δ, $CDCl_3$): 170.0 (-CO), 77.8 (C of Cp), 71.7 (2,2′-C of Cp), 70.9 (3,3′-C of Cp), 41.3 (CH_2 attached to NH), 38.4 (CH_2 attached to S).

2.3.3.2. Fc[CO-Gly-CSA]$_2$ (6): Silica gel column, EtOAc : MeOH 93:7, R_f = 0.35, Yellow solid. Yield = 14 % (15 mg). FT-IR (KBr, cm^{-1}): 1720, 1680 (C=O). UV-vis (λ in nm, [ε in $M^{-1}cm^{-1}$]): 440 [250]. HRMS (ES): calc. for $C_{20}H_{25}N_4O_4FeS_2$ 505.0666, observed 505.0647 $[M+1]^+$. ^{1}H-NMR (δ $CDCl_3$): 7.71 (t, 1H, NH Fc), 6.24 (s, 1H, NH CSA), 4.74 (s, 2H, 2,2'-CH Cp), 4.41 (s, 2H, 3,3'-CH Cp), 4.14 (d, 2H, J = 6 Hz, α-CH_2 of Gly), 3.49 (d, 2H, J = 5 Hz, CH_2 attached to N), 2.93 (br s, 2H, CH_2 of CSA attached to S). ^{13}C-NMR (δ, $CDCl_3$): 180.3 (-CO Gly), 178.5 (-CO Fc) 104.2 (ipso C of of Cp), 74.2 (2,2′-C of Cp), 72.3 (3,3′-C of Cp), 47.0 (α-C of Gly), 35.0 (CH_2 attached to NH), 36.3 (CH_2 attached to S).

2.3.3.3. Fc[CO-Ala-CSA]$_2$ (7): Silica gel column, EtOAc : Hexanes 97:3, R_f = 0.32, Yellow solid. Yield = 21% (22 mg). FT-IR (KBr, cm^{-1}): 1780, 1680 (two C=O s). UV-vis (λ in nm, [ε in $M^{-1}cm^{-1}$]): 440 [230]. HRMS (ES): calc. for $C_{22}H_{29}N_4O_4FeS_2$ 533.0979, observed 533.0960 $[M+1]^+$. ^{1}H-NMR (δ, $CDCl_3$): 7.20 (s, 1H, NH Fc), 6.70 (d, 1H, J = 8 Hz, NH CSA), 4.67 (m, 1H, CH of Ala), 4.54 (s, 2H, 2,2'-Cp CH), 4.47 (s, 2H, 3,3'-Cp CH), 3.65 (m, 2H, CH_2 attached to N), 2.89 (m, 2H, CH_2 attached to S), 1.56 (d, 3H, J = 4 Hz, CH_3 of Ala). ^{13}C-NMR (δ, $CDCl_3$): 173.0 (-CO CSA), 170.8 (-CO Fc) 115.7 (ipso C of of Cp), 72.0 (2-2′C of Cp), 71.3 (3-3′ C of Cp), 49.8 (α-C of Ala), 39.4 (CH_2 attached to NH), 38.8 (CH_2 attached to S), 18.0 (CH_3 in Ala).

2.3.3.4. Fc[CO-Val-CSA]$_2$ (8): Silica gel column, EtOAc 100%, R_f = 0.35, Orange solid. Yield = 21 % (25 mg). FT-IR (KBr, cm^{-1}): 1750, 1690 (C=O). UV-vis (λ in nm, [ε in $M^{-1}cm^{-1}$]): 445 [250]. HRMS (ES+): calc. for $C_{26}H_{37}N_4O_4FeS_2$ = 589.1605; observed 589.1517 $[M+1]^+$. ^{1}H-NMR (δ, $CDCl_3$): 7.32 (s, 1H, NH Fc), 6.54 (d, 1H, J =

9 Hz, NH CSA), 4.67 (s, 2H, 2,2'-CH Cp), 4.56 (s, 2H, 3,3'-CH Cp), 4.47 (m, 1H, α-CH of Val), 3.73 (m, 2H, CH_2 attached to N), 2.85 (m, 2H, CH_2 attached to S), 2.45 (m,1H, CH of Val), 1.08 (s, 3H, CH_3 of Val), 1.07 (s, 3H, Me of Val). ^{13}C-NMR (δ, $CDCl_3$): 172.1 (-CO CSA), 171.1 (-CO Fc) 105.5 (ipso C of Cp), 72.3 (2,2′-C of Cp), 71.8 (3,3′-C of Cp), 70.6 (α-C of Val), 60.5 (CH Val), 39.2 (CH_2 attached to NH), 38.0 (CH_2 attached to S), 29.1 (CH_3 Val), 19.4 (Me Val).

2.3.3.5. Fc[CO-Leu-CSA]$_2$ (9) : Silica gel column, EtOAc : Hexanes 9:1, R_f = 0.32. Yellow solid. Yield = 28% (31 mg). FT-IR (KBr, cm^{-1}): 1720, 1770 (two C=O s). UV-vis (λ in nm, [ε in $M^{-1}cm^{-1}$]): 445 [340]. HRMS (ES): calc. for $C_{28}H_{40}N_4O_4FeS_2$ 617.1918, observed 617.1890 $[M+1]^+$. ^{1}H-NMR (δ $CDCl_3$): 7.32 (s, 1H, amide NH of Leu linked to ferrocene), 6.35 (d, 1H, J = 7Hz, NH CSA), 4.60 (m, 1H, αCH of Leu), 4.47 (s, 2H, 2,2'-CH Cp), 4.37 (s, 2H, 3,3'-CH Cp), 3.65 (m, 2H, CH_2 attached to N), 2.82 (m, 2H, CH_2 attached to S), 1.80 (m, 1H, CH Leu), 1.62 (m, 2H, CH_2 Leu), 0.98 (d, 3H, J = 4 Hz, Me Leu), 0.95 (d, 3H, J = 6 Hz, Me Leu). ^{13}C-NMR (δ, $CDCl_3$): 172.6 (-CO CSA), 170.9 (-CO Fc), 96.5 (ipso C of of Cp), 72.3 (2,2′-C of Cp), 71.9 (3,3′-C of Cp), 70.8 (α-C of Leu), 64.7 (C Leu), 52.9 (C of Leu) 40.9 (CH_2 attached to NH), 38.9 (CH_2 attached to S), 21.4 (Me of Leu) 19.5 (Me of Leu).

2.3.4. Electrochemical Studies: All solution electrochemical experiments were carried out using a CV-50W Voltammetric Analyzer (BAS) at room temperature (20 ± 2^{o}C). Tetrabutylammonium perchlorate was used as supporting electrolyte (0.2 M in MeCN). A glassy carbon electrode was used as a working electrode (BAS, diameter 3mm) and a platinum wire was used as a counter electrode. The glassy carbon working electrode was polished with alumina (3 μm followed by 1 μm, then 0.5 μm) prior to use to remove any

surface contaminants. The reference electrode was a Ag/AgCl electrode (BAS, 3M NaCl). iR compensation was applied. Backgrounds of the solvent containing the supporting electrolyte were collected before each set of experiments and then subtracted from the CVs. The experiment was repeated at least 10 times to get reliable values for $E_{1/2}$.

2.3.5. X-ray crystallography: Suitable crystals of compounds **5** (orange prisms 0.40 x 0.38 x 0.28 mm) and **6** were obtained from a ether-layered solution of the compounds in dichloromethane. Data for **5** and **6** were measured using a Siemens Smart CCD diffractometer or a Bruker PLATFORM diffractometer/SMART 1000 equipped with a CCD area detector, respectively, using Mo-Kα radiation (graphite monochromated) with ω scans. An empirical absorption correction (SADABS)[7] was applied to **5** and **6**. The

Table 2.1. Summary of crystallographic data for compounds **5** and **6**.

	5	**6**
Chemical Formula	$C_{32}H_{36}Fe_2N_4O_4S_4$	$C_{20}H_{24}FeN_4O_4S_2$
FW	780.59	504.40
Crystal size/mm	0.40 x 0.38 x 0.28	0.25 x 0.25 x 0.20
Crystal system	monoclinic	monoclinic
Space group	I 2/a	P21/c
a/Å	25.1400(10)	12.4840(2)
b/ Å	10.7111(4)	13.3040(2)
c/ Å	24.2720(10)	26.4780(3)
α/°	90	90
β/°	93.0975(7)	106.1200(8)
γ/°	90	90
V/Å^3	6526.3(4)	4224.75(10)
Z	8	8
D(calcd.), g/cm^3	1.589	1.586
T/K	193(2)	173(2)
λ/Å	0.71073	0.71073
μ/mm^{-1}	1.190	0.948
R (I>2σ(I))[a]	0.0349	0.0645

structures were solved using direct methods.[8] In both cases, for one of the molecules, the podand chain displays a significant positional disorder, which was modeled by assuming an occupancy of 50:50 (for **5**) and 40:60 (for **6**) for the two positions. The ordered ferrocene molecule in **5** and the ferrocene group of the disordered molecule were refined anisotropically, while the disordered chain was refined isotropically using full-matrix least-squares on F^2. For **6**, all atoms were refined anisotropically on F^2. H-atoms were placed in calculated positions and included in the refinement. The final R value for **5** was R1 = 0.0349 and wR2 = 0.0870 for 6693 reflection with $I > 2\sigma(I)$ (20739 total reflections). And for compound **6**, R1 = 0.0645 and wR2 = 0.1087 for 6532 reflections with $I > 2\sigma(I)$ (8632 total reflections). Crystallographic details for both structures are found in Table 2.1. CCDC reference numbers 227645 (Compound **5**) and 227646 (Compound **6**).

2.4. Results and Discussions

The ferrocene-peptide macrocyles **5** – **9** are readily obtained as crystalline yellow to orange solids in low to moderate yields by the reaction of ferrocenedicarboxylic acid with the appropriate amino acid-cystamine conjugate for **6** - **8** or with cystamine in the case of compound **5** in the presence of carbodiimide and HOBt under high dilution conditions (Scheme 2.1). At concentrations above 2 mmol in ferrocenedicarboxylic acid the yields are decreased significantly, as expected for the synthesis of macrocycles. All compounds were fully characterized spectroscopically.

In the ^{1}H-NMR spectrum, all macrocycles exhibit the expected 2:2 signal pattern for disubstituted Fc-systems with the four ortho protons on the two Cp rings shifted downfield compared to the meta-Hs.[3] The α-Hs are observed at δ 4.23 for **6**, δ 4.47 for **7**, δ 4.62 for **8**, and δ 4.44 for **9**. This compares favorably to related mono-substituted Fc-peptides described in the literature.[9]

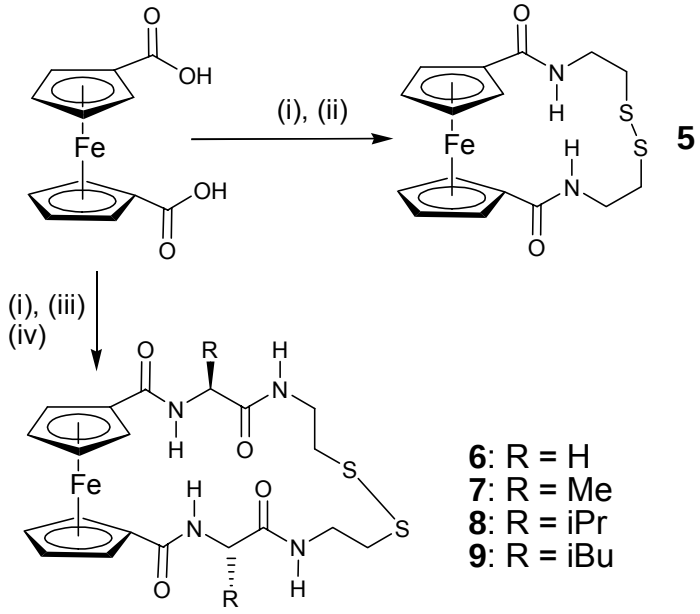

Scheme 2.1. Synthesis of redox active cyclopeptides : (i) EDC, HOBt, CH_2Cl_2, (ii) CSA• 2HCl, CH_2Cl_2, (iii) (a) Boc-amino acid CSA dimer, TFA, (b) Et_3N, CH_2Cl_2, (iv) dilution.

In order to investigate the H-bonding behaviour of these systems, we decided to carry out a VT-NMR study in $CDCl_3$. Figure 2.1 shows a partial ^{1}H-NMR spectrum of the amide region of compound **9** at various temperatures. Both amide protons display a temperature dependent chemical shift, indicating their involvement in H-bonding. For compound **9**, the amino acid NH at δ 7.44 and the cystamine NH at δ 6.52 experience an upfield shift as the temperature increases. The temperature influence is higher for the Fc-NH^B than for the CSA NH^A. The temperature behavior for all compounds is summarized in Table 2.2.

Table 2.2. Temperature behavior of the amide NH for Fc-compounds **5** – **9** in $CDCl_3$ (1 mM).

Compound	NH^A	NH^B
Fc[CO-CSA]$_2$ (**5**)	-	3.3
Fc[CO-Gly-CSA]$_2$ (**6**)	0.8	7.0
Fc[CO-Ala-CSA]$_2$ (**7**)	1.5	5.4
Fc[CO-Val-CSA]$_2$ (**8**)	2.0	3.5
Fc[CO-Leu-CSA]$_2$ (**9**)	0.7	5.3

The temperature coefficient for the Fc-amino acid NH is invariably higher than that of the cystamine NH for all compounds investigated. The temperature behavior compares well with other H-bonded peptide systems.[10] The CSA NH only displays a shallow temperature dependence, which may indicate only weak H-bonding. IR also supports the presence of H-bonding. For example, compound **6** displays two NH stretching vibrations at 3391 (H-bonded) and 3443 cm^{-1} (non H-bonded). Similarly, compounds **7** – **9** exhibit two NH bands. The presence of H-bonding involving the Fc-amide is supported by the structural investigation of compounds **5** and **6**.

a)

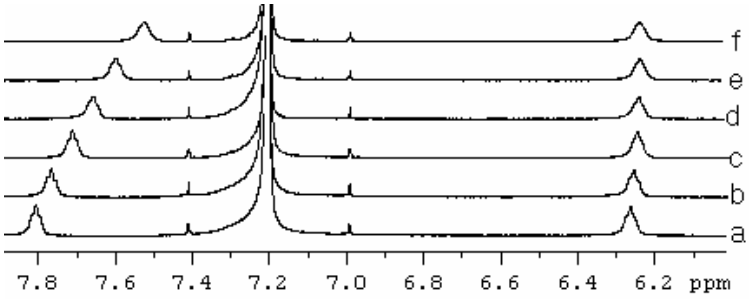

b)

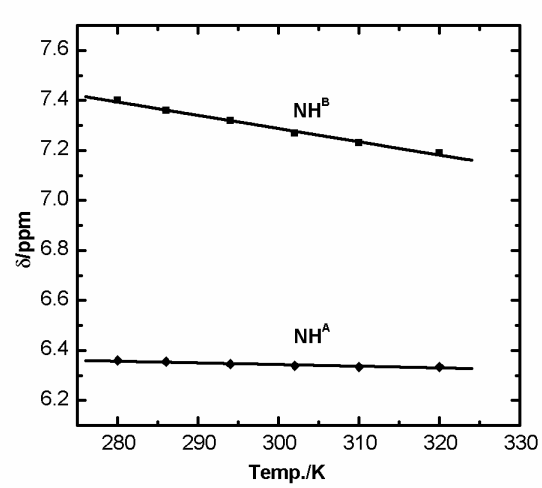

Figure 2.1. (a) Stackplot showing the amide NH region of the ^1H NMR spectrum of compound **9** in $CDCl_3$ (1 mM); a = 280K, b = 286K, c = 294K, d = 302K, e = 310K and f = 320K and (b) showing the temperature behaviour of the Fc-amide NH^B and the CSA amide NH^A. The temperature coefficients are evaluated from the slope.

Our X-ray crystallographic investigations of compounds **5** and **6** show the presence of two crystallographically independent molecules within the asymmetric unit. The two molecules within the asymmetric unit display slightly different bond distances and angles. The molecular structure of one of the molecules of compound **5** is shown in Figure 2.2. Both Fc molecules adopts a 1,2'-conformation with the amide C=O pointing towards the outside of the macrocycle, enabling it to interact with the adjacent molecule via an intermolecular H-bond (N···O contact 3.027(4) Å). Intramolecular H-bonding interactions, often observed for bis-substituted Fc-amino acid and peptide conjugates are not observed.[3]

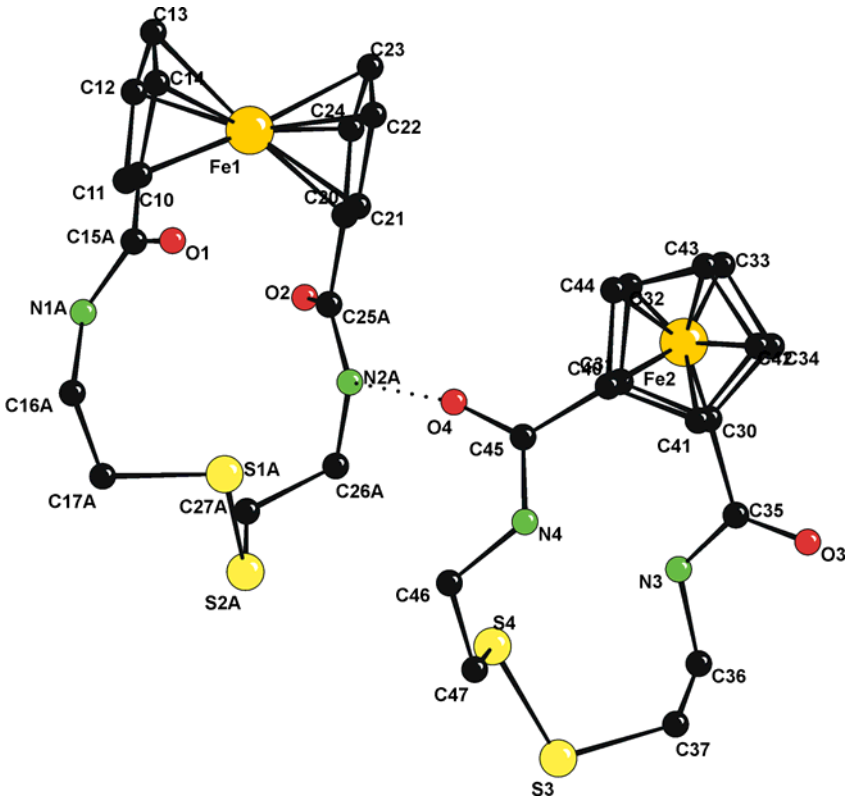

Figure 2.2. Molecular structure of compound **5** showing the two adjacent molecules in the asymmetric unit. Please note the weak H-bonding interaction involving N(2A) and O(4). The CSA chain of molecule 1 is disordered over two positions both having 50/50 occupancy. Only one of the two conformations is shown. Selected bond distances: d(S(1A)-S(2A) = 2.0329(18) Å, d(S(1B)-S(2B) = 2.043(3) Å; d(S(3)-S(4)) = 2.0326(9) Å, d(S(4)-C(47) = 1.821(3) Å, d(O(3)-C(35) = 1.237(3) Å, d(O(4)-C(45) = 1.239(3) Å (see supplemental material). H-bonding contact: N(1A)···O(3) =2.980(4)Å, N(2A)···O(4) = 3.027(4)Å, N(3)···O(2) = 2.821(3)Å, N(4)···O(1) = 2.884(3)Å.

Orientation and presumably the size of the macrocycle do not allow formation of any intramolecular N···O H-bonding interactions involving the amide groups. The S-S distances are S(1A)-S(2A) = 2.0329(18) Å and S(1B)-S(2B) = 2.043(3) Å and S(3)-S(4) 2.0326(9) Å. C-O bond distances are typical for carbonyl C=O distances found in Fc-amides. Both Fc molecules in **5** have virtually co-planar Cp rings (Cp-Fe1-Cp: 2.4º and Cp-Fe2-Cp = 0.6º).[11] For the disordered Fc1 system, the amide-Cp twists are 25.5º and 15.3º for Cp1 (C10-C14) and chain A and chain B, respectively, and 16.5º and 19.9º for Cp2 (C20-C24) and chain A and chain B, respectively. For Fc2, the amide twists are slightly higher with 26.5º for Cp3 and 21.5º for Cp4. Compound **6** displays the same basic structural features. The system adopts a 1,2'-configuration, having both Fc-C=O pointing outwards and are engaged in intermolecular H-bonding interactions. But in contrast to compound **5**, both amide NH in $[FcCO\text{-}Ala\text{-}CSA]_2$ (**6**) are engaged in strong intramolecular H-bonding to the opposite peptide C=O across the ring (d(N(11)···O(22) = 2.862(4)Å, d(N(21)···O(12)) = 2.873(4) Å, d(N(31)···O(42) = 2.959(4)Å, d(N(41)···O(32)) = 2.815(4) Å). The molecular structure of one of the two molecules within the asymmetric unit of compound **6** is shown in Figure 2.3. **6** possesses the same intramolecular H-bonding as displayed by the open-chain ferrocene dipeptide conjugates reported by Hirao and Metzler-Nolte.[3] Hirao's $Fc[CO\text{-}Glu\text{-}Leu\text{-}OEt]_2$ displays an asymmetric H-bonding interaction of the two podand peptide chains involving the carbonyl of the Gly of one chain and the NH of Gly of the other podand dipeptide chain with distances of d(N···O) = 3.042(3) Å and 2.753(4) Å.[3b] For the related system, $Fc[CO\text{-}Gly\text{-}Phe\text{-}OEt]_2$, the H-bonding is symmetrical (d(N···O) = 2.84(1)Å). In Metzler-Nolte's $Fc[CO\text{-}Ala\text{-}Phe\text{-}OMe]_2$, two intramolecular cross-strand H-bonds were observed (d(N···O) = 2.921 Å, 2.924 Å, 2.901 Å, and 2.893Å for the two independent molecules).[3g] In all three systems the second amino acid possesses the ability to enage in additional intermolecular H-bonding to four neighboring molecules. In contrast the lack of N···O H-

bonding ability of Pro in Fc[CO-Gly-Pro-OEt]$_2$ and Fc[CO-Ala-Pro-OEt]$_2$ restrict the H-bonding pattern to intramolecular cross-strand H-bonding (for Fc[CO-Gly-Pro-OEt]$_2$: 2.910(4), 2.898(5), 2.85(1), 2.87(1) for two independent molecules; for Fc(Ala-Pro-OEt)$_2$: d(N···O) = 2.981(8) Å).[3f, g] Variation of the ester group for Fc(Ala-Pro-OR)$_2$ with R = Me, Et, Pr, Bz show no changes in the intramolecular H-bonding between Ala NH and Ala CO with distances ranging from 3.030(9) Å to 2.925(9) Å.[3e] As exemplified by Fc[CO-Ala-Pro-NHPyMe]$_2$, the structural motif is not even perturbed in the presence of other external H-bonding interactions, such as those caused by the interaction of the Fc-peptide-pyridine conjugate with (1*R*,3*S*)-camphoric acid, indicating its remarkable stability even in the presence of other highly H-bonding agents (d(N···O) = 2.97Å and 2.95Å).[3e]

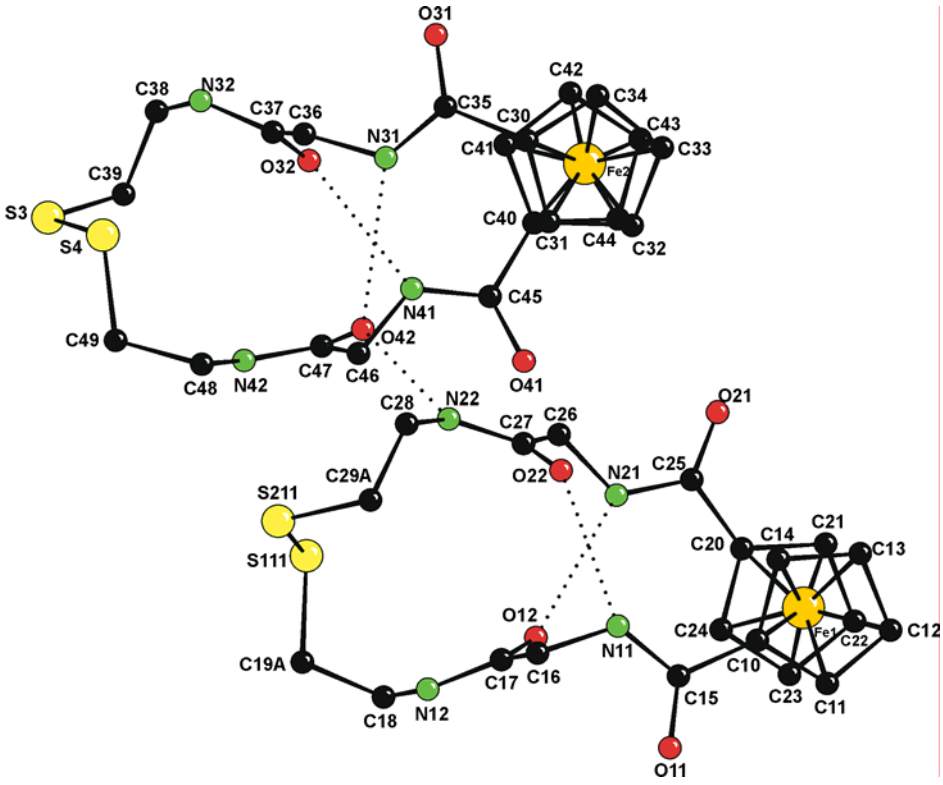

Figure 2.3. Molecular structure of compounds **6** showing the intra- and intermolecular H-bonding interactions a) intramolecular H-bonding: d(N(11)···O(22) = 2.862(4) Å, d(N(21)···O(12)) = 2.873(4) Å, d(N(31)···O(42) = 2.959(4) Å, d(N(41)···O(32)) = 2.815(4) Å; b) intermolecular contacts: d(N(22)···O(42) = 2.974(5) Å, d(N(12)···O(31)* = 2.836(4) Å, d(N(32)···O(11)** = 2.843(4) Å, d(N(42)···O(41)$^{\#}$ = 2.867(4) Å. Symmetry transformations used to generate equivalent atoms: * : +x, -y+0.5, +z+0.5; **: +x, -y+0.5, +z-0.5; $^{\#}$: -x+1, +y-0.5, -z+0.5.

Despite numerous reports on the stability of the cross-strand H-bonding motif, it is also noteworthy that the simple amino acid conjugate Fc[CO-Phe-OMe]$_2$, reported by Metzler-Nolte, displays only a single intramolecular H-bond (d(N···O) = 2.832 Å) and in addition engages in intermolecular H-bonding with an adjacent molecule (d(N···O) = 2.935Å), showing the ability of the molecule to switch between two intramolecular and more intemolecular H-bonding.[3g] This of course is in contrast to earlier reports by Erker and Mingos who found the conventional cross-strand H-bonding motif in Fc[CO-Val-OMe]$_2$[12] and Fc[CO-GlyNH$_2$]$_2$.[13] However, the example of Fc[CO-Phe-OMe]$_2$ is certainly instructive in showing that this class of compounds may possess a richer richer supramolecular chemistry than was initially thought.

The redox behaviour of compounds **5** – **9** was investigated by cyclic voltammetry (CV). A typical CV curve is shown in Figure 4.

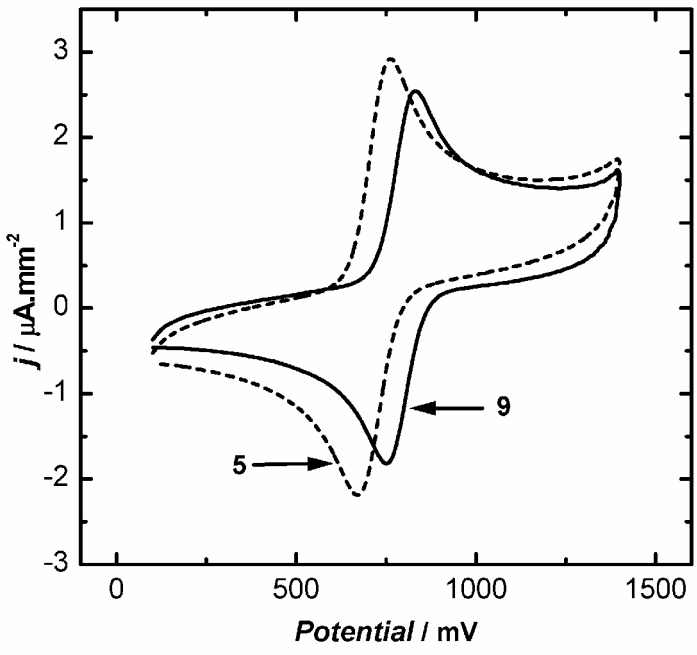

Figure 2.4. Cyclic voltammogram of compounds **5** and **9** in MeCN (0.1 mM, 0.2 M TBAP) at a scan rate of 100 mVs^{-1} on a glassy carbon (BAS) working electrode.

All compounds exhibit a fully reversible one electron oxidation, with Faradaic current ratios close to unity and peak separations ranging from 76 – 95 mV. Table 2.3 summarizes the electrochemical behaviour. Redox potentials in general are similar to those reported before for H-bonded and non-H-bonded peptides.[3,14] There are some noticeable variations in the $E_{1/2}$ of the Fc-peptide macrocycles. Whereas the $E_{1/2}$ of compound **5** is observed at 740 mV (versus Ag/AgCl), those of the Fc-peptide macrocycles **6** – **9**, which show $E_{1/2}$ between 773 and 794 mV (vs. Ag/AgCl). This increase coincides with an increase in the number of intramolecular H-bonds, which is in contrast to Maran's Fc-Aib peptides,[15] which show that an decreasing oxidation potential with an increase in the number of H-bonds.

Table 2.3. Electrochemical data for compounds **5** – **9**.[a]

Compound	$E_{1/2}$ (mV)	ΔE (mV)	i_c/i_a
Fc[CO-CSA]$_2$ (**5**)	740	80	0.91
Fc[CO-Gly-CSA]$_2$ (**6**)	773	77	0.92
Fc[CO-Ala-CSA]$_2$ (**7**)	780	95	0.80
Fc[CO-Val-CSA]$_2$ (**8**)	789	76	0.92
Fc[CO-Leu-CSA]$_2$ (**9**)	794	92	0.88

[a] 1 mM solution in MeCN, 0.2 M TBAP, scan rate = 100 mVs^{-1}, glassy carbon (BAS) working electrode, Pt counter electrode, Ag/AgCl reference electrode.

Cheng andcoworkers also observed small changes of the redox potential in their Fc–cystine systems that are explained as amino acid specific changes.[5] Similar effects were reported earlier for monosubstituted systems[9,16] and maybe rationalized in terms of small differences in solvation for the various peptide systems.[9d] However, at the present time no rationale backed by solid high-level quantum chemical calculationsis available to explain these observations in detail.

2.5. Acknowledgments: The authors would like to acknowledge the financial support from NSERC in the form of an operating grant. H.B.K is Canada Research Chair in Biomaterials. We grateful to Ken Thoms for running the MS spectra, and to the SSSC for instrument time (NMR, X-ray).

2.6. References

[1] a) M. Amorin, L. Castedo, and J.R. Granja, *J. Am. Chem. Soc.* **2003**, 125, 2844-2845; b) W.S. Horne, C.D. Stout, M.R. Ghadiri, *J. Am. Chem. Soc.* **2003**, 125, 9372-9376; c) H. Okamoto, T. Nakanishi, Y. Nagai, M. Kasahara, K. Takeda, *J. Am. Chem. Soc.* **2003**, 125, 2756-2769; d) T.D. Clark, J.M. Buriak, K. Kobayashi, M.P. Isler, D.E. McRee, M.R. Ghadiri, *J. Am. Chem. Soc.* **1998**, 120, 8949-8962; e) D. Ranganathan, C. Lakshmi, I.L. Karle, *J. Am. Chem. Soc.* **1999**, 121, 6103-6107; f) D. Ranganathan, V. Haridas, R. Gilardi, I.L. Karle, *J. Am. Chem. Soc.* **1998**, 120, 10793-10800; g) D. Ranganathan, *Acc. Chem. Res.* **2001**, 34, 919-930; h) Theoretical Study Nanotubes: F. Ferrante, G. La Manna, *J. Phys. A*. **2003**, 107, 91-96.

[2] a)`R.P. Lyon and W.M. Atkins, *J. Am. Chem. Soc.*, **2001**, 123, 4408; b) J.H. Collier, B.-H. Hu, J.W. Ruberti, J. Zhang, P. Shum, D.H. Thompson and P.B. Messersmith, *J. Am. Chem. Soc.*, **2001**, 123, 9463; c) T.C. Holmes, S. deLasalle, X. Su, G. Liu, A. Rich and A. Zhang, *Proc. Natl. Acad. Sci. USA*, **2000**, 97, 6728.

[3] a) A. Nomoto, T. Moriuchi, S. Yamazaki, A. Ogawa, T. Hirao, *Chem. Commun*. 1998, 1963-1964; b) T. Moriuchi, A. Nomoto, K. Yoshida, K.; Ogawa, A.; Hirao, T. *J. Am. Chem. Soc.* **2001**, 123, 68-75; c) T. Moriuchi, A. Nomoto, K. Yoshida, T. Hirao *J. Organomet. Chem.* **1999**, 589, 50-58; d) T. Moriuchi, K. Yoshida, T. Hirao, *Organometallics* **2001**, 20, 3101-3105; e) T. Moriuchi, K. Yoshida, T. Hirao, J. Organomet. Chem. **2003**, 668, 31-34; f) T. Moriuchi, A. Nomoto, K. Yoshida, T. Hirao Organometallics **2001**, 20, 1008-1013; g) D.R. van Staveren, T. Weyhermüller, N. Metler-Nolte, Dalton Trans. **2003**, 210-220.

[4] R.S. Herrick, R.M. Jarret, T.P. Curran, D.R. Dragoli, M.B. Flaherty, S.E. Lindyberg, R.A. Slate and L.C. Thornton, *Tetrahedron Lett.*, **1996**, 37, 5289-5292.

[5] H. Huang, L. Mu, J. He and J.-P. Cheng. *J. Org. Chem.*, **2003**, 68, 7605-7611.

[6] a) T.J. Katz, N. Acton and G. Martin, *J. Am. Chem. Soc.,* **1969**, 91, 2804-2805; b) P.J. Hamond, P.D. Beer and C. D. Hall, *Chem. Commun.,* **1983**, 1161-1163 ; c) M. Hisatome, M. Yoshihashi, K. Masuzoe and K. Yamakawa, *Organometallics,* **1987**, 6, 1498-1502 ; d) M.C. Grossel, M.R. Goldspink, J.P. Knychala, A.K. Cheetham and J.A. Hrilijac, *J. Organomet. Chem.,* **1988**, 352, C13-16; e) C.D. Hall, I.P. Danks, S.C. Nyburg, A.W. Parkins and N.W. Sharpe, *Organometallics,* **1990**, 9, 1602-1607; f) M.C. Grossel, M.R. Goldspink, J.A. Hriljac and S.C. Weston, *Organometallics,* **1991**, 10, 851-860; g) W. Finckh, B.-Z. Tang, A. Lough and I. Manners, *Organometallics,* **1992**, 11, 2904-2911; h) S. Barlow and D. O'Hare, *Organometallics,* **1996**, 15, 3885-2890; i) R. Rulkens, D.P. Gates, D. Balaishis, J.K. Puelski, D. F. McIntosh, A.J. Lough and I. Manners, *J. Am. Chem. Soc.,* **1997**, 119, 10976-10986; j) M. Herberhold, H.-D. Brendel, A. Hofmann, B.

Hofmann and W. Milius, *J. Organomet. Chem.,* **1998**, 556, 173-187; k) Review: R.W. Heo and T.R. Lee, *J. Organomet. Chem.,* **1999**, 578, 31-42; l) T. Sakano, H. Ishii, I. Yamaguchi, K. Osakada and T. Yamamoto, *Inorg. Chim. Acta,* **1999**, 296, 176-182 ; m) B. Delavauz-Nicot and S. Fery-Forgues, *Eur. J. Inorg. Chem.,* **1999**, 1821-1825 ; n) T. Mizuta, M. Onishi and K. Miyoshi, *Organometallics,* **2000**, 19, 5005-5009 ; o) A. Tarraga, P. Molina and J.L. Lopez, *Tetrahedron Lett.,* **2000**, 41, 2479-2482; p) K. Hassenberg, J. Pickardt and R. Steudel, *Organometallics,* **2000**, 19, 5244-5246 ; q) P. Liptau, S. Knüppel, G. Kehr, O. Kateva, R. Fröhlich and G. Erker, *J. Organomet. Chem.,* **2001**, 637-639, 621-630; r) K.H.H. Fabian, H.-J. Linder, N. Nimmerfroh and K. Hafner, *Angew. Chem. Int. Ed.,* **2001**, 40, 3402-3405; s) R. Steudel, K. Hassenberg, J. Pickardt, E. Grigiotti and R. Zanello, *Organometallics,* **2002**, 21, 2604-2608; t) O. Kadkin, C. Näther and W. Freidrichsen, J. *Organomet. Chem*., **2002**, 649, 161-172; u) A. Tarrage, P. Molina, J.L. Lopez, M.D. Velasco, D. Bautista, P.C. Jones, *Organometallics*, **2002**, 21, 2055-2065.

[7] *SHELXTL-NT 5.1, Program Library for Structure Solution and Molecular Graphics*; Bruker AXS, Inc.: Madison, WI, **1998.**

[8] G. M. Sheldrick, *SHELXL97, Program for the Solution of Crystal Structures;* University of Göttingen, Göttingen, Germany **1997**.

[9] a) I. Bediako-Amoa, T.C. Sutherland, C.-Z. Li, R. Silerova and H.-B. Kraatz *J. Phys. Chem. B,* **2004***,* 108, 704-714; b) H.S. Mandal, H.-B. Kraatz *J. Organomet. Chem.,* 2003, 674, 32-37; c) K. Plumb, H.-B. Kraatz *Bioconjugate Chem.,* **2003**, **4,** 601-606; d) M.V. Baker, H.-B. Kraatz and J.W. Quail *New J. Chem.,* **2001**, 25, 427-433.

[10] a) I. Bediako-Amoa, R. Silerova and H.-B. Kraatz, *Chem. Commun.* **2002**, 2430-2431; b) P. Saweczko, G. D. Enright and H.-B. Kraatz, *Inorg. Chem.,* **2001**, 40*,* 4409-4419.

[11] L. Lin, A. Berces and H.-B. Kraatz *J.Organomet.Chem* ,**1998**, 556, 11-20.

[12] M. Oberhoff, L. Duda, J. Karl, R. Mohr, G. Erker, R. Fröhlich and M. Grehl, *Organometallics*, **1996**, 15, 4005-4011.

[13] A.S. Georgopoulou, D.M.P. Mingos, A.J.P. White, D.J. Williams. B.R. Horrocks and A. Houlton, *Dalton Trans.,* **2000**, 2969-2974.

[14] Y. Xu, P. Saweczko, H.B. Kraatz *J. Organomet. Chem.,* **2001**, 637-639, 335-342.

[15] Antonello, S.; Formaggio, F.; Moretto, A.; Toniolo, C.; Maran, F. *J. Am. Chem. Soc.,* **2003**, 125, 2874-2875.

[16] H.-B. Kraatz, J. Lusztyk and G. E. Enright, Inorg. Chem., **1997**, 36,2400–2405.

Chapter 3

Discovery of the first Pseudo β-Barrel: Synthesis and Formation by Tiling of Ferrocene cyclopeptides.

3.0. Connecting Text

This chapter describes the preparation of synthetic models of a secondary structural domain of protein, the β-barrel. Because of the complexity associated in managing the β-strand peptides, it was not possible to prepare the synthetic model of this important structural motif. By using Fc as a molecular scaffold and Macrocyclization, we were able to maintain the β-sheet characteristics of the peptides and moreover, we were able to align them in a suitable fashion and assemble through H-bonding providing a β-barrel like architecture. Therefore, it demonstrates a critical method for controlling the structure of peptides making it relevant to my Ph.D. research objective.

This paper was reproduced with the permission from *Angew. Chem. Int. Ed* **2006**, 45, 751-754, Copyright 2006, Wiley VCH. This paper was co-authored by D. A. R. Sanders, G. Schatte and H.-B. Kraatz. All experimental works with the exception of crystallographic analysis were carried out by me. In addition I wrote the initial draft of the manuscript. The text below is a *verbatim* copy of the published paper.

3.1. Introduction

Inspired by channel-forming proteins involved in trans membrane transport and controlling biological functions,[1] the construction of porous organic architectures with well-defined shapes and sizes from simple building blocks has emerged as an important subject in biological chemistry as well in material science.[2-8] In this regard recently

introduced peptide-derived materials are used to mimic biological channels and serve as models for trans-membrane pores or as antibacterial pore-forming agents,[9-10] with potential applications in drug delivery or as constrained chiral reaction environments.[2, 11-12] These channels are mainly self-assembled from cyclopeptides, which stack on top of each other to give large hollow tubes, having the individual cyclopeptides connected via H-bonding akin to that found in antiparallel β-sheets. Peptide β-barrel presents a particular challenge. This ubiquitous structural motif is present in a wide range of proteins, including pore forming proteins present as membrane proteins of gram negative bacteria, mitochondria and chloroplast and control many sophisticated biological functions.[13] In β-barrel the peptide strands are arranged more or less parallel to the axis of the barrel. To date it has not been possible to synthesize a model for such an ubiquitous biological structural motif.[14] Here, we report the synthesis and the structure of first artificial β-barrel obtained by self-assembly from smaller bio-organometallic ferrocene-peptide conjugates. In this model, eight β-strands are arranged almost parallel to the axis of the channel having an internal pore diameter of 8Å. Experimental evidence shows that the pore appears to be filled with water molecules (see below). Our approach offers the potential to exploit such structures for the *de novo* design of functional trans-membrane channels. Such structures may also find applications in separation science, supramolecular host-guest chemistry and in molecular electronics.

3.2. Results and Discussion

The structure of 1-1′ bis-substituted ferrocene-peptide conjugates is controlled by a fine balance between inter- and intramolecular H-bonding and attached peptide strands attain

β-sheet conformation.[15-18] In general, *P*-helical and *M*-helical conjugates with respect to ferrocene are formed if L-amino acids and D-amino acids are respectively attached to the metallocene and the substituents adopt a flexible *anti* conformation, which is not suitable for sheet-like intramolecular interaction of the elongated peptide strands. We decided to force the attached strands arrange parallel to each other by chemically linking the two podant peptide chains with cysteamine, a disulfide linker, thereby restricting the mobility of the strands. We expected this to have a profound consequence in that this chemical modification should foster intermolecular hydrogen bonding, which is akin to that found in antiparallel β-sheets.

In order to optimize intramolecular H-bonding between the two peptide substituents, a small twist of the Cp-amide planes is required, resulting in the peptide strands to turn towards each other.[19] From this observation we predicted that restricting the formation of a "flat" β-sheet by tying the two peptide substituents via a cystamine linker will induce additional curving of the peptide strands and thus may allow to create hollow H-bonded assemblies based on a β-sheet motif. For this purpose, we designed the two ferrocene cyclopeptides, Fc[CO-Gly-Val-CSA]$_2$(**5**) and Fc[CO-Gly-Ile-CSA]$_2$(**6**) (Gly = glycine, Val = valine, Ile = isoleucine, CSA = cysteamine), each having glycine as the first amino acid to be attached to the ferrocene, giving maximum flexibility to the podant peptide chains, followed by valine or isoleucine, the amino acids with very high propensity to form β-sheets. Compounds **5** and **6** were synthesized by the cyclization of 1-1′ ferrocene dicarboxylic acid and cysteamine peptide conjugates at very high dilution

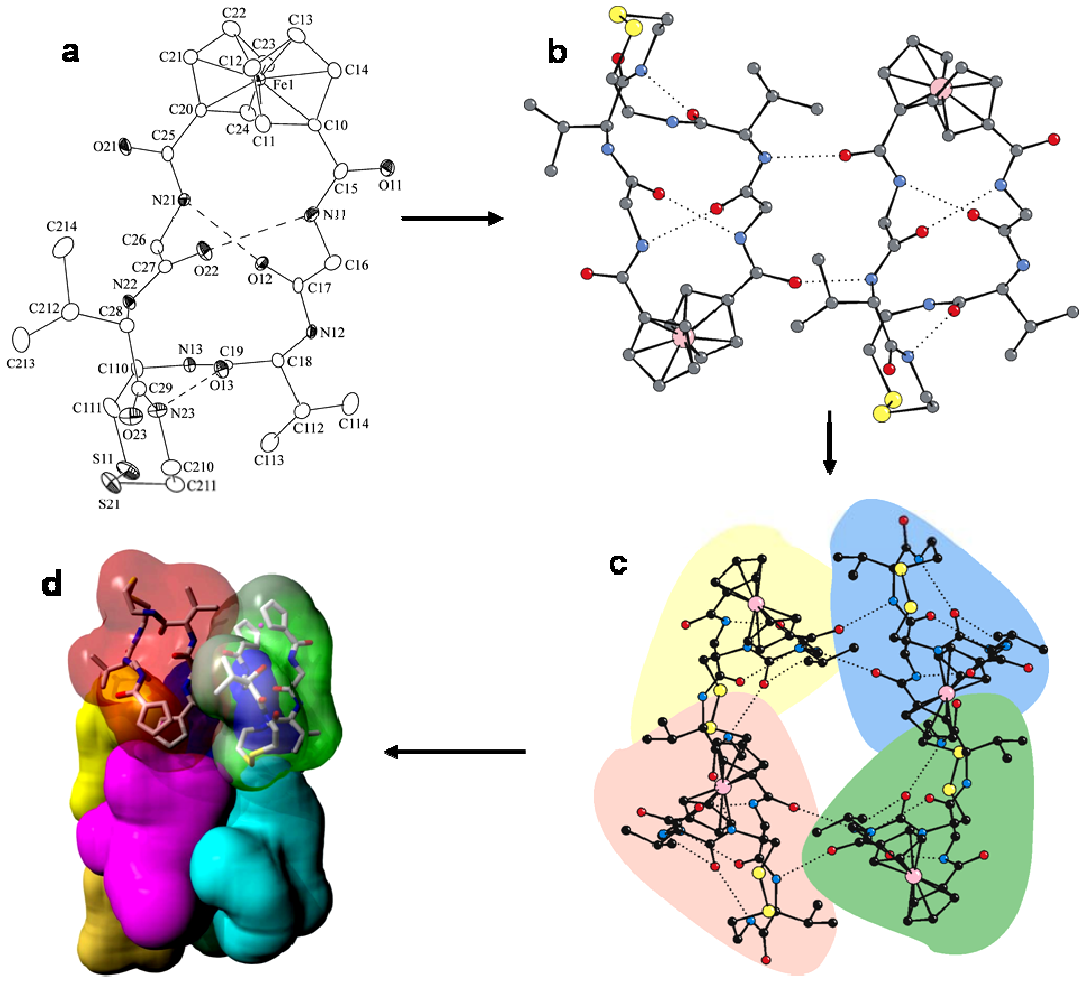

Figure 3.1. The crystal structure of Fc[CO-Gly-Val-CSA]$_2$(**5**) and schematic view of the formation of the pseudo β-barrel: a) molecular structure of compound 5 showing the *P*-helicity of the ferrocene unit and the intramolecular H-bonding between the two podant peptide strands. The geometry of the Fc group, the amide substitutents and bond lengths and angles are well within established parameters for Fc-peptide conjugates;[20] b) formation of β-sheets through intermolecular N(H)•••O=C hydrogen bonding. The head-to-tail interaction of the molecules results in an unusual up-up-down-down arrangement of the peptide strands. The arrangement between the two peptide strands on the two Fc conjugates is antiparallel; c) four molecules interact via H-bonding to form a β-barrel. A view down the *c*-axis is shown. The disordered water molecules inside the cavity of the barrel were omitted for clarity; d) molecular surface representation showing a side view of the half barrel viewed along the *c*-axis formed by tiling of cyclic ferrocene peptides. *Crystal data for* ***5***: $C_{30}H_{42}Fe_1N_6O_6S_2$; formula weight: 702.67; crystal system: orthorhombic; space group: $P2_12_12_1$; cell dimensions: a = 14.4808(4) Å, b = 16.2650(5) Å, c = 16.4770(4) Å, $\alpha = \beta = \gamma = 90°$, $Z = 4$; $\mu = 0.543$ mm^{-1}, $d_{calc.} = 1.209$ Mg/m^3.

and were characterized spectroscopically. They are poorly soluble in organic solvents, as expected for strongly H-bonded materials.[21] Compound **5** is readily obtained in a crystalline form suitable for structural analysis by X-ray diffraction from solutions at low concentrations. The molecular structure of compound 5, together with its supramolecular arrangement is shown in Figure 3.1.

There are three different types of H-bonding present in the structure of **5**. Intramolecular H-bonding is observed between the C=O group and the adjacent (H)N group [N(21)-O(12), 2.7848(4) Å; N(23)-O(13), 2.848(3) Å and N(11)-O(22), 3.013(4) Å]. The Fc[CO-Gly-Val-CSA]$_2$ units are liked via intermolecular H-bonding (2.898(4) and 3.036(4) Å). The intermolecular H-bonding interactions between head-to-tail connected ferrocene peptides results in the formation of a 14-membered ring, as expected for two peptides interacting in an antiparallel *β*-sheet fashion (see Figure 3. 1b).[16] The *β*-sheets are parallel to the *bc*-plane. Additional H-bonding (2.824(4) Å; involving the atoms O23 and N13) between adjacent sheets results in the formation of *β*-barrels with a diameter of ca 8 Å (measured between adjacent oxygen atoms of the C=O groups, see Figure 3.1c). Importantly, the structural rigidity allows the molecules to act as tiles forming what can be described as pseudo-barrels. (Figure 3.1d).

Figure 3.2 gives a stereoview of a pseudo-barrel formed by tiling of the Fc-conjugates and superimposed the direction of the individual *β*-strands. The barrel is formed by eight β-strands arranged in a up-up-down-down-up-up-down-down pattern. The axis of the barrel is parallel to the *ac*-plane and perpendicular to the *bc*-plane. The φ/Φ angles for the four residues are (Gly1 -134°/194°, Val1 -56°/146°, Gly2 -76°/161° ,

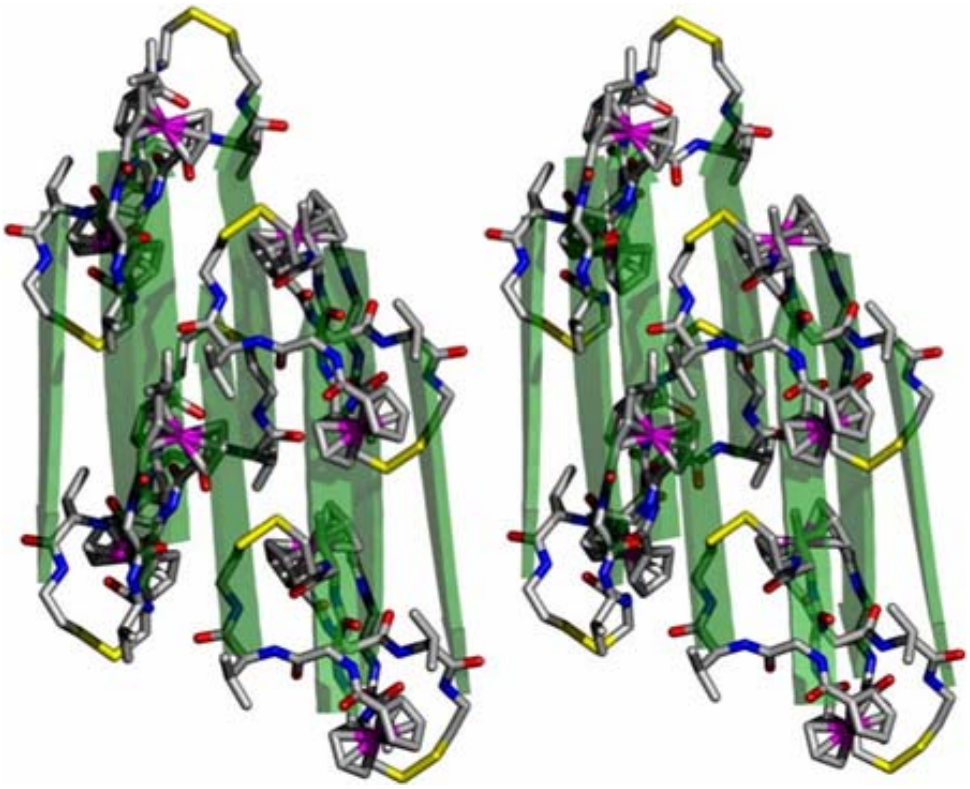

Figure 3.2. Stereoview of the pseudo-barrel formed by tiling of compound **5**. Indicated are the individual molecules as well as the direction of the individual β-strands. The φ/Φ angles for the four residues are (Gly1 -134°/194°, Val1 -56°/146°, Gly2 -76°/161° , Val2 -115°/64°). These residues all fit close to the theoretical region of β-sheet conformations (φ : -180° to -45° and Φ : 45° to 225°). As is seen with naturally occurring β-sheets, there is distortion, but the angles still fall within the "allowed" Ramachandran region associated with beta-sheet structures. The third "residue" (the cystamine) of one substituent (chain 1) has a φ value of approx. –97°, making the one substituent of the molecule a fairly close approximation of a β-strand.[22]

Val2 -115°/64°). These residues all fit close to the theoretical region of β-sheet conformations (φ : -180° to -45° and Φ : 45° to 225°).[22] As is seen with naturally occurring β-sheets, there is distortion, but the angles still fall within the "allowed" Ramachandran region associated with beta-sheet structures.[23-27] The third "residue" (the cystamine) of one substituent (chain 1) has a φ value of approx. –97°, making the one substituent of the molecule a fairly close approximation of a β-strand.

There is precedence for naturally occurring an eight-stranded β-barrels. For example, OmpX[28], OmpA[29], PagP[30] are all eight stranded barrels with various biological functions, ranging from toxin binding, to controlling enzymatic activity. Another example is NspA from *N. meningitides,* which is involved in cell adhesion and which has potential applications in structure-based vaccine design.[31] In these natural β-barrel the β- strands are tilted from the barrel axis where as in our pseudo β-barrel the β-strands are almost parallel to the barrel axis.

Figure 3.3a provides a view of the interior surface of the pseudo barrel, showing hydrophilic and hydrophobic characteristics. Some of the peptide carbonyls point towards the inside of the pseudo-barrel. We assume that this imparts sufficient hydrophilic character on the interior of the barrel to enable water to be inside the pseudo-barrels. An X-ray analysis shows a significant amount of residual electron density inside the pore, which is best modeled as approximately 12 disordered water molecules, with adjacent water molecules separated from each other by approximately 2.8 Å, which corresponds to strong H-bonding. The closest contact between the water and the interior walls of the pseudo barrel is 3.5 Å, indicating weak H-bonding interactions with the walls. The solution ^{1}H-NMR of compound 5 in clearly indicates the presence of water as part of the crystalline solid. The NMR indicates the presence of approximately 1.2 - 1.5 molecules of water per molecule of Fc-peptide for a total of approximately 9 to 12 molecules of water per 8-mer or pseudo-barrel. Since the space within the barrel is 386 Å^3, theoretically ten water molecules, each occupying 40 Å^3, could fit the pore. Therefore, a model including only water molecules inside the pore best fits all the experimental evidence. This compares well with pore-forming

cyclopeptides, described before by Ghadiri, who has interpreted residual electron density present within the pores of the cylindrical β-sheet peptide as water molecules.[32]

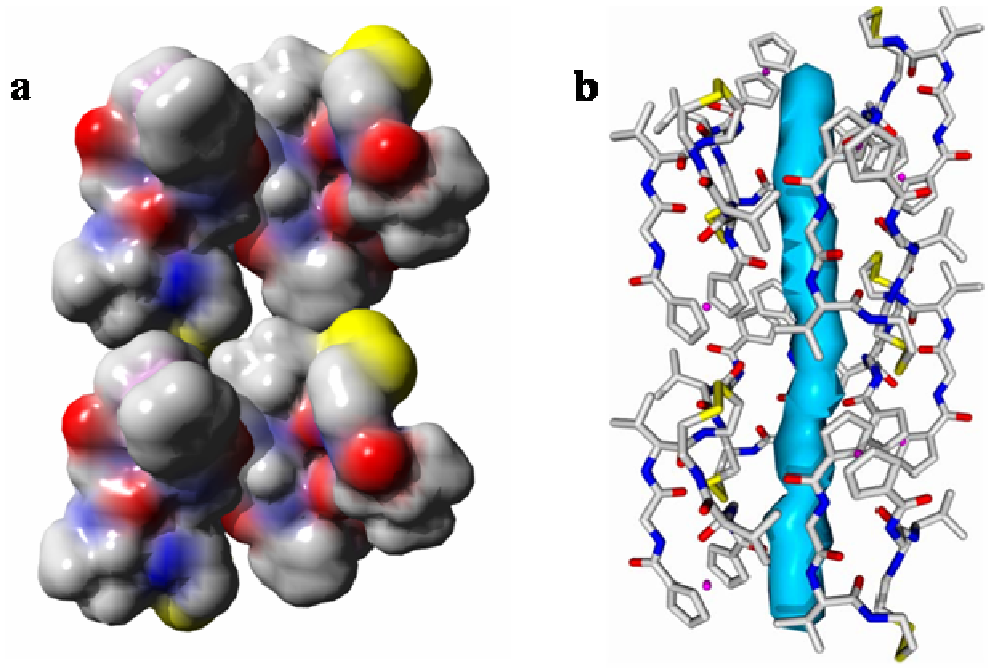

Figure 3.3. a) van der Waals surface representation of a cut-away side view of the interior of the pseudo-barrel showing the hydrophilic and hydrophobic characteristics. The colour coding corresponds to atoms: red (oxygen), blue (nitrogen), yellow (sulphur), gray (carbon); b) The same side view of the pseudo-barrel is presented as in Fig 3a generated by tiling of molecules of compound **5**. This channel has an interior diameter of ca 8Å. The residual electron density within this channel is interpreted as water molecules which are disordered over several positions and only the approximate envelope of the channel content is shown.

FT-IR is also a powerful technique in examining the secondary structure of peptides.[33] In particular, the Amide-I region offers a characteristic footprint that allows to distinguish between an α-helix, a β-sheet and a random coil conformation. The FT-IR spectrum of compound **5** in the solid state exhibits amide-I bands at 1640cm^{-1} and 1682 cm^{-1} and an amide-II at 1536 cm^{-1} which are the characteristic peaks for β-sheet.[33,34] Importantly, the IR absorptions are virtually identical for the Ile derivative 6 (1640 cm^{-1},

1680 cm^{-1} and 1535 cm^{-1} respectively) (see 3.S1), indicating that the structures of **5** and **6** are similar in the solid state. As expected, the amide N-H are involved in H-bonding and absorptions are observed in the Amide-A region at 3280 cm^{-1} and 3282 cm^{-1} for 5 and 6, respectively. Our observations are closely related to those made by Ghadiri and co-workers who showed that cyclo-peptides having an alternating D- and L amino acid sequence, assemble via intermolecular H-bonding into peptide nanotubes where the individual building blocks have antiparallel β-sheet conformation.[5]

3.3. Conclusions

In summary, we outline a potential strategy for the design of porous peptide materials, in which the barrel-like pores are formed by the self-assembly of bio-organometallic peptide conjugates. Although solubility of these systems is at present a challenge, the use of hydroxyl-containing amino acids such as serine and threonine should allow us to study the self-assembly in solution. Our approach may hold promise for the assembly of large porous peptide materials from readily available starting materials, which may find applications in biological chemistry as well as materials science. If successful, the strategy described here should lend itself to the preparation of *de novo* proteins incorporating the *β*-barrel motif.

3.4. Acknowledgements: We acknowledge support from NSERC in the form of an operating grant. H.-B. K. is the Canada Research Chair in Biomaterials.

Supporting information describing synthesis characterization of **5** , **6** and intermediates, IR spectra of **5** and **6** and X-ray structural data for compound **5** is presented below, after references.

3.5. References

[1] M. H. Saier, *J. Membrane Biol.* **2000**, 175, 165-180
[2] D. T. Bong, , T. D. Clark, J. R. Granja, M. R. Ghadiri, *Angewandte Chemie* **2001**, 113, 1016-1041 *Angew.Chem. Int. Edn.* **2001**, 40, 988-1011.
[3] D. Venkataraman, S. Lee, J. S. Zhang, J. S. Moore, *Nature* **1994**, 371, 591-593.
[4] A. Harada, J. Li, M. Kamachi, *Nature* **1993**, 364, 516-518.
[5] M. R. Ghadiri, J. R. Granja, R. A. Milligan, D. E. McRee, N. Khazanovich, *Nature* **1993**, 366, 324-327.
[6] M. R. Ghadiri, J. R. Granja, L. K. Buehler, *Nature* **1994**, 369, 301-304.
[7] J. C. Nelson, J. G. Saven, J. S. Moore, P. G. Wolynes, *Science* **1997**, 277, 1793-1796.
[8] D. Ranganathan, C. Lakshmi, I. L. Karle, *J. Am. Chem. Soc.* **1999**, 121, 6103-6107.
[9] J. R. Granja, M. R. Ghadiri, *J. Am. Chem. Soc.* **1994**, 116, 10785-10786.
[10] S. Fernandez-Lopez, H. S. Kim, E. C. Choi, M. Delgado, J. R. Granja, A. Khasanov, K. Kraehenbuehl, G.Long, D. A. Weinberger, K. M. Wilcoxen, M. R. Ghadiri, *Nature* **2001**, 414, 329-329.
[11] J. Sanchez-Quesada, H. S. Kim, M. R. Ghadiri, *Angewandte Chemie* **2001**, 113, 2571-2574 *Angew. Chem. Int. Edn.* **2001**, 40, 2503-2506.
[12] B. Eisenberg, *Acc. Chem. Res.* **1998**, 31, 117-123.
[13] W. C. Wimley, *Curr. Opin. Struct. Biol.* **2003** 13, 404-411.

[14] N. Sakai, J. Mareda, S. Matile, *Acc. Chem. Res.* **2005**, 38, 79-87.
[15] D. R. van Staveren, N. Metzler-Nolte, *Chem. Rev.* **2004**, 104, 5931-5985.
[16] T. Moriuchi, A. Nomoto, K. Yoshida, A. Ogawa, T. Hirao, *J. Am. Chem. Soc.* **2001**, 123, 68-75.
[17] T. Moriuchi, K. Yoshida, T. Hirao, *Org. Lett.* **2003**, 5, 4285-4288.
[18] A. Nomoto, T. Moriuchi, S. Yamazaki, A. Ogawa, T. Hirao, *Chem. Commun.* **1998**, 1963-1964.
[19] S. Chowdhury, G. Schatte, H. B. Kraatz, *Dalton Trans.* **2004**, 1726.
[20] L. Lin, A.Berces, H. B. Kraatz, *J. Organomet. Chem.* **1998**, 556, 11-20
[21] D. Gauthier, P. Baillargeon, M. Drouin, Y. L. Dory, *Angewandte Chemie* **2001**, 113, 4771-4774 *Angew. Chem. Int. Edn.* **2001**, 40, 4635-4638.
[22] G.N. Ramachandran, V. Sasisekharan, *Adv. Protein Chem.* **1968**, 23, 283-437.
[23] M.R. Betancourt, J. Skolnick, *J. Mol. Biol.* **2004**, *343*, 635-649.
[24] S. Hovmoller, T. Zhou, T. Ohlson, *Acta Cryst.* **2002**, *D58*, 768-776.
[25] P.A. Karplus, *Prot. Sci.* **1996**, *5*, 1406-1420.
[26] A.D. Solis, S. Rackovsky, *Proteins: Struct. Funct. Genet.* **2002**, *48*, 463-486.
[27] W. Kabsch, C. Sander, *Biopolymers* **1983**, *22*, 2577-2637.

[28] J. Vogt, G. E. Schulz, *Structure with Folding & Design* **1999**, 7, 1301-1309.
[29] A. Pautsch, G. E. Schulz, *Nature Struct. Biol.* **1998**, 5, 1013-1017
[30] P. M. Hwang, R. E. Bishop, L. E. Kay, *Proc. Natl. Acad. Sci. U SA* **2004**, 101, 9618-9623.
[31] L.Vandeputte-Rutten, M. P.Bos, J. Tommassen, P. Gros, *J. Biol. Chem.* **2003**, 278, 24825-24830.
[32] T. D. Clark, J. M. Buriak, K. Kobayashi, M. P. Isler, D. E. McRee, M. R. Ghadiri, *J. Am. Chem. Soc.* **1998**, 120, 8949-8962
[33] S. Krimm, J. Bandekar, *Adv. Protein Chem.* **1986**, 38, 181-364.
[34] A. Barth, C. Zscherp, *Quart. Rev. Biophys.* **2002**, 35, 369-430.

3.6. Supporting Information

3.6.1. Experimental

3.6.1.1. General: All syntheses were carried out in air unless otherwise indicated. CH_2Cl_2 (BDH; ACS grade) used for synthesis was dried (CaH_2) and distilled prior to use. $CDCl_3$ (Aldrich) were dried by, and stored over molecular sieves (8-12 mesh; 4Å effective pore size; Fisher) before use. CD_3CN (Aldrich) was used immediately opening the sealed ampoule. EDC, HOBt, BOP, CSA·2HCl (Aldrich), $MgSO_4$, $NaHCO_3$ (VWR), and 1,1'-$Fc(OH)_2$ was synthesised by known method. Et_3N (BDH; ACS grade) used in the synthesis was used as received. For column chromatography, a column with a width of 2.7 cm (ID) and a length of 45 cm was packed 18-22 cm high with 230-400 mesh silica gel (VWR). For TLC, aluminum plates coated with silica gel 60 F_{254} (EM Science) were used. NMR spectra were recorded on a Bruker AMX-500 spectrometer operating at 500 MHz (^1H) and 125 MHz ($^{13}C\{^1H\}$). Peak positions in both ^1H and ^{13}C spectra are reported in ppm relative to TMS. The ^1H-NMR spectra are referenced to the residual $CHCl_3$ signal at δ 7.27. All $^{13}C\{^1H\}$-NMR spectra are referenced to the $CDCl_3$ signal at δ 77.23 ppm.

3.6.1.2. Synthesis of Cysteamine -Amino acid conjugates

3.6.1.2.1. [Boc-Val-CSA]$_2$ (1): Boc-Val-OH (1.89 g; 10 mmol) was dissolved in 30 ml of DCM. Solid HOBt (1.68 g; 11 mmol) and of EDC•hydrochloride (2.10 g; 11 mmol) were added sequentially. After 20 minutes, the reaction mixture was cooled in an ice bath. To the reactions solution, a solution of CSA dihydrochloride (1.12 g; 5 mmol) in 50 ml of DCM and 2 ml Et_3N was added dropwise over 5 minutes. After completion, the reaction mixture was allowed to warm up and was kept at room temperature for 10 hours under constant stirring. The resulting solution was then washed successively with saturated $NaHCO_3$, 10% citric acid, saturated $NaHCO_3$ and then water. Then it was evaporated under reduced pressure in a rotorvap. The product was purified by column chromatography Silica gel column, (ethyl acetate : hexane =50:50, R_f = 0.33) yellowish white powder. Yield = 79%. ^{1}H NMR (δ, $CDCl_3$) 7.13 (d, 1H, amide NH), 5.80 (m 1H NH attached to Boc), 4.26(s 1H α H of Val), 3.60 (d, 2H, CH_2 attached to NH), 2.80 (m, 2H, CH_2 attached to S), 2.10 (m, 1H, β-H of Val), 1.56 (s, 9H, Boc), 0.97 (d, 3H, Val CH_3), 0.95 (d, 3H, another Val CH_3)

3.6.1.2.2. [Boc-Ile-CSA]$_2$ (2): Procedure for the synthesis is similar to **1**. Column (ethyl acetate: hexane = 75 : 25, R_f = 0.28) white powder. Yield = 82%. ^{1}H-NMR (δ, $CDCl_3$) 7.13 (d 1H amide NH), 5.80 (m 1H NH attached to Boc), 4.26(s 1H α H of Ile), 3.60 (d 2H CH_2 attached to NH), 2.80 (m 2H CH_2 attached to S), 2.10 (m 1H sec. H of Ile. side chain),1.56 (s 9H Boc), 1.3 (2H, CH_2 of Ile) 0.97 (d 3H Ile CH_3), 0.95 (d 3H another Ile CH_3)

3.6.1.2.3. [Boc-Gly-Val-CSA]$_2$ (3): Boc-Gly-OH (0.95 g; 5 mmol) was dissolved in 30 ml of DCM. Solid HOBt (0.84 g; 5.5 mmol) and of EDC•hydrochloride (1.05 g; 5.5 mmol) were added sequentially. After 20 minutes, the reaction mixture was cooled in an ice bath. To the reactions solution, a solution of [Boc-Val-CSA]$_2$ (**1**) (1.38 g; 2.5 mmol) deprotected by the treatment with TFA followed by basification by the addition of tryethyl amine in 50 ml of DCM was added dropwise over 5 minutes. After completion, the reaction mixture was allowed to warm up and was kept at room temperature for 10 hours under constant stirring. The resulting solution was then washed successively with saturated $NaHCO_3$, 10% citric acid, saturated $NaHCO_3$ and then water. Then it was evaporated under reduced pressure in a rotorvap. The product was purified by column chromatography (silica gel ethyl acetate 100%, $R_f = 0.28$) to get the pure product in 60% yield (1.02 g). ^{1}H NMR (δ, $CDCl_3$) 7.33(s, 1H, NH close to Cp) , 7.25 (s, 1H, NH form Val), 6.53 (s, 1H, NH of CSA) 4.02 (d, 1H, α-H of Val), 3.86 (m, 2H, α-H of Gly), 3.57 (d, 2H, CH_2 attached to NH of CSA), 2.84 (d, 2H, CH_2 attached to S of CSA), 1.91(d, 1H, β-H of Val), 1.46 (s, 9H, CH_3 of Boc), 0.96 (d, 3H, CH_3 of Val), 0.94 (d, 3H, another CH_3 of Val)

3.6.1.2.4. [Boc-Gly-Ile-CSA]$_2$ (4): Procedure for the synthesis is similar to **3**. Column, (ethyl acetate : hexane = 75:25, $R_f = 0.31$) white powder. Yield = 82%. ^{1}H-NMR (δ, $CDCl_3$) 7.21(s, 1H, NH close to Cp) , 7.15 (s, 1H, NH form Ile) , 5.68 (s, 1H, NH of CSA) 4.51 (d, 1H, α-H of Ile), 3.69 (m, 2H, α-H of Gly), 3.59 (d, 2H, CH_2 attached to NH of CSA), 2.85 (d, 2H, CH_2 attached to S of CSA), 1.90 (d, 1H, β-H of Ile), 1.59 (m, 2H, CH_2 of Ile) 1.44 (s, 9H, CH_3 of Boc), 0.96 (d, 3H, CH_3 of Ile), 0.91 (d, 3H, another CH_3 of Ile)

3.5.1.3. Synthesis of Macrocycles

3.5.1.3.1. Fc[CO-Gly-Val-CSA]$_2$ (5): In an ice-bath, ferrocenedicarboxylic acid (0.055 g; 0.2 mmol) was dissolved in dichloromethane (10 mL), followed by the addition of HOBt (0.062 g; 0.4 mmol) and EDC (0.078 g; 0.4 mmol). After half an hour, the reaction mixture was diluted to 300 ml by dichloromethane. In another flask, cystamine dihydrochloride (**2**) (0.045 g; 0.2 mmol) was dissolved in 10 ml of dichloromethane and 1 ml of triethylmine.The resulting solution was diluted to 100ml. In another 2L flask 0.132 g (0.2 mmol) of [Boc-Gly-Val-CSA]$_2$(**3**) deprotected by the treatment with TFA followed by basification by the addition of triethylamine. Then it was diluted to 1400ml by dry DCM. To this solution was added the first solution over 5 minutes in ice bath. Stirring was continued for 48 hours at room temperature. Then the solution was washed consecutively with saturated $NaHCO_3$, 10% aqueous citric acid, saturated aqueous $NaHCO_3$ and water. The organic phase was then dried over anhydrous Na_2SO_4, and then evaporated at 25^0C under reduced pressure to get the crude product. It was then purified by flash chromatography on silica (EtOAc:MeOH = 95:5 v/v, R_f = 0.30) to get 77 mg (42 %) of the desired compound. FTIR (Resolusion 1 cm^{-1}) : 1640 cm^{-1}, 1682 cm^{-1} (C=O), 1536 cm^{-1} (C-N of amide) 3280 cm^{-1} (N-H stretching) UV-vis: (λ in nm, [ε in $M^{-1}cm^{-1}$]): 442 [280] HRMS (ES): Calc. for $C_{30}H_{42}N_6O_6FeS_2$ $[M]^+$, 702.6870 observed mass $[M+1]^+$ 703.6921; ^{1}H NMR (δ, CD_3CN): 8.27 (s, 1H, NH closest to Cp), 7.18 (s, 1H, NH form Val), 6.76 (d J=1.7Hz NH from CSA), 4.86 (d *j*=12.6Hz 1H αH of Val), 4.61 (s 1H *ortho*-H of Cp), 4.54 (s, 1H, another *ortho*-H of Cp), 4.37 (s, 1H, *meta*-H of Cp), 4.35 (s, 1H, another *meta*-H of Cp), 3.67 (m, 2H, α-H of Gly) 3.47 (m, 2H, CH_2

attached to NH of CSA), 2.83 (m, 2H, CH_2 attached to S of CSA), 2.12 (m, 1H, β-H of Val), 0.93 (d, 3H, CH_3 of side chain of Val) 0.92 (d, 3H, another CH_3 of side chain of Val); $^{13}C\{^1H\}$-NMR (δ, CD_3CN): 172.1 (C=O closest to Cp), 171.9 (C=O from Gly), 169.8 (C=O of Val), 76.4 (*ipso*-C of Cp), 72.3 (*ortho*-C Cp), 71.6 (another *ortho*-C Cp), 71.3 (*meta*-C Cp), 70.1 (another *meta*-C Cp), 59.1 (α-C of Val), 42.6 (αC of Gly), 38,5 (CH_2 of CSA attached to NH), 38.1 (CH_2 of CSA attached to S), 30.7 (β-C of Val), 18.9 (CH_3 of Val), 17.5 (another CH_3 of Val).

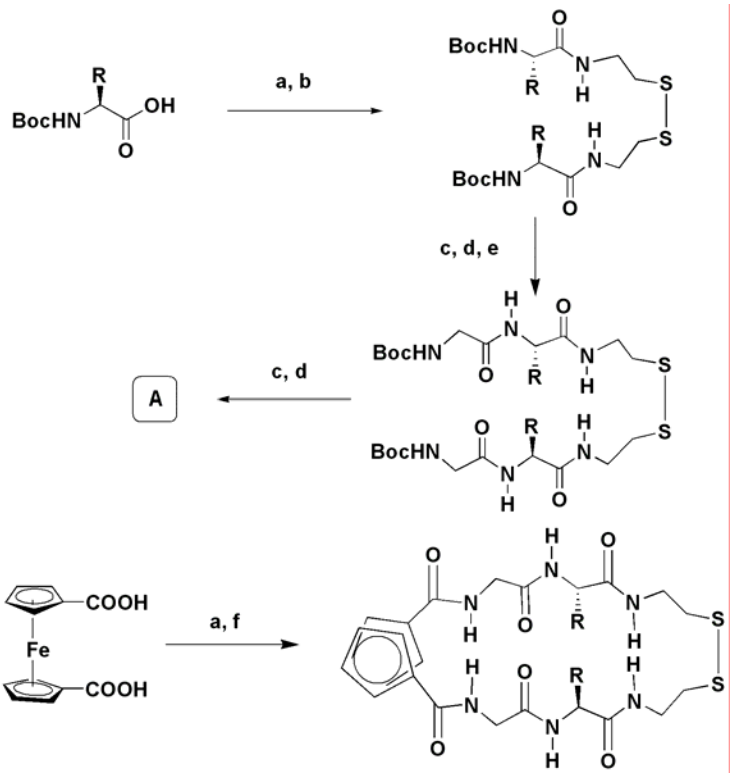

R=isopropyl (**5**) and isobutyl (**6**)

Scheme 3.S1. Synthesis of ferrocene-cyclopeptides : (a) EDC/HOBt in CH_2Cl_2; (b) CSA• 2HCl and TEA solution in CH_2Cl_2; (c) 50% TFA in CH_2Cl_2, stirred for half an hour (d) TEA in ice bath (e) Boc-amino acid activated by EDC/HOBT (f) solution of A at 0.05mM dilution and stirred for 48 hours.

3.5.1.3.2. Fc[CO-Gly-Ile-CSA]$_2$ (**6**): Synthesis procedure is similar to **5**. Column on silica (EtOAc:MeOH = 95:5 v/v, R_f = 0.30), yield 49 %. FTIR: 1640 and 1680 cm^{-1} (C=O), 1535 cm^{-1} (C-N of amide) 3282 cm^{-1} (N-H stretching); UV-vis: (λ in nm, [ε in $M^{-1}cm^{-1}$]): 441 [278]; HRMS (ES): Calc. for $C_{32}H_{46}N_6O_6FeS_2$ $[M]^+$ 730.4221 observed mass $[M+1]^+$ 731.4256 ; ^{1}H-NMR (δ, CD_3CN): 8.41 (s, 1H NH closest to Cp), 7.35 (s, 1H NH form Ile), 6.70 (d, J = 5.7 Hz, NH from CSA), 4.87 (d, J = 12.6 Hz, 1H, αH of Ile), 4.61 (s, 1H, *ortho*-H of Cp), 4.53 (s, 1H, another *ortho*-H of Cp), 4.36 (s, 1H, *meta*-H of Cp), 4.34 (s, 1H, another *meta*-H of Cp), 3.71 (m, 2H αH of Gly), 3.64 (m, 2H, CH_2 attached to NH of CSA), 2.85 (m, 2H, CH_2 attached to S of CSA), 1.88 (m, 1H, β-H of Ile), 1.54 (d, 2H, CH_2 of Ile), 0.95 (m, 2H, CH_3 of Ile), 0.87 (d, 2H, CH_3 of Ile) ; $^{13}C\{^1H\}$-NMR (δ, CD_3CN): 172.5 (C=O closest to Cp), 171.2 (C=O from Gly), 170.9 (C=O from Ile), 76.0 (*ipso*-C of Cp), 72.4 (*ortho*-C Cp), 71.7 (another *ortho*-C Cp), 71.4 (*meta*-C Cp), 70.2 (another *meta*-C Cp), 58.4 (αC of Ile), 43.3 (αC of Gly), 39.1 (CH_2 of CSA attached to NH), 38.8 (CH_2 of CSA attached to S), 37.6 (β-C of Ile), 25.0 (CH_2 of Ile) 15.9 (CH_3 of Ile), 12.6 (another CH_3 of Ile).

3.6.2. Structural Study

3.6.2.1. FT-IR study

FT-IR spectra were recorded in BIO-RAD, FTS-40 in solid state (KBr) from 400 cm^{-1} to 4000cm^{-1}.

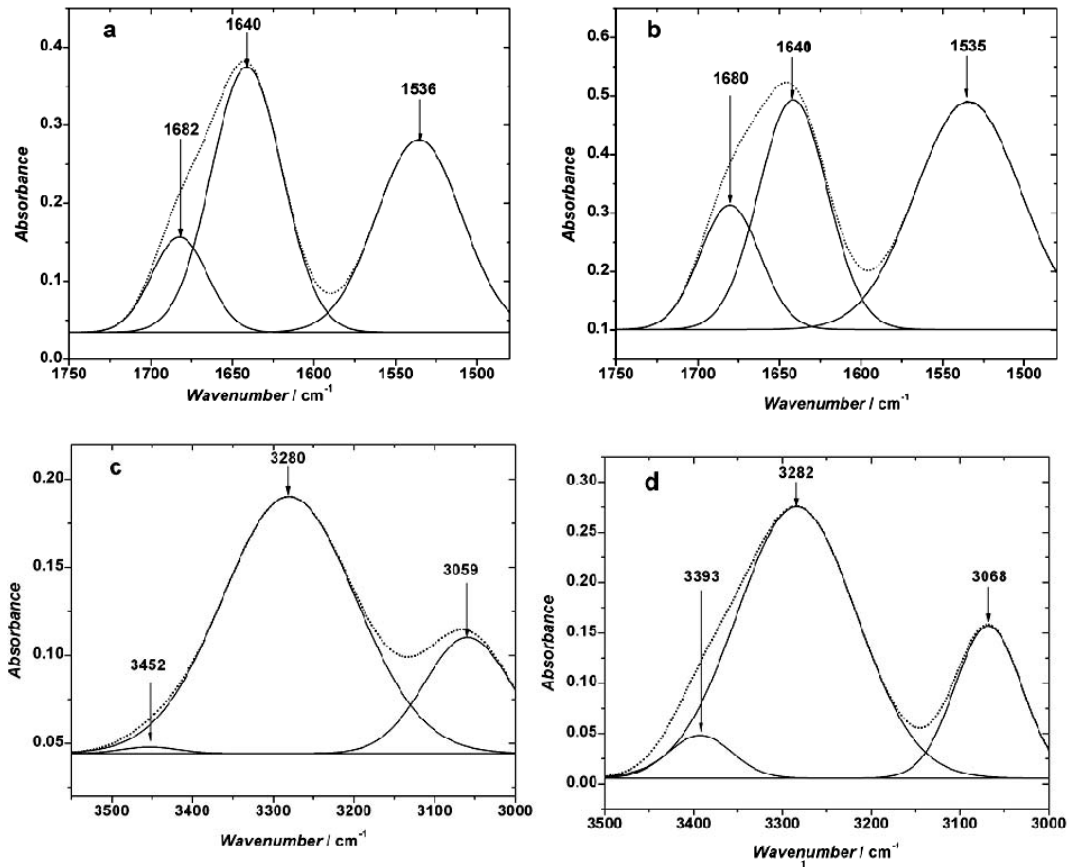

Figure 3.S1. Representative partial FT-IR spectrum (1 cm^{-1} resolution) for Fc[Gly-Val-CSA]$_2$(**5**) and Fc[Gly-Ile-CSA]$_2$(**6**), in the solid state (KBr). Components peaks are obtained by deconvolution of the original spectrum with single component Gaussian function using origin software (a) amide-I and amide-II region of **5**, (b) amide-I and amide-II region of 6 and (c) amide-A region of 5 (d) amide-A region of 6.

3.6.2.2. Determination of Water Content in the Crystals by ^{1}H-NMR Spectroscopy

NMR Spectra were obtained in DMSO-D6.Crystals were made by the same method as was used to prepare the crystal for X-ray diffraction i.e. by diffusing hexanes in the 1 mM solution of 5% methanol in chloroform (all solvents used were undistilled).

Crystallization was done in crystallization tubes of approximate same dimension as an NMR tube. After one day crystals were taken out washed by ether, dried under vacuum and put in NMR tube. 400μL of DMSO was added. In an another blank NMR tube, 400μL of DMSO was taken from the same bulk. Immediately tubes were closed and wrapped carefully to avoid air entry.

For blank solvent the integration of water peaks were calibrated to 1 and the corresponding value for the solvent residual peaks were noted. In sample solution the integration of solvent residual peak were calibrated to the value of the blank. Thus the integration of corresponding water peak was the summation of water in the solvent plus the water from the crystal. In this case the two protons from cysteamine residue were merging to the water peak and was taken into consideration. The integration of the α-proton of Valine residue was taken as standard and each molecule contains two alpha protons. Calibrating the integration of α-protons of Valine to two, the amount of water per molecule was calculated.

3.6.2.3. X-ray Crystallography

Crystalllization of Fc[Gly-Val-CSA]$_2$(**5**) was done by slowly diffusing hexane to the very dilute solution in metanol and chloroform mixture. Yellow rod shaped crystal of approximate dimension of 0.15 × 0.15 × 0.15 mm suitable for x-ray crystallography was deposited after 3 days. All measurements were made on a Nonius KappaCCD 4-Circle Kappa FR540C diffractometer using monochromated Mo K_α radiation (λ = 0.71073 Å) at -100 °C. An initial orientation matrix and cell was determined from 10 frames using ϕ scans.[S1] Data were measured using ϕ- and ω-scans. [S1] Data reduction

was performed with the HKL DENZO and SCALEPACK software [S2], which corrects for beam inhomogeneity, possible crystal decay, Lorentz and polarisation effects. A multi-scan absorption correction was applied (SCALEPACK,).[S2]

The 20276 collected reflections were merged (R_{int} = 0.0704) to provide 6518 data, of which all were unique (R_{sigma} = 0.0640) and 5690 observed ($I > 2\sigma(I)$) reflections (SHELXL97-2).[S5] The ranges of indices were $-16 \le h \le 16$, $-19 \le k \le 15$, $-16 \le l \le 19$ corresponding to a θ-range of 1.88 to 24.71°. The structure was solved using direct methods (SIR-97 [S4]) and refined by full-matrix least-squares method on F^2 with SHELXL97-2.[S5] The non-hydrogen atoms were refined anisotropically. Hydrogen atoms were included at geometrically idealized positions (C-H bond distances 0.95/0.98/0.99 Å) and were not refined. The isotropic thermal parameters of the hydrogen atoms were fixed at 1.2 times that of the preceding carbon atom. Attempts to refine peaks of residual electron density as water were unsuccessful. The data were corrected for disordered electron density through use of the SQUEEZE [S7] procedure as implemented in PLATON.[S8] A total solvent-accessible void volume of 774.9 Å^3 (20.1% of the unit cell volume) with a total electron count of 241 was found in the unit cell. Electron density identified in solvent accessible areas are given in Table S1.

Table 3.S1. Electron density per void and volumes.

No. of Void	Centre of Void			Volume [Å^3]	% volume	Electron Count/void
	X_{av}	X_{av}	X_{av}			
1	-0.024	0.025	0.000	386	7.5	120
2	0.007	0.7504	0.500	386	1.2	120

Table 3.S2. Crystal data and structure refinement for compound **5**.

Empirical formula	$C_{30}H_{42}FeN_6O_6S_2$
Formula weight	702.67
Temperature	173(2) K
Wavelength	0.71073 Å
Crystal system	orthorhombic
Space group	$P2_12_12_1$ (No. 19; Hall: P2ac 2ab)
Unit cell dimensions	a = 14.4080(4) Å b = 16.2650(5) Å c = 16.4770(4) Å; α= 90° β= 90°γ = 90°
Volume	3861.32(19) $Å^3$
Z	4
Density (calculated)	1.209 Mg/m^3
Absorption coefficient	0.543 mm^{-1}
F(000)	1480
Crystal size	0.15 x 0.15 x 0.15 mm^3
Theta range for data collection	1.88 to 24.71°.
Index ranges	-16<=h<=16, -19<=k<=15, -16<=l<=19
Reflections collected	20274
Independent reflections	6518 [R(int) = 0.0704]
Completeness to theta = 24.71°	99.7 %
Max. and min. transmission	0.9230 and 0.9230
Refinement method	Full-matrix least-squares on F^2
Data / restraints / parameters	6518 / 0 / 410
Goodness-of-fit on F^2 [6]	1.087
Final R indices [I>2sigma(I)]	R1 = 0.0485, wR2 = 0.0983
R indices (all data)	R1 = 0.0612, wR2 = 0.1021
Absolute structure parameter	0.046(19)
Largest diff. peak and hole	0.397 and -0.421 $e.Å^{-3}$

Expected volume for H_2O solvent molecules is 40 $Å^3$. The modified data improved the *R*-factors (before SQUEEZE: R_1 = 0.1010, wR_2 = 0.2631; largest difference peak and hole, 3.07 and -0.81 $e^-/Å^3$; after SQUEEZE: R_1 = 0.0485, wR_2 = 0.1021; largest difference peak and hole, 0.397 and -0.421 $e^-/Å^3$). Derived values (formula weight, density, absorption coefficient) do not contain the contribution of the disordered solvent. The final cycle of full-matrix least squares refinement using F^2 (SHELXL97-2,)[S5] was

based on 6518 reflections and 410 variable parameters. Neutral atom scattering factors for non-hydrogen atoms and anomalous dispersion coefficients are contained in the SHELXTL-NT 6.14[S3] program library.

Table 3.S3. Hydrogen bond distances [Å] for compound **5**.

Intramolecular:	
N(21)(H)····O(12)	2.784(4)
N(11)(H) ····O(22)	3.013(4)
N(23)(H) ····O(13)	2.848(4)
Intermolecular:	
O(23)····(H)N(13))*	2.823(4)
N(13)(H)····O(23)**	2.823(4)
O(11)····(H)N(22)'	3.036(4)
N(12)(H)····O(21)'	2.898(4)
N(22)(H)····O(11)"	3.036(4)
O(21)····(H)N(12)"	2.898(4)

Symmetry transformations used to generate equivalent atoms:

*:	-x, y - 0.5, -z + 0.5
**:	-x, y + 0.5, -z + 0.5
':	-x + 0.5, -y + 1, z - 0.5
":	-x + 0.5, -y + 1, z + 0.5

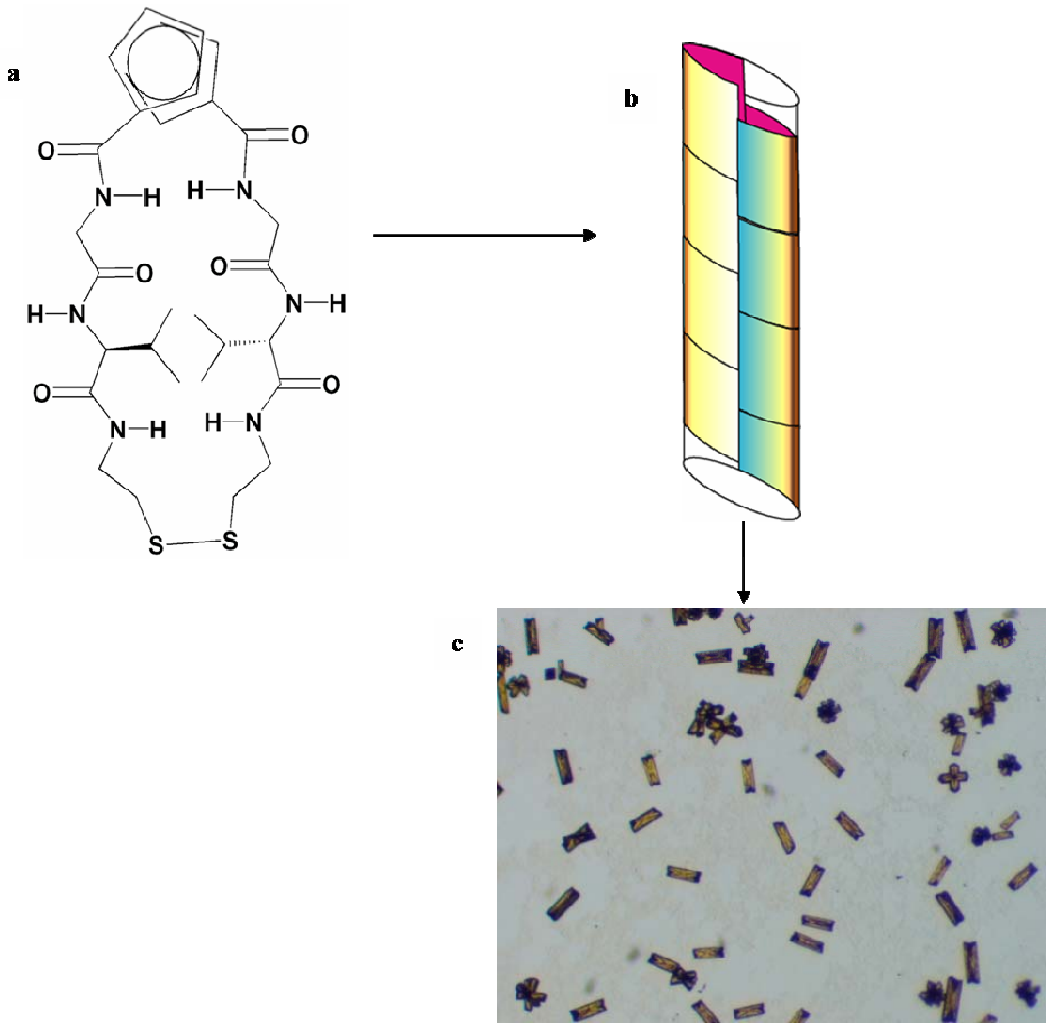

Figure 3.S2. (a) Molecular structure of compound Fc[CO-Gly-Val-CSA]$_2$(**5**), (b) Representation of barrel formed by the tiling of the cyclopeptides and (c) Picture of the crystals of compound five formed by slow evaporation of solvent from the solution in methanol and chloroform on glass slide. For slow evaporation the glass slide was put inside a beaker, covered by aluminium foil.

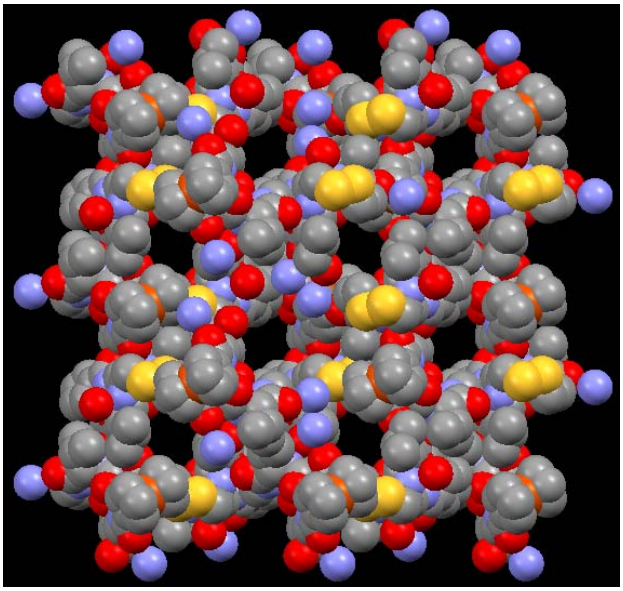

Figure 3.S3. Crystal structure of Fc[CO-Gly-Val-CSA]$_2$(**5**) in space filling mode, diffused water molecules are taken out (a) Showing the three dimensional network of pores.

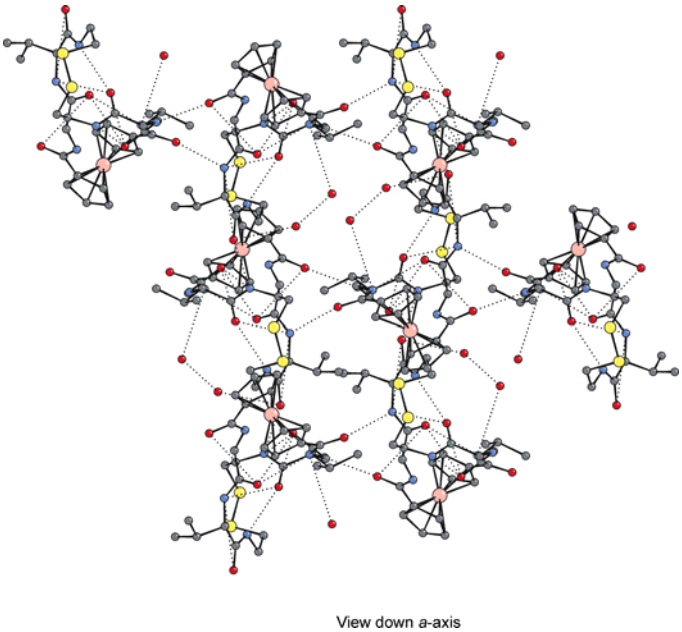

Figure 3.S4. Crystal structure of Fc[CO-Gly-Val-CSA]$_2$(**5**) showing the hydrogen bonding between diffused water molecules, between the molecules of the barrel and the diffused water molecules and the molecules of the barrel.[S9]

3.6.3 Supplementary References

[S1] *COLLECT* data collection software, Nonius B.V., **1998**.

[S2] *HKL DENZO and SCALEPACK v1.96*: Z. Otwinowski, W. Minor, *Processing of X-ray Diffraction Data Collected in Oscillation Mode, Methods in Enzymology*, Volume 276: *Macromolecular Crystallography*, Part A, Carter, C. W., Jr., Sweet, R. M., Eds.; Academic Press: San Diego, CA, **1997**; pp. 307-326.

[S3] *SHELXTL-NT 6.14, XPREP, Program Library for Structure Solution and Molecular Graphics*; Bruker AXS, Inc.: Madison, WI, **2000-2003**.

[S4] A. Altomare, G. Cascarano, C. Giacovazzo, A. Guagliardi, A. G. G. Moliterni, M.C. Burla, G. Polidori, M. Camalli, R. Spagna, *SIR-97, A package for crystal structure solution by direct methods and refinement*; *J. Appl. Crystallogr.* **1999**, *32*, 115.

[S5] G. M. Sheldrick, *SHELXL97-2, Program for the Solution of Crystal Structures;* University of Göttingen, Göttingen, Germany **1997**.
Function minimized: $\Sigma w(|F_o|^2-|kF_c|^2)^2$; k: overall scale factor. Refinement on F_o^2 for all reflections (all of these having $F_o^2 \geq -3\sigma(F_o^2)$). Weighted R-factors wR_2 and the values for *GooF* are based on F_o^2; conventional R-factors R_1 are based on F_o,with F_o set to zero for negative F_o^2. The observed criterion of $F_o^2 > 2\sigma(F_o^2)$ is used only for calculating R_1, and is not relevant to the choice of reflections for refinement. R-factors based on F_o^2 are statistically about twice as large as those based on F_o, and R-factors based on ALL data will be even larger.

[S6] Standard deviation of an observation of unit weight (*goodness-of-fit* on F^2):
$GooF = \{\Sigma[w(F_o^2-F_c^2)^2]/(n - p)\}^{1/2}$
n: number of reflections, p: number of parameters

[S7] *SQUEEZE*: P. Sluis, A. L. van der Spek, *Acta Crystallogr.* **1990**, 46A, 194.

[S8] *PLATON*: A Multipurpose Crystallographic Tool, Utrecht University, Utrecht, The Netherlands; A. L. Spek, *Acta Crystallogr.*, **1990**, 46A, C34.

[S9] I.A. Karle, J.L. Flippen-Anderson, S. Agarwalla, P. Balaram, *Biopolymers* **1994**, 34, 721-735.

Chapter 4

Synthesis and Structure of Extended *β*-Sheet Like Peptides Using Ferrocene as Molecular Scaffold

4.0. Connecting Text

Acyclic Fc-peptide conjugates do not form inter-strand intramolecular H-bond beyond the first amino acid. They even adopt γ-turn through the formation of intra-strand H-bonding. In this chapter, we have described the rational design and preparation of two Fc-tripeptide conjugates, Fc[CO-Gly-Val-Cys(Bz)-OMe]$_2$ and Fc[CO-Gly-Ile-Cys(Bz)-OMe]$_2$. Structural studies in solution and solid states showed the formation of extended β-sheet-like structures. This shows that, by selecting the proper sequence of amino acids, it would be possible to extend the inter-strand H-bonding in acyclic Fc-peptide conjugates and longer β-sheet like structures could be achieved. Hence, this is a critical method for controlling the structure of peptides.

This chapter is the reproduced from the prepared manuscripts to be submitted to Organic Letters. Permissions have been obtained from the co-authors G. Schatte and H.-B. Kraatz. All experimental works with the exception of crystallographic analysis were carried out by me. In addition I wrote the initial draft of the manuscript.

4.1. Introduction

β-sheets are the crucial secondary structural elements of proteins. Due to a very high tendency of self-aggregation and complexity of their folding, *β*-sheet models are difficult to study. Out of numerous attempts in preparing the *β*-sheet models of

peptides,[5] conjugation of peptides with non-natural scaffolds has been a successful strategy.[6] Ferrocene, an organometallic molecule having two easily rotating parallel cyclopentadiene (Cp) rings, has been widely explored as a molecular scaffold to impart a specific secondary structure to the attached peptide.[7] These conjugates self-assemble through H-bonding, resulting in novel and interesting supramolecular architectures. It has been found that podant amino acids and peptide attached to the two different Cp rings engage in H-bonding interaction akin to that found in *β*-sheet peptides. The design of these Fc-conjugates have been systematically studied by various researchers.[8] It is observed that when a single amino acid is linked to each Cp ring of ferrocene dicarboxylic acid through an amide bond, they form 10-member intramolecularly H-bonded rings, as is found in antiparallel *β*-sheets (**1** in Figure 4.1).

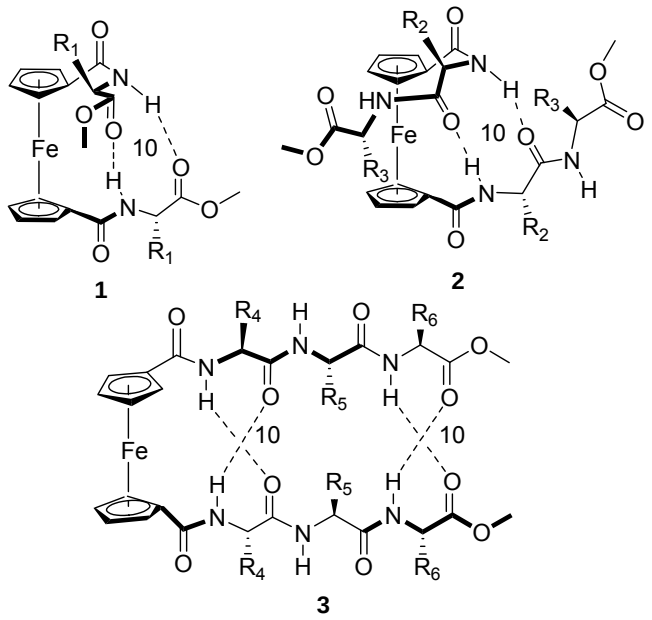

Figure 4.1. Formation of *β*-sheet-like conformations of disubstituted ferrocene-peptide conjugates with the different lengths of peptide strands.

However, as the peptide chain is extended to a dipeptide, the two peptide chains point in opposite directions, giving rise to a helical arrangement with respect to Fc moiety (**2** in

Figure 4.1). Hirao and co-workers have reported Fc-dipeptide-heterocycle conjugates, where the peptide strands are engaged in intrastrand H-bonding with the formation of γ-turn motifs.[9] Apparently, it seems that it is not possible to align the conjugated peptide strands in an extended interstrand H-bonded conformation. Here, we report the design of two peptide conjugates of ferrocene that adopt a β-sheet-like conformation through the formation of extended intramolecular interstrand H-bonding (**3** in Figure 4.1).

4.2. Results and Discussions

In our earlier study,[10] we attempted to get extended H-bonded β-sheet-like structures by cyclization, and we realized that it might be possible to prepare acyclic Fc-peptide conjugates in extended H-bonded form if the proper sequence of amino acids is chosen. The systems with Gly as the first amino acid attached to Fc provide the maximum flexibility to the podand peptide chains. The following the amino acids with high propensity for β-sheet seemed to be able to maintain β-sheet-like conformation in extended form. In this present study we have explored that hypothesis. With the aforementioned idea, we selected the sequences Gly-Val-Cys and Gly-Ile-Cys and conjugated to 1,1'-Fc-dicarboxylic acid through Gly. Structural investigation of these conjugates has been performed in the solution and solid states, which reveal the formation of extended β-sheet-like conformation of the peptide backbone.

Suitably protected dipeptides, Boc-Val-Cys(Bz)-OMe (**4**) and Boc-Ile-Cys(Bz)-OMe(**6**) and tripeptides Boc-Gly-Val-Cys(Bz)-OMe (**5**) and Boc-Gly-Ile-Cys(Bz)-OMe (**7**) were synthesized by the standard solution peptide coupling method using HBTU as a coupling reagent. The target compounds Fc[CO-Gly-Val-Cys(Bz)-OMe]$_2$ (**8**) and

Fc[CO-Gly-Val-Cys(Bz)-OMe)$_2$ (**9**) were synthesized by coupling the tripeptides to ferrocene dicarboxylic acid using the same coupling techniques. All the compounds were fully characterized spectroscopically (see section 4.6.1.2.). In compound **8,** the ^{1}H-NMR spectrum shows that the NH of both Gly and Cys resonates at down fields, respectively at 8.64 ppm and 7.14 ppm which indicates their strong involvement in H-bonding. This is expected for the proposed structure, where these NHs are supposed to participate in intramolecular H-bonding. The NH of Val resonates at higher field, δ 6.55, suggesting its weaker involvement in H-bonding. This fact also correlates with the proposed structure. A similar ^{1}H-NMR resonance pattern has been observed in compound **9** (where chemical shifts are δ 8.68, 7.20 and 6.63 respectively for Gly, Cys and Ile). This hypothesis was further tested by a variable concentration ^{1}H-NMR study (see Figure 4.2).

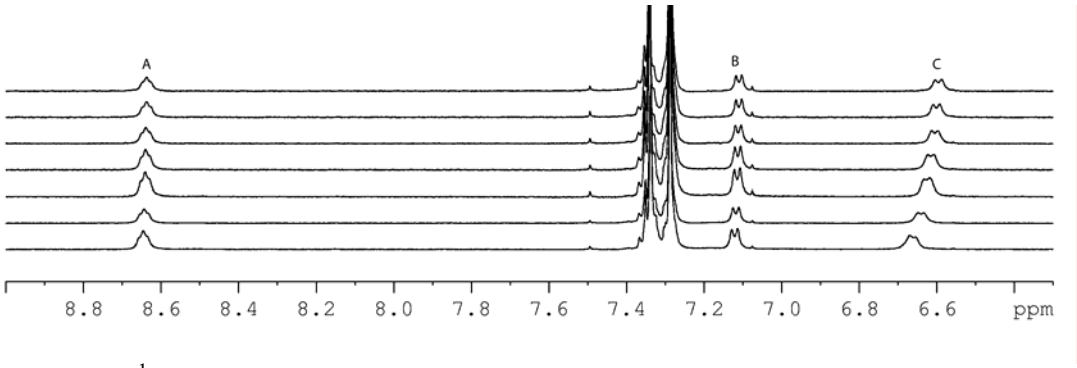

Figure 4.2. ^{1}H-NMR spectra of the amide regions of compound **8**, Concentration (mM) from bottom to top; 2.00, 1.60, 1.33, 1.14, 1.00, 0.98 and 0.80. Peak A for Gly NH, B for Cys NH and C for Val NH.

In this study, it is observed that as the concentration of the solution decreases, the chemical shifts for NHs of Val in **8** and Ile in **9**, shift towards upfield, suggesting their involvement in intermolecular hydrogen bonding. On the other hand, the chemical shifts

for NHs of Gly and Cys, in both the compounds remain almost constant with the variation of concentration.

Circular dichroism (CD) spectroscopy is a reliable tool to evaluate the conformation of Fc-conjugates by using the Fc band (+ or –) at about 450 nm and has been extensively used to determine the conformation of Fc-peptide conjugates. CD spectral study (Figure 4.3) of our proposed *β*-sheet-like peptide conjugates show the positive absorption for ferrocene d-d transition at around 480 nm, which is the indication of the formation of *P*-helical structure as expected for intramolecularly hydrogen bonded L-amino acid conjugates of disubstituted ferrocene. The negative absorption bands around 217 and 219 nm respectively in **8** and **9** indicate the presence of *β*-sheet conformation of the peptide backbones.

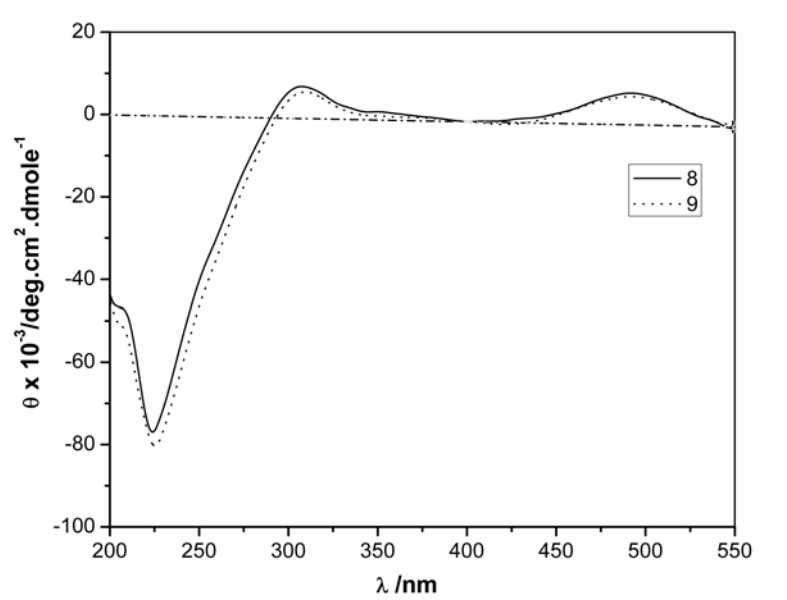

Figure 4.3. CD spectra of compound **8** and **9** in CH_3CN solution at 25ºC, showing the presence of *P*-helical arrangement of podand peptides with respect to ferrocene and signature of *β*-sheet conformations.

Suitable crystals of compound **8** and **9** were obtained by slow evaporation of solvents from solutions in chloroform at 0ºC temperature. Single crystal structural analysis by X-ray diffraction show that both of the compounds crystallize in the $P2_12_12_1$ space group. The molecular structures of the compounds **8** and **9**, are shown in Figure 4.4.

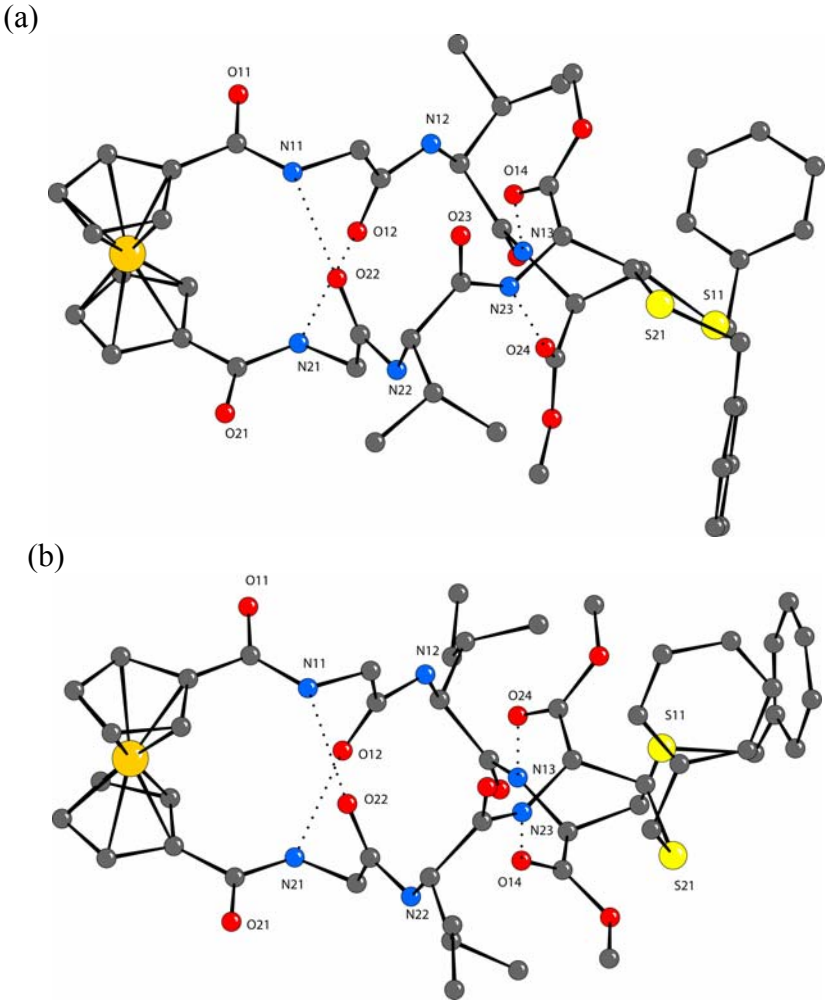

Figure 4.4. Molecular structures of compounds **8** (a) and **9** (b) as obtained from single crystal X-ray diffraction study, showing the extended β-sheet-like forms. Hydrogen atoms are omitted for clarity. Grey spheres represent carbon, red spheres oxygen, blue spheres nitrogen, yellow spheres sulfur and orange spheres represent iron atoms.

The crystal structures clearly show the formation of extended β-sheet conformation. In both the molecules **8** and **9**, several intramolecular H-bondings are observed between the C=O group of one peptide strand and the (H)N group of other strand (O12···N21 = 2.846 Å, O22···N12 = 2.915 Å, O14···N23 = 3.082 Å and O24···N13 = 3.054 Å in **8** and O12···N21 = 2.825 Å, O22···N12 = 2.887 Å, O24···N13 = 3.341 Å and O14···N23 = 3.125 Å in **9**). It is observed that the H-bond distances involving Gly-NH are shorter, which correlates with the downfield shift of the resonances in ^{1}H-NMR spectroscopy. The longer H-bonds involving Cys-NH may be due to the steric repulsion between the bulky protecting groups on Cys.

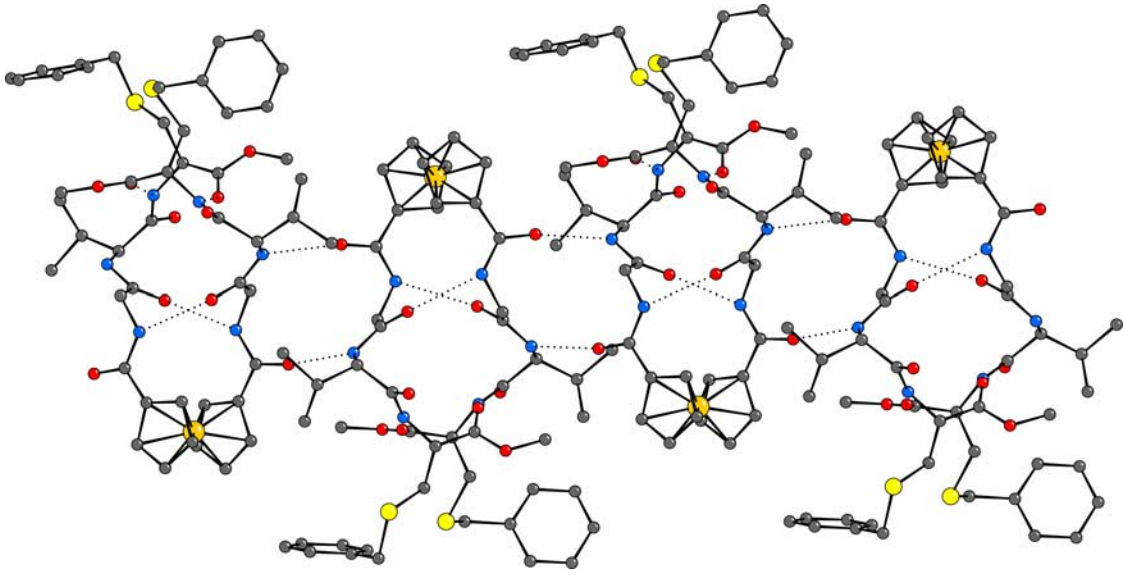

Figure 4.5. Intermoleculecular arrangement of **8** showing the formation of sheet-like assembly. The intermolecular hydrogen bonding distances are O11···N22* = 2.869 Å, and N12···O22** = 3.064 Å; * = -x + ½, -y, z - ½, ** = -x + ½, -y, z + ½.
Compound **9** shows the identical supramolecular assembly. The intermolecular hydrogen bonding distances are O11···N22* = 2.926 Å, and N12···O22** = 2.894 Å; * = -x + 1, y + ½, -z + ½, ** = -x + 1, y - ½, -z + ½.

Each single molecule is linked to two other molecules via intermolecular H-bonding (O11···N22* = 2.869 Å, and N12···O22** = 3.064 Å in **8** and O11···N22* = 2.926 Å and N12···O22** = 2.894 Å in **9**) to form the sheet like continuous assembly (Figure 4.4). The intermolecular H-bonding interactions between head-to-tail connected ferrocene peptides results in the formation of a 14-member antiparallel β-sheet like structure.

FT-IR is also a powerful technique in examining the secondary structure of peptides.[11] Absorptions in the Amide-I region offer a characteristic signature that allows to distinguish an α-helix, a β-sheet and a random coil

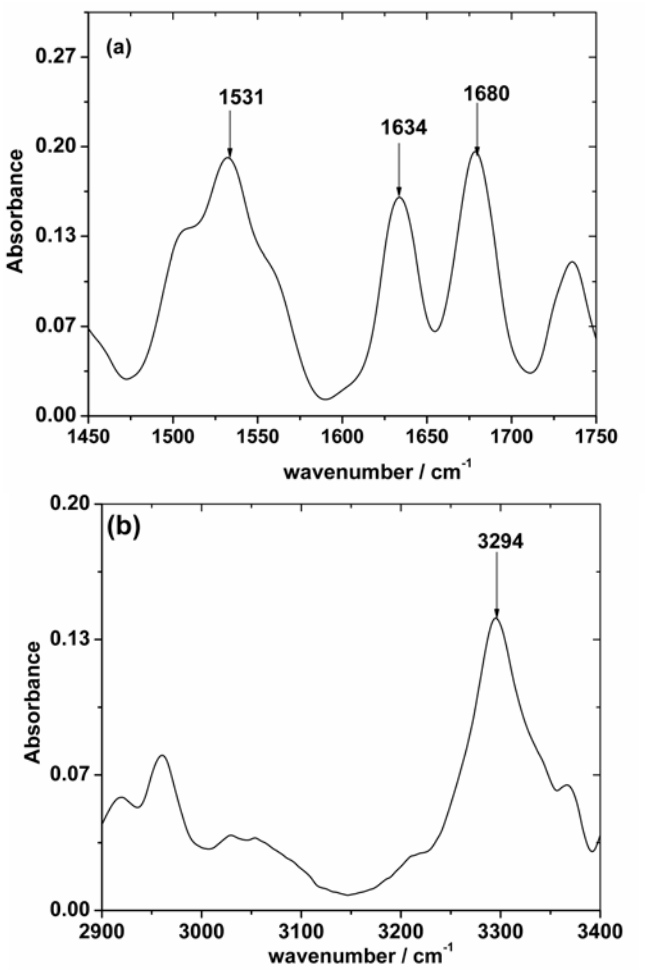

Figure 4.6. FTIR spectroscopy of **8** showing (a) amide-I, amide-II and (b) amide-A regions.

conformation. The FT-IR spectrum of compound **8** in the solid state exhibits amide-I bands at 1634 cm^{-1} and 1680 cm^{-1} and an amide-II at 1531 cm^{-1}, which are the characteristic peaks for β-sheet conformation.[11,12] The IR absorptions of **9** (1638 cm^{-1}, 1679 cm^{-1} and 1533 cm^{-1} respectively) are identical to those of compound **8** (see Figure 4.S1).This also indicates that the structures of **8** and **9** are similar in the solid state. In Amide-A regions the absorptions are 3294 cm^{-1} and 3282 cm^{-1} for **8** and **9** respectively suggesting the involvement of N-Hs in H-bonding which is expected in the proposed structures.

4.3. Conclusions

In conclusion, we have designed the Fc-peptides conjugates which can adopt extended β-sheet-like conformations. The proposed structures have been confirmed by NMR, CD and, IR and X-ray crystallography. These are the first examples of extended β-sheet conformation in acyclic Fc-peptide conjugates.

4.4. Acknowledgements: We acknowledge support from NSERC in the form of an operating grant. H.-B. K. is the Canada Research Chair in Biomaterials.

Supporting information describing synthesis characterization of **8** , **9** and intermediates, IR spectra of **9** and X-ray structural data for compound **8** and **9** is presented below, after references.

4.5. References

[1] J. J. Osterhout, *Protein Peptide Lett.* **2005**, *12*, 159-164

[2] (a) M. A. Shogren-Knaak, P. J. Alaimo, K. M. Shokat, *Annu. Rev. Cell Dev. Biol.* **2001**, 17, 405-433; (b) J. D. Sadowsky, M. A. Schmitt, H. S. Lee, N. Umezawa, S. M. Wang, Y. Tomita, S. H. Gellman, *J. Am. Chem. Soc.* **2005**, 127, 11966-11968.

[3] (a) M. Zasloff, *Nature* **2002**, 415, 389-395; (b) M. A. Schmitt, B. Weisblum, S. H. Gellman, *J. Am. Chem. Soc.* **2004**, 126, 6848-6849; (c)S. Fernandez-Lopez, H. S. Kim, E. C. Choi, M. Delgado, J. R. Granja, A. Khasanov, K. Kraehenbuehl, G. Long, D. A. Weinberger, K. M. Wilcoxen, M. R. Ghadiri, *Nature* **2001**, 412, 452-455.

[4] (a) V. Balzani, A. Credi, F. M. Raymo and J. F.Stoddart, *Angew. Chem. Int. Ed.* **2000**, 39, 3349-3391.(b) S. G. Zhang, *Nature Biotech.* **2003**, 21, 1171-1178; (c) S. Hecht, *Mater. Today* **2005**, 48-55.

[5] (a) J. P. Schneider, J. W. Kelly, *Chem. Rev.* **1995**, 95, 2169-2187; (b) T. A. Martinek, G. K. Toth, E. Vass, M. Hollosi, F. Fulop, *Angew. Chem. Int. Ed.* **2002**, 41, 1718-1721; (c) W. A. Loughlin, J. D. A. Tyndall, M. P. Glenn, D. P. Fairlie, *Chem. Rev.* **2004**, 104, 6085-6117; (d) S. Aravinda, N. Shamala, R. Rajkishore, H. N. Gopi, P. Balaram, *Angew. Chem. Int. Ed* **2002**, 41, 3863; (e) J. Venkatraman, G. A. N. Gowda, P. Balaram, *J. Am. Chem. Soc.* **2002**, 124, 4987.

[6] R. M. Hughes, M. L. Waters, *Current Opin. Struct. Biol.* **2006**, 16, 514; (b) T. Moriuchi, T. Hirao, *Chem. Soc. Rev.* **2004**, 33, 294.

[7] (a) R. S. Herrick, R. M. Jarret, T. P. Curran, D. R. Dragoli, M. B. Flaherty, S. E. Lindyberg, R. A. Slate, L. C. Thornton, *Tetrahedron Lett.* **1996**, 37, 5289-5292; (b) T. Moriuchi and T. Hirao, *Chem. Soc. Rev.*, **2004**, 33, 294–301.

[8] (a) D. R. van Staveren, N. Metzler-Nolte, *Chem. Rev.* **2004**, 104, 5931; (b) S. I. Kirin, H. B. Kraatz, N. Metzler-Nolte, *Chem. Soc. Rev.* **2006**, *35*, 348; (c) T. Moriuchi, A. Nomoto, K. Yoshida, A. Ogawa, T. Hirao, *J. Am. Chem. Soc.* **2001**, 123, 68; (d) D. R. van Staveren, T. Weyhermuller, N. Metzler-Nolte, *Dalton Trans.* **2003**, 210-217; (e) L. Barisic, M. Dropucic, V. Rapic, H. Pritzkow, S. I. Kirin, N. Metzler-Nolte, *Chem. Commun.* **2004**, 2004-2005; (f) S. Chowdhury, K. A. Mahmoud, G. Schatte, H. B. Kraatz, *Org. Biomol. Chem.* **2005**, 3, 3018-3023.

[9] (a) T. Moriuchi, T. Nagai, T. Hirao, *Org. Lett.* **2005**, 7, 5265-5268; (b) T. Moriuchi, T. Nagai, T. Hirao, *Org. Lett.* **2006**, 8, 31-34.

[10] S. Chowdhury, D. A. R. Sanders, G. Schatte, H. B. Kraatz, *Angew. Chem. Intl. Ed.* **2006**, 45, 751.

[11] S. Krimm, J. Bandekar, *Adv. Protein Chem.* **1986**, 38, 181-364.

[12] A. Barth, C. Zscherp, *Quart. Rev. Biophys.* **2002**, 35, 369-430.

4.6. Supporting Information

4.6.1. Experimental

4.6.1.1. General: All syntheses were carried out in air unless otherwise indicated. CH_2Cl_2 (BDH; ACS grade) used for synthesis, was dried (CaH_2) and distilled prior to use. $CDCl_3$ (Aldrich) was dried and stored over molecular sieves (8-12 mesh; 4Å effective pore size; Fisher) before use. CD_3CN (Aldrich) was used immediately opening the sealed ampoule. BocGly-OH, BocVal-OH, H-Cys(Bz)-OMe (Advanced Chemtech), HOBt, HBTU, (Aldrich), $MgSO_4$, $NaHCO_3$ (VWR), and 1,1'-$Fc(OH)_2$ was synthesised by known method. Et_3N (BDH; ACS grade) used in the synthesis was used as received. For column chromatography, a column with a width of 2.7 cm (ID) and a length of 45 cm was packed 18-22 cm high with 230-400 mesh silica gel (VWR). For TLC, aluminum plates coated with silica gel 60 F_{254} (EM Science) were used. NMR spectra were recorded on a Bruker AMX-500 spectrometer operating at 500 MHz (^1H) and 125 MHz ($^{13}C\{^1H\}$). Peak positions in both ^1H and ^{13}C spectra are reported in ppm relative to TMS. The ^1H-NMR spectra are referenced to the residual $CHCl_3$ signal at δ 7.27. All $^{13}C\{^1H\}$-NMR spectra are referenced to the $CDCl_3$ signal at δ 77.23.

4.6.1.2. Synthesis and Characterization

4.6.1.2.1. Boc-Val-Cys(Bz)-OMe (4): Boc-Val-OH (1.09 g; 5 mmol) was dissolved in 200 ml of DCM 1.00 ml (7.5 mmol) of triethyl amine was added in ice cold condition. In another flask 1.31 g (5 mmol) of HCl·HCys(Bz)-OMe was dissolved in 50 ml DCM and 1.40 ml (10 mmol) of triethylamine was added and stirred for 10 minutes. Then the second solution was added to the first solution in ice cold condition. After 5 minutes,

3.79 g of solid HBTU (10mmol) was added and after 30 minutes the ice bath was taken away and the reaction mixture was stirred for 6 hours at room temperature. The reaction mixture was worked up by washing sequentially with saturated aqueous $NaHCO_3$, 10% aqueous citric acid, saturated aqueous $NaHCO_3$ and water.

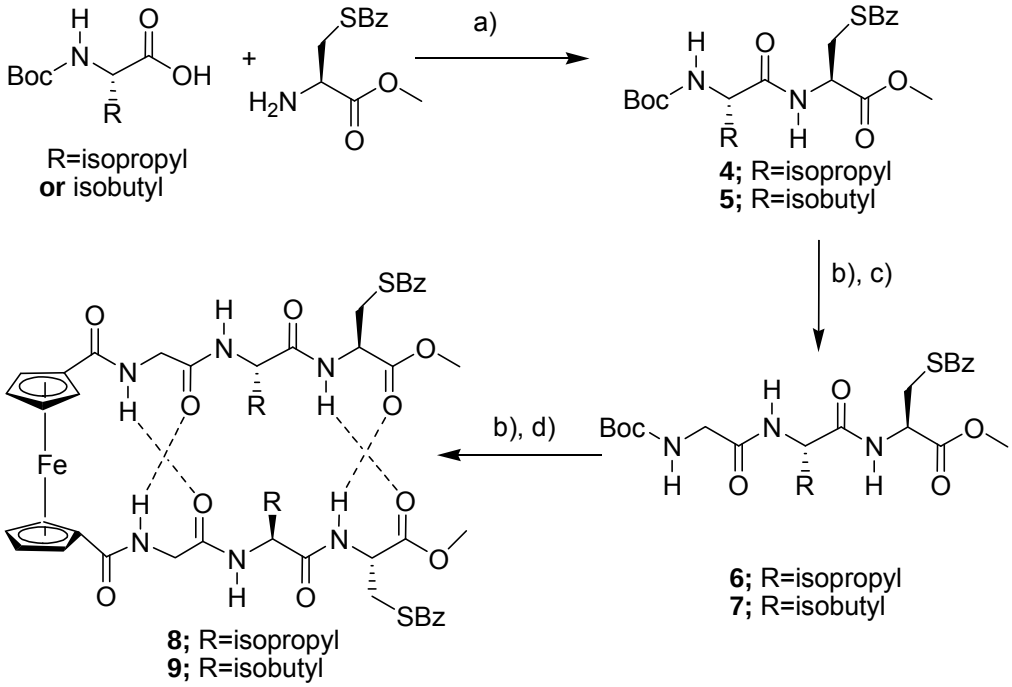

Scheme 4.S1. Synthesis of dipeptides, tripeptides and the ferrocene dicarboxylic acid conjugates of the tripeptides. a) TEA, HBTU in DCM, (b) TFA, evaporate after 20 minutes to completely remove TFA and suspended in DCM and TEA added, c) Boc Gly-OH, HBTU in DCM stirring for 5 hrs, d) Ferrocene dicarboxylic acid /TEA/ HBTU in DCM stirring 10hrs.

Then it was dried with anhydrous sodium sulfate and evaporated under reduced pressure. The product was purified by column chromatography using silica gel column, (ethyl acetate : hexane =50 : 50, R_f = 0.51) to get 1.81 g (85%) of white solid. ^{1}H-NMR (δ, $CDCl_3$) 7.32 (m, 5H, H of Ph), 6.71 (d 1H, NH attached to Boc), 4.78 (d, 1H, α-H of Val) 4.26 (m, 1H, α-H of Cys), 3.76 (s, 3H, ester OCH_3) 3.72 (s, 2H, CH_2 attached Ph),

2.88-2.86 (m, 2H, β-H of Cys), 2.10(m, 1H, β-H of Val), 1.56 (s, 9H, Boc), 0.96 (d, 3H, Val CH_3), 0.95 (d, 3H, another Val CH_3)

4.6.1.2.2. Boc-Gly-Val-Cys(Bz)-OMe (5): 1.07 g (2.5 mmol) of Boc-Val-Cys(Bz)-OMe (**4**) was treated with minimum amount of TFA (50% in DCM). After 30 minutes TFA was completely removed in rotovap. Then it was suspended in 50 ml of DCM followed by dropwise addition of tryethyl amine in ice cold condition to make the solution basic. 0.43 g (2.5 mmol) of Boc-Gly-OH was added to the solution followed by addition of 0.70 ml (5mmol) of TEA in ice bath. Then 1.9 g (5 mmol) of HBTU was added. After 30 minutes the reaction mixture was allowed to warm up to room temperature and kept for 7 hours under constant stirring. The resulting solution was then washed successively with saturated $NaHCO_3$, 10% citric acid, saturated $NaHCO_3$ and water. Then it was evaporated under reduced pressure in a rotorvap. The product was purified by column chromatography using silica gel column (ethyl acetate $R_f = 0.28$) to get the pure product in 75% yield (0.91 g). ^{1}H-NMR (δ, $CDCl_3$): 7.37-7.28 (m, 5H, of Ph) 6.69 (d, J = 7Hz, 1H, NH of Val) , 6.58 (d, J = 5 Hz, NH of Cys), 5.14 (s, 1H, NH of Gly), 4.79-4.75 (m, 1H, α-H of Val), 4.34 (dd, 1H, α-H of Cys), 3.89-3.81 (dd, 2H α-H of Gly), 3.75(s, 3H, ester OCH_3), 3.72 (s, 2H, CH_2 attached Ph), 2.90-2.88 (dd, 2H, β-H of Cys), 2.16 (m, 1H, β-H of Val), 1.46 (s, 9H, CH_3 of Boc), 1.00 (d, J = 8.7 Hz, 3H, CH_3 of Val), 0.96 (d, J = 7.2 Hz, 3H another CH_3 of Val)

4.6.1.2.3. Boc-Ile-Cys(Bz)-OMe (6): The procedure is identical to that used for the preparation of **4**. Column (ethyl acetate : hexane =40 : 60, $R_f = 0.45$), white solid, yield

= 81% (0.88 g). ^{1}H-NMR (δ, $CDCl_3$) : 7.32-7.30 (m, 5H, Ph), 7.10 (d, 1H, NH of Cys), 6.69 (d, 1H, NH attached to Boc), 4.77 (m, 1H, α H of Ile), 4.10 (m, 1H, α-H of Ile), 3.77 (s, 3H, CH_3 of ester), 3.73 (s, 2H, CH_2 attached to Ph), 2.90 (d, 2H, β-H of Cys), 1.90 (m, 1H, β-H of Ile), 1.52 (m, 1H, one γ-H of Ile), 1.45 (s, 9H, CH_3 of Boc), 1.18 (m, 1H, another γ-H of Ile), 0.98 (d, 3H, CH_3 of Ile), 0.96 (d, 3H, another CH_3 of Ile).

4.6.1.2.4. Boc-Gly-Ile-Cys(Bz)-OMe (**7**): The procedure is identical to that used for the preparation of **5**. column (ethyl acetate 100%, R_f = 0.36) to get the pure product in 71% yield (0.87 g). ^{1}H-NMR (δ, $CDCl_3$) 7.37-7.31 (m, 5H, Ph), 6.67 (d, 1H, NH of Ile), 6.56 (d, 1H, NH of Cys), 5.11 (s, 1H, NH of Gly), 4.79 (dd, 1H, α-H of Val), 4.35 (dd, 1H, α-H of Cys), 3.86 (dd, 2H, α-H of Gly), 3.76 (s, 3H, CH_3 of ester), 3.72 (s, 2H, CH_2 attached to Ph), 2.89 (d, 2H, β-H of Cys), 1.91 (dd, 1H, β-H of Ile), 1.53 (m,1H, one γ-H of Ile), 1.44 (s, 9H, CH_3 of Boc), 1.17 (m, 1H, another γ-H of Ile), 0.97 (d, 3H, CH_3 of Ile), 0.94 (d, 3H, another CH_3 of Ile).

4.6.1.2.5. Fc[CO-Gly-Val-Cys(Bz)OMe]$_2$ (8): 0.48 g (1 mmol) of Boc-Gly-Val-Cys(Bz)-OMe (**5**) was treated with 2 ml of TFA (50% in DCM). After 30 minutes TFA was completely removed in rotovap. Then it was suspended in 50 ml of DCM followed by dropwise addition of triethyl amine in ice cold condition to make the solution basic. 0.14 g (0.5 mmol) of ferrocene dicarboxylic acid was added to the solution followed by addition of 0.42 ml (3mmol) of TEA in ice bath. Then 1.1 g (3 mmol) of HBTU was added. After 30 minutes the reaction mixture was allowed to warm up to room temperature and kept for 7 hours under constant stirring. The resulting solution was then

washed successively with saturated $NaHCO_3$, 10% citric acid, saturated $NaHCO_3$ and water. Then it was evaporated under reduced pressure in a rotoevaporator. The product was purified by column chromatography using silica gel column (ethyl acetate : methanol = 95 : 5, R_f = 0.31) to get the pure product in 65% yield (0.32 g). FTIR in KBr (resolution 4 cm^{-1}) : 1634 cm^{-1}, 1680 cm^{-1} (C=O), 1531 cm^{-1} (C-N of amide), 3294 cm^{-1} (N-H stretching); UV-vis: (λ in nm, [ε in $M^{-1}cm^{-1}$]): 442 [280]; HRMS (ES): Calc. for $C_{48}H_{60}N_6O_{10}FeS_2$ $[M]^+$, 1000.3162 observed mass $[M+1]^+$ 1001.4221; ^{1}H-NMR (δ, $CDCl_3$): 8.64 (t, 1H, NH of Gly), 7.33-7.32 (m, 5H, of Ph), 7.12 (d, J = 5.7Hz, 1H, NH of Cys), 6.68 (d, J = 7 Hz, 1H, NH of Val), 4.85 (s, br, 2H, *ortho*-H of Cp), 4.75-4.71 (q, 1H, α-H of Cys), 4.44-4.42 (q, 1H, α-H of Val), 4.38 (s, br, 2H, *meta*-H of Fc) 4.04-3.79 (dd, 2H α-H of Gly), 3.73 (s, 2H, CH_2 attached Ph), 3.72(s, 3H, ester OCH_3), 2.90 (d, J = 9.1 Hz, 2H, β-H of Cys), 2.35 (m, 1H, β-H of Val), 1.04 (d, J = 6.2Hz, 3H, CH_3 of Val), 0.99 (d, J = 6.0 Hz, 3H another CH_3 of Val); $^{13}C\{^1H\}$-NMR (δ, $CDCl_3$): 172.3, 171.7, 171.5, 171.3, 137.9, 129.3, 129.1, 127.7, 75.9, 72.1, 71.9, 71.2, 70.7, 59.0, 53.0, 52.2, 43.8, 36.7, 33.2, 30.7, 19.8, 17.8.

4.6.1.2.6. Fc[CO-Gly-Ile-Cys(Bz)OMe]$_2$ (9): The procedure is identical to that used for the preparation of **8**. Column on silica (EtOAc : MeOH = 95:5 v/v, R_f = 0.35), yield 59 %. FTIR: 1638cm^{-1} and 1679cm^{-1} (C=O), 1533 cm^{-1} (C-N of amide), 3282 cm^{-1} (N-H stretching); UV-vis: (λ in nm, [ε in $M^{-1}cm^{-1}$]): 441 [278]; HRMS (ES): Calc. for $C_{32}H_{46}N_6O_6FeS_2$ $[M]^+$ 1028.3475 observed mass $[M+1]^+$ 1029.4228; ^{1}H-NMR (δ, $CDCl_3$): 8.67 (t, 1H, NH of Gly), 7.49-7.34 (m, 5H, Ph), 7.21 (d, J = 8.5 Hz, 1H, NH of Cys), 6.55 (d, J = 5.8 Hz, NH of Ile), 4.86 (d, J = 9.6 Hz, 2H, *ortho*-H of Cp), 4.73 (dd, 1H, α-

H of Cys), 4.50 (q, 1H, α-H of Ile), 4.40 (d, J = 7.0 Hz, 1H, *meta*-H of Cp), 3.84 (m, 2H, α-H of Gly), 3.76 (s, 2H, CH_2 attached to Ph), 3.74 (s, 3H, CH_3 of ester), 2.98 (dd, 2H, β-H of Cys), 2.14 (s, br, 1H, β-H of Ile), 1.54-1.21 (dd, 2H, CH_2 of Ile), 1.02 (m, 2H, CH_3 of Ile), 0.97 (d, 2H, CH_3 of Ile) ; $^{13}C\{^1H\}$-NMR (δ, $CDCl_3$): 172.0, 171.4, 171.1, 171.0, 137.7, 128.9, 128.7, 127.4, 75.5, 75.4, 71.8, 71.4, 70.8, 70.5, 58.5, 52.6, 51.9, 43.6, 36.8, 36.2, 32.7, 29.7, 24.7, 15.9, 11.8.

4.6.2. FT-IR Study

FT-IR spectra were recorded in BIO-RAD, FTS-40 in solid state (KBr) from 400 cm^{-1} to 4000cm^{-1} with 4 cm^{-1} resolution.

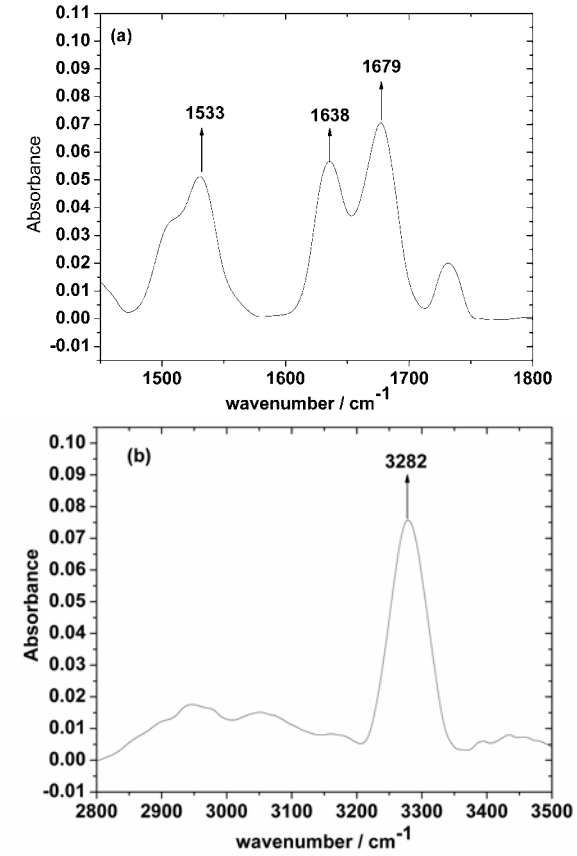

Figure 4.S1. Representative partial FT-IR spectrum (4 cm^{-1} resolution) for Fc[CO-Gly-Ile-Cys(Bz)OMe]$_2$ (**9**), in the solid state (KBr). (a) amide-I and amide-II region of **9** and (b) amide-A region of **9**.

4.6.3. X-ray Crystallography

Crystallization of Fc[CO-Gly-Val-Cys(Bz)OMe]$_2$ (**8**) and Fc[CO-Gly-Ile-Cys(Bz)OMe]$_2$ (**9**) were carried out by slowly diffusing the solvent from the solution in chloroform in refreegerator. Orange rod shaped crystals suitable for x-ray crystallography were deposited after 3-4 days. All measurements were made on a Nonius KappaCCD 4-Circle Kappa FR540C diffractometer using monochromated Mo K_α radiation (λ = 0.71073 Å) at -100 °C. An initial orientation matrix and cell was determined from 10 frames using ϕ scans.[S1] Data were measured using ϕ- and ω-scans. [S1] Data reduction was performed with the HKL DENZO and SCALEPACK software [S2], which corrects for beam inhomogeneity, possible crystal decay, Lorentz and polarisation effects. A multi-scan absorption correction was applied (SCALEPACK,).[S2]

The structures were solved using direct methods (SIR-97 [S4]) and refined by full-matrix least-squares method on F^2 with SHELXL97-2.[S5] The non-hydrogen atoms were refined anisotropically. Hydrogen atoms were included at geometrically idealized positions (C-H bond distances 0.95/0.98/0.99 Å) and were not refined. The isotropic thermal parameters of the hydrogen atoms were fixed at 1.2 times that of the preceding carbon atom.

Table 4.1. Summary of crystallographic Data of Fc[CO-Gly-Val-Cys(Bz)OMe]$_2$ (**8**) and Fc[CO-Gly-Ile-Cys(Bz)OMe]$_2$ (**9**).

	8	**9**
Chemical formula	$C_{48}H_{60}Fe_1N_6O_{10}S_2$	$C_{50}H_{64}Fe_1N_6O_{10}S_2$
FW	1000.99	1029.04
Crystal system	orthorhombic	orthorhombic
Space group	$P2_12_12_1$ [No. 19]	$P2_12_12_1$ [No. 19]
a/ Å	16.2410(7)	13.5790(4)
b/ Å	17.8260(9)	16.5860(5)
c/ Å	16.8370(7)	22.5580(7)
α/°	90.00	90.00
β/°	90.00	90.00
γ/°	90.00	90.00
V/Å^3	4878.5(4)	5080.5(3)
Z	4	4
D(calcd)/g cm^{-3}	1.364	1.345
T/K	173(2)	173(2)
λ/ Å	0.71073	0.71073
μ/mm^{-1}	0.458	0.442
R_1 ($I > 2\,\sigma(I)$)[a]	0.0670	0.0483
wR (all data)[b]	0.1252	0.1306
GOOF on F^2	0.935	1.093

$R_1=[\Sigma||F_o|-|F_c||]/[\Sigma|F_o|]$; $wR_2 = \{[\Sigma w(F_o^2-c^2)^2]/[\Sigma w(F_o^2)^2]\}^{1/2}$; $w = [\sigma(F_o^2) + (aP)^2 + (bP)]^{-1}$ where $P = [\mathrm{Max}(F_o^2,0) + 2\,F_c^2]/3$.

Table 4.S2. Inter and intramolecular hydrogen bonding distances of **8**.

N(11)(H)····O(22)=C	2.916(8)
N(13)(H)····O(24)=C	3.082(8)
N(21)(H)····O(12)=C	2.846(7)
N(23)(H)····O(14)=C	3.054(8)
N(22)(H)····O(11)*=C	3.064(8)
O(11)=C····N(22)**(H)	3.064(8)
N(12)(H)····O(21)**=C	2.869(8)
O(21)=C····N(12)*(H)	2.868(82)

Symmetry transformations used to generate equivalent atoms:

*: -x + ½, -y, z - ½
**: -x + ½, -y, z + ½

Table 4.S3. Inter and intramolecular hydrogen bonding distances of **9**.

N(11)(H)····O(22)=C	2.887(4)
N(21)(H)····O(12)=C	2.758(5)
N(22)(H)····O(11)*=C	2.926(4)
O(11)=C····N(22)**(H)	2.926(4)
N(12)(H)····O(21)**=C	2.894(4)
O(21)=C····N(12)*(H)	2.894(4)

Symmetry transformations used to generate equivalent atoms:

*: -x + 1, y + ½, -z + ½
**: -x + 1, y - ½, -z + ½

Supramolecular arrangments of the molecules in the crystals: Through intermolecular hydrogen bonding both the molecules assemble into pleated beta-sheet like archetechtures. Views of these supramolecular arrangements in different directions are presented in the following figures (Figure 4.S2 to Figure 4.S7).

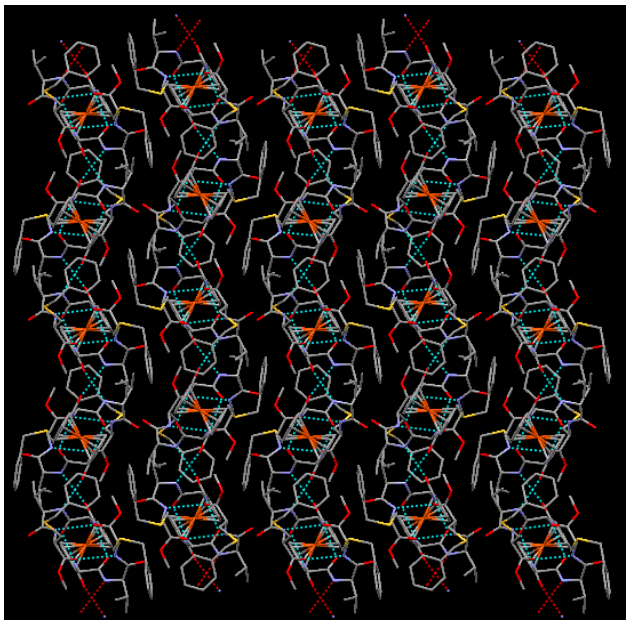

Figure 4.S2. Packing of Fc[CO-Gly-Val-Cys(Bz)OMe]$_2$ (**8**), view along x axis.

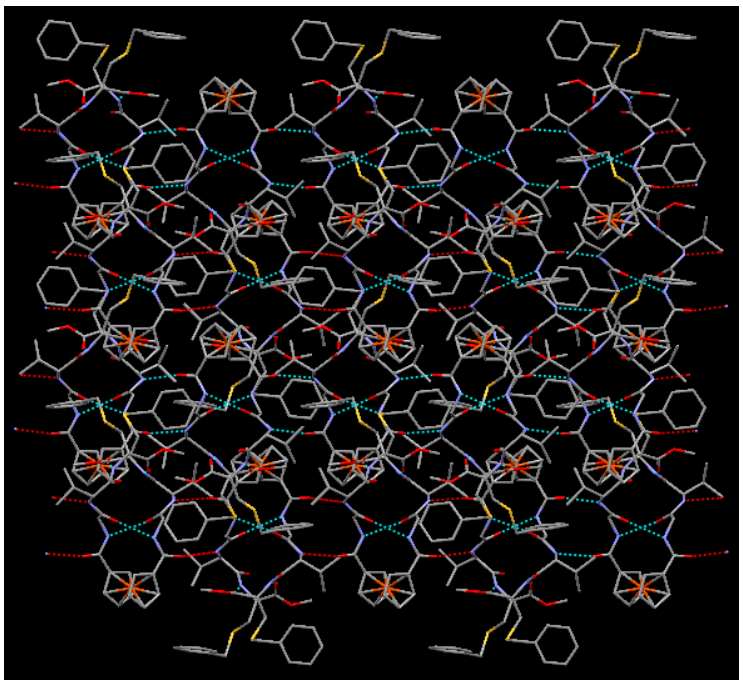

Figure 4.S3. Packing of Fc[CO-Gly-Val-Cys(Bz)OMe]$_2$ (**8**), view along y axis.

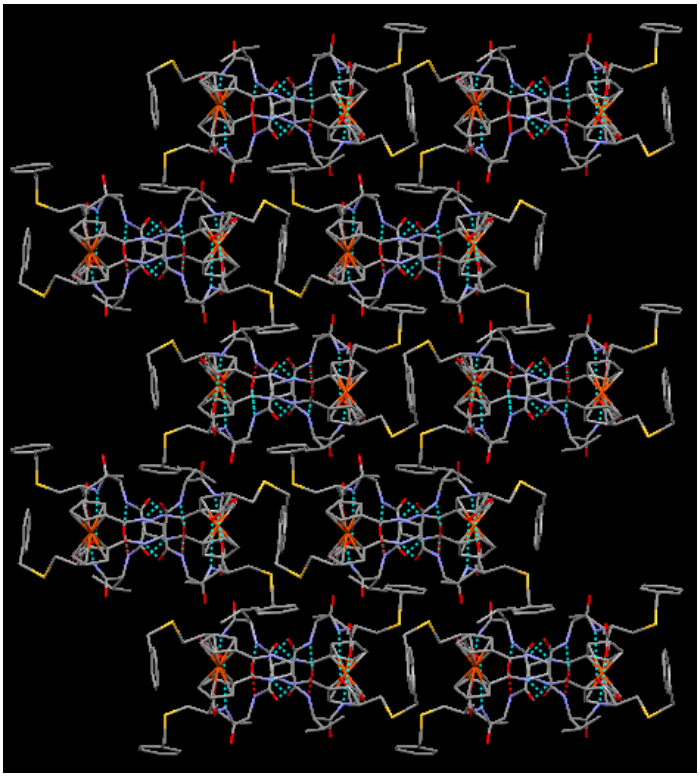

Figure 4.S4. Packing of Fc[CO-Gly-Val-Cys(Bz)OMe]$_2$ (**8**), view along z axis.

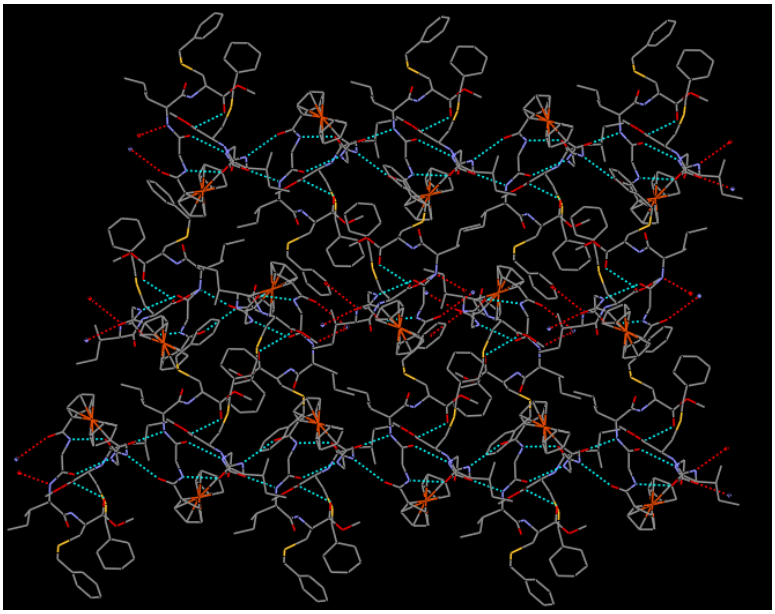

Figure 4.S5. Packing of Fc[CO-Gly-Ile-Cys(Bz)OMe]$_2$ (**9**), view along x axis.

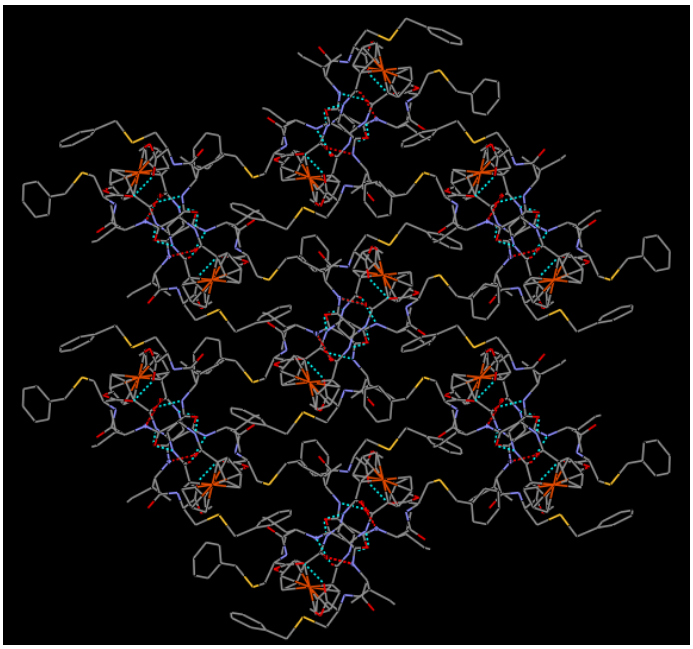

Figure 4.S6. Packing of Fc[CO-Gly-Ile-Cys(Bz)OMe]$_2$ (**9**), view along y axis.

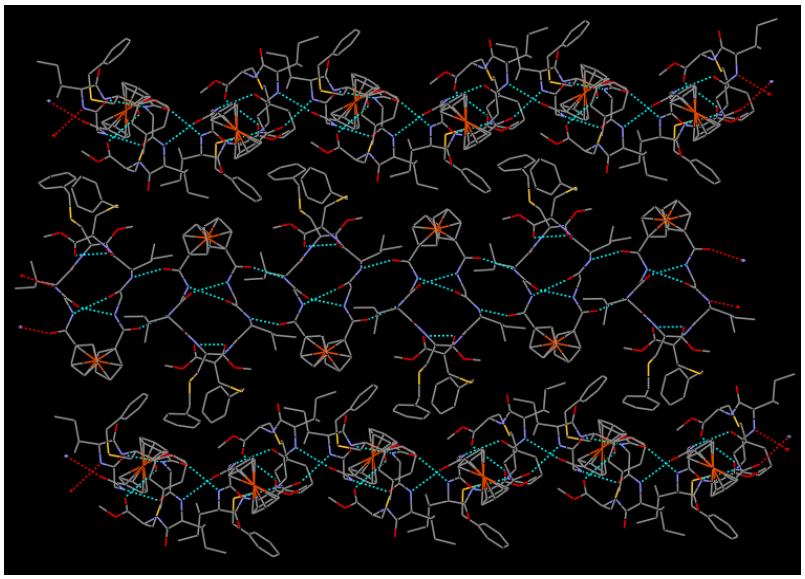

Figure 4.S7. Packing of Fc[CO-Gly-Ile-Cys(Bz)OMe]$_2$ (**9**), view along z axis.

4.7. Supporting References

[S1] *COLLECT* data collection software, Nonius B.V., **1998**.

[S2] *HKL DENZO and SCALEPACK v1.96*: Z. Otwinowski, W. Minor, *Processing of X-ray Diffraction Data Collected in Oscillation Mode, Methods in Enzymology*, Volume 276: *Macromolecular Crystallography*, Part A, Carter, C. W., Jr., Sweet, R. M., Eds.; Academic Press: San Diego, CA, **1997**; pp. 307-326.

[S3] *SHELXTL-NT 6.14, XPREP, Program Library for Structure Solution and Molecular Graphics*; Bruker AXS, Inc.: Madison, WI, **2000-2003**.

[S4] A. Altomare, G. Cascarano, C. Giacovazzo, A. Guagliardi, A. G. G. Moliterni, M.C. Burla, G. Polidori, M. Camalli, R. Spagna, *SIR-97, A package for crystal structure solution by direct methods and refinement*; *J. Appl. Crystallogr.* **1999**, *32*, 115.

[S5] G. M. Sheldrick, *SHELXL97-2, Program for the Solution of Crystal Structures;* University of Göttingen, Göttingen, Germany **1997**.

Chapter 5

Amino Acid Conjugates of 1,1'-Diaminoferrocene. Synthesis and Chiral Organization

5.0. Connecting Text

In this chapter, the preparation of $Fc[NH\text{-}Boc]_2$ and its amino acid conjugates is described. To date, only 1,1'-Fc dicarboxylic acid and 1-amino-1'-Fc carboxylic acid have been exploited for the preparation of peptide conjugates, exhibiting specific H-bonding pattern associated with the *β*-sheet-like structure. Peptide conjugates of 1,1'-diaminoferrocene display the illusive 14-membered H-bonding with an anti-parallel alignment of the peptide strands, which adds a new scaffold for controlling the structures of peptides.

This paper was reproduced with the permission from *Org. Biomol. Chem*. **2005**, 3, 3018-3013. Copyright 2005, Royal Society of Chemistry. It was co-authored by K. A. Mahmoud, G. Schatte and H.-B. Kraatz. The major part of it was contributed by me. The text below is a *verbatim* copy of the published paper.

5.1. Abstract

1,1'-Bis(*tert*-butoxycarbonylamino)ferrocene (**6**), a protected derivative of 1,1'-diaminoferrocene, has been synthesized by a very convenient method and serves as a synthon for 1,1-diaminoferrocene. Its structure in solid state and in solution has been studied by NMR and X-ray crystallography. 1,1'-bis(*tert*- butoxycarbonylamino) ferrocene serves as starting material for the synthesis of amino acid conjugates of L- and D-alanine. The structures of these bioconjugates have been studied by NMR and CD spectroscopy and X-ray crystallography and reveal that the chiral organization of the

podant amino acid chains is controlled by the chirality of the attached amino acid. The substituents engage in strong intramolecular H-bonding generating 14-membered H-bonded rings, a motif previously unrealized in ferrocene–amino acid and peptide conjugates

5.2. Introduction

Controlling the secondary structures of peptides is of great importance in designing functional peptidic materials[1,2] and understanding the function of proteins and enzymes.[3] Among various means, use of molecular scaffolding has attracted greatattention in achieving specific secondary structures.[4] In this context, ferrocene (Fc) derivatives **1**–**3** are widely used as a redox active scaffold. Having the cyclopentadienyl rings separated by 3.3 Å , allows effective intramolecular interstrand H-bonding in peptide conjugates of disubstituted Fc, where the peptide strands are on the two different cyclopentadienyl (Cp) rings. Hydrogen bonding imposes a specific secondary structure onto the bioconjugates, first described by Herrick and co-workers.[5] The particular choice of Fc-scaffold will influence the ability for forming H-bonded assemblies. For example, conjugates of 1 often give rise to one dimensional H-bonded chains, whereas **2** and **3** can give rise to H-bonded b-sheet like structures or even engage in chiral helical arrangements.[6–12] It is also observed that, based on the torsional twist about the Cp(centroid)–Fe–Cp(centroid) axis, conformational enantiomerization is possible for the case of 1,1'-disubstituted ferrocene[13] and the conformations can be stabilized by intramolecular hydrogen bonding between the two peptides strands, when the substituents are peptides, as described by Hirao using **2** as a scaffold.[10] Given the general difficulty in preparing mono- and diaminoferrocene derivatives in sufficiently

high yields,[14–17] peptide derivatives of 1,1'-diaminoferrocene (**4**) are completely absent from the literature. We set out to develop a synthetic procedure that circumvents the use of the explosive 1,1'-diazoferrocene.[18]

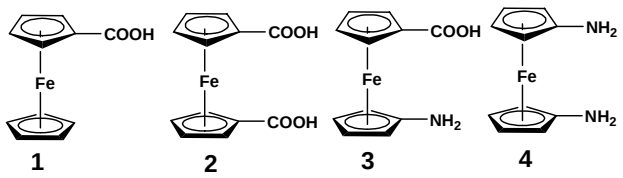

Here, we report the convenient synthesis of 1,1-bis(*tert*butoxycarbonylamino) ferrocene (**6**), a convenient synthon of 1,1-diaminoferrocene (**4**). The bis-Boc derivative is compatible with the peptide synthesis protocol, as is demonstrated by the preparation of its first amino acid conjugates. To test the chiral organization pattern of the Fc conjugate, L- and D-alanine conjugates were prepared. Importantly, the systems exhibit a previously unknown H-bonding motif for Fc–peptide conjugates.

5.3. Results and Discussions

1,1ʳ-bis(carbonylazido)ferrocene (**5**) was synthesized from 1,1ʳ-ferrocenedicarboxylic acid (**2**) by treatment with ethyl chloroformate, followed by the reaction with sodium azide. The reaction of the carbonylazido compound **5** with tertiary butanol at 80°C for 8 hours cleanly leads to the desired bis-Boc-protected compound **6** in 72 % yield (Scheme 5.1). The material is stable in solution and in the solid state and does not decompose in solution even after several months. Compound **6** was characterized spectroscopically and by single-crystal X-ray analysis. The ^{1}H-NMR spectrum shows the two carbamide NHs upfield from typical amide at δ6.06.

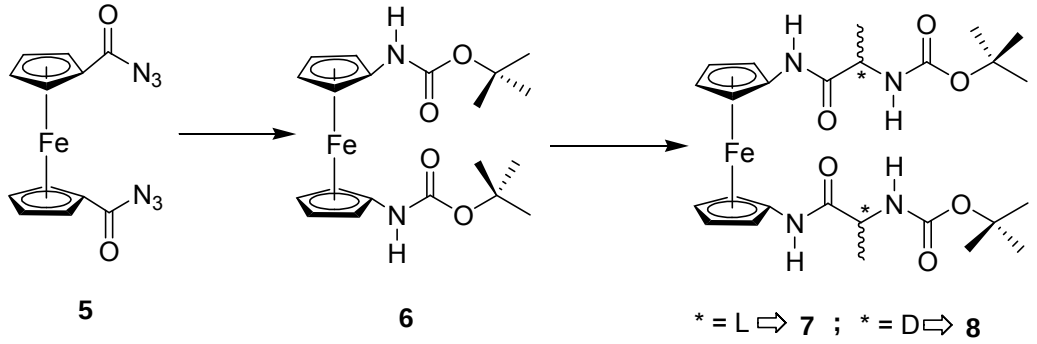

5 6 * = L ⇨ 7 ; * = D ⇨ 8

Scheme 5.1. Synthesis of 1,1'-bis(Boc-amino)ferrocene (**6**) via 1,1'-bis(carbonylazido)ferrocene (**5**) and its amino acid derivatives with L-Ala (**7**) and D-Ala (**8**). (i) Reflux in *tert*-BuOH, 80ºC, 8 hrs (ii) a) TFA, b)TEA, c) Boc-Ala-OH activated by EDC/HOBt.

Similarly, the ^{13}C-NMR exhibitis a resonance at δ153.2, typical for the Boc carbonyl. The IR spectrum shows a strong absorption for the C=O group at 1695 cm^{-1}. Single crystals of compound **6** were obtained by slow diffusion of hexane into a chloroform solution. The X-ray diffraction study reveals the presence of three independent rotamers having the two substituents at different rotational angles (70º, 144º, 180º) with an approximate 1,2' and 1,3' conformation. Two molecules in general positions in the asymmetric unit and one molecule with its Fe atom on an inversion centre. All three rotamers are linked via intermolecular N(H)•••O=C bonding. In one of the rotamers, strong intramolecular H-bonding is present (see Figure 5.1, ferrocene Fe(1)). The ^{1}H-NMR provides an indication for the presence of more than one rotamer even in solution. At 250 K, the ^{1}H-NMR spectrum shows the presence of three N-H signals of different intensities. Upon increasing the temperature to 295 K, the signals merge to a single peak, indicating rapid interconversion of the rotamers on the NMR time scale (Figure 5.1b).

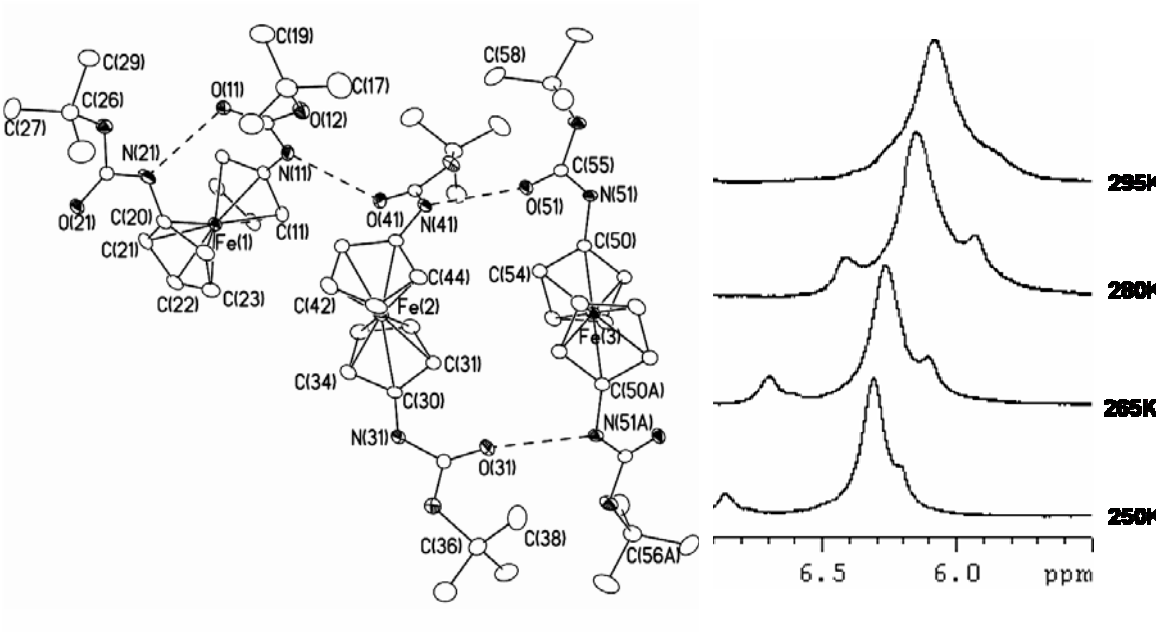

Figure 5.1. (a) ORTEP diagram of 1,1'-bis(tert-butoxycarbonylamino)ferrocene (**6**) showing three rotamers and intra- and intermolecular hydrogen bonds are indicated by dotted lines. Relevant bond distances [Å] and angles [º]: Fe(3)-C(Cp)$_{av.}$,1,99(6); N(31)-C(30), 1.509(4); N(31)-C(35), 1.417(4); N(41)-C(40), 1.423(4); N(41)-C(45), 1.471(4); C(35)-O(31) 1.203(4); C(35)-O(32), 1.411(4); C(45)-O(41) 1.217(3), C(45)-O(42), 1.384(3); Cp/Cp twist angle, 0.3(1); $\beta_{av.}$, 4.7(2) [A: 1-x, 1-y,-z]. (b) Partial ^{1}H NMR spectrum recorded at different temperatures showing the amide N-H region of compound 6, indicating the presence of at least three distinct rotamers in solution at low temperatures and facile interconversion between the rotamers at high temperatures.

Compound **6** is a convenient starting material for the preparation of amino acid bioconjugates. The synthesis of the L-Ala and D-Ala conjugates 1,1'-bis(*tert*-butoxycarbonyl-L-alanine-amido)ferrocene (**7**) and 1,1'-bis(*tert*-butoxycarbonyl-D-alanine-amido)ferrocene (**8**) were readily achieved after deprotection of the amino group, followed by coupling with the corresponding Ala derivatives in the presence of a carbodiimide under inert atmosphere, to prevent the oxidation of the diaminoferrocene formed *in situ* (see Scheme 5.1). Compounds **7** and **8** were characterized by spectroscopic methods. Both compounds display a single broad absorption in the visible region with λ_{max} = 448 nm due to the Fc-based d-d transition, which experiences a

bathochromic shift compared to the Boc-protected **6**. In the IR, a new signal appears at 1671 cm^{-1} due to the presence of the Fc-amide C=O, in addition to the signal due to the Boc C=O group at 1575 cm^{-1}. Similarly, the ^{13}C-NMR spectrum exhibits two resonances in the carbonyl region at δ171.7 (Fc-amide C=O) and at δ155.5 (Boc C=O). The corresponding NH signals are observed at δ9.00 for the Fc-NH-CO group and at δ5.11 for the Boc-protected Ala. The α-H of Ala is observed at as a multiplet at δ 4.35, while the Ala-CH_3 is observed upfield at δ17.5.

The compound readily crystallizes from a chloroform solution by slow diffusion of hexanes to produce yellow-orange needles. Two single crystal X-ray diffraction studies of these compounds were carried out showing that the compounds crystallize in the space group C_2.‡ A graphical representation of compound **8** is shown in Figure 5.2. The Cp rings in both ferrocenoyl groups are co-planar (angle between Cp planes: 2.8(2)°). The amide and Cp rings are twisted by 18.9(2)°. Importantly, the molecules maximize their H-bonding through formation of intermolecular and intramolecular N(H)•••O=C bonding. Two intramolecular H-bonds (2.805(6) Å) are formed between the amide groups connected to the Cp rings and the adjacent carbonyl of the Boc causing *M*-helicity of the compound. Thus, the two podand amino acid substituents have the same arrangement as was observed for L- and D-amino acid conjugates of ferrocenedicarboxylic acid **2**[9] and for the conjugates offerroceneamino acid **3**.[12] Importantly, for amino acid conjugates of compound **4** intramolecular NH•••O=C H-bonding results in the formation of a previously unobserved 14-membered H-bonded ring. Thus, the nature of the parent Fc derivative (**2** – **4**) appears to direct the size of the H-bonded ring, as depicted in Scheme 5.2. The bonded ring size in peptide conjugates

increases from 10 for the derivatives of **2**[5], to 12 for the derivatives of **3**[12] to 14 for the derivatives of **4**.

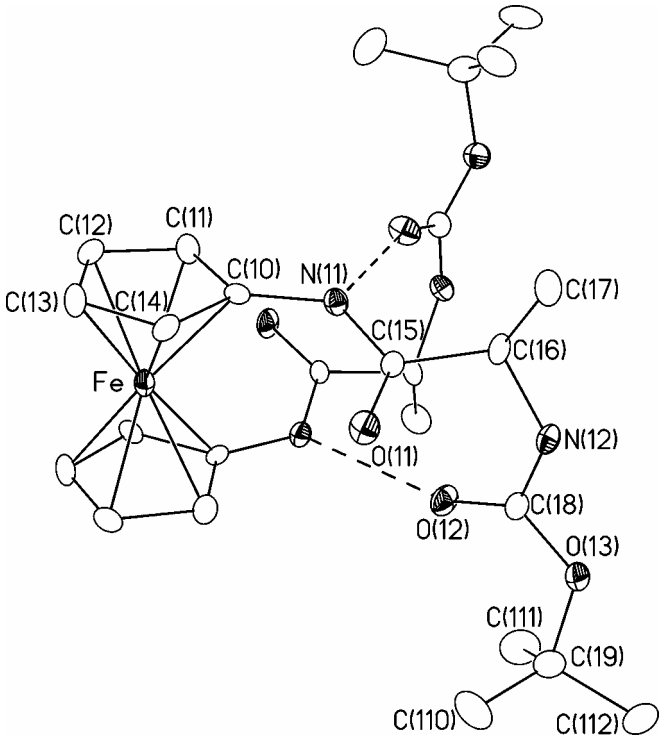

Figure 5.2. ORTEP diagram of the X-ray single crystal structure of **8** (30% probability) showing intramolecular hydrogen bonds. Relevant bond distances [Å] and angles [º]: Fe-C(Cp)$_{av.}$, 2.040(5); N(11)-C(10), 1.419(4); N(11)-C(15), 1.349(3); C(15)-O(11), 1.224(3); C(15)-C(16), 1.536(4) C(16)-N(12) 1.445(3); Cp/Cp twist angle, 3.43(9); ct(Cp)-Fe-ct(Cp*), 159.7(9); β, 19.08(9) [*:-x+1, y, -z+1].

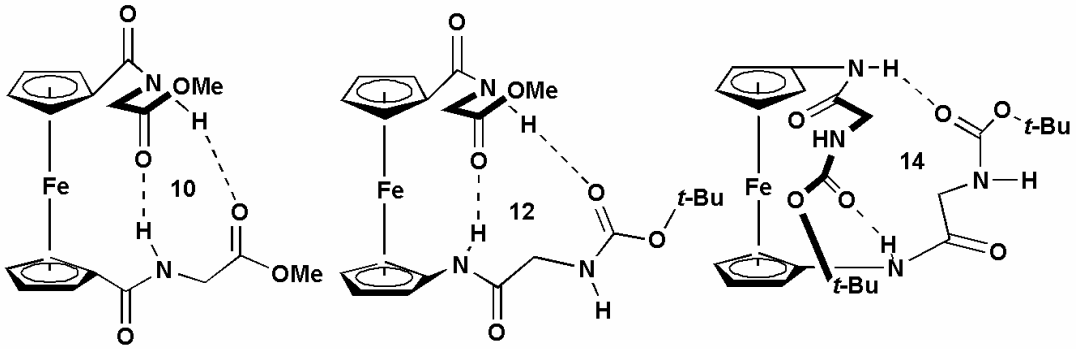

Scheme 5.2. Intramolecular H bonding pattern in amino acid conjugates of disubstitued Fc derivatives results in the formation of 10-membered rings for conjugates of **2**, 12-membered rings for conjugates of **3** and novel 14-membered rings for conjugates of **4**.

Table 5.1. Summary of crystallographic data for 1,1'-bis(tert-butoxycarbonylamino)ferrocene (**6**), 1,1'-bis(*tert*-butoxycarbonyl-L-alanine-amido)ferrocene (**7**) and 1,1'-bis(*tert*-butoxycarbonyl-D-alanine-amido)ferrocene (**8**).

	6	**7**	**8**
Chemical formula	$C_{22}H_{31}Fe1N_2O_4$	$C_{26}H_{38}FeN_4O_6$	$C_{26}H_{38}FeN_4O_6$
FW	416.31	558.45	558.45
Crystal system	Monoclinic	Monoclinic	Monoclinic
Space group	$P2_1/n$	$C2$	$C2$
a/ Å	10.8116(1)	15.4790(8)	15.490(3)
b/ Å	11.8065(1)	9.3380(5)	9.3390(19)
c/ Å	40.9023(4)	11.0340(9)	11.036(2)
α/°	90.00	90.00	90.00
β/°	91.0490(4)	117.034(2)	117.09(3)
γ/°	90.00	90.00	90.00
V/Å^3	5220.19(8)	1420.62(16)	1421.3(6)
Z	10	2	2
D(calcd)/g cm^{-3}	1.324	1.306	1.305
T/K	173(2)	173(2)	173(2)
λ/ Å	0.71073	0.71073	0.71073
μ/mm^{-1}	0.748	0.575	0.575
R ($I > 2\ \sigma(I)$)[a]	0.0636	0.0614	0.0393
wR (all data)[b]	0.1134	0.1846	0.0755
GOOF on F^2	0.935	1.123	1.058

$R_1 = [\Sigma||F_o|-|F_c||]/[\Sigma|F_o|]$; $wR_2 = \{[\Sigma w(F_o^2-F_c^2)^2]/[\Sigma w(F_o^2)^2]\}^{1/2}$; $w = [\sigma(F_o^2) + (aP)^2 + (bP)]^{-1}$ where $P = [\mathrm{Max}(F_o^2,0) + 2\ F_c^2]/3$.

This is an important result, which may allow the use of ferrocenediamine as a scaffold for in the rational design of structurally well-defined peptide assemblies.

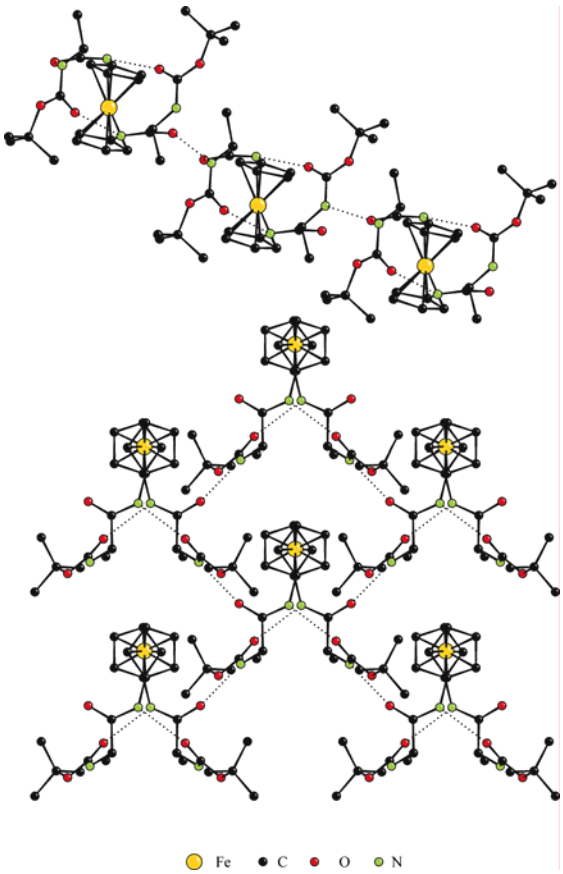

Figure 5.3. Crystal structure of **8** showing the intramolecular H-bonding, interaction between ferrocene moiety and *tert*-butyl group (viewed down the *a*-axis (top and down the *c*-axis (bottom)). Dotted lines indicate hydrogen bonding.

In addition, the molecules are engaged in intermolecular NH•••O=C hydrogen bonds (2.825(6) Å), see Figure 5.3), showing a honeycomb structure, which contrasts the helical arrangement for ferrocenedicarboxylic acid derivatives observed by Hirao and coworkers.[7] We decided to study the H-bonding ability of compounds **7** and **8** in solution. Variable temperature ^{1}H-NMR at various concentrations allows the detection of both inter- and intramolecular H-bonding (see Figure 5.4). Upon increasing the temperature, intermolecular H-bonding is weakened (-6.9 ppb/K for N(12)), while the intramolecular H-bonding, responsible for stabilizing the particular helicity about the Fc core exhibits a positive temperature behaviour (+4.2 ppb/K) (Figure 5.4), which may

indicate that as the intermolecular H-bonding is broken, the intramolecular H-bonding may be strengthened.

(a)

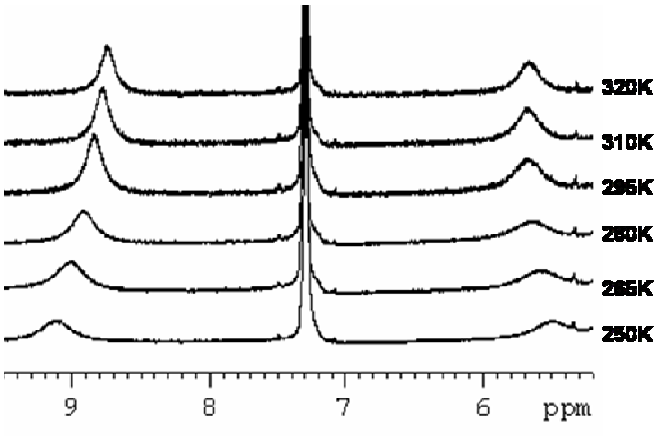

(b)

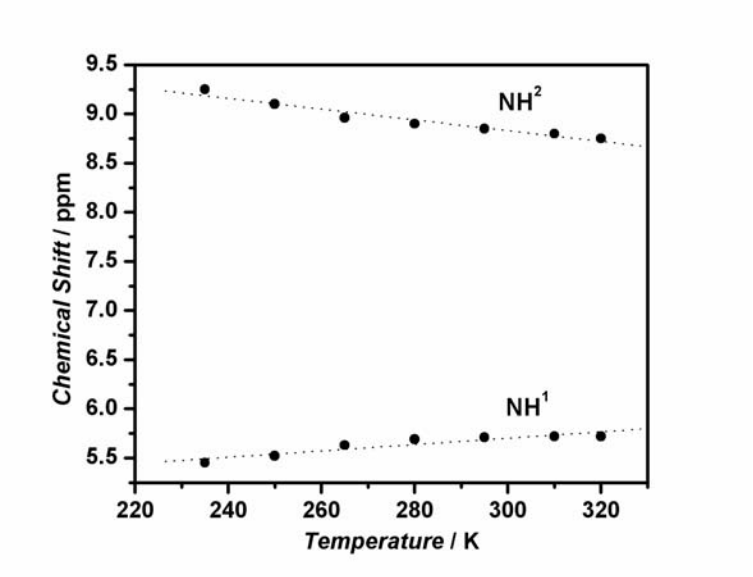

Figure 5.4. (a) ^{1}H-NMR spectra compound **8** at different temperature in 1mM solution in $CDCl_3$ (b) Corresponding plot of chemical shift vs. temperature compound **8**, NH^1 (slope=+4.2 ppb/K) amide hydrogen attached to Cp ring of ferrocene and NH^2 (slope =-6.9 ppb/K) is the amide proton from alanine.

CD provides evidence that compounds **7** and **8** maintain their helicity in solution. The CD spectra for compounds **7** and **8** were measured in CH_2Cl_2 at a concentration of

1mM and are shown in Figure 5.5. As expected for the D and L form, the two compounds give CD spectra that are the exact opposite of each other, indicating that a chiral rigid structure is maintained in solution. This necessitates the absence of free roation about the Cp-Fe-Cp axis and the lack of free rotation of the podant ligand about the Cp-N bond. Thus, the presence of the intramolecular H-bonding between the amino acid substituents is crucial for maintaining the structure in solution and is seen as the major cause for chirality organization in these systems. **7** is found to form a *P*-helical structure as indicated from the positive Cotton effect at the ferrocene function region (480 nm) as was observed by Metzler-Nolte for L-amino acids conjugates with 1,1'-ferrocedicarboxylic acid.

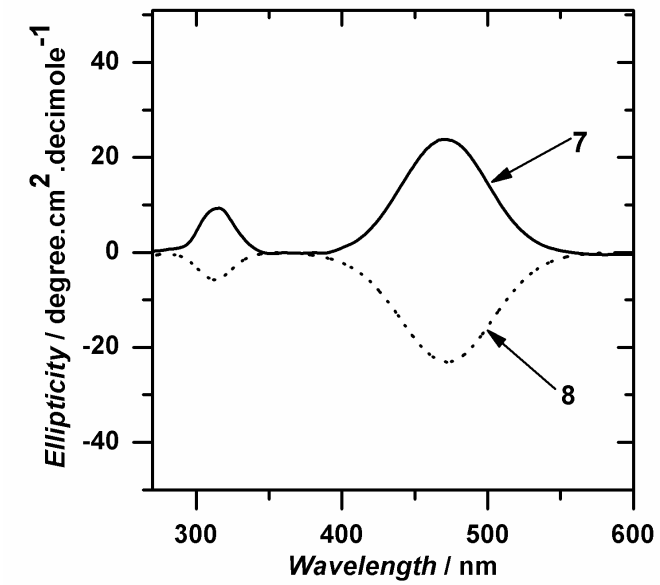

Figure 5.5. CD Spectra of 1,1́-bis(*tert*-butoxycarbonyl-L-alanine-amido)ferrocene (**7**) and 1,1́-bis(*tert*-butoxyarbonyl-D-alanine-amido)ferrocene (**8**) in 1mM solution in CH_2Cl_2 showing opposite chirality with respect to ferrocene.

A negative Cotton effect of same intensity and in the same region for **8** was observed which corresponds to the observation of Hirao's D-amino acid conjugates.[9] The

electrochemical behavior of compounds **6** – **8** was studied by cyclic voltammetry (CV) and differential pulse voltammetry (DPV) in CH_2Cl_2. The electrochemical parameters for compounds **6** - **8** are summarized in Table 5.2. All three compounds exhibit only quasi-reversible behavior with a Faradic current ratio of close to unity by large peak separations. The halfwave potential, $E_{1/2}$, for the Boc-derivative is observed at 306 mV (vs Ag/AgCl), while the a redox potential for compounds **7** and **8** are shifted to higher oxidation potential.

Table 5.2. Electrochemical data of compounds **6-8**[a].

Compound	$E_{1/2}$(mV)	ΔE_p(mV)	i_a/i_c
6	306 (±5)	361	1.06
7	366 (±5)	151	1.11
8	370 (±5)	154	1.10

[a] measured using GCE working electrode vs. Ag/AgCl , scan rate 0.1 V s^{-1}, compounds **6**, **7**, **8** at 0.1 M in CH_2Cl_2 0.1 M TBAP. The $E_{1/2}$ of the Fc/Fc^+ couple under the experimental conditions is 448(+/-5) mV (vs. Ag/AgCl). The $E_{1/2}$ of the Fc/Fc^+ couple under the experimental conditions is 448(+/-5) mV.

5.4. Conclusions

In conclusion, we provide a new synthetic approach to bis-Boc protected 1,1'-diaminoferrocene, a very convenient derivative of unstable diamino ferrocene and show that this novel ferrocene compound can be converted cleanly to amino acid conjugates. Thus resulting bioconjugates show a specific secondary structure through the involvement of strong intramolecular H-bonding in the solid state as well as in solution, forming a 14 membered ring as is seen in antiparallel beta sheet peptide. The chirality of amino acid is found to change the chiral organization of peptide strands with respect to ferrocene.

5.5. Experimental

5.5.1. Synthesis and Characterization: All syntheses were carried out in air unless otherwise indicated. CH_2Cl_2 (BDH; ACS grade) used for synthesis was dried (CaH_2) and distilled prior to use. $CDCl_3$ (Aldrich) was dried (CaH_2), and stored over molecular sieves (8-12 mesh; 4Å effective pore size; Fisher) before use. EDC·HCl, HOBt (Quantum), $MgSO_4$, and $NaHCO_3$ (VWR) were used as received. For column chromatography, a column with a width of 2.7 cm (ID) and a length of 45 cm was packed 18-22 cm high with 230-400 mesh silica gel (VWR). For TLC, aluminum plates coated with silica gel 60 F_{254} (EM Science) were used. NMR spectra were recorded on a Bruker Avance 500 MHz spectrometer using a 5-mm broadband probe operating at 500.134 MHz (^{1}H) and 125.766 MHz (^{13}C $\{^1$H$\}$). Peak positions in both ^{1}H and ^{13}C spectra are reported in ppm relative to TMS. The ^{1}H-NMR spectra are referenced to the residual $CHCl_3$ signal at δ 7.27. All ^{13}C $\{^1$H$\}$ spectra are referenced to the $CDCl_3$ signal at δ 77.23. Mass spectrometry was carried out on a VG Analytical 70/20 VSE instrument. Infrared spectra were obtained in KBr and recorded with a Perkin-Elmer model 1605 FT-IR (resolution: 4 cm^{-1}).

5.5.1.1. 1,1'-bis(*tert*-butoxycarbonylamino)ferrocene (6): 1,1'-bis(azidocarbonyl)ferrocene (1.52 g, 10 mmol) was refluxed in *tert*-butanol at 80°C for 12 hours. After rotorevaporation of butanol, the crude product was purified by flash column chromatography using hexane/ethyl acetate (3.5/1.0; R_f = 0.35), and dried under reduced pressure to give 1.70 g (72%) of compound **6**. HRMS (ES): calc for $C_{20}H_{28}N_2O_4Fe$: 416.1449; found: 416.1410 $[M]^+$. FT-IR (KBr, cm^{-1}): 3316 (b, s, N-H),

1695 (s, C=O), 1542 (s, Amid I). UV-vis (CH_2Cl_2; λ in nm [ε in $Lmol^{-1}cm^{-1}$]: 442[154]. ^{1}H-NMR ($CDCl_3$, δ/ppm): 6.06 (br, s, 2H, NH) 4.36(s, 4H, *ortho*-H of Cp), 3.99 (s, 4H, *meta*-H of Cp) 1.49 (s, 18H, CH_3 of Boc). $^{13}C\{^1H\}$-NMR ($CDCl_3$, δ/ ppm): 153.2 (C=O), 95.0 (*ipso*-C Fc) 79.3 (*ortho*-C of Fc), 68.3 (*ortho*-C of Fc), 64.4 (*meta*-C of Fc), 62.1 (*meta*-C of Fc), 62.0 (tertiary C of Boc), 27.1 (CH_3 of Boc).

5.5.1.2. 1,1'-bis(*tert*-Butoxycarbonyl-L-alanine-amido) ferrocene (**7**): 1,1'- bis-(butoxycarb onylamino) ferrocene (6) (0.42 g 1 mmol) was dissolved in CH_2Cl_2 (2 ml) and cooled to 0 °C. TFA (2 mL) was added dropwise under a nitrogen atmosphere. Then the ice bath was removed and stirring was continued. After 30 min, CH_2Cl_2 (10 mL) was added and the solution was cooled before an excess Et_3N was added dropwise. To this mixture, a solution of Boc-L-Ala-OH (0.38 g 2 mmol), HOBt (0.38 g 2.5 mmol), and EDC•HCl (0.48 g 2.5 mmol) in dry CH_2Cl_2) was added. The reaction mixture was stirred for 12 hours at room temperature and then washed consecutively with saturated aqueous sodium bicarbonate, 10% aqueous citric acid, saturated sodium bicarbonate, and water. The organic phase was separated and dried over Na_2SO_4, filtered and then evaporated to dryness. After purification by flash column chromatography (hexane/ethyl acetate 3/1; R_f = 0.3) the product was obtained in 77 % yield (0.43 g) (77%) as an orange crystalline solid. HRMS (ES): calc for $C_{26}H_{38}N_4O_6Fe$: 558.2210; found: 558.2181 $[M]^+$. FT-IR (KBr, cm^{-1}): 3284 (b, s, N-H), 1671 (s, C=O), 1575 (s, C=O), 1549 (s, Amid II). UV-vis (CH_2Cl_2; λ in nm [ε in $M^{-1}cm^{-1}$]): 448[250]. ^{1}H-NMR ($CDCl_3$, δ/ppm) : 9.00 (1H, s, NH of Fc), 5.39 (1H, s, *ortho*-H of Fc), 5.11 (1H, d, *J* = 7 Hz, NH Ala), 4.36 (1H, m, α CH Ala), 4.11 (1H, s, *ortho*-H of Fc), 3.93 (1H, s, *meta*-H of Cp), 3.93 (1H, s, *meta*-H of Cp), 1.48 (9H, s, CH_3 of Boc), 1.35 (3H, d, J = 7 Hz, CH_3 of

Ala). $^{13}C\{^{1}H\}$-NMR ($CDCl_3$, δ/ppm): 171.7 (C=O), 155.5 (C=O of Boc), 95.1 (*ipso*-C of Cp), 80.2 (tertiary C of Boc), 64.8 (*ortho*-C of Cp), 63.8 (*ortho*-C of Cp), 61.7 (*meta*-C of Cp), 60.0 (*meta*-C of Cp), 50.1(α-C of Ala), 27.6 (CH_3 of Boc), 16.7 (CH_3 of Ala)

5.5.1.3. 1,1'-bis(tert-Butoxycarbonyl-D-Alanine-amido)ferrocene (**8**): The synthetic procedure was identical to that reported for the synthesis of compound **7**. Column chromatography using hexane/ethyl acetate 3/1; R_f = 0.35. HRMS (ES): calc for $C_{26}H_{38}N_4O_6Fe$: 558.2210; found: 558.2182 $[M]^+$. FT-IR (KBr, cm^{-1}): 3284 (b, s, N-H), 1671 (s, C=O), 1575 (s), 1548 (s, Amid II). UV-vis (CH_2Cl_2; λ in nm [ε in $M^{-1}cm^{-1}$]: 448 [240]. ^{1}H-NMR $CDCl_3$, δ/ppm): 9.00 (1H, s, NH of Fc), 5.39 (1H, s, ortho-H of Cp), 5.11 (1H, d, J = 7 Hz, NH Ala), 4.36 (1H, m, α-CH of Ala), 4.11 (1H, s, ortho-H of Cp), 3.98 (1H, s, meta-H of Cp), 3.93(1H, s, 1H, s, meta-H of Cp), 1.49 (9H, s, CH_3 of Boc), 1.35 (3H, d, J = 7 Hz, CH_3 Ala). $^{13}C\{^{1}H\}$-NMR ($CDCl_3$, δ/ppm): $^{13}C\{^{1}H\}$-NMR ($CDCl_3$, δ/ppm): 171.7 (C=O), 156.7 (C=O of Boc), 95.2 (*ipso*-C of Fc), 80.7 (tertiary C of Boc), 65.6 (*ortho*-C of Cp), 64.5 (*ortho*-C of Cp), 62.5 (*meta*-C of Cp), 60.9 (*meta*-C of Cp), Cp), 50.8 α CH Ala, 28.4 (CH_3 of Boc), 17.5 (CH_3 of Ala).

5.5.2. CD Measurements: CD spectra were recorded using a PiStar-180 spectropolarimeter (from Applied Biophysics) in the CH_2Cl_2 solution with the concentration (1.0×10^{-3} M) by using quartz cell of path length 1cm under an argon atmosphere at 25 ^{0}C.

5.5.3. X-ray Crystallography: Suitable crystals of compound **6** (yellow; 0.14 × 0.11 × 0.09 mm), **7** (reddish yellow; 0.12 × 0.14 × 0.09 mm) and **8** (reddish yellow crystal; 0.25

× 0.20 × 0.13 mm) were obtained from a hexane-layered solution of the compounds in chloroform. All measurements were made on a Nonius Kappa CCD 4-Circle Kappa FR540C diffractometer using monochromated Mo K_α radiation (λ = 0.71073 Å) at -100 °C. An initial orientation matrix and cell was determined from 10 frames using ϕ scans. Data were measured using φ- and ω-scans and were processed using the standard Nonius software.[19-20] The structures were solved using direct methods (2: SIR-97; 3: SHELXS-97) and refined by full-matrix least-squares method on F^2 with SHELXL97-2.[21] The non-hydrogen atoms were refined anisotropically. Hydrogen atoms were included at geometrically idealized positions (C-H bond distances 0.95/0.99 Å; N-H bond distances 0.88 Å) and were not refined. The isotropic thermal parameters of the hydrogen atoms were fixed at 1.2 times that of the preceding carbon or nitrogen atoms.[22-23]

5.5.4. Electrochemical Measurements: The electrochemical experiments were carried out at room temperature using CV-50W voltammetric analyzer. A gold electrode (diameter 50 μm) was used as working electrode. 1 mM solutions of compounds **6 - 8** were prepared in 0.1 M tetrabutylammonium perchlorate (TBAP) in CH2Cl2. Cyclic voltammetry (CV) experiments were carried out at a scan rate of 100 mV/s. Differential Pulse Voltammetry (DPV) was carried out at 10 mV/s. A platinum wire (1 mm) was used as the counter electrode and a Ag/AgCl (BAS) was used a the reference electrode. The $E_{1/2}$ of the Fc/Fc+ couple under the experimental conditions is 448(+/-5) mV (vs. Ag/AgCl).

5.6. Acknowledgements: The authors would like to acknowledge the financial support from NSERC, the Canada Foundation for Innovation (CFI) and the Saskatchewan Innovation Fund (SIF). H.-B.K is Canada Research Chair in Biomaterials. We are grateful to Ken Thoms for running the MS spectra and to the SSSC for instrument time (NMR, X-ray).

Supporting information containing intermolecular arrangement of **6** and VT-NMR plots of **8** and CV and DPV plots of **6**, **7** and **8** has been presented below after references.

5.7. References

[1] S. G. Zhang, *Nat. Biotechnol.*, **2003**, 21, 1171–1178.
[2] V. Balzani, A. Credi, F. M. Raymo and J. F. Stoddart, *Angew. Chem. Int. Ed.*, **2000**, 39, 3349–3391.
[3] M. A. Shogren-Knaak, P. J. Alaimo and K. M. Shokat, *Annu. Rev.Cell Dev. Biol.*, **2001**, 17, 405–433.
[4] T. Moriuchi and T. Hirao, *Chem. Soc. Rev.*, **2004**, 33, 294–301.
[5] R. S. Herrick, R. M. Jarret, T. P. Curran, D. R. Dragoli, M. B.Flaherty, S. E. Lindyberg, R. A. Slate and L. C. Thornton, *Tetrahedron Lett.*, **1996**, 37, 5289–5292.
[6] I. Bediako-Amoa, R. Silerova and H. B. Kraatz, *Chem. Commun.*, **2002**, 2430–2431.
[7] A. Nomoto, T. Moriuchi, S. Yamazaki, A. Ogawa and T. Hirao, *Chem. Commun.*, **1998**, 1963–1964.
[8] T. Moriuchi, A. Nomoto, K. Yoshida and T. Hirao, *Organometallics*, **2001**, 20, 1008–1013.
[9] T. Moriuchi, A. Nomoto, K.Yoshida, A. Ogawa and T. Hirao, *J. Am. Chem. Soc.*, **2001**, 123, 68–75.
[10] T. Moriuchi, K. Yoshida and T. Hirao, *Organometallics*, **2001**, 20, 3101–3105.
[11] D. R. van Staveren, T. Weyhermuller and N. Metzler-Nolte, *Dalton Trans.*, **2003**, 210–220.
[12] L. Barisic, M. Dropucic, V. Rapic, H. Pritzkow, S. I. Kirin and N. Metzler-Nolte, *Chem. Commun.*, **2004**, 2004–2005.
[13] G. Cerichelli, B. Floris and G. Ortaggi, *J. Organomet. Chem.*, **1974**, 76, 73.
[14] E. M. Acton and R. M. Silverstein, *J. Org. Chem.*, **1959**, 24, 1487– 1490.
[15] F. S. Arimoto and A. C. Haven, *J. Am. Chem. Soc.*, **1955**, 77, 6295.
[16] W. E. Parham and V. J. Trynelis, *J. Am. Chem. Soc.*, **1955**, 77, 68.
[17] G. R. Knox and P. L. Pauson, *J. Chem. Soc.*, **1961**, 4615.

[18] A. Shafir, M. P. Power, G. D. Whitener and J. Arnold, *Organometallics*, **2000**, 19, 3978.
[19] *COLLECT data collection software*, Nonius, Delft, The Netherlands, **1998**.
[20] SCALEPACK v1.96: Z. Otwinowski and W. Minor, Processing of Xray Diffraction Data Collected in Oscillation Mode, *Methods Enzymol.*, **1998**, 276, 302; Z. Otwinowski and W.Minor, *Macromolecular Crystallography, Part A*, ed. C. W. Carter, Jr. and R. M. Sweet, Academic Press, San Diego, CA, **1997**.
[21] G. M. Sheldrick, *SHELXS-97, Program for solution of crystal structures*, University of Göttingen, Germany, **1997**.
[22] A. Altomare, M. C. Burla, M. Camalli, G. L. Cascarano, C. Giacovazzo, A. Guagliardi, A. G. G. Moliterni, G. Polidori and R. Spagna, *J. Appl. Crystallogr.*, **1999**, 32, 115.
[23] G. M. Sheldrick, *SHELXL-97-2, Program for refinement of crystal structures*, University of Göttingen, Germany, **1998**.

5.8. Supporting Information

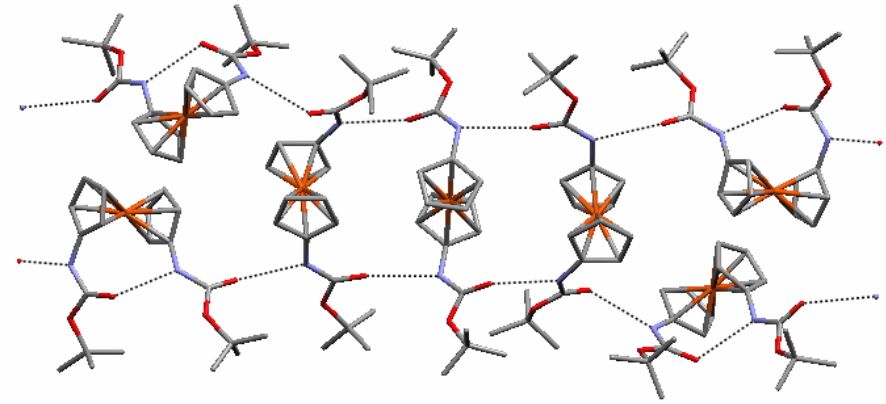

Figure 5. S1. Sheet like arrangement in the X-ray single crystal structure of compound **6** involving three different rotamers present in the asymmetric unit cell and their linkages though hydrogen bonding. Selected hydrogen bond distances are O51····N41 = 2.709Å, N51A····O31 = 2.763Å, N51····O31A = 2.763Å, O51A····N41A = 2.709Å, O41····N11 = 2.781Å, N31····O21B = 2.735Å, O11····N21 = 2.614Å, O21····N31B = 2.735Å . [A =1-x,1-y,-z B=1.5-x,1/2+y,1/2-z]

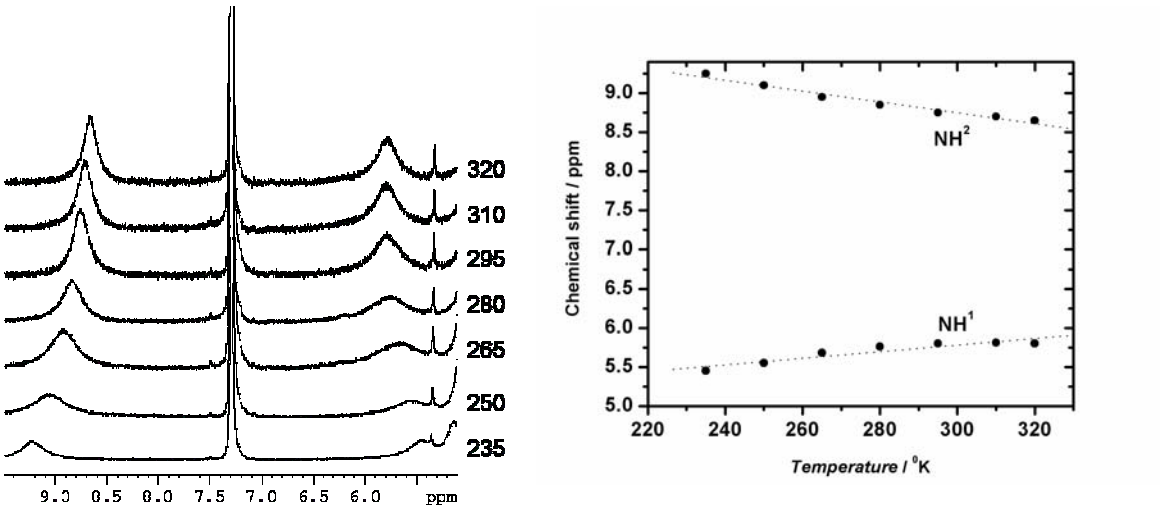

Figure 5.S2. Variable NMR study of 1,1'-bis(*tert*-Butoxycarbonyl-L-Alanine-amido) ferrocene (**7**), NH^1 is close to ferrocene and NH^2 is the one which is attached to Boc.

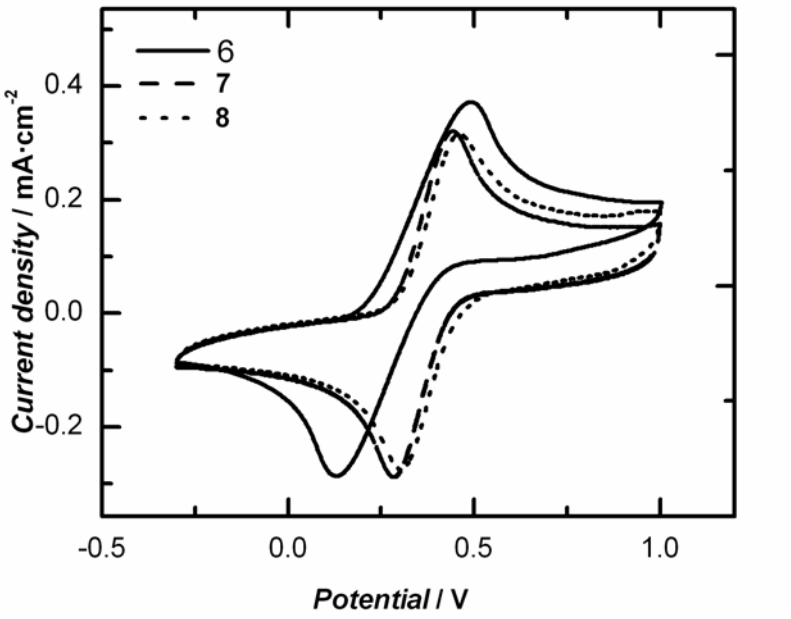

Figure 5.S3. Cyclic voltammogram SWV spectra of 0.1 M compounds **6-8** measured using GCE electrode vs. Ag/AgCl , scan rate 0.1 v/s, in CH_2Cl_2 /0.1 M TBAP. The $E_{1/2}$ of the Fc/Fc^+ couple under the experimental conditions is 448(+/-5) mV (vs. Ag/AgCl).

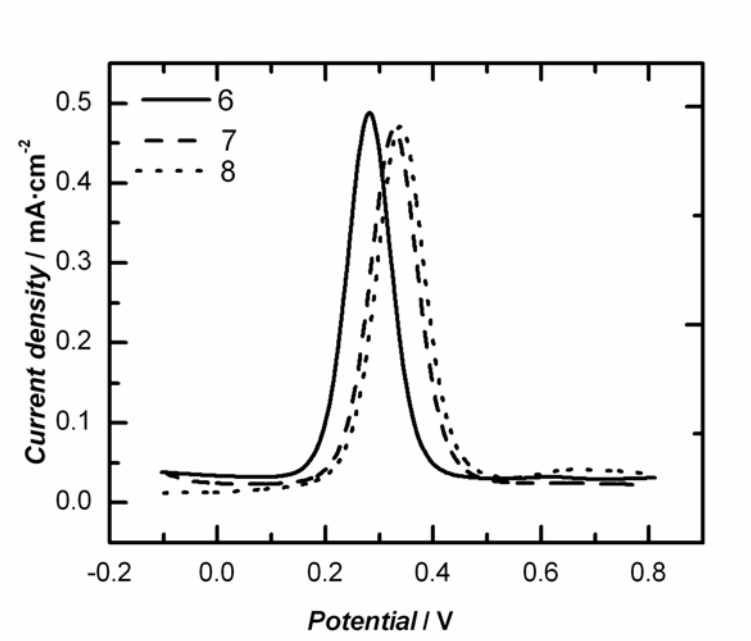

Figure 5.S4. SWV spectra of 0.1 M compounds **6-8** measuredusing GCE electrode vs. Ag/AgCl , scan rate v/s, in CH_2Cl_2 /0.1 M TBAP. The $E_{1/2}$ of the Fc/Fc^+ couple under the experimental conditions is 448(+/-5) mV (vs. Ag/AgCl).

Chapter 6

Rational Design of a New Class of Bioorganometallic Foldamers: A Potential Model for Parallel β-Helical Peptides.

6.0. Connecting Text

This chapter describes the synthesis of a series of Fca-peptide conjugates which can adopt the *β*-helical conformation, a critical structural domain of proteins. It is known that peptide conjugates of disubstituted Fc are capable of providing *β*-sheet motif to the attached peptide strands and in the same time the peptides align themselves in helical fashion with respect to Fc. In this attempt, we exploited both these charteristics in extended form. Structural studies of the Fca-peptide conjugates in solution and solid states indicated the formation of *β*-helical conformation. Thus, it is an efficient novel method to control the structure of peptides using molecular scaffold.

 This paper was co-authored by G. Schatte and H.-B. Kraatz. All experimental works with the exception of crystallographic analysis were carried out by me. In addition I wrote the initial draft of the manuscript. The text below is a *verbatim* copy of the published paper.

6.1. Introduction

The design of structurally well-defined peptide motifs has been an active area of research aimed at gaining a deeper understanding of biochemical processes,[1] to generate molecules with potential biological applications,[2] or to develop novel biomaterials.[3] Synthetic foldamers that resemble the structure of helical[4] and sheet conformations,[5] two of the major secondary structural motifs in proteins, can now be

designed de novo using non-proteinogenic amino acids or molecular scaffold. Alternating D- and L-amino acid sequences have been found to generate helical conformations maintaining the β-sheet in the same time so called β-helix as is seen in Gramicidin A.[6] In 1993, a new kind β-helix formed only from the sequence of L-amino acids, was discovered in bacterial *Pectate Lyase C*.[7] and was recognized to play various important roles in biological systems.[8] In this structural motif, a series of β-strands are linked by a turn-region, resulting in a virtually perpendicular arrangement of the individual β-strands with respect to the axis of the helix. Little effort has been dedicated in designing the model for this important secondary structural domain. In 2001, Nolte and coworkers reported the synthetic analogue, where peptide strands are attached to a central polyiscyanide backbone and adopt a β-sheet running the length of the central helical core.[9] Disubstituted ferrocenes, and ferrocene amino acid (Fca) in particular, are known to induce β-turns in peptide conjugates and have the appropriate structural rigidity due to efficient H-bonding interactions between the peptide chains attached to the two Cp rings.[10] Thus, we hypothesized that it should be possible to design helical foldamer exploiting the turn-inducing properties of Fca and linking them to α-amino acids. It was thought that the H-bonding interactions between the peptide substituents on opposite Cp rings would favor the formation of a helical foldamer which displays the main features of the natural β-helical motif. Here, we wish to present the results of a synthetic and structural study of a series of helical foldamers formed from L- and D-alanine and Fca. Our results unequivocally show the utility of our design approach for the formation of a series of unprecedented helical foldamers displaying right- and left-handedness.

6.2. Results and Discussions

Starting from the fully protected Fca derivative **1**,[11] the desired "monomers" Fca-L-alanine (**2**) and Fca-D-alanine (**3**), their corresponding oligomers **6-11**, and poly(Fca-L-alanine) **12** were synthesized in solution by peptide coupling strategies as indicated in Scheme 6.1 and were characterized spectroscopically (see section 6.6.1.2.). The ^{1}H-NMR spectra of **2** and **3** in $CDCl_3$ show the presence of amide NH signal at δ 7.61 (NH of Fca) and δ 6.50 (NH of Ala). As the length of the peptide increases, the amide resonances gradually shift downfield, indicating an increasingly H-bonded system (see Figure 6.S1). In the case of the polymeric **12**, the two amide NH resonances are observed δ 10.87 (for NH attached to Cp) and δ 9.07 (for NH of Ala) as is expected for strongly H-bonded systems.

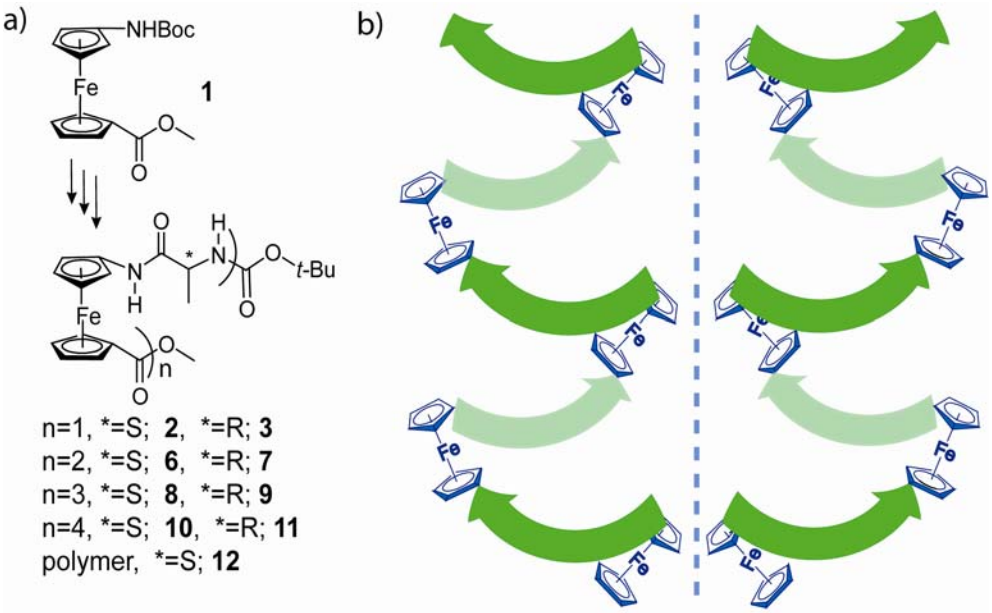

Scheme 6.1. a) Preparation of P and M helical foldamers from the conjugates of Fca with L- and D-alanine respectively (detail description of the synthesis and characterization is given in section 6.6.1.2.); b) Schematic representation of the formation of right and left handed beta helical structures from the alternating conjugates of Fca and L-amino acids and D- amino acids respectively which are mirror image of each other.

Structural studies in solution by ROESY-NMR of the Fca-foldamers **6**, **8**, and **10** show the cross correlations between the Fc-NH_i and the β-H of Ala_{i+1}, between the Ala-NH_{i+1} and the α-H of Ala_i and between β-H of Ala_{i+1} and the α-H of Ala_i (see Figure 6.S2 - Figure 6.S4), which correspond to the β-helical conformations. Circular dichroism (CD) spectroscopy is a reliable tool to evaluate the conformation of chiral Fc-conjugates displaying a band (+ or –) at about 450 nm. CD studies of our foldamers in acetonitrile solution (Figure 6.1) show that the oligomers **6**, **8**, and **10**, derived from L-Ala, exhibit a weak positive Cotton effect (*P*-helicity) in the ferrocene region at λ = 450 nm, while the D-Ala derivatives **7**, **9** and **11** exhibit a negative Cotton effect (*M*-helicity).

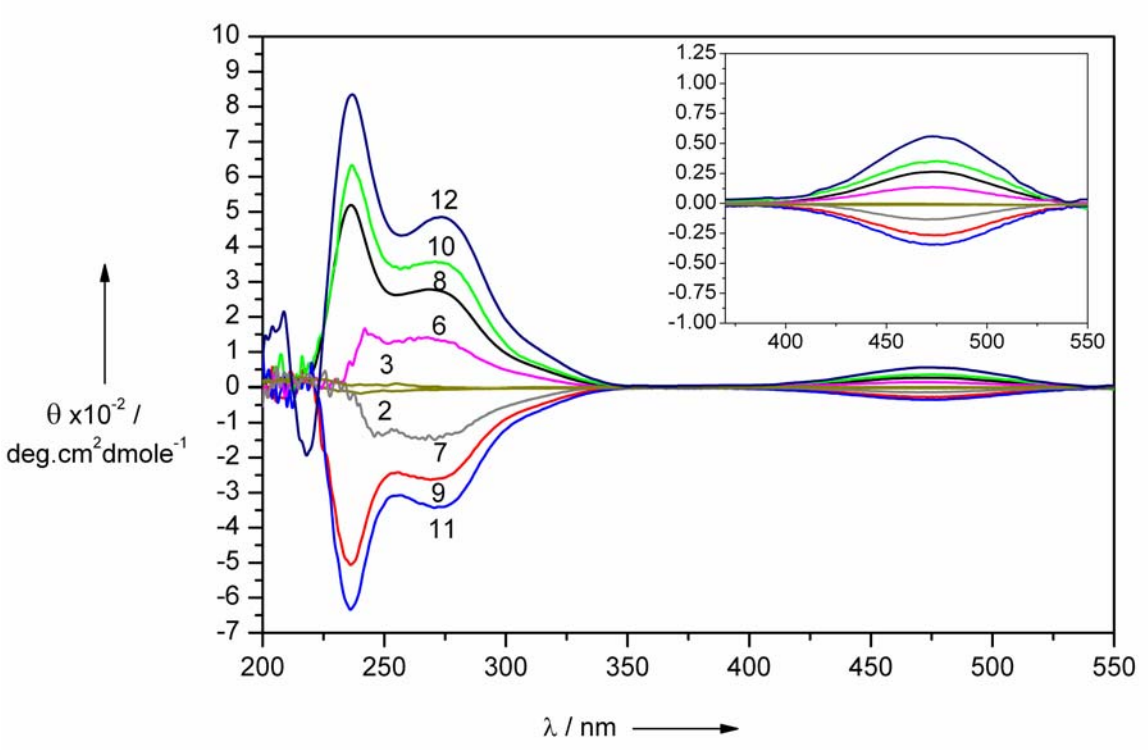

Figure 6.1. Circular dichroism spectra of the Fca-Ala "monomers" **2** and **3** and the right handed and left handed parallel β-helical Fca-Ala oligomers (**6**-**11**) and polymer (**12)** in acetonitrile at 25°C. Intensity is normalized for one repeating unit.

The Fca-Ala "monomers" **2** and **3** do not exhibit any Fca-based band, but display a weak signal in the peptide region, which are mirror images of each other. The absence of the band in the Fca region is not surprising, since the intramolecular H-bonding required to establish a stable secondary structure is not possible in these "monomers". For the dimers **6** and **7** in which two Fca-Ala units are connected to each other through an Ala unit, strong intramolecular H-bonding (see Figure 6.2, vide infra) exists between the two Ala groups. The resulting effect on the CD spectrum normalized to a single Fca-Ala is significant enhancement of the bands. Additional Fca-Ala units increase the signal intensity of the normalized CD spectrum in both the Fca and peptide region. Peptides of equal length have CD signals of equal magnitude but of opposite sign, indicating that the helicity pattern is identical but of opposite handedness. Upon elongation, the conjugates are able to establish stronger intramolecular H-bonding between adjacent Ala units resulting in more rigid helical arrangement. Importantly, the polymer displays a characteristic band at 215 nm indicative of β-sheet peptides, which is absent in the smaller oligomers. The helices are stable at elevated temperatures and do not show a distinct melting behavior at temperatures up to 70˚C (see Figure 6.S5).

The dimers (**6** and **7** in $P2_12_12_1$ space group) and trimers (**8** in $P4_12_12$ and **9** in $P4_32_12$ space group) were easily crystallized either by slow diffusion of non solvent into the sample solution or by slow evaporation of solvent from the solution (see section 6.6.6). The single crystal structure analyses of those show the expected axial chirality for each of the Fca residues. All systems derived from L-Ala adopt a P-helical conformation, while D-Ala gives rise to M-helicity, corroborating the CD results. The amino acid residues are involved in intramolecular H-bonding, forming parallel β-sheet-like structure with 12-membered H-bonded rings.

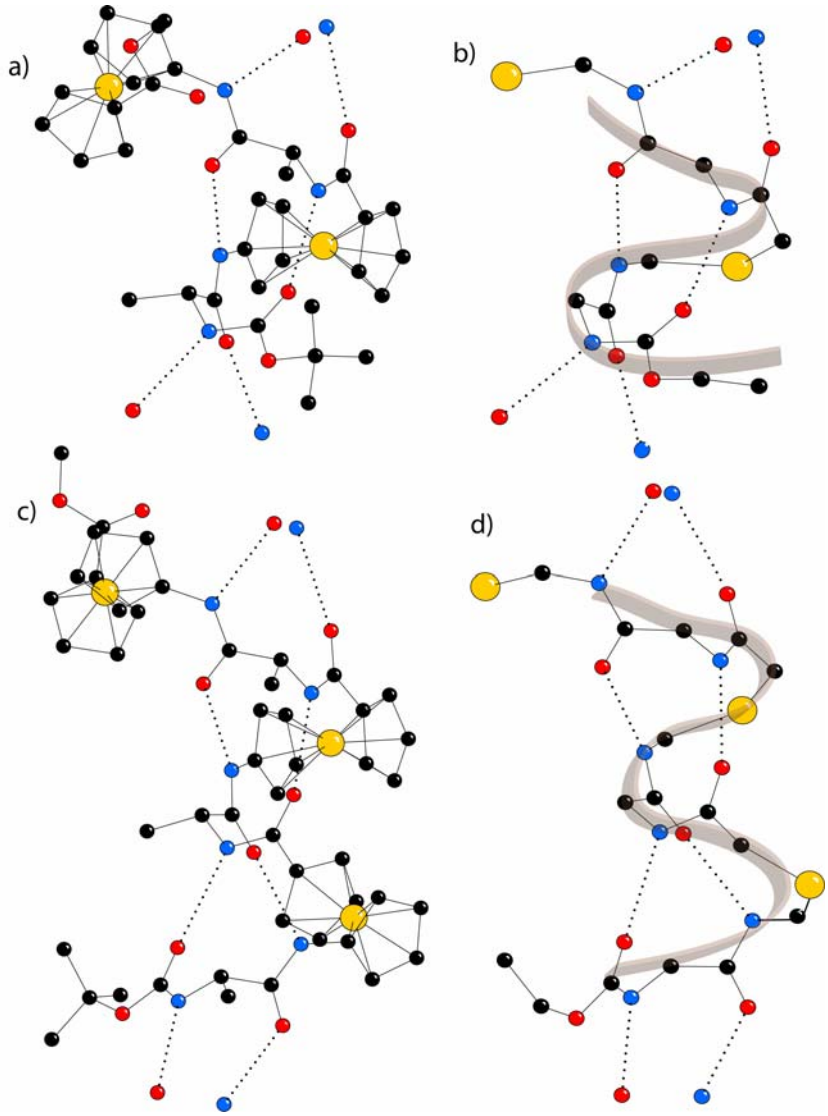

Figure 6.2. a) Crystal Structure of 6, b) Showing the helical backbone of 6, c) Crystal Structure of 8, d) Showing the helical backbone of 8. Black spheres are carbon, blues are nitrogen, reds are oxygen and yellows are iron. Hydrogen atoms are omitted for clarity. Dashed lines represent H-bond. The intramolecular and intermolecular H-bonding patterns are identical (12-membered rings including the H-atoms, parallel β-sheet like). Crystal structure of 7 is the mirror image of 6 and 9 is the mirror image of 8 (see Figure 6.S15).

As the length of the helix increases, the number of 12-membered H-bonded rings increases. The intramolecular H-bonding distances (N-O) are 2.95-2.92 Å between the NH of Fca and C=O of Ala and 2.99-2.97Å between the NH of Ala and C=O of Fca.

The dihedral angles of all peptide segments for compounds **6** and **8** are -79 > φ > -67° and 155 < ψ < 138°, which fall within the regions of the Ramachandran plot (φ = -180° to - 45° and ψ = 45° to 225°) assigned to β-sheet conformations although it deviates from the perfect parallel β-sheet conformation.[13] For the foldamers **7** and **9** derived from D-Ala, the dihedral angles are similar in magnitude but of opposite in sign. Importantly, on the supramolecular level, the same H-bonding pattern as intramolecular (12 membered parallel beta sheet like ring formation and similar N-O distances) is propagated forming a continuous helical structure. The individual supramolecular helices arrange parallel to each other to generate solvent filled hydrophobic pockets (CH_2Cl_2 for **6** and **7**, hexane for **8**, $CHCl_3$ for **9**). FTIR of the foldamers in KBr (see Figure 6.S6 – Figure 6.S9) show the amide A absorption in the range 3266-3272 cm^{-1} which clearly indicates the involvement of the amide NH in H-bonding. The Amide I and II regions of the conjugates are complex and show a series of bands (1627-1639 cm^{-1} and 1680-1690 cm^{-1}) that may be attributed to a β-sheet conformation.[14]

6.3. Conclusion

In conclusion, we presented the results of a study into the preparation and structural properties of organometallic peptide conjugate foldamers which adopt a structure that shows some structural similarities to the β-helical motif found in naturally occurring proteins, exploiting the turn-inducing ability of Fca. This novel redox active β-helical system may have potential for the electrochemical screening of "beta-breakers". We are now exploring the electronic and electrochemical properties of these systems in solution and surface using surface-supported helical foldamers. In addition, we are

expanding our approach to include other amino acids, such as glutamic acid, which should allow us to synthesize and study artificial anti-freeze peptides.

6.4. Acknowledgements: We acknowledge support from NSERC in the form of an operating grant. H.-B. K. is the Canada Research Chair in Biomaterials.

Supporting Information containing Experimental and spectroscopic details; IR spectra for all compounds; VT-CD spectra and NMR stack plot for L-series; ROESY spectra of **6**, **8** and **10**; single crystal data and intermolecular arrangements of compounds **6-9**. is presented below, after references.

6.5. References

[1] a) M. A. Shogren-Knaak, P. J. Alaimo, K. M. Shokat, *Annu. Rev. Cell Dev. Biol.* **2001**, *17*, 405-433; b) J. D. Sadowsky, M. A. Schmitt, H. S. Lee, N. Umezawa, S. M. Wang, Y. Tomita, S. H. Gellman, *J. Am. Chem. Soc.* **2005**, *127*, 11966-11968.

[2] a) M. Zasloff, *Nature* **2002**, *415*, 389-395; b) M. A. Schmitt, B. Weisblum, S. H. Gellman, *J. Am. Chem. Soc.* **2004**, *126*, 6848-6849; c)S. Fernandez-Lopez, H. S. Kim, E. C. Choi, M. Delgado, J. R. Granja, A. Khasanov, K. Kraehenbuehl, G. Long, D. A. Weinberger, K. M. Wilcoxen, M. R. Ghadiri, *Nature* **2001**, *412*, 452-455.

[3] a) S. G. Zhang, *Nature Biotech.* **2003**, *21*, 1171-1178; b) S. Hecht, *Mater. Today* **2005**, 48-55.

[4] a) D. Seebach, M. Overhand, F. N. M. Kuhnle, B. Martinoni, L. Oberer, U. Hommel, H. Widmer, *Helv. Chim. Acta* **1996**, *79*, 913-941; b) S. H. Gellman, *Acc. Chem. Res.* **1998**, *31*, 173-180; c) J. S. Nowick, *Acc. Chem. Res.* **1999**, *32*, 287-296; d) D. H. Appella, L. A. Christianson, I. L. Karle, D. R. Powell, S. H. Gellman, *J. Am. Chem. Soc.* **1999**, *121*, 6206-6212; e) R. P. Cheng, S. H. Gellman, W. F. DeGrado, *Chem. Rev.* **2001**, *101*, 3219-3232; f) D. J. Hill, M. J. Mio, R. B. Prince, T. S. Hughes, J. S. Moore, *Chem. Rev.* **2001**, *101*, 3893-4011; g)J. Venkatraman, S. C. Shankaramma, P. Balaram, *Chem. Rev.* **2001**, *101*, 3131-3152; h) J.-M. L. Joachim Garric, Ivan Huc, *Angew. Chem. Intl. Ed.* **2005**, *44*, 1954-1958, *Angew. Chem.* **2005,** 117, 1990-1994; i) W. S. Horne, M. K. Yadav, C. D. Stout, M. R. Ghadiri, *J. Am. Chem. Soc.* **2004**, *126*, 15366-15367; j) G. V. M. Sharma, P. Nagendar, P. Jayaprakash, P. R. Krishna, K. V. S.

Ramakrishna, A. C. Kunwar, *Angew. Chem. Intl. Ed.* **2005**, *44*, 5878-5882. *Angew. Chem.* **2005,** 117, 6028-6032; k) M. A. Schmitt, S. H. Choi, I. A. Guzei, S. H. Gellman, *J. Am. Chem. Soc.* **2005**, *127*, 13130-13131; l) C. Baldauf, R. Gunther, H. J. Hofmann, *Angew. Chem. Intl. Ed.* **2004**, *43*, 1594-1597, *Angew. Chem.* **2005,** 116, 1621-1624; m) G. V. M. Sharma, K. R. Reddy, P. R. Krishna, A. R. Sankar, P. Jayaprakash, B. Jagannadh, A. C. Kunwar, *Angew. Chem. Intl. Ed.* **2004**, *43*, 3961-3965, *Angew. Chem.* **2004,** 116, 4051-4055; n) A. Hayen, M. A. Schmitt, F. N. Ngassa, K. A.Thomasson, S. H. Gellman, Angew. Chem. 2004, 116, 511; Angew. Chem. Int. Ed. 2004, 43, 505-510, Angew. Chem. 2004, 116, 511 –516; o) S. De Pol, C. Zorn, C. D. Klein,O. Zerbe, and O. Reiser, Angew. Chem. Int. Ed. 2004, 43, 511 –514, Angew. Chem. 2004, 116, 517 –520. p) C. Baldauf, R. Gunther, H.-J. Hofmann, *J. Org. Chem.* **2006**, *71*, 1200-1208.

[5] a) J. P. Schneider, J. W. Kelly, *Chem. Rev.* **1995**, *95*, 2169-2187; b) T. A. Martinek, G. K. Toth, E. Vass, M. Hollosi, F. Fulop, *Angew. Chem. Intl. Ed.* **2002**, *41*, 1718-1721, *Angew. Chem.* **2002,** 114, 1794-1797; c) W. A. Loughlin, J. D. A. Tyndall, M. P. Glenn, D. P. Fairlie, *Chem. Rev.* **2004**, *104*, 6085-6117.

[6] a) B. A. Wallace, *Biophys. J*. **1986**, 49, 295-306; b) G. N. Ramachandran, R. Chandrasekaran, *Ind. J. Biochem. Biophys*, **1972**, 9, 1-11; c) E. Navarro, E. Fenude, B. Celda, *Biopolymers* **2002**, *64*, 198; d) C. Baldauf, R. Gunther, H. J. Hofmann, *Biopolymers* **2005**, *80*, 675; e) P. De Santis, S. Morosetti, R. Rizzo, *Macromolecules*, **1974**, 7, 52-58

[7] M. D. Yoder, N. T. Keen, F. Jurnak, *Science* **1993**, *260*, 1503.

[8] a) Y. C. Liou, A. Tocilj, P. L. Davies, Z. C. Jia, *Nature* **2000**, *406*, 322; b) J. Jenkins, R. Pickersgill, *Prog. Biophys. Mol. Biol.* **2001**, *77*, 111.

[9] J. Cornelissen, J. Donners, R. de Gelder, W. S. Graswinckel, G. A. Metselaar, A. E. Rowan, N. Sommerdijk, R. J. M. Nolte, *Science* **2001**, *293*, 676.

[10] a) T. Moriuchi, A. Nomoto, K. Yoshida, A. Ogawa, T. Hirao, *J. Am. Chem. Soc.* **2001**, *123*, 68-75; b) D. R. van Staveren, N. Metzler-Nolte, *Chem. Rev.* **2004**, *104*, 5931-5985; c) T. Moriuchi, T. Hirao, *Chem. Soc. Rev.* **2004**, *33*, 294; d) L. Barisic, M. Dropucic, V. Rapic, H. Pritzkow, S. I. Kirin, N. Metzler-Nolte, *Chem. Commun.* **2004**, 2004-2005; e) S. Chowdhury, K. A. Mahmoud, G. Schatte, H. B. Kraatz, *Org. Biomol. Chem.* **2005**, *3*, 3018-3023.

[11] L. Barisic, W. Rapic, V. Kovac, *Croat. Chem. Acta* **2002**, *75*, 199-210.

[12] S. I. Kirin, H. B. Kraatz, N. Metzler-Nolte, *Chem. Soc. Rev.* **2006**, *35*, 348-354.

[13] G. N. Ramachandran, V. Sasisekharan, *Adv. Protein Chem.* **1968**, 23, 283-437.

[14] a) S. Krimm, J. Bandekar, *Adv. Protein Chem.* **1986**, 38, 181-364; b) A. Barth, C. Zscherp, *Quart. Rev. Biophys.* **2002**, *35*, 369-430; c) M. R. Ghadiri, J. R. Granja, R. A. Milligan, D. E. McRee, N. Khazanovich, *Nature* **1993**, *366*, 324-327.

6.6. Supplementary Information

6.6.1. Experimental

6.6.1.1. General: All syntheses were carried out in air unless otherwise indicated. CH_2Cl_2 (BDH; ACS grade) used for synthesis was dried (CaH_2) and distilled prior to use. $CDCl_3$ (Aldrich) was dried (CaH_2) , and stored over molecular sieves (8-12 mesh; 4Å effective pore size; Fisher) before use., Amino Acids, HBTU (Advanced Chemtech), $MgSO_4$, Citric Acid and $NaHCO_3$ (VWR), TFA, TEA, DIEPA (Aldrich) were used as received. For column chromatography, a column with a width of 2.7 cm (ID) and a length of 45 cm was packed 18-22 cm high with 230-400 mesh silica gel (VWR). For TLC, aluminum plates coated with silica gel 60 F_{254} (EM Science) were used. NMR spectra were recorded on a Bruker Avance-500 spectrometer using a 5-mm broadband probe operating at 500.134 MHz (^1H) and 125.766 MHz (^{13}C $\{^1H\}$). Peak positions in both ^1H and ^{13}C spectra are reported in ppm relative to TMS. The ^1H NMR, COSY, TOCSY, HMQC, HMBC and ROESY spectra are referenced to the residual $CHCl_3$ signal at δ 7.27. All ^{13}C $\{^1H\}$, HMQC and HMBC spectra are referenced to the $CDCl_3$ signal at δ 77.23. ROESY spectra were taken using spin lock period 200msec and relaxation delay 3.5sec. Mass spectrometry was carried out on a VG Analytical 70/20 VSE instrument. Infrared spectra were obtained with a Perkin-Elmer model 1605 FT-IR at 4 cm^{-1} resolution.

6.6.1.2. General Procedure for the Synthesis of the Monomers and Oligomers

Boc protected precursors*, were stirred in 60% of trifluoroacetic acid (TFA) in dichloromethane for 30 minutes in nitrogen atmosphere. The TFA was completely

removed as an azeotrope by repeated evaporation using a rotovap using dichloromethane. The remaining solid material was dissolved in dichloromethane, placed in an ice bath (0-5°C) and was made basic using *N*-*N*-diisopropylethylamine in an approximately 1: 2.5 molar ratio. Then the acid component was added in a 1:1 molar ratio. After 15 minutes, HBTU (1:1.4 molar ratio) was added and stirred for 7-8 hours. The reaction mixture was washed sequentially with saturated aqueous sodium bicarbonate, 10% aqueous citric acid, saturated sodium bicarbonate and then water. The organic phase was dried over anhydrous sodium sulfate, filtered and then evaporated to dryness. The crude product was purified by flash column chromatography.

*Boc protected ferrocene-1-amino-methyl carboxylate(**1**) in 10 mmol scale for the preparation of monomers(**2** and **3**), monomers in 2.5mmol scale for the preparation of dimmer (**6** and **7**), dimers in 1mmol scale for the preparation of trimers (**8** and **9**) and trimer in 0.5 mmol scale for the tetramer (**10** and **11**))

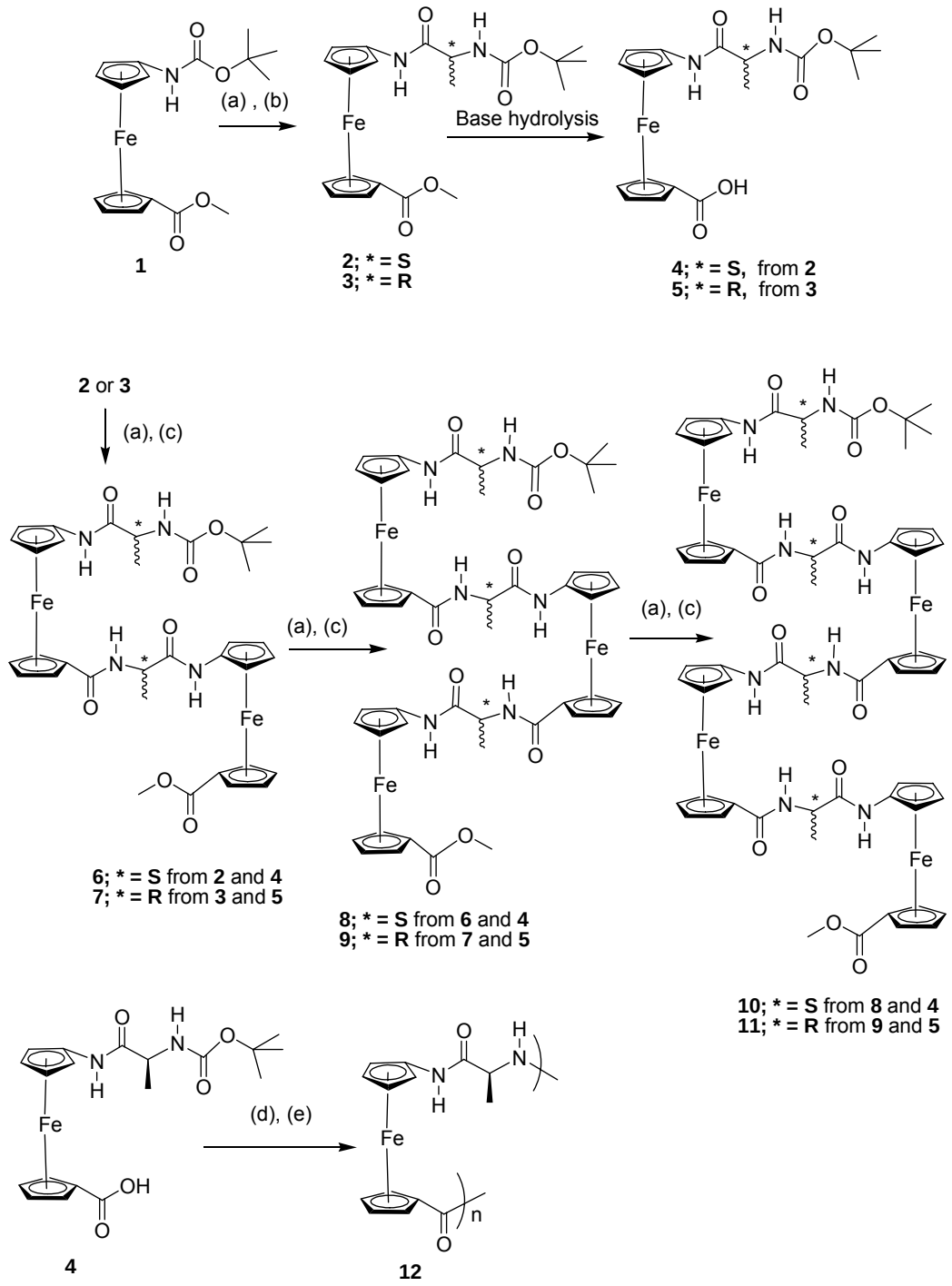

Scheme 6.S1. Synthesis of monomers, oligomers and polymers (a) Stirring in 60% TFA in DCM, (b) TFA removed, dissolved in DCM, made basic by DIEPA, add Boc protected D- or L-Ala, add HBTU and stir overnights under N_2 atmosphere. (c) TFA removed, dissolved in DCM, made basic by DIEPA, added respective carboxylic acid, added HBTU and stirred for 7 hours.(d) Along with 5 mol % of **2** stirred in 60% TFA in DCM, (e) TFA removed, dissolved in DCM, made alkaline by DIEPA, added respective carboxylic acid, added HBTU and stirred for 10 hours then 5 % (mol) of **4** was added and stirred foe 2 hours.

6.6.1.2.1. 1-Boc-L-Alanino-n'-methyl-ferrocene-carboxylate (2): Flash column chromatography using ethylacetate/hexanes (1/1) (R_f = 0.35). Yield (75%), orange powder**.** HRMS (ES): calc for $C_{20}H_{28}N_2O_4Fe$: 430.1449; found: 430.1410$[M]^+$. FT-IR (KBr, cm^{-1}): 3322 (b, s, N-H), 1711 (s, ester C=O), 1688 (s, amide I), 1519 (s, Amid II). UV-vis (CH_3CN; λ in nm [ε in $Lmol^{-1}cm^{-1}$]: 443 [280], ^{1}H-NMR ($CDCl_3$, δ/ppm): 7.65 (1H, s, br, NH attached to Cp), 5.16 (1H, d, *J* = 6 Hz, NH of Ala), 4.77 (2H , s, Cp), 4.65 (1H, s, Cp), 4.57 (1H, s, br, α-H of Ala), 4.36 (2H, s, Cp), 4.21 (1H, s, br, Cp), 4.02 (2H, d, *J* = 6 Hz, Cp), 3.80 (3H, s, CH_3 of ester), 1.49 (9H, s CH_3 of Boc), 1.45 (3H, d, *J* = 7 Hz, CH_3 of Ala). $^{13}C\{^1H\}$-NMR ($CDCl_3$, δ/ppm): 172.1 (C=O of ester), 171.4 (C=ONH), 156.2 (C=ONH of Boc), 95.4 (Fc C attached to carbonyl), 80.8, 72.9, 72.9 , 72.3, 71.6, 71.4, 66.9, 66.6, 63.5, 63.2 (different Cs of Cps), 52.0 (CH_3 of ester), 51.2 (α-C of Ala), 80.8(tertiary C of Boc), 28.7 (CH_3 of Boc), 18.4 (CH_3 of Ala).

6.6.1.2.2. 1-Boc-D-Alanino-n'-methyl-ferrocene-carboxylate (3): Flash column chromatography using ethylacetate/hexanes (1/1) (R_f = 0.35). Yield (70%), orange powder**.** HRMS (ES): calc for $C_{20}H_{28}N_2O_4Fe$: 430.1449; found: 430.1421$[M]^+$. FT-IR (KBr, cm^{-1}): 3314 (b, s, N-H), 1717 (s, ester C=O), 1689(s, amide I), 1515 (s, Amid II). UV-vis (CH_3CN; λ in nm [ε in $Lmol^{-1}cm^{-1}$]: 443 [282], ^{1}H-NMR ($CDCl_3$, δ/ppm): 7.64 (1H, s, br, NH attached to Cp) 5.15 (1H, d, *J* = 6.5 Hz, NH of Ala), 4.75 (2H , s, Cp), 4.65 (1H, s, Cp), 4.56 (1H, s, br, α-H of Ala), 4.40 (2H, s, Cp), 4.22 (1H, s, br, Cp), 4.05(2H, d, *J* = 7 Hz, Cp), 3.80 (3H, s, CH_3 of ester), 1.49 (9H, s CH_3 of Boc) 1.45 (3H, d, *J* = 7 Hz, CH_3 of Ala). $^{13}C\{^1H\}$-NMR ($CDCl_3$, δ/ppm): 172.2 (C=O of ester), 171.4 (C=ONH), 156.2(C=ONH of Boc) 95.3 (Fc C attached to carbonyl), 80.7, 72.5, 72.8 ,

72.3, 71.7, 71.4, 66.8, 66.5, 63.5, 63.2 (different Cs of Cps), 52.0 (CH_3 of ester), 51.2 (α-C of Ala), 81.0 (tertiary C of Boc), 28.2 (CH_3 of Boc), 18.3 (CH_3 of Ala).

6.6.1.2.3. 1-Boc-L-Alanino-n'-methyl-ferrocene-carboxylic Acid (4): 5 mmol (2.15g) **2** was dissolved in 200 mL of dioxane. To it was added the solution of 5mmol of sodium hydroxide in 10ml of water. It was stirred at 50°C for one hour. Then the solvent was removed by rotovaporation and 100 ml of water was added, and washed with dichloromethane to remove unreacted ester. The aqueous layer was cooled in ice bath and acidified by 2N HCl and the precipitate was extracted by DCM, dried by sodium sulfate and evaporated to get, orange red powder, 1.84 g (89%) of **4.** ^{1}H-NMR ($CDCl_3$, δ/ppm): 7.67 (1H, s, br, NH attached to Cp), 5.29 (1H, d, *J* = 6 Hz, NH attached to Boc), 5.21 (1H, s) 4.94 (2H, s) 4.61 (1H, s), 4.50 (3H, s, br, α-H and of 2H Cp), 4.14 (1H, s, br, Cp), 4.06 (1H, s, br, Cp) 1.49 (9H, s, CH_3 of Boc), 1.45 (3H, d, *J* = 7 Hz, CH_3, of Ala).

6.6.1.2.4. 1-Boc-D-Alanino-n'-methyl-ferrocene-carboxylic Acid (5): Same procedure like **4** was used. Yield (84%)**,** ^{1}H-NMR ($CDCl_3$, δ/ppm): 7.68 (1H, s, br, NH attached to Cp), 5.29(1H, d, *J* = 6 Hz, NH attached to Boc), 5.22 (1H, s), 4.94 (2H, s) 4.63 (1H, s), 4.50 (3H, s, br, α-H and of 2H Cp) 4.16 (1H, s, br, Cp), 4.07 (1H, s, br, Cp), 1.49 (9H, s, CH_3 of Boc), 1.45(3H, d, *J* = 7 Hz, CH_3, of Ala).

6.6.1.2.5. 1-Boc-L-Alanino-ferrocene-n'-L-Alanino-1-ferrocene-n'-methyl-carboxylate (6): Flash column chromatography by using ethylacetate/hexanes (2/1, R_f = 0.35) (70%) reddish yellow colored compound **6**. HRMS (ES): calc for $C_{26}H_{38}N_4O_6Fe$:

728.2210; found: 728.2128[M]$^{+}$. FT-IR (KBr, cm^{-1}): 3340 (br, N-H), 3273 (br, N-H hydrogen bonded) 1715 (s, ester C=O) 1686 (s, Amid I), 1662 (s, Amid I), 1639 (s, Amid I), 1524 (s, Amid II). UV-vis (CH_3CN; λ in nm [ε in $M^{-1}cm^{-1}$]): 448 [580] ^{1}H-NMR ($CDCl_3$, δ/ppm) : 9.94 (1H, s, NH of Cp), 9.17 (1H s, NH of another Cp), 8.06 (1H, d, *J* = 3 Hz, NH of Ala), 5.47(1H, s, Cp), 5.28(1H, s, NH of other Ala attached to Boc) , 4.95 (1H, s, Cp), 4.80 (2H, d, *J* = 6 Hz , Cp), 4.76 (2H, s, Cp), 4.75 (H, d, *J* = 6.5 Hz, α-H of Ala between two Cp), 4.57 (1H, s, Cp), 4.43 (2H, s, Cp), 4.35 (2H, m, Cp), 4.31(1H, s, α-H of other Ala) 4.11 (1H, s, Cp), 4.02 (2H, d, *J* = 7.5 Hz, Cp), 3.98 (1H, s, Cp), 3.94 (1H, s, Cp), 3.79 (3H, s, ester), 1.56 (3H, d, *J* = 7 Hz, CH_3 of Ala between Fc), 1.49 (9H, s, CH_3 of Boc), 1.45 (3H, d, *J* = 7.0 Hz, CH_3). $^{13}C\{^{1}H\}$-NMR ($CDCl_3$, δ/ppm): 174.6, 172.6, 172.3, 171.6, 156.5, 96.5, 95.9, 80.9, 73.2, 73.1, 72.0, 71.5, 71.3, 70.9, 70.0, 66.9, 66.8, 65.8, 65.7, 64.3, 63.5, 63.1, 52.0, 51.5, 50.5, 30.0, 28.8, 18.4, 17.9.

6.6.1.2.6. 1-Boc-D-Alanino-ferrocene-n'-D-Alanino-1-ferrocene-n'-methyl-carboxylate (7): Flash column chromatography by using ethylacetate/hexanes (2/1, R_f = 0.35) (70%) reddish yellow colored compound 7. HRMS (ES): calc for $C_{26}H_{38}N_4O_6Fe$: 728.2210; found: 728.2181[M]$^{+}$.]$^{+}$. FT-IR (KBr, cm^{-1}): 3360 (br, N-H), 3273 (br, N-H hydrogen bonded) 1715 (s, ester C=O) 1681 (s, Amid I), 1658 (s, Amid I), 1639 (s, Amid I), 1525 (s, Amid II). UV-vis (CH_3CN; λ in nm [ε in $M^{-1}cm^{-1}$]): 448 [582] ^{1}H-NMR ($CDCl_3$, δ/ppm) : 9.93 (1H, s, NH of Cp), 9.14 (1H s, NH of another Cp), 8.07 (1H, d, *J* = 3.5 Hz, NH of Ala), 5.46(1H, s, Cp), 5.27(1H, s, NH of other Ala attached to Boc) , 4.91 (1H, s, Cp), 4.79 (2H, d, *J* = 6 Hz , Cp), 4.75 (2H, s, Cp), 4.74 (H, d, *J* = 6.5 Hz, α-H of Ala between two Cp), 4.56 (1H, s, Cp), 4.43 (2H, s, Cp), 4.35 (2H, m, Cp),

4.31(1H, s, α-H of other Ala) 4.10 (1H, s, Cp), 4.00 (2H, d, *J* = 7.5 Hz, Cp), 3.99 (1H, s, Cp), 3.95 (1H, s, Cp), 3.79 (3H, s, ester), 1.56 (3H, d, *J* = 7 Hz, CH_3 of Ala between Fc), 1.49 (9H, s, CH_3 of Boc), 1.45 (3H, d, *J* = 7.0 Hz, CH_3). $^{13}C\{^1H\}$-NMR ($CDCl_3$, δ/ppm): 175.1, 172.6, 172.3, 171.5, 156.4, 96.5, 95.7, 81.0, 73.2, 73.1, 72.0, 71.5, 71.3, 70.9, 70.0, 66.9, 66.8, 65.8, 65.7, 64.4, 63.4, 63.0, 52.0, 51.5, 51.7, 30.0, 28.8, 18.0, 17.8.

6.6.1.2.7. 1-Boc-L-Alanino-ferrocene-n'-L-Alanino-1-ferrocene-n'-L-Alanino-1-ferrocene-n'-methyl-carboxylate (8): Flash column chromatography by using ethylacetate/hexanes (2/1, R_f = 0.3), (77%) reddish yellow powder. HRMS (ES): calc for $C_{26}H_{38}N_4O_6Fe$: 1026.2414; found: 1026.2151$[M]^+$. FT-IR (KBr, cm^{-1}): 3324 (b, N-H), 3274 (b, N-H hydrogen bonded) 1714 (s, ester C=O) 1691 (s, Amid I), 1661(s, Amid I), 1629 (s, Amid I), 1528 (s, Amid II). UV-vis (CH_3CN; λ in nm [ε in $M^{-1}cm^{-1}$]): 448 [881] ^1H-NMR ($CDCl_3$, δ/ppm) : 10.48 (1H, s, NH of Cp in the middle), 10.20 (1H, s, NH of Cp which is attached to Boc Ala), 8.87 (1H, d, *J* = 7 Hz, amide NH of Ala in the middle), 8.76 (1H, s, NH of Cp with methyl ester), 8.11 (1H, d, *J* = 7 Hz, amide NH of Ala), 5.49(1H, s, Cp), 5.45 (1H, s, Cp), 5.16(1H, s, amide NH of Ala attached to Boc), 4.97 (1H, s, Cp), 4.90 (1H, s, Cp), 4.78(1H, s, Cp), 4.71 (1H m, α-H of Ala), 4.69 (1H, s, Cp), 4.50 (2H, s, Cp), 4.37(1H, s, Cp) 4.30 (1H, d, *J* = 1.8 Hz, α-H of Ala), 4.24 (1H, s, Cp), 4.20 (1H, d, *J* = 8.4 Hz, α-H of Ala), 4.13 (1H, s, Cp), 4.08 (1H, s, Cp), 4.04 (1H, s, Cp), 3.96 (2H, d, *J* = 11 Hz, Cp), 3.86 (2H, s, Cp), 3.75 (3H, s, CH_3 of ester), 1.55 (3H, d, *J* = 7 Hz, CH_3 of Ala in the middle), 1.52 (3H, d, *J* = 7.5 Hz, CH_3 of Ala in one end), 1.49 (9H, s, CH_3 of Ala of Boc), 1.45 (3H, d, *J* = 7 Hz, CH_3 of Ala attached to Boc). $^{13}C\{^1H\}$-NMR ($CDCl_3$, δ/ppm): 175.3, 174.9, 172.4, 171.7, 171.5, 156.4, 96.7,

96.2, 95.4, 80.9, 73.3, 72.7, 71.6, 71.4, 71.4, 70.8, 70.2, 67.1, 66.9, 65.5, 63.9, 63.8, 63.2,52.1, 51.8, 51.7, 50.8, 28.8, 18.2, 17.8, 16.9

6.6.1.2.8. 1-Boc-D-Alanino-ferrocene-n'-D-Alanino-1-ferrocene-n'-D-Alanino-1-ferrocene-n'-methyl-carboxylate (9): Flash column chromatography by using ethylacetate/hexanes (2/1, R_f = 0.3), (77%) reddish yellow powder. HRMS (ES): calc for $C_{26}H_{38}N_4O_6Fe$: 1026.2414; found: 1026.2177$[M]^+$. FT-IR (KBr, cm^{-1}): 3326 (b, N-H), 3270 (b, N-H hydrogen bonded), 1712 (s, ester C=O) 1689 (s, Amid I), 1659 (s, Amid I), 1629 (s, Amid I), 1529 (s, Amid II). UV-vis (CH_3CN; λ in nm [ε in $M^{-1}cm^{-1}$]): 448 [890] ^{1}H-NMR ($CDCl_3$, δ/ppm) : 10.46 (1H, s, NH of Cp in the middle), 10.24 (1H, s, NH of Cp which is attached to Boc Ala), 8.80 (1H, d, *J* = 7 Hz, amide NH of Ala in the middle), 8.69 (1H, s, NH of Cp with methyl ester), 8.09 (1H, d, *J* = 7 Hz, amide NH of Ala), 5.49(1H, s, Cp), 5.45 (1H, s, Cp), 5.14(1H, s, amide NH of Ala attached to Boc), 4.96 (1H, s, Cp), 4.91(1H, s, Cp), 4.78(1H, s, Cp), 4.71 (1H m, α-H of Ala), 4.69 (1H, s, Cp), 4.51 (2H, s, Cp), 4.35(1H, s, Cp) 4.30 (1H, d, *J* = 2 Hz, α-H of Ala), 4.24 (1H, s, Cp), 4.20 (1H, d, *J* = 8.4 Hz, α-H of Ala), 4.13 (1H, s, Cp), 4.08 (1H, s, Cp), 4.04 (1H, s, Cp), 3.96 (2H, d, *J* = 11 Hz, Cp), 3.86 (2H, s, Cp), 3.75 (3H, s, CH_3 of ester), 1.55 (3H, d, *J* = 7 Hz, CH_3 of Ala in the middle), 1.52 (3H, d, *J* = 7.5 Hz, CH_3 of Ala in one end), 1.49 (9H, s, CH_3 of Ala of Boc), 1.45 (3H, d, *J* = 7 Hz, CH_3 of Ala attached to Boc). $^{13}C\{^1H\}$-NMR ($CDCl_3$, δ/ppm): 175.1, 174, 172.5, 171.5, 171.5, 156.4, 96.6, 96.4, 95.4, 80.7, 73.3, 72.7, 71.6, 71.4, 71.4, 70.8, 70.2, 67.1, 66.9, 65.5, 63.9, 63.8, 63.2,52.1, 51.9, 51.9, 50.8, 28.7, 18.1, 17.8, 17.

6.6.1.2.9. 1-Boc-L-Alanino-ferrocene-n'-L-Alanino-1-ferrocene-n'-L-Alanino-1-ferrocene-n'-L-Alanino-1-ferrocene -n'-methyl-carboxylate (10): Flash column chromatography by using ethyl acetate/hexanes (3/1, R_f = 0.28) to get 429mg (79%) redish orange powder. HRMS (ES): calc for $C_{26}H_{38}N_4O_6Fe$: 1324.2527; found: 1324.2491$[M]^+$. FT-IR (KBr, cm^{-1}): 3324 (b, N-H), 3272 (b, N-H hydrogen bonded) 1720 (s, ester C=O), 1681 (s, Amid I), 1660 (s, Amid I), 1628 (s, Amid I), 1528 (s, Amid II). UV-vis (CH_3CN; λ in nm [ε in $M^{-1}cm^{-1}$]): 448 [1188] ^{1}H-NMR ($CDCl_3$, δ/ppm) : 10.78 (1H, s, NH of Cp in the middle), 10.56 (1H, s, amide NH of Cp in the middle), 10.24 (1H, s, amide NH of Cp which is attached to Boc Ala), 9.01 (1H, d, *J* = 5.5Hz, amide NH of Ala in the middle), 8.90 (1H, s, br, amide NH of Ala in middle), 8.77 (1H, s, br, amide NH of Cp) 8.24(1H, br, amide NH of Ala in the middle), 5.60 (2H, s, br, Cp), 5.56 (2H, s, Cp), 5.20 (1H, s, Cp),, 5.16 (1H, NH attached to Boc), 5.09 (1H, s, Cp), 5.00(1H, s, Cp), 4.89 (1H, s, Cp), 4.82(1H, d, J = 2.5 Hz, α-H of Ala), 4.76(1H, m, α-H of Ala), 4.74(1H, m, α-H of Ala), 4.69 (2H, s, Cp), 4.67 (1H, s, Cp), 4.53 (2H, s, Cp), 4.49 (2H, s, Cp), 4.46 (1H, s, Cp), 4.37 (2H, s, Cp), 4.35 (1H, s, Cp), 4.34 (3H, s, br, Cp), 4.32 (3H, s, Cp), 4.29 (1H, m, α-H of Ala), 4.22 (3H, s, Cp), 4.10 (2H, m, *J* = 1.5Hz, Cp), 3.97 (1H, s, Cp), 3.80 (3H, s, CH_3 of ester), 1.59 (3H, s, br CH_3 of Ala), 1.54 (6H, d, *J* = 7 Hz, br CH_3 of Ala), 1.49 (9H, s, CH_3 of Boc), 1.46 (3H, d, *J* = 6.5Hz CH_3 of Ala). $^{13}C\{^1H\}$-NMR ($CDCl_3$, δ/ppm):, 175.3, 174.9, 172.4, 171.7, 171.6, 156.3, 96.5, 96.4, 96.3, 95.5, 80.9, 75.6, 75.3, 73.4, 73.2, 72.9, 72.7, 72.2, 72.1, 71.6, 71.5, 70.9, 70.8, 70.7, 70.3, 70.2, 69.7, 68.6, 68.4, 67.1, 67.0, 66.4, 66.3, 65.8, 65.5, 64.7, 64.0, 63.8, 63.7, 63.3, 63.2, 52.1, 51.9, 51.8, 51.7, 51.5, 30.2, 29.7, 28.8, 20.0, 18.2, 17.8, 17.2.

6.6.1.2.10. 1-Boc-D-Alanino-ferrocene-n'-D-Alanino-1-ferrocene-n'-D-Alanino-1-ferrocene-n'-D-Alanino-1-ferrocene -n'-methyl-carboxylate (11): Flash column chromatography by using ethylacetate/hexanes (3/1, R_f = 0.28) to get 429mg (79%) redish orange powder. HRMS (ES): calc for $C_{26}H_{38}N_4O_6Fe$: 1324.2527; found: 1324.2485$[M]^+$. FT-IR (KBr, cm^{-1}): 3324 (b, N-H), 3270 (b, N-H hydrogen bonded) 1721 (s, ester C=O) 1680 (s, Amid I), 1658(s, Amid I), 1628 (s, Amid I), 1528 (s, Amid II). UV-vis (CH_3CN; λ in nm [ε in $M^{-1}cm^{-1}$]): 448 [1177] ^{1}H-NMR ($CDCl_3$, δ/ppm) : 10.79 (1H, s, NH of Cp in the middle), 10.52 (1H, s, amide NH of Cp in the middle), 10.26 (1H, s, amide NH of Cp which is attached to Boc Ala), 9.05 (1H, d, *J* = 5.5Hz, amide NH of Ala in the middle), 8.90 (1H, s, br, amide NH of Ala in middle), 8.76 (1H, s, br, amide NH of Cp) 8.25 (1H, br, amide NH of Ala in the middle), 5.65 (2H, s, br, Cp), 5.56 (2H, s, Cp), 5.20 (1H, s, Cp),, 5.14 (1H, NH attached to Boc), 5.00 (1H, s, Cp), 5.00(1H, s, Cp), 4.89 (1H, s, Cp), 4.82(1H, d, J = 3 Hz, α-H of Ala), 4.76(1H, m, α-H of Ala), 4.74(1H, m, α-H of Ala), 4.69 (2H, s, Cp), 4.67 (1H, s, Cp), 4.53 (2H, s, Cp), 4.49 (2H, s, Cp), 4.46 (1H, s, Cp), 4.37 (2H, s, Cp), 4.35 (1H, s, Cp), 4.34 (3H, s, br, Cp), 4.35 (3H, s, Cp), 4.29 (1H, m, α-H of Ala), 4.21 (3H, s, Cp), 4.10 (2H, m, *J* = 1.5Hz, Cp), 3.98 (1H, s, Cp), 3.79 (3H, s, CH_3 of ester), 1.60 (3H, s, br CH_3 of Ala), 1.55 (6H, d, *J* = 7 Hz, br CH_3 of Ala), 1.49 (9H, s, CH_3 of Boc), 1.46 (3H, d, *J* = 7 Hz CH_3 of Ala). $^{13}C\{^1H\}$-NMR ($CDCl_3$, δ/ppm):, 175.2, 174.5, 172.4, 171.7, 171.5, 156.0, 96.2, 96.0, 96.3, 95.5, 80.8, 75.5, 75.3, 73.4, 73.2, 72.9, 72.6, 72.2, 72.0, 71.5, 71.1, 70.8, 70.7, 70.3, 70.2, 69.7, 68.6, 68.4, 67.1, 67.0, 66.4, 66.3, 65.8, 65.5, 64.7, 64.0, 63.8, 63.7, 63.3, 63.2, 52.1, 51.9, 51.9, 51.8, 51.8, 30.2, 29.6, 28.8, 20.1, 18.2, 17.8, 17.1.

6.6.1.2.11. 1-Boc-poly-L-Alanino-ferrocene -n'-methyl ester(12): 41 mg of ferrocene 1-Boc-L-Alanino-n'-ferrocene-carboxylic Acid (**4)** alongwith **5%** of 1-Boc-L-Alanino-n'-methyl-ferrocene-carboxylate (**2**) were mixed with 2ml of 60% TFA solution in dichloromethane and stirred for 30 minutes.Then it was dried in rotovap to remove TFA completely putting dichoromethane several times. It was dissolved in 100 ml of dichloromethane. Making alkaline with 0.5 ml of DIEPA it was placed in ice bath then at 0°C 0.1mmol (5eqv.) of BOP was added. After 5 hours 5% of **4** was added and stirred for 4 more hours. Then washed successively with $NaHCO_3$, 10% citric acid solution, NaHCO3 solution and then by distilled water. DCM layer was dired by sodium sulfate and evaporated in rotovap.Then the solid was washed by cold ethyl acetate to get the 28mg of yellow polymer **12**. FT-IR (KBr, cm^{-1}): 3272 (b, N-H hydrogen bonded) 1721 (s, ester C=O) 1680 (s, Amid I), 1658 (s, Amid I), 1628 (s, Amid I), 1528 (s, Amid II). UV-vis (CH_3CN; λ in nm [ε in M^{-1} (monomer)cm^{-1}]): 448 [290] ^{1}H-NMR ($CDCl_3$, δ/ppm) : 10.89-10.84 (1H, m, NH of Cp), 9.09-8.90 (1H, m, amide NH of Ala), 5.79-3.78 (~9H, m, Cp and α-H of Ala), 1.63 (3H, br CH_3 of Ala).

6.6.3. NMR Study

6.5.3.1. Stack plot of ^{1}H-NMR spectra of compounds **2**, **6**, **8**, **10**, **12** (L-series).

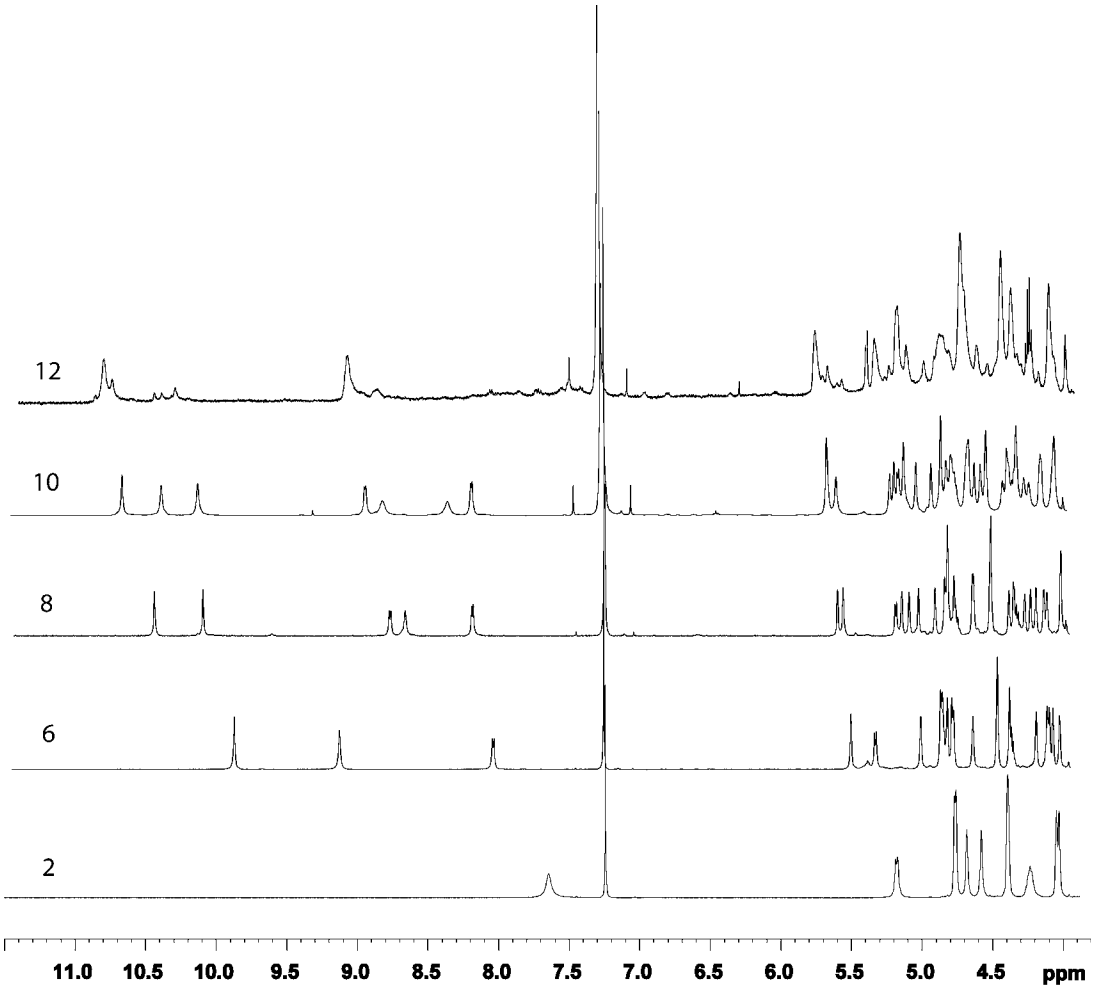

Figure 6.S1. NMR plot of L series monomer (**2**), dimmer (**6**), trimer (**8**), tetramer (**10**) and polymer (**12**) showing that as the number of repeating unit increases the amide proton shifts towards down field indicating their stronger involvement in hydrogen bonding. For the case of polymer only one set of amide proton attached to ferrocene and one set attached to alanine are found which implies that almost all protons are hydrogen bonded and in the same environment.

6.6.3.2. ROESY Study of Compounds **6**, **8,** and **10 (**the L-series of foldamers)

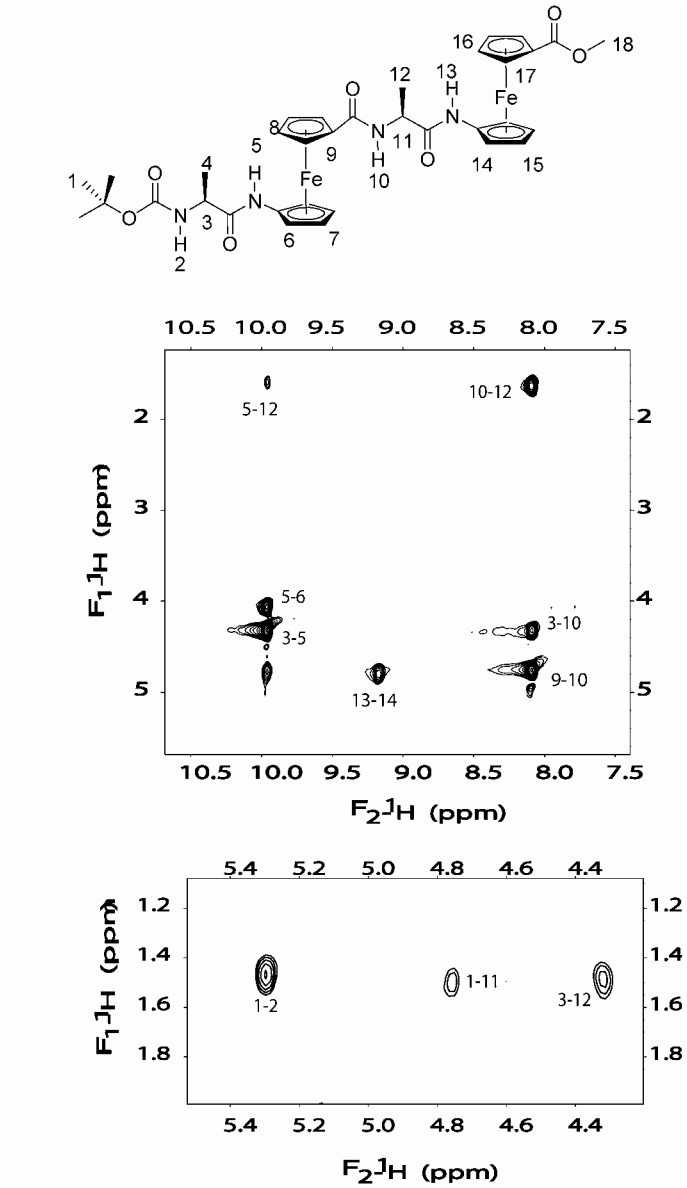

Figure 6.S2. Selected region of ROESY plot of **6,** showing the interactions of Fc-NH (i) with β-H Ala(i+1), Ala-NH (i+1) with α -H of Ala(i) and β -H of Ala(i+1) with α -H of Ala(i).

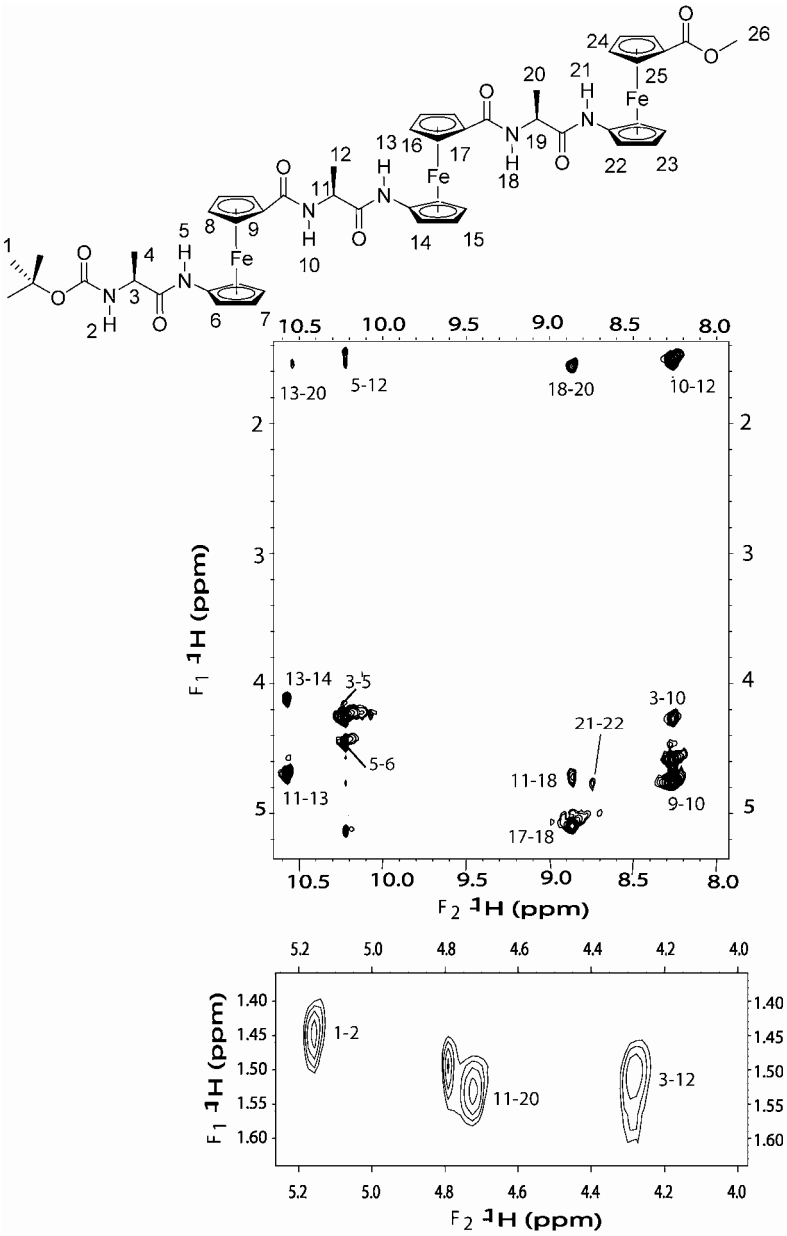

Figure 6.S3. Selected region of ROESY plot of **8,** showing the interactions of Fc-NH (i) with β-H Ala (i+1), Ala-NH (i+1) with α -H of Ala (i) and β -H of Ala (i+1) with α -H of Ala (i).

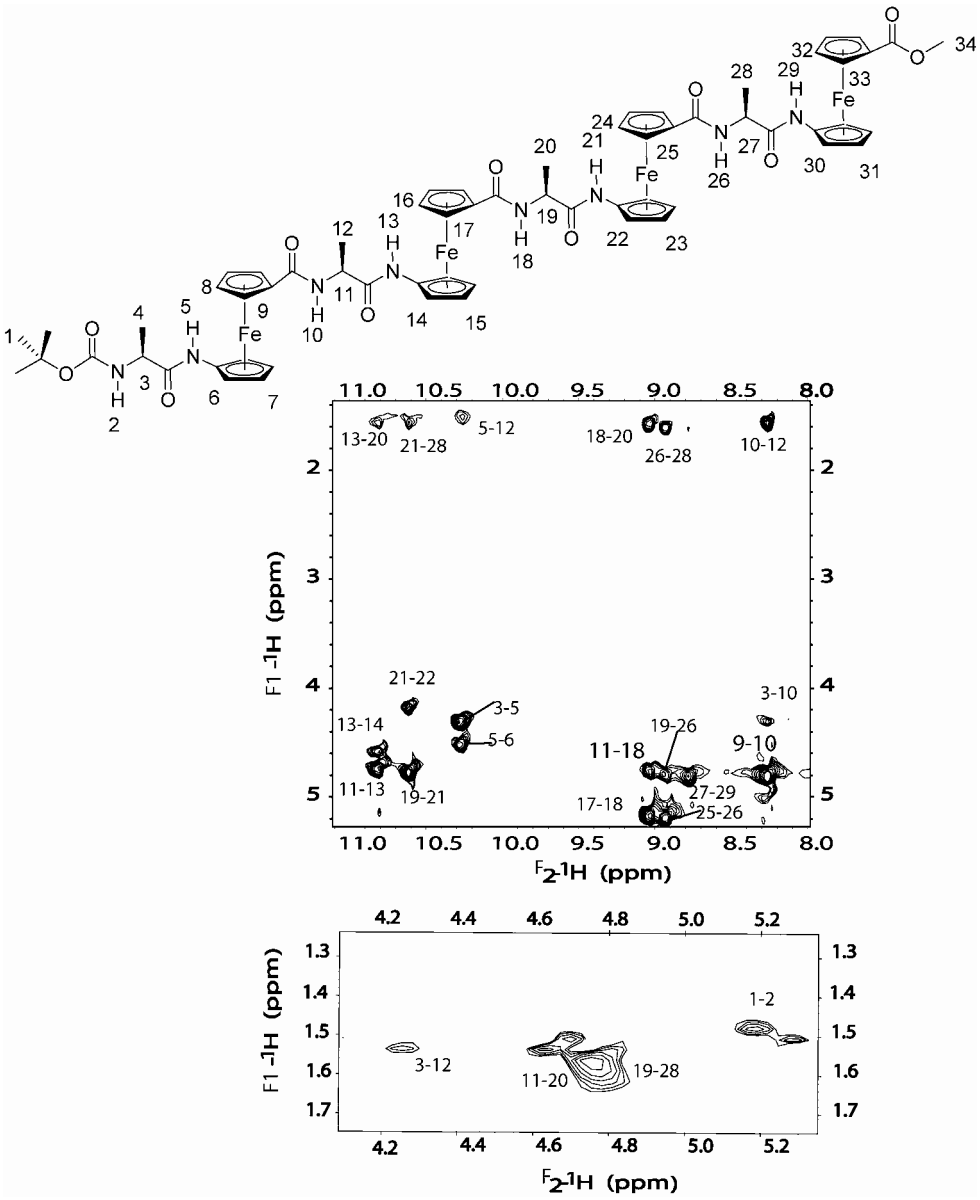

Figure 6.S4. Selected region of ROESY plot of **10,** showing the interactions of Fc-NH (i) with β-H Ala (i+1), Ala-NH (i+1) with α -H of Ala (i) and β -H of Ala (i+1) with α -H of Ala (i).

6.6.4. CD Spectroscopy:

CD spectra were recorded using a PiStar-180 spectropolarimeter (from Applied Biophysics) under an argon atmosphere in the CH_3CN solution at the concentrations (1.0 x 10^{-5} M) with respect to repeating unit.

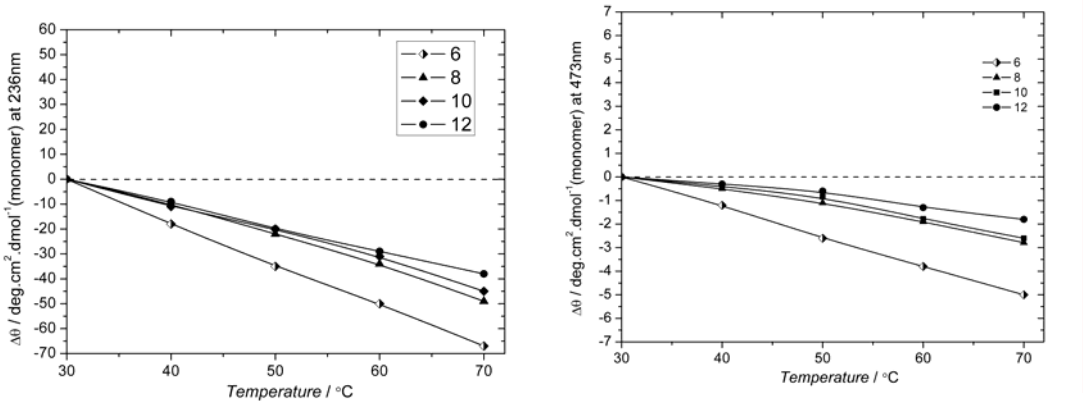

Figure S5. Normalized plot of variable temperature circular dichroism spectra.

6.6.5. FT-IR Study

FT-IR Spectra in the regions of 1500-1800 cm^{-1}(Amide I and Amide II) showing the signature for beta sheet peptide for dimmer to polymer and 3000-3300 cm^{-1} (Amide a) showing the involvement of amide NH in H-bonding.

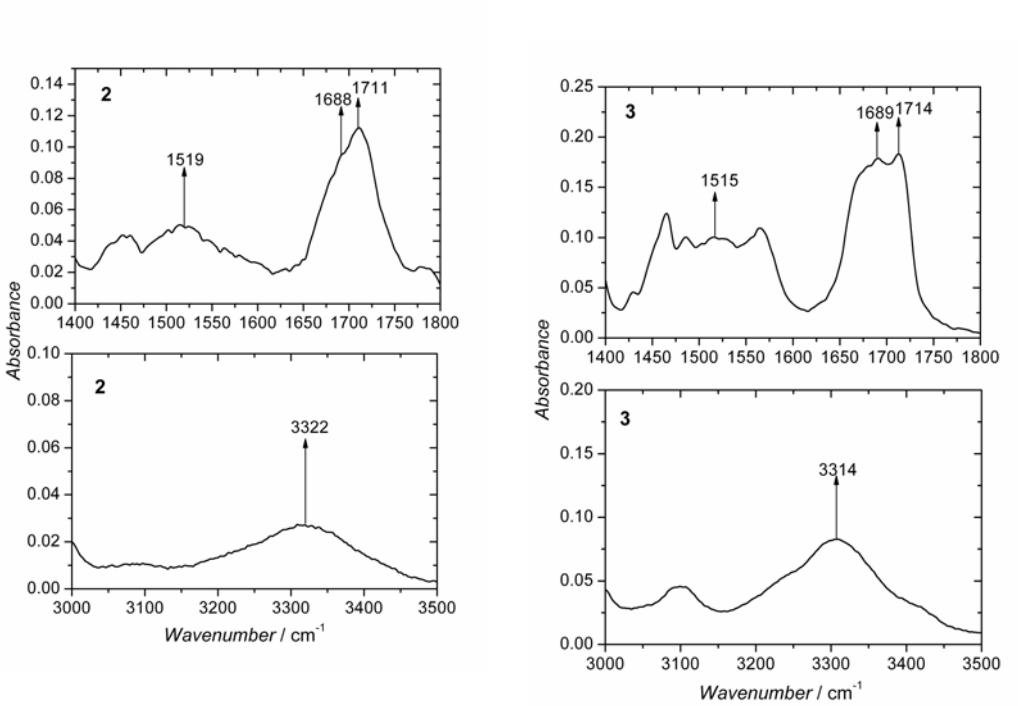

Figure 6.S6. FT-IR spectra of monomers (**2** and **3**) showing the amide-I, amide-II and amide-A regions.

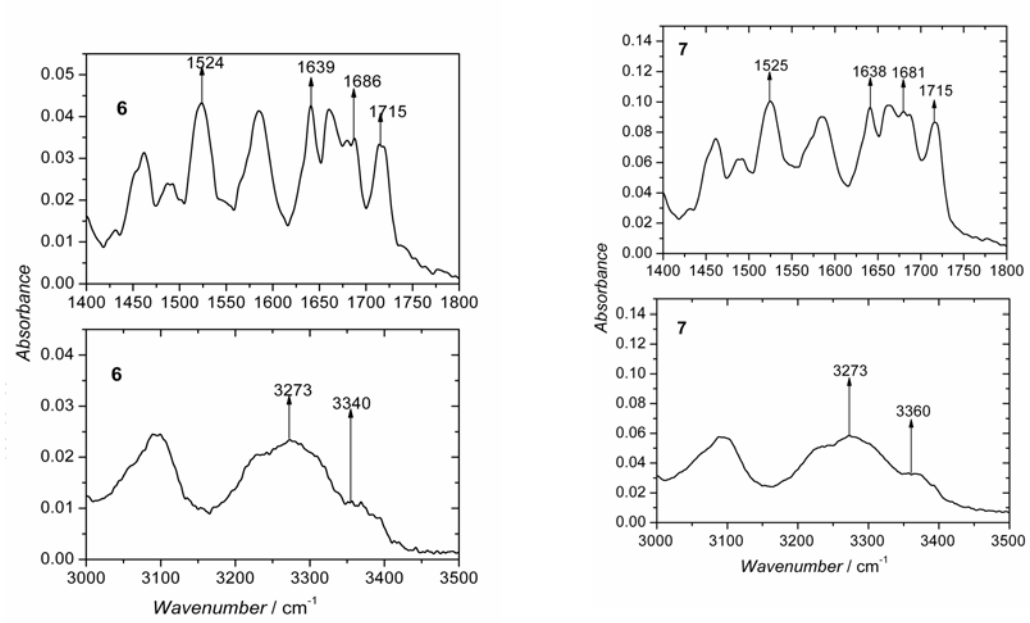

Figure 6.S7. FT-IR spectra of dimers (**6** and **7**) showing the amide-I, amide-II and amide-A regions.

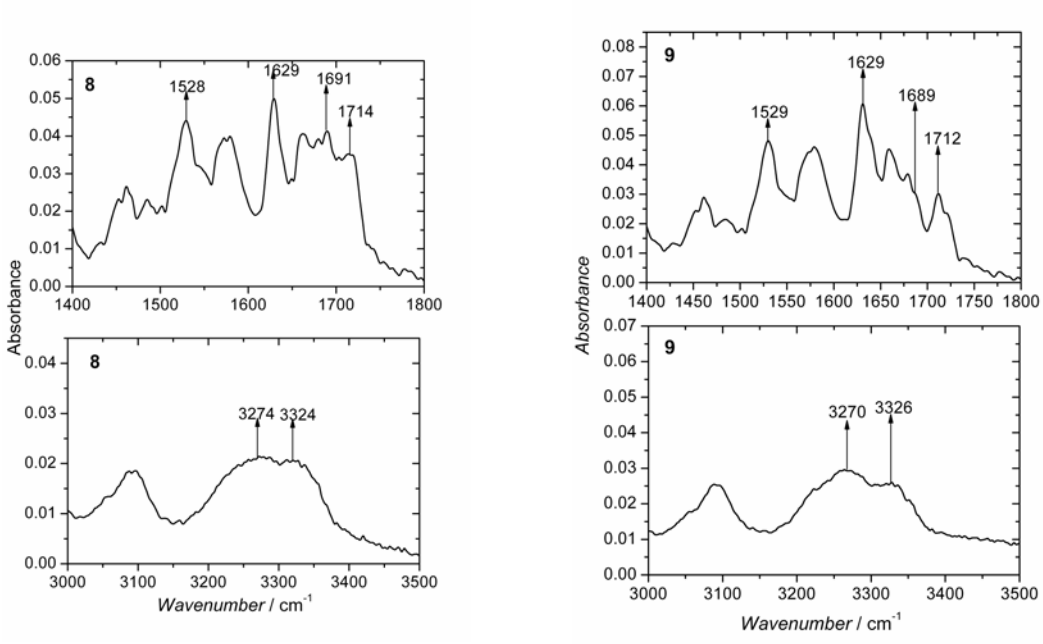

Figure 6.S8. FT-IR spectra of trimers (**8** and **9**) showing the amide-I, amide-II and amide-A regions.

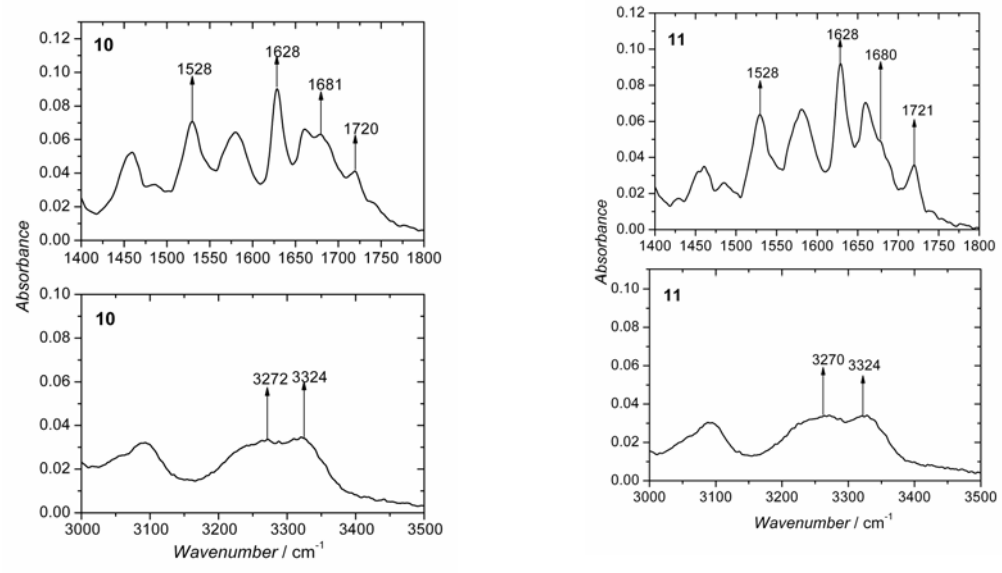

Figure 6.S9. FT-IR spectra of tetramers (**10** and **11**) showing the amide-I, amide-II and amide-A regions.

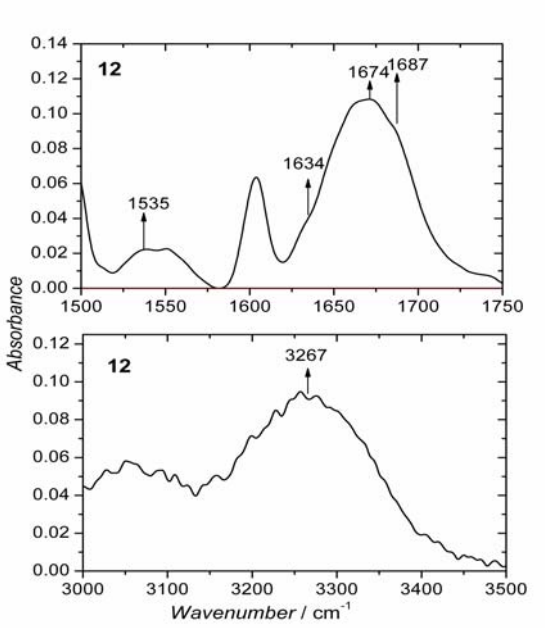

Figure 6.S10. FT-IR spectra of polymer (**12**) showing the amide-I, amide-II and amide-A regions

6.6.6. X-ray Crystallography:

Suitable crystals of compounds **6** (yellow; 0.14 × 0.11 × 0.09 mm), **7** (reddish yellow; 0.12 × 0.14 × 0.09 mm) and **8** (yellow; 0.07 × 0.07 × 0.10 mm were obtained by slowly diffusing hexanes in the solution in dichloromethane and of **9** (reddish yellow crystal; 0.08 × 0.09 × 0.09 mm) was obtained by slow evaporation of chloroform from the solution. All measurements were made on a Nonius KappaCCD 4-Circle Kappa FR540C diffractometer using monochromated Mo K_α radiation (λ = 0.71073 Å) at -100 °C. An initial orientation matrix and cell was determined from 10 frames using ϕscans.[S1-S4] Data were measured using ω-scans.[S1] The data were processed using the standard

Nonius software.[S4] The structures were solved using direct methods (**2**: SIR-97; **3**: SHELXS-97)[S3,S5] and refined by full-matrix least-squares method on F^2 with SHELXL97-2.[S2]

Table S1. Crystal data and structure refinement for compounds **6 - 9**.

Compound	**6**	**7**	**8**	**9**
Empirical formula	$C_{35}H_{42}Cl_2Fe_1N_4O_7$	$C_{35}H_{42}Cl_2Fe_2N_4O_7$	$C_{51}H_{61}Fe_3N_6O_9$	$C_{49}H_{55}Cl_3Fe_3N_6O_9$
Formula weight	813.33	813.33	1069.61	1145.89
Crystal Color, Habit	yellow-orange, plate	yellow-orange, plate	orange, plate	yellow-orange, plate
Crystal dimensions (mm)	0.13 × 0.08 × 0.08	0.12 × 0.12 × 0.12	0.18 × 0.18 × 0.15	0.10 × 0.10 × 0.10
Crystal system	monoclinic	orthorhombic	tetragonal	tetragonal
Space group	$P2_12_12_1$ [No. 19]	$P2_12_12_1$ [No. 19]	$P4_12_12$ [No. 92]	$P4_32_12$ [No. 96]
a (Å)	13.4220(3)	13.376(2)	13.997(5)	14.0740(2)
b (Å)	16.7930(4)	16.7560(15)	13.997(5)	14.0740(2)
c (Å)	16.7920(3)	16.7840(11)	52.108(5)	51.9910(9)
α (°)	90	90	90	90
β (°)	90	90	90	90
γ (°)	90	90	90	90
V (Å^3)	3784.84(14)	3761.8(7)	10209(5)	10298.2(3)
Z^b	4	4	8	8
F(000)	1688	1688	4472	4736
Density (ρ_{calcd})	1.427 Mg/m^3	1.436 Mg/m^3	1.392 Mg/m^3	1.478 Mg/m^3
Absorption coefficient (μ)	0.959 mm^{-1} (= 9.59 cm^{-1})	0.965 mm^{-1} (= 9.65 cm^{-1})	0.902 mm^{-1} (= 9.02 cm^{-1})	1.050 mm^{-1} (= 10.50 cm^{-1})

The non-hydrogen atoms were refined anisotropically. Hydrogen atoms were included at geometrically idealized positions (C-H bond distances 0.95/0.99 Å; N-H bond distances

0.88 Å) and were not refined. The isotropic thermal parameters of the hydrogen atoms were fixed at 1.2 times that of the preceding carbon or nitrogen atom.

Table 6.S2. Data collection and refinement conditions for compounds **6-9**.

Compound	**6**	**7**	**8**	**9**
Theta range for data collection	3.27 to 27.49°	3.90 to 24.71°	2.14 to 21.95°	1.50 to 24.72°
Completeness to theta = 27.49°	99.5%	98.1%	99.4%	97.5%
Reflections collected[d]	15746	6024	11895	16805
Independent reflections $[F_o^2 \geq -3\sigma(F_o^2)]$[e]	8639 [R_{int} = 0.0287][f]	6024 [R_{int} = 0.0000][f]	6191 [R_{int} = 0.0427][f]	8627 [R_{int} = 0.1072][f]
Observed reflections $[F_o^2 > 2\sigma(F_o^2)]$[g]	7741	5179	4915	5268
Reflection (observed)/parameter ratio	17:1	12:1	8:1	9:1
Reflection (data)/parameter ratio	19:1	14:1	10:1	14:1
Goodness-of-fit on F^2	1.047	1.140	1.048	1.028
R_1	0.0361	0.0871	0.0505	0.0725
wR_2	0.0845	0.1932	0.1210	0.1558
Max. Shift/Error in Final Cycle	0.001	0.000	0.000	0.001
Largest difference peak and hole	0.351 and -0.590 $e^-/Å^3$	0.925 and -0.527 $e^-/Å^3$	0.422 and -0.244 $e^-/Å^3$	0.818 and -0.688 $e^-/Å^3$

All data were collected in Nonius KappaCCD difractometer, using Graphite-monochromated Mo Kα radiation of wave length 0.71073 Å at -100(2) °C. $R_1 = [\Sigma||F_o|-|F_c||]/[\Sigma|F_o|]$ for $[F_o^2 > 2\sigma(F_o^2)]$[i] $wR_2 = \{[\Sigma w(F_o^2-F_c^2)^2]/[\Sigma w(F_o^2)^2]\}^{1/2}$ [all data] $GooF = \{\Sigma[w(F_o^2-F_c^2)^2]/(n-p)\}^{1/2}$, n: number of reflections, p: number of parameters

Table 6.S3. Intra and intermolecular N(H)···O=C contacts [Å] of **6**.

r_{vdW}(N) + r_{vdW} (O) = (1.55 + 1.50) [Å] = 3.05 [Å]

Intramolecular contacts:

N(21)(H) ····O(12)=C	2.990(3)
N(11)(H) ····O(22)=C	2.819(3)

Intermolecular contacts:

N(22)(H)····O(11)*=C	2.881(3)
N(12)*(H)····O(21)=C	2.930(3)
N(12)(H)····O(11)**=C	2.930(3)
N(22)** ····(H)O(11)=C	2.881(3)

Symmetry transformations used to generate equivalent atoms:

*: -x + ½, -y + 2, z - ½
**: -x + ½, -y + 2, z + ½

Table 6.S4. Intra and intermolecular N(H)···O=C contacts [Å] of **7**.

r_{vdW}(N) + r_{vdW} (O) = (1.55 + 1.50) [Å] = 3.05 [Å]

Intramolecular contacts:

N(21)(H)····O(12)=C	2.98(1)
N(11)(H)····O(22)=C	2.824(9)

Intermolecular contacts:

N(12)(H)····O(21)*=C	2.93(1)
N(22)*(H)····O(11)=C	2.87(1)
N(22)(H)····O(11)**=C	2.87(1)
N(12)**(H)····O(21)=C	2.93(1)

Symmetry transformations used to generate equivalent atoms:

*: -x + ½, -y + 1, z - ½
**: -x + ½, -y + 1, z + ½

Table 6.S5. Intra and intermolecular N(H)···O=C contacts [Å] for **8.**

r_{vdW}(N) + r_{vdW} (O) = (1.55 + 1.50) [Å] = 3.05 [Å]

Intramolecular contacts:

N(11)(H)····O(22)=C	2.931(6)
N(21)(H)····O(12)=C	2.977(6)
N(41)(H)····O(21)=C	2.971(6)
N(22)(H)····O(42)=C	2.943(6)

Intermolecular contacts:

N(42)*(H)····O(11)=C	2.854(7)
N(12)(H)····O(41)*=C	2.882(7)
N(12)′(H)····O(41)=C	2.882(7)
N(42)(H)····O(11)′=C	2.854(7)

Symmetry transformations used to generate equivalent atoms:

*: y - ½, -x + 1.5, z - ¼
′: -y + 1.5, x + ½, z + ¼

Table 6.S6. Intra and intermolecular N(H)···O=C contacts [Å] of **9**.

r_{vdW}(N) + r_{vdW} (O) = (1.55 + 1.50) [Å] = 3.05 [Å]

Intramolecular contacts:

N(11)(H)····O(22)=C	2.929(8)
N(21)(H)····O(12)=C	2.967(8)
N(41)(H)····O(21)=C	2.957(8)
N(22)(H)····O(42)=C	2.995(8)

Intermolecular contacts:

N(42)*(H)····O(11)=C	2.885(8)
N(12)(H)····O(41)*=C	2.883(8)
N(12)′(H)····O(41)=C	2.883(8)
N(42)(H)····O(11)′=C	2.885(8)

Symmetry transformations used to generate equivalent atoms:

*: y + ½, -x + ½, z + ¼
′: -y + ½, x - ½, z - ¼

Table 6.S7. Dihedral angles of the selected peptide bonds.

Dihedral angles of **6** for the amide portions

1	C18	N12	C16	C15	-72.38
2	N12	C16	C15	N11	146.93
3	C25	N21	C26	C28	-79.98
4	N21	C26	C28	N22	155.41

Dihedral angles of **7** for the amide portions

1	C18	N12	C16	C15	70.49
2	N12	C16	C15	N11	-145.49
3	C25	N21	C26	C28	82.90
4	N21	C26	C28	N22	-155.43

Dihedral angles of **8** for the amide portions

1	C18	N12	C16	C15	-68.46
2	N12	C16	C15	N11	138.38
3	C25	N21	C26	C28	-68.25
4	N21	C26	C28	N22	145.73
5	C45	N41	C46	C48	-74.96
6	N41	C46	C48	N42	143.64

Dihedral angles of **9** for the amide portions

1	C18	N12	C16	C15	67.70
2	N12	C16	C15	N11	-137.16
3	C25	N21	C26	C28	68.02
4	N21	C26	C28	N22	-147.13
5	C45	N41	C46	C48	74.39
6	N41	C46	C48	N42	-142.25

6.5.6.1. ORTEP diagrams and intermolecular arrangements of **6-9** in crystal:

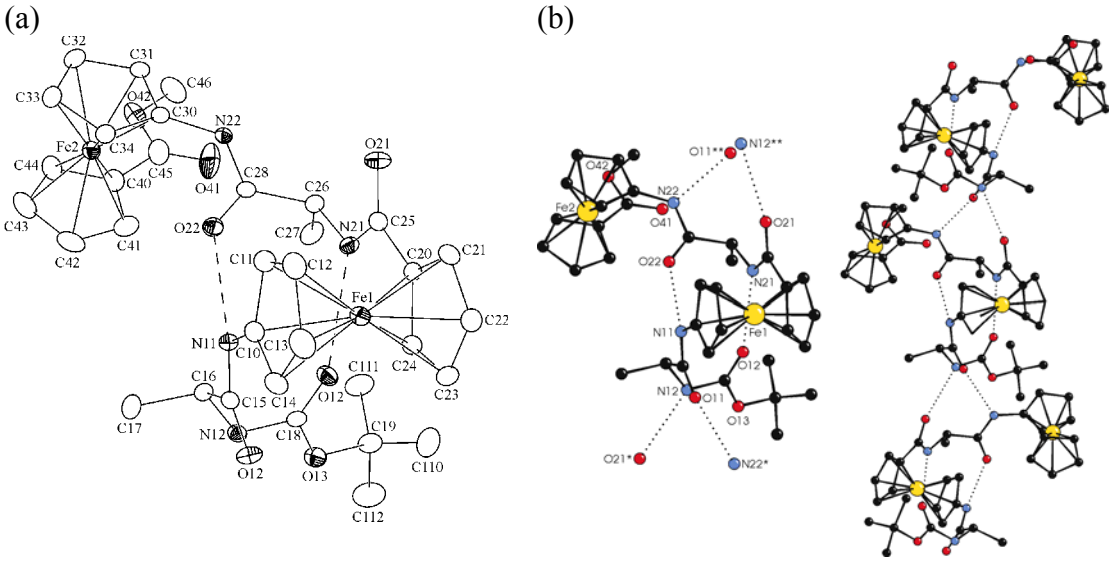

Figure 6.S11. Plot of **6** showing (a) ORTEP diagram and (b) the formation of supramolecular helical strand.

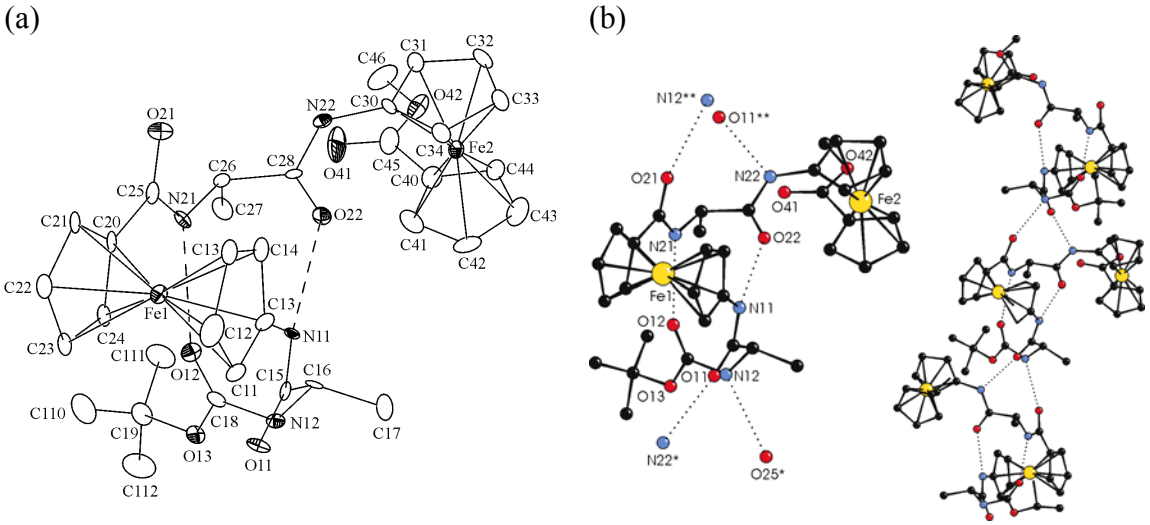

Figure 6.S12. Plot of **7** showing (a) ORTEP diagram and (b) the formation of supramolecular helical strand.

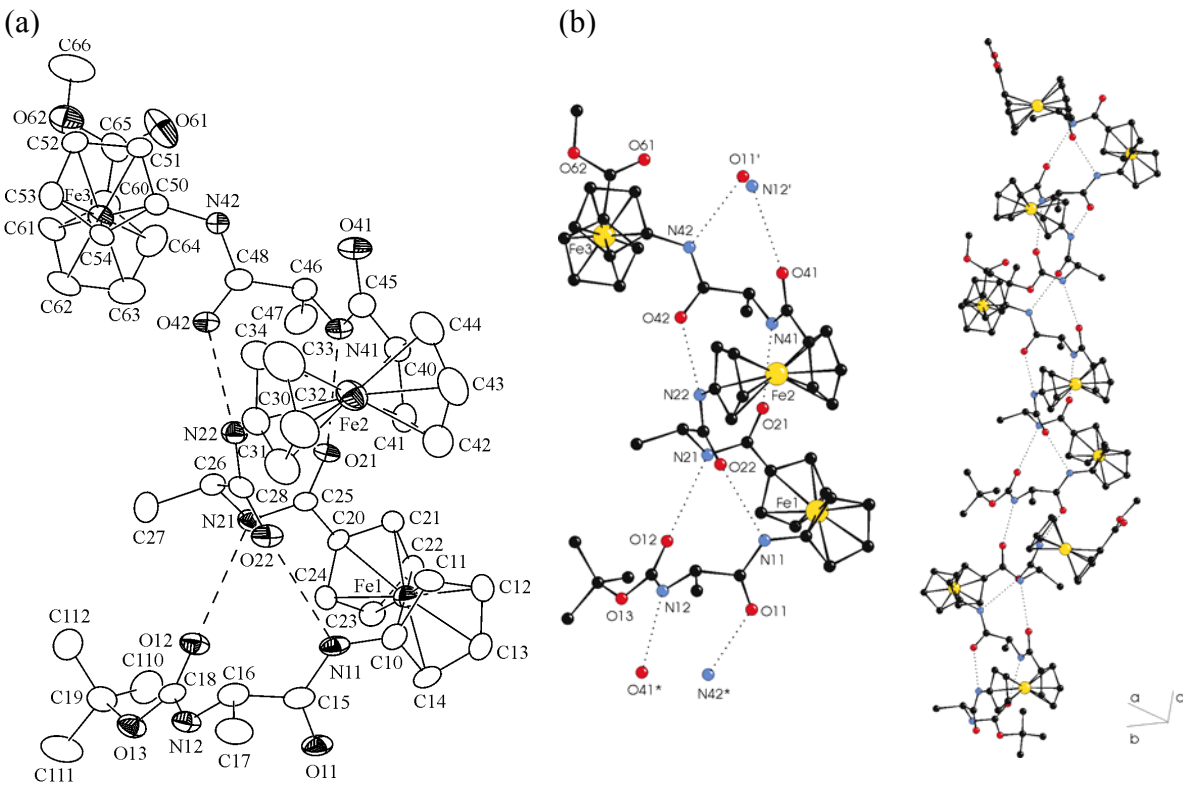

Figure 6.S13. Plot of **8** showing (a) ORTEP diagram and (b) the formation of supramolecular helical strand.

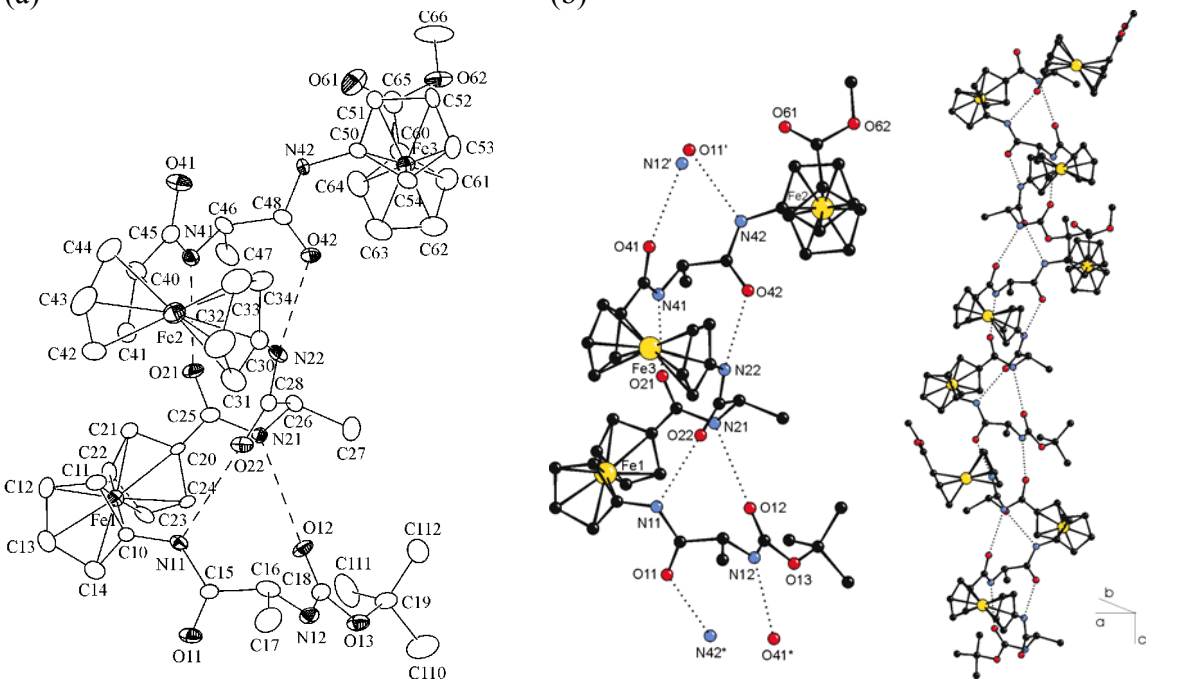

Figure 6.S14. Plot of **9** showing (a) ORTEP diagram and the formation of supramolecular helical strand.

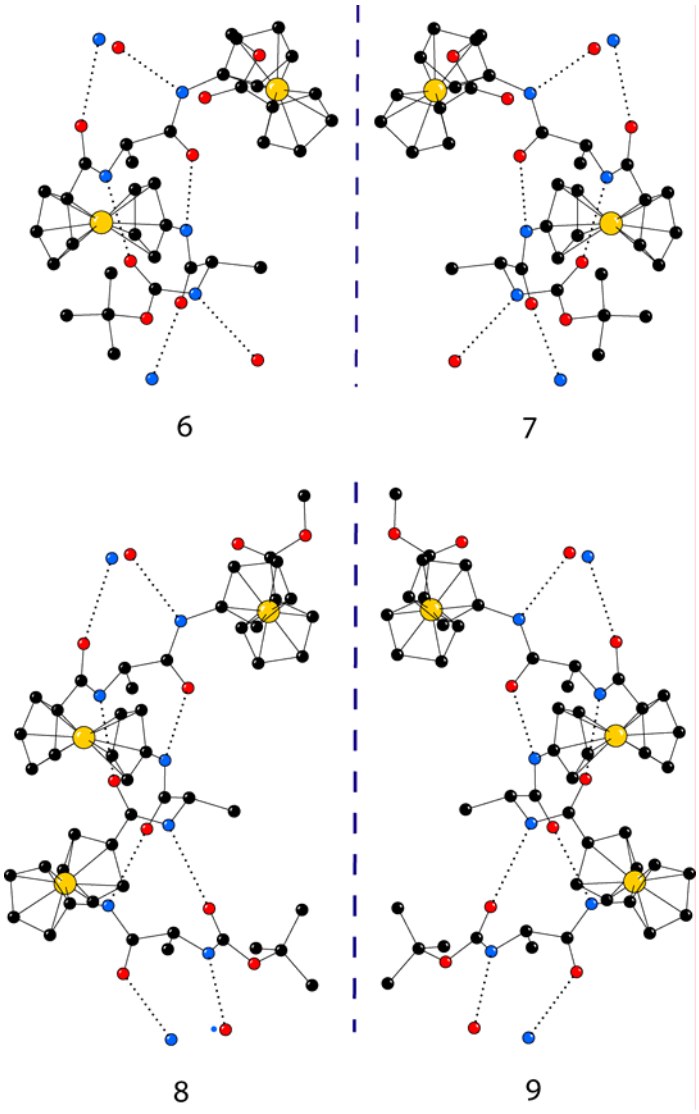

Figure 6.S15. Crystal structures of L-series dimer **6** and trimer **8** are mirror images of corresponding D-series dimer **7** and trimer **9**.

6.5.6. Supporting References

[S1] *COLLECT data collection software*, Nonius, Delft, The Netherlands, **1998**.

[S2] SCALEPACKv1.96: Z. Otwinowski and W. Minor, Processing of X-ray Diffraction Data Collected in Oscillation Mode, *Methods Enzymol.*,**1998**, 276, 302; Z. Otwinowski and W. Minor, *Macromolecular Crystallography, Part A*, ed. C. W. Carter, Jr. and R. M. Sweet, Academic Press, San Diego, CA, **1997**.

[S3] G. M. Sheldrick, *SHELXS-97, Program for solution of crystal structures*, University of Göttingen, Germany, **1997**.

[S4] Altomare A., Burla M. C., Camalli M., Cascarano G. L., Giacovazzo C., Guagliardi A., Moliterni A. G. G., Polidori G. and Spagna R. *J. Appl. Crystallogr.*, **1999**, 32, 115.
[S5] Sheldrick G. M., *SHELXL-97-2, Program for refinement of crystal structures*, University of Göttingen, Germany, **1998**.

Chapter 7

General Discussion and Conclusion

In my work, I have exploited various 1,n'-disubstituted ferrocene derivatives ($Fc[COOH]_2$, $Fc[NH_2]_2$ and $Fc[NH_2][COOH]$) for the preparation of peptide conjugates. The purpose of this work was to explore the use of the organometallic group as a scaffold for stabilizing β-sheets, a ubiquitous secondary structural element found in proteins. While there are a number of approaches available, as described in Chapter 1, the approach detailed in Chapters 2 – 6, is highly versatile and enabled me to prepare not only simple models for β-sheets, but also the first synthetic model for a β-barrel-like structure and even parallel β-helices. In my work, I have provided a series of design examples, which illustrate the versatility of the ferrocene scaffold for designing some challenging secondary and even tertiary structural motifs.

As was shown in the introduction to my thesis, peptide conjugates of 1,1'-Ferrocenedicarboxylic acid have been found to arrange in an interesting β-sheet like structure, forming a 10-member intramolecular H-bonding. However, in these conjugates, the carboxyl ends of the amino acids point away form each other. [1-6] As a result, the second amino acid attached to it, does not form any intramolecular inter-strand H-bonds. Therefore, this simplistic approach appears not to be very promising for the design of extended β-sheets. In Chapter 2, I have introduced the concept of

cyclization, in order to restrict the flexibility of the podant peptide chains, forcing them into a specific conformation that facilitates their interaction by H-bonding. A series of pseudocyclopeptides of general formula Fc[AA-CSA]$_2$ were prepared. It is observed that they adopted β-sheet like 10-membered intramolecular H-bonded ring and arrange themselves in 1,2'-conformation akin to that found in the non-cyclic analogues. ^{1}H-NMR in chloroform showed that the NHs originated from the conjugated amino acids were involved in intramolecular hydrogen bonding, where as the NHs of cysteamine formed intermolecular hydrogen bonds. FTIR spectroscopy also revealed the presence of strong H-bonding. From the crystal structure of Fc[CO-Gly-CSA]$_2$ described in Chapter 2, it was observed that the intramolecular H-bonding distances (*d* N-O = ~2.832Å) were shorter than the corresponding acyclic analogue, Fc[CO-Gly-NH$_2$]$_2$ (*d* N-O = ~2.884 Å), prepared earlier by Erker.[7] This indicated the presence of a strong interstrand attraction and provided structural rigidity, which is maintained in solution. Variable temperature ^{1}H-NMR experiment showed that the resonances of NHs involved in the intramolecular H-bonding, did not change with the increase in temperature. This result proved that the cyclization through the carboxyl ends was a promising strategy to control the alignment of the ends, without disturbing the β-sheet forming characteristics.

The concept of cyclization was developed further in Chapter 3 for the purpose of designing a new structural motif based on a β-sheet-like structure. Intramolecular β-sheet-like H-bonding pattern has been successfully extended, which allowed me to prepare the first model of a β-barrel structure. From the rigidity of the system and an inward twisting in peptide strands, it was hypothized that if the proper sequence of amino acids was attached next to the Fc group, in the cyclic systems, it would be

possible to extend the β-strand characteristics and develop an interface that enables intermolecular H-bonding interactions. In addition, the Fc scaffold in such cyclopeptide conjuguates provides sufficient flexibility for the peptide strands to rotate out of the Cp plane allowing the conjugates to associate into hollow pore-like structures. This is an entirely new concept and further demonstrates the utility of the Fc scaffold.

This hypothesis has been tested in Chapter 3 by designing two pseudocyclopeptides, Fc[Gly-Val-CSA]$_2$ and Fc[Gly-Ile-CSA]$_2$. From X-ray crystal structure it was observed that the amino acids in the backbone maintained β-strand characteristics. They arranged themselves in parallel and anti-parallel fashions through intra- and intermolecular H-bonding, forming a barrel like structure with an internal diameter of 8 Å. To the best of our knowledge, this is the only example of "a synthetic β-barrel", although this secondary structural domain has been ubiquitous and known for a long time in biological systems. The inside of the barrel is filled with water as evidenced from NMR and crystal structure studies.

In addition to cyclization, I have discovered that it is also possible to form acyclic Fc-conjuguates, which have the podant peptide chains arranged in a β-sheet-like fashion. For this approach to work, it is necessary to have glycine as the proximal amino acid. Gly provides sufficient flexibility. Furthermore, my studies indicate that it is necessary to pay particular attention to the amino acid sequence for this strategy to succeed. Taking this into consideration, the two tripeptide conjugates Fc[CO-Gly-Val-Cys(Bz)-OMe] and Fc[CO-Gly-Ile-Cys(Bz)-OMe] were prepared as described in Chapter 4. After the Fc-proximal Gly, the β-strand forming amino acids, Val and Ile were chosen. The CD spectral study showed P-helical conformation in the Fc region, as

expected for the L-amino acid conjugates. A negative absorbance at 215 nm proved the formation β-sheet conformation of the peptide strands. NMR study indicated that the NHs of Gly and Cys formed intramolecular hydrogen bond, where as the Val NH formed intermolecular hydrogen bonding, which was expected for the proposed extended β-sheet conformation. IR spectra showed two absorbance peaks in the amide-I region (at around 1630 cm^{-1} and 1680 cm^{-1}), which was the indication of the presence of β-strand conformation. Finally, the X-ray crystal structures of both the compounds were found to coincide well with the proposed structures. Thus, in the acyclic systems, we were also able to achieve the extended β-sheet like conformation. In light of earlier reports by Hirao, my results described in Chapter 4 are very surprising and indicate that it is possible to prepare acylic Fc-peptide conjugates in which the podant peptide chains adopt a β-sheet-like structure.

In my work, I also used a the ferrocene diamine derivative $Fc[NH\text{-}Boc]_2$, which is suitable for making Fc-peptide conjugates by amide bond formation. So far, the amino acid of 1,1'-Fc dicarboxylic acid and 1-amino-1'-Fc carboxylic acid have been exploited for the formation of peptide conjugates. As shown in the introduction, 1,1'-Fc dicarboxylic acid was found to form anti-parallel β-sheet-like 10-membered hydrogen bonded rings, whereas 1-amino-1'-Fc carboxylic acid forms parallel β-sheet-like 12-membered hydrogen bonded rings. This indicates that amino acid conjugates of 1,1'-diaminoferrocene may align the peptide strands in an anti-parallel β-sheet. Motivated by this hypothesis, I set out to prepare such conjugates. But the chemical instability of the necessary intermediate, 1,1'-diaminoferrocene, created a hurdle. This obstacle was overcome by synthesizing a very stable derivative $Fc[NH\text{-}Boc]_2$, which was compatible

with common peptide synthesis protocols. By exploiting this derivative, the conjugates with D- and L-alanine were successfully prepared. CD spectroscopic studies demonstrated the formation P-helical structure for the L-alanine conjugates and M-helical alignment for the D, similar to the fact as observed in the conjugates of 1,1'-ferrocnedicarboxylic acid and 1-amino-1'-ferrocenecarboxylic acid. NMR spectral studies showed that the NHs of Fc formed intra-molecular hydrogen bonding as expected for the proposed structure. X-ray crystal structure study clearly showed the formation of well organized structure through the formation of anti-parallel β-sheet-like 14-member hydrogen bonded ring. They arranged in a helical fashion assuming respectively 1,2'- and 1,5'-conformation. Therefore, we suggest that this is a novel method for controlling the peptide structure.

In my work, I have also demonstrated a unique methodology for preparing a model system for β-helical peptides. In Chapter 6, I have described the first *de novo* model for this secondary structural motif, which is present in the tail-spike of several bacteriophages and which plays an important role in the transfer of genetic information from the phage to the bacteria. Once more, the scaffolding behavior of Fc was exploited demonstrating its versatility. It is well known that peptide conjugates of disubstituted ferrocenes are capable of providing both β-sheet motif and helical arrangement to the attached amino acids.[1,5,6] In our attempt, we exploited both of these characteristics in an extended form. Using 1-amino-1'-ferrocenecarboxylic acid as a helical turning motif, a series peptide conjugates were prepared, using alternating sequence of Fc amino acid and alanine amino acids. In solution, NMR and CD spectral studies indicated the formation of proposed β-helical conformation. FTIR spectroscopic study in solid-state

showed the signature of β-sheet conformation and the involvement of the amide proton with strong hydrogen bonding. The strength of the H-bonding within the molecules was found to increase incrementally with increasing length of the Fc-conjugate. X-ray crystal structure studies on a series of models demonstrate the presence of 12-membered H-bonded rings as would be expected in a parallel β-sheet-like structure, which extends throughout the length of the conjugates and is even propagated on the supramolecular level providing a continuous β-helical structure.

In conclusion, I have achieved my objectives described in section 1.5 in Chapter 1 and succeeded in developing the general strategies that allowed me to prepare the models of β-sheets and structures that contain this important secondary structural element. Specifically, I prepared models for β-barrels and β-helices applying the ferrocene group as an integral design element. It is hoped that the methodology developed in this thesis will be useful for preparing other challenging structural models which will be useful in biological and materials sciences and also will find application in *de novo* protein design.

In addition, the importance of this work is that it provides access to a range of structural motifs that can be investigated separately and in isolation of a protein for their individual stability to solvents, pH, temperature, and other effects. In essence it will be possible to carry out comparative studies of the relative stabilities of various β-sheet-like models and draw conclusions that will be of relevance to β-sheets and to various other structural motifs present in proteins. Therefore, these systems may provide a route, in the future, to address the protein folding problem using well-defined model systems.

References:

[1] R. S. Herrick, R. M. Jarret, T. P. Curran, D. R. Dragoli, M. B. Flaherty, S. E. Lindyberg, R. A. Slate, L. C. Thornton, *Tetrahedron Lett.* **1996**, 37, 5289-5292;

[2] T. Moriuchi, A. Nomoto, K. Yoshida, A. Ogawa, T. Hirao, *J. Am. Chem. Soc.* **2001**, 123, 68-75.

[3] D. R. van Staveren, T. Weyhermuller, N. Metzler-Nolte, *Dalton Trans.* **2003**, 210-220.

[4] D. R. van Staveren, N. Metzler-Nolte, *Chem. Rev.* **2004**, 104, 5931

[5] L. Barisic, M. Dropucic, V. Rapic, H. Pritzkow, S. I. Kirin, N. Metzler-Nolte, *Chem. Commun.* **2004**, 2004-2005.

[6] T. Moriuchi, T. Nagai, T. Hirao, *Org. Lett.* **2005**, 7, 5265-5268;

[7] M. Oberhoff, L. Duda, J. Karl, R. Mohr, G. Erker, R. Fröhlich and M. Grehl, *Organometallics*, **1996**, 15, 4005-4011.

Appendices

A.1. Publications

[7] S. K. Dey, Y.-T. Long, **S. Chowdhury,** T. C.Sutherland, H. S. Mandal, and H.-B. Kraatz, Study of Electron Transfer in Ferrocene-Labeled Collagen-like Peptides. *Langmuir*, **2007**, 23, 6475-6477

[6] **S. Chowdhury**, G. Schatte, H.-B. Kraatz, Rational Design of A New Class of Bioorganometallic Foldamers: Potential Model For Parallel Beta-Helical Peptides, *Angew. Chem. Int. Ed*. **2006**, 45, 6882-6884**.**

[5] **S. Chowdhury**, D. A. R. Sanders, G. Schatte, H.-B. Kraatz, Discovery of a Pseudo-Beta Barrel, Synthesis and Formation by Tiling Ferrocene Cyclopeptides, *Angew. Chem. Int. Ed*, **2006**, 45, 751-754.

[4] **S. Chowdhury**, K. A. Mahmoud, G. Schatte, H.-B. Kraatz, Amino Acids Conjugates of 1,1'-Diamino Ferrocene, Synthesis and Chiral Organization, *Org. Biomol. Chem*. **2005**, 3, 3018-3013.,

[3] **S. Chowdhury**, G. Schatte, H.-B. Kraatz, A cyclic Ferrocene Histidine Conjugate: Interaction with Alkali Metal Ions, *Eur. J. Inorg. Chem*. **2006**, 988-993

[2] G. Orlowski, **S. Chowdhury**, Y. Long, T. C. Sutherland, H.-B. Kraatz, Electrodeposition of Ferrocene Peptide Disulfide, *Chem. Commun.* **2005**, 1330-1332.

[1] **S. Chowdhury**, G. Schatte, H.-B. Kraatz, Synthesis, structure and electrochemistry of ferrocene-peptide macrocycles *Dalton Trans*. **2004**, 1726-1730.

A.2. Curriculum Vitae

Somenath Chowdhury
Son of Kalimati Chowdhury and Late Abanikanta Chowdhury
Born in Village: Majirdanga, Dist: Bankura, West Bengal, India

Academic Qualification

(a) From May 2003 to April 2007, worked for my **Ph.D.** with professor Heinz-Bernhard Kraatz, in the Department of Chemistry, University of Saskatchewan, Canada. Average grade in Course works: 88.5%

(b) M.Tech. in polymer from Indian Institute of Technology, Kharagpur, India in 1997 (CGPA: 8.59/10)

(c) M.Sc. in Chemistry from Indian Institute of Technology, Kharagpur, India in 1995. (CGPA: 7.38/10)

Research experience

May 2003-April 2007: *At the Department of Chemistry, University of Saskatchewan.*
Worked on controlling the secondary structure of peptides, mainly to achieve β-sheet conformation, using molecular scaffold and by cyclization. I have designed and synthesized different model peptides and carried out their extensive conformational study, mainly by NMR, CD and XRD.

Aug 2002- April 2003: *At the Department of Chemistry, University of Saskatchewan.*
Design and synthesis of various heterocylic conjugates with the aim of site specific DNA binding.

Jan 1998-July 2002: *At the Institute of Science and Technology for Advanced Studies and Research, Vallabh Vidyanagar, India.*
Synthesis of various anhydride group containing monomers and their copolymers with the aim of controlling the release of primary amino group containing drugs.

June 1995-Feb 1997: *At Indian Institute of Technology, Kharagpur, India.*
Imparting polarophilicity to hydrocarbon polymers to improve compatibility with polyamides.

Awards and Scholarships

(**6**) Herzberg Award in 2006 at the University of Saskatchewan.
(**5**) Graduate Teaching Fellowship award in 2005-2006 at the University of Saskatchewan.
(**4**) Graduate Teaching Fellowship award in 2004-2005 at the University of Saskatchewan.
(**3**) Graduate Scholarship by the Department of Chemistry, University of Saskatchewan 2003-2004.
(**2**) Full Institutional Schlorship based on GATE (Graduate Aptitude Test in Engineering) percentile, during my M.Tech. (1995-1997), at Indian Institute of Technology, Kharagpur, India.
(**1**) Junior Research Fellowship from Council of Scientific and Industrial Research, India.

Tests Qualified:

(a) Graduate Aptitude Test in Engineering (percentile 98.85) in 1995, Conducted by HRD, India
(b) National Eligibility Test in Chemical Sciences with junior research fellowship From Council of Scientific and industrial research, conducted by HRD, India.
(c) Graduate Record Examination (GRE) general, conducted by ETS, score 1970/2400 (V-480, Q-790, A-700).
(d) TOEFL, conducted by ETS, score of 277/300.